Lubrication and Cooling in Creep Feed Grinding

by

Melanie Grace Gibbs

A dissertation submitted for the degree of Doctor of Philosophy at the University of Bristol, Department of Mechanical Engineering, May 1988.

CONTENTS

SUMMARY

The technique of continuous dressing has been used to isolate the lubricating and cooling properties of a range of grinding fluids. Continuous dressing has been shown to control the wheel surface, and hence the grinding process, under a range of conditions. The specific grinding energy has been used to define and rank the lubricity of fluids and has been shown to be sensitive enough to distinguish not only between oil and water based fluids but also between a micro- and a macroemulsion. It has been shown that oil can reduce the specific energy requirement to one third of that with a soluble oil macroemulsion on a difficult-to-grind Nimonic alloy, and to one half on an easy-to-grind steel. The microemulsion investigated has been shown to have superior lubricating abilities to other water based fluids studied, being able to reduce the specific energy for grinding Nimonic at high removal rates to two-thirds of the energy required with a macroemulsion.

It has been demonstrated that it is reasonable to model the specific energy requirements of surface creep feed grinding as a series of contiguous plunge grinding operations. Plunge grinding has then been used to study the cooling abilities of fluids. These have been ranked according to the proportion of grinding energy which enters the workpiece under continuously dressed conditions.

The proportion of energy entering the workpiece has been estimated by comparing workpiece temperatures to an extant model of the grinding process. The technique revealed clear differences between oil and water based fluids, but was not sensitive enough to distinguish well between the water based fluids.

MEMORANDUM

The accompanying dissertation, entitled "Lubrication and Cooling in Creep Feed Grinding", is submitted in support of an application for the degree of Doctor of Philosophy in Engineering at the University of Bristol.

The dissertation is based on independent work by the candidate and all contributions from others have been acknowledged fully within the dissertation. The supervisor's contribution was that normally made in a British University.

None of the work described has been, or is being, submitted for any other degree or diploma to this or any other University.

I hereby declare that the above statements are true.

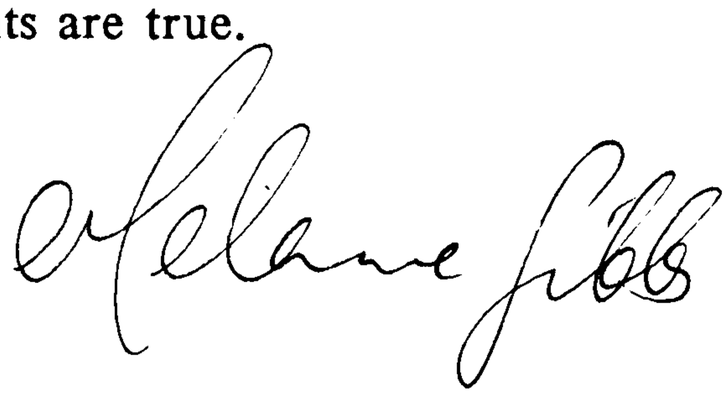

M. G. Gibbs

May, 1988

ACKNOWLEDGEMENTS

I would like to thank my supervisor, Dr. Trevor Howes, Dr. Kevin Neailey for help with the residual stress measurements, and the technicians of the Mechanical Engineering workshop, particularly Mr. Clive Calder and Mr. Ian Chalmers.

Financial support from the S.E.R.C. and Esso Petroleum is gratefully acknowledged and, in addition, I must thank Mr. John Russell for providing industrial liaison.

Finally, special thanks to David for helping me to get it together.

for my parents

LIST OF TABLES

Numbers in bold text denote the pages on which the tables and figures are referred to.

LIST OF FIGURES

NOMENCLATURE

The following terms are used in the main text of this dissertation. Additional notation in the Appendices is fully explained where it appears.

a	depth of cut (mm)
C_L	heat loss coefficient ($W/m^2/K$)
C_P	specific heat capcity (J/kg/K)
d	diameter of plunge ground pin (mm)
d_W	wheel diameter (mm)
F_N , F_T	normal and tangential force components per workpiece width (N/mm)
h	chip thickness (mm)
k	thermal conductivity (W/m/K)
N_P , N_S	normal forces owing to ploughing (P) and to sliding (S) between wear flats and the workpiece (N)
Q_W	percentage of the energy entering the workpiece (%)
Q_V	rate of decrease of Q_W with increasing surface temperature (%/K)
r	grit radius (mm)
R	ratio of depth to width of cut for individual grits
R_a	surface roughness average (μm)
S	grinding wheel structure factor
T_P, T_S	tangential forces owing to ploughing (P) and to sliding (S) between wear flats and the workpiece (N)
u	grit separation (mm)
U	specific energy (J/mm^3)
U_C	cutting energy (J/mm^3)
V_D	dresser infeed rate (μm/rev)
V_N	maximum normal workpiece infeed rate (mm/min)
V_P	workpiece plunge feed rate (mm/min)
V_S	wheel surface speed (m/s)

V_W	workpiece feed rate (table speed) (mm/min)
W_P	various wheel parameters
Z'	stock removal rate per workpiece width (mm^3/mm/sec)
α	theoretical distance between independent profiles on the grinding wheel (mm)
μ	friction coefficient
ρ	density (kg/m^3)

1. INTRODUCTION

The principal objective of the research described in this thesis was to investigate the lubricating and cooling properties of various generic types of grinding fluid in the 'creep feed' grinding process. Therefore, in this first chapter background information on different types of grinding fluids and then on the creep feed grinding process will be given. Subsequently the role and requirements for fluids under creep feed grinding conditions will be discussed and hence the need for assessing their lubricating and cooling abilities.

1.1. GRINDING FLUIDS

1.1.1. Types of grinding fluid and their compositions.

Grinding fluids can be divided into two categories: oils and water based fluids.

Oil grinding fluids may be 'straight' mineral oils or may be blended with oiliness additives and may contain 'extreme pressure' (or E.P.) additives in addition in order to improve performance at high temperatures and pressures. These 'E.P. oils' typically contain up to 10% E.P. and oiliness additives, with the balance being made up of mineral oil. Mineral oils are mixtures of three main types of hydrocarbon - paraffins, napthenes, and aromatics - and, because they are mixtures, do not have well defined boiling points. Typical viscosities are in the range 5 to 20 cStokes depending on the intended application.

The function of oiliness additives (or 'lubricity additives') is to improve the boundary lubrication properties of the fluid. Typically, fatty acid esters, fatty acids, alcohols and fatty oils are used as such additives. In general, they are only physically adsorbed onto the metal surface by virtue of their polar (i.e. electrically charged) head groups. They have oily hydrocarbon tails which aid

lubricity. However, fatty acids can react chemically with a metal surface to form metallic soaps and so aid lubrication. Oiliness additives are only effective at low loads and temperatures, so they are often used in conjunction with E.P. additives, which are effective at higher temperatures and pressures. E.P. additives aid boundary lubrication by chemically reacting preferentially with the nascent, freshly cut metal surface. It has been shown that grinding chips are very prone to redeposition on the metal surface and to forming what are known as 'loading' patches on the grinding wheel, unless the highly reactive metal surfaces can easily form bonds with other substances rather than rebonding to the parent metal [1]*. Indeed it is impossible to grind successfully in an inert atmosphere, without the presence of oxygen [2]. Oxygen reacts with the nascent metal surface, forming the metal oxide, and E.P. additives work by enabling the fast production of a surface film on the metal, usually of the metal chloride, sulphide or phosphide. Chlorine additives are useful for temperatures in the range 150 to 300°C. Metal sulphide films are less effective in reducing grinding forces than chlorides, and sulphides may cause staining of some metals although they operate to a temperature of about 700°C. Thus these two types of E.P. additive are usually used together to aid performance over a wide range of temperature and, additionally, they seem to behave synergetically.

Water based (or 'watermix') fluids are so named because they are sold as concentrates which are diluted with water before use. They are very widely used and the UK consumption of water based fluids was recently estimated as 20 000 tonnes/annum [3]. They can usefully be divided here into three categories - 'soluble oils', 'semi-synthetics' and 'synthetics' - although definitions and nomenclature vary but usually depend upon the oil content.

Soluble oils contain 50 to 80% oil in their concentrated form, whereas semi-synthetics contain between 5 and 30% oil and synthetic fluids have less than 5%

* Numbers in brackets correspond to references listed at the end of the text.

oil or none at all. The oil portion may or may not contain E.P. and oiliness additives. The typical compositions of the different types of water based fluids are summarised in Table 1. It is important to remember that these can be very complex mixtures of up to two dozen components, and several compounds with the same function may be used to complement each other as an aid to efficiency over a wider range of conditions, temperature and pH, for example. However some compounds can offer several useful properties: benzylamines, for example, although more expensive corrosion inhibitors than sodium nitrite, are also useful as biocides, emulsifiers and viscosity improvers [4].

Emulsifiers are added in order to disperse the oil content in the main water phase of the fluid. In simple terms, emulsifiers can be thought of as large linear tadpole-shaped molecules. The 'head' of the molecule has an affinity for water. This may be, as in the case of anionic emulsifiers, because it has a charge associated with it which enables it to form weak bonds with the water molecules. Alternatively, as in the case of non-ionic emulsifiers, the molecules have a similar structure to that of water so that weak 'hydrogen bonds', like those between water molecules, are formed. The 'tail' end of the molecule has an affinity for oil because it has a similar hydrocarbon structure to oils. Emulsifier molecules of this type are called 'surface active agents', or 'surfactants', because they are active at the surfaces formed between two substances (oil and water in this case). The hydrophilic (water-loving) head sits in the water phase and the hydrophobic tail sits in the oil phase. Thus surfactants affect the thermodynamics of the interface, stabilising it, so that a much larger interface can be supported in the form of droplets of oil in a continuous water phase. Without an emulsifier the surface tension between the two fluids rapidly causes them to separate into two layers, in order to minimise the interfacial area and hence the associated free energy. This is why oil and water do not normally mix. Figure 1 is a schematic two dimensional diagram of the interface between an emulsified oil droplet and water.

The emulsifiers for soluble oils are usually anionic surfactants, such as tall oil soaps, cresols, sulphated fish oil, sodium or potassium naphthenates and sodium sulphonate. Synthetic and semi-synthetic concentrates may also, or solely, contain non-ionic surfactants which are usually polyethoxylated phenols and are comparatively expensive.

Semi-synthetic fluids are often called 'microemulsions' because they contain very small oil droplets. These are thermodynamically stable because the microemulsion contains a relatively large ratio of emulsifier to oil. Microemulsions appear transparent because the .01 to .1 μm diameter oil droplets are too small to diffract light. Soluble oils have droplet diameters of about 1 μm and hence are opaque. They are known as 'macroemulsions', because of their larger oil droplet size (in comparison to microemulsions). Synthetics can be further subdivided into 'chemical emulsions', with either a finely divided low oil content or with colloidal surfactant aggregates, and into true 'chemical solutions', where all of the components are dissolved in the water.

'Coupling agents' or 'co-surfactants' are bulky molecules which fit between the charges on the surfactant molecules, screening them so that they can pack together more closely and therefore be more effective. Isopropyl alcohol and diethylene alcohol are common coupling agents.

The presence of water requires the inclusion of corrosion inhibitors in the fluid formulation and the most simple form of chemical grinding solution consists of water and rust inhibitor only. Sodium nitrite was a universally used corrosion inhibitor but can react with triethanolamine, a common major constituent of synthetic fluids, to form potentially carcinogenic nitrosamine. Organic amines, organic amides and borates are common corrosion inhibiting additives. They adsorb onto the metal surface to form a protective film to prevent corrosive substances from making contact with the metal surface.

Biocides must also be added to water based fluids to control fungal and bacterial growth. Fungi need more alkaline conditions than bacteria so usually only one of these two will predominate, depending on the conditions. Phenols are particularly effective against fungus but are ineffective against bacteria and are expensive. Other biocides work by releasing formaldehyde but lose their effectiveness with time and are ineffective at raised temperatures. This means that a dose of 'kill all' biocide must often be added to a comparatively fresh fluid in order to keep fungal and bacterial growth under control.

Whilst the foaming tendency of oils is directly related to their viscosity and temperature it is a minor problem when compared to the foaming of watermix fluids, where the surfactant stabilises the air/fluid interface. This effect necessitates the addition of antifoams. Silicones are often added as antifoams but they have a dewetting action and do not completely dissolve in the fluid. Waxy polymers are also used but, where possible, it is preferable to avoid their use because they necessarily counter the action of the emulsifier and are inclined to leave sticky deposits on the machine tool. They are often added in situ where there is a specific foaming problem but, because of the aforementioned disadvantages, some manufacturers forbid their use.

1.1.2. The advantages and disadvantages of the different types of grinding fluids.

Properties other than those directly affecting metal removal rates will be discussed in this section.

The most striking difference between oil and water based fluids is in the cost, both of the fluid itself (dilution with water brings the cost down !) and of housekeeping procedures and disposal. Whereas the recycling of straight lubricating oils is an established process, oils containing fatty and E.P. additives are very difficult to recycle [5]. Soluble oils (macroemulsions) and semi-synthetics

(microemulsions) can easily be split to produce a water component, pure enough to be disposed of down the drain, and a small amount of oil and precipitated waste. A disadvantage of some synthetics is that they cannot be disposed of in this way.

The major disadvantage of water based fluids is their susceptibility to microbial contamination which can cause expensive problems. Some water must be present for bacterial growth to take place, so unless oils become contaminated they are unlikely to suffer from this problem. Oil, some emulsifiers, and salts in the diluting water act as nutrients for bacteria [6]. This means that housekeeping procedures must be strict to avoid bacterial and fungal build-up, despite the inclusion of biocides in fluid formulations. Apart from the health and safety aspects described in Section 1.2.5, bacterial action can cause corrosion due to the foaming of acid by-products, which leads to fluid spillages and emulsion breakdown.

In addition to providing food for bacteria, hard water soon consumes the emulsifier and causes scummy deposits. However, very soft water will tend to foam. Therefore it is necessary to control the water hardness, especially where there is excessive evaporation and topping up. A hardness of 50 ppm is optimum [7]. Control of neat oils is simpler and their stability is only affected by tramp oil which becomes inseparable. Contamination by tramp oil should also be avoided with water based fluids because this upsets the chemical balance and can destroy the effectiveness of the emulsifier.

It has been shown that the rust preventatives and surfactants in watermix fluids cause increased tool wear [8]. Fluids containing water are also known to increase the rate of wheel wear by reacting chemically with the bond [9] and matrix [10] materials to reduce their fracture strength, whilst oil does not do this [11].

An uncontaminated watermix fluid is much more acceptable on health and safety grounds than oil, because of the reduction of oil misting and fuming and

the absence of a fire hazard. More seriously, mineral oil was identified as a carcinogen as long ago as the last century and was known to cause scrotal cancer in particular. Spillages of watermix fluids are less difficult to deal with and cleaning is easier.

Chemical fluids (synthetics) in particular are claimed to have advantages in terms of cleanliness of operation, although all watermix fluids may leave sticky deposits on machine tool components. Watermix fluids also leave much cleaner and easier to handle components than oil, although the claim that the transparent fluids enable better visibility is not valid for creep feed grinding where there is excessive turbulence.

1.2. RATIONALE FOR THE WORK

1.2.1. Creep feed grinding and its advantages.

Creep feed grinding is now a well established high stock removal process, where a large depth of cut, typically of between 1 and 10mm, is taken at a low relative speed between the grinding wheel and the work. Table speeds in the range 50 to 500 mm/min are common and the stock is usually removed in one pass, although sometimes a shallow finishing pass is used for better surface quality and dimensional consistency. Figure 2 shows the essential features of the process. The wheel may be dressed with a single point diamond, or with a diamond or crusher roller. The geometry of the process allows for in-process, as well as between-process, dressing with a roller and this is particularly advantageous in the form grinding of difficult to machine materials.

Creep feed grinding has been compared to climb milling as a high stock removal, one pass process [12]; however it has two major advantages over milling. The first of these is that creep feed grinding can tackle much harder to machine materials than milling; indeed it is often used to grind prehardened materials

rather than the time consuming process of 'roughing-out', heat treating and then finish machining. It has traditionally been used in the aerospace industry, where high-temperature, exotic materials such as nickel alloys, cobalt steels and titanium are commonly machined. The other major advantage is the comparative ease with which the form of a component can be changed in grinding, simply by redressing the wheel to a new shape, whereas milling requires costly retooling to achieve this.

Direct comparisons can also be drawn with conventional grinding. In conventional, reciprocating, surface grinding the workpiece and table must reverse direction at the end of each stroke and this time spent 'grinding air' makes the process inefficient in comparison to creep feed grinding, especially for short workpieces.

The large depth of cut used in creep feed grinding - typically two or three orders of magnitude greater than in conventional grinding - means that there is a much larger area of contact between the wheel and the work. Thus the force per grit in the grinding zone is lower than in shallow cut grinding. It has been argued that this means that lower temperatures are generated and that the integrity of the ground surface is therefore improved [13]. Others have suggested that the longer arc of cut and hence longer contact time allows more effective cooling to take place [14]. A consequence of the lower forces is that softer and more porous wheels can be used. This provides more chip clearance for the long chips and better fluid delivery through the increased arc of contact.

The long interface, whilst increasing the difficulties of delivering an adequate supply of grinding fluid to the cutting zone, does have the advantage of suppressing and stabilising vibration [15] which it is particularly important to eliminate when grinding components such as cams. The immunity to vibration also enables the use of wheels made from ultra-hard abrasives, such as cubic boron nitride, which are keener and therefore, although more expensive than aluminium

oxide wheels, are sometimes more economic to use because they require less in-process dressing and wheel changing. Creep feed grinding also gives better form holding, therefore requiring less in-process dressing, than conventional surface grinding. This is partly owing to more gentle impacts with the edge of the work at the start of each cut because of the lower grit forces and slower table speeds, and also because there is only one impact per cycle. Trmal [16] has shown that this is not the only factor however, so that cylindrical creep feed grinding also shows benefits in this respect over shallowcut cylindrical grinding.

1.2.2. The importance and widespread use of creep feed grinding.

At first the use of creep feed grinding was restricted to difficult to machine materials, as described previously. However it now sees much more widespread use, even to the grinding of glass fibre and wood [17], although the predominant use is for operations where there is a large quantity of stock to be removed, or where high profile accuracy is required. Thus creep feed grinding is used in the auto-industry to produce such items as rocker arms, steering racks, cam shafts, con-rods and end caps. It is also used to manufacture tools like drills, thread cutting dies, broaches and punches. It is even used to re-grind aero parts after they have been built up again by welding [18]. In the rotary mode creep feed grinding is used to machine recirculating ball races [19] and for precision joints and couplings in pipes [20,21]. However the major impetus to develop the creep feed grinding process has come from the aero industry where quality and reliability are so essential. It is claimed to have been first discovered as a technique about thirty years ago in Germany [22] and rose to importance in this country in the late 60s when Rolls Royce successfully used it to machine turbine blades, with huge savings in process time. By the end of the 70s a technique called 'continuous dressing' was implemented with further savings. The next development was multi-wheeled grinding 'centres' which could grind the root, shroud and seals of a turbine blade in a sequence of three

operations, where previously this had taken place on seven separate machines. This development meant that the whole process now needed to be automated, as manual loading of parts, dressing, wheel changing and gauging could not keep pace with it. The manufacture of nozzle guide vanes and titanium compressor blades is also being automated in the same way. Machine tool manufacturers are now developing fully automated creep feed grinding machines which can be integrated into complete manufacturing systems. Novel features, such as vertical spindles for ease of automated wheel changing and narrow radiused wheels driven by CNC to generate profiles [23] have recently been introduced. Flexibility, in terms of ease of altering component geometry, is also being designed-in. All of these developments mean that creep feed grinding is finding more and more widespread use, and not only in large batch production. However, this rapidly changing technology is still dependent on fluids, the action of which is not adequately understood and the correct application of which is vital to the success of the machining operation [12].

1.2.3. The role of grinding fluids.

The two primary and interdependent reasons that grinding fluids are used are cost reduction and quality maintenance. The fluid has been shown to play a critical role in determining the economics of the machining process [11] by its influence both on direct and indirect costs. It influences the cost of a grinding operation by its effect on the following:

1) **Wheel life.** - usually described in terms of the 'grinding ratio', which is the ratio of the ground volume to the wheel volume consumed. In addition to the cost of the wheel itself, in a non-automated process the downtime during wheel dressing and changes, which has been shown to be 19% of the total grinding time in some industries [24], adds to the operational costs.

2) **Stock removal rate.** The fluid has a profound effect on the rate at which stock can be removed, which is limited by the desired workpiece quality. In creep feed grinding the ultimate limitation to the stock removal rate is the occurrence of workpiece 'burn' [25] which is described below.

3) **Fluid cost.** This is usually small compared to the total manufacturing costs, but varies by about an order of magnitude between different water based fluids. Where neat oil fluids are used the cost can be significant. The indirect costs of fluid housekeeping, disposal and the frequency of cleaning procedures for the fluid and environment must also be considered. Expensive air extraction systems are more likely to be needed when neat oils are used.

Achievable quality and stock removal rate are interdependent, tending to act in opposition to each other. Thus, an optimum balance should be established, depending on the the quality requirements for the product. Aspects of the quality, affected by the fluid, which should be considered are:

1) **Surface finish.** The overall 'smoothness' of the surface generated depends upon the lubricating ability of the fluid, but ineffective washing away of swarf and inappropriate cooling (i.e. quenching) can lead to macroscopic scratches and cracks respectively [26]. The fluid lubricity also influences the redeposition of 'loading' patches from the wheel onto the workpiece [1]. Workpiece burn causes surface oxidation and irregularities due to cyclic temperature changes. Chemical reactions with the fluid can cause workpiece staining.

2) **Workpiece size.** Heating up of the workpiece during grinding may produce a finished product which is out of tolerance and hence scrapped.

3) **Workpiece distortion.** Residual stresses are mainly thermally induced [27]. They may result in distortion of the workpiece if later relieved and are particularly undesirable in high temperature applications.

All of these factors (except for the cleaning away of swarf) are dependent on what can loosely be categorised as the lubricating and cooling properties of the fluid. Briefly, lubrication of the wheel/work interface reduces the forces developed during grinding, reducing the power developed. This means that there is less heat energy to be dissipated to the workpiece. Cooling, on the other hand, removes the heat generated by the grinding forces. Thus, both the lubricating and the cooling properties of the fluid affect the temperature of the workpiece and, hence, the occurrence of workpiece 'burn'. Burn is said to have occurred when the material ground undergoes a metallurgical change. For steels this is understood to be when the austenitising temperature is reached [28] and is accompanied by a visible oxidation of the surface. (Thermal softening can occur at lower temperatures, and is also deleterious [29].)

The lubricating and cooling processes will be described in more detail in Chapter 2.

1.2.4. The importance of grinding fluids in creep feed grinding.

The role of grinding fluids in general has been described; however, as was explained in Section 1.2.1, creep feed grinding is a comparatively arduous operation and, as such, puts heavy demands on the fluid. Indeed, as stated before, correct fluid application is vital for successful creep feed grinding [12]. The

exception to this is where very easy to grind non-metals, developing low forces, are ground - glass fibre composites, for example [17].

Whilst Section 1.2.2 described the widespread use of creep feed grinding, surprisingly very little work has been done to develop fluids specifically for creep feed grinding or for rationalised use in automated systems, which often run virtually unmanned and continuously. This further complicates the requirements on a fluid which must already satisfy the arduous demands of creep feed grinding, for which the fluids currently available are by no means ideal [30].

Owing to the large depths of cut employed in creep feed grinding, a large proportion of the wheel circumference is grinding at any one time, with a corresponding increase in the production of heat, if all other parameters remain constant. In conjunction with this it is difficult to deliver an adequate supply of fluid along the long contact arc; the fluid has been shown to cool less well at the end of the arc, causing premature burning of the workpiece [31]. This means that a fluid with good wetting properties, or one which can overcome these geometrical constraints, is needed. Not only is more heat generated, but the heat source is slow moving, causing a build up of heat in the grinding zone [32].

1.2.5. The initial assessment of fluid acceptability.

There are numerous pass/fail criteria against which a fluid is measured, both by the supplier and the user, before it can even be considered in terms of its machining ability. Some of the tests carried out by the manufacturer when a new fluid is developed are described in Appendix 1. However, whilst these tests are performed under laboratory conditions, poor housekeeping procedures can radically alter the properties of a grinding fluid in factory use.

The most important criterion is user acceptability, which will depend upon smell, colour and perceived health risks. The most important health

considerations are skin irritation, misting (which is caused by a fine suspension of fluid particles in the air and can enter the lungs), and bacteria, which may produce an unpleasant smell and can enter the body through cuts and inhalation of contaminated mist [33].

Compatibility with machine tool elements is the next criterion. The fluid must not cause erosion of bare metal, staining, paint stripping or leave sticky deposits which dry hard and are then difficult to remove or which can gum up a machine. A fluid which foams excessively will spill over the top of the tank onto the floor, and can cause expensive problems when filtration is used for swarf removal. Foaming is a particular problem in creep feed grinding because of the high fluid pressures used, especially if a high pressure jet is used to remove loose grits when continuous dressing is employed. At least one major user screens all new fluids for foaming before they are allowed onto the shop floor [30]. Factors such as disposability of waste fluid and the rationalisation of the cutting and lubricating fluids used must also be considered. Maintaining the correct dilution of water based fluids is particularly important as the additives will only work in a narrow range of concentrations. In spite of this, fluids are often mistreated and expected to perform at elevated bulk temperatures, low concentrations, and poorly cleaned, which encourages bacteria. This, in conjunction with incorrect dilution procedures, means that fluids need to be very tolerant of their operating conditions and is why biostable fluids, and those which do not emulsify tramp oil, are being widely developed.

So it can be seen that, whilst the role of grinding fluids depends upon the terms loosely classified as lubrication and cooling, there are other properties which must be taken into consideration.

1.2.6. The selection of a grinding fluid based on performance in use.

On the shop floor, once the basic acceptability criteria have been satisfied, fluids tend to be selected by trial and error. Assessment of performance in use is then based on stock removal rates, surface finish, workpiece damage in terms of burning and cracking and the scrap rate - in other words, on the influence the fluid exerts over cost reduction and quality maintenance. These assessments will usually be qualitative and subjective and, as with the criteria not directly related to performance, can be significantly affected by housekeeping procedures. In practice a user will usually go to tender to decide from which manufacturer to buy. Then the fluid for a new line will commonly undergo field trials and be altered several times until the best fluid for the operating conditions is found.

Under conventional grinding conditions using alumina wheels, several researchers have shown that oil, which is associated with superior lubricating ability, performs better than water based fluids (e.g. [11,34,35,36,37]). This means that, for the more severe types of conventional grinding, oil has generally been preferred unless conditions allow the use of the technologically inferior, but cheaper and environmentally preferable, watermix fluids. However, under creep feed grinding, the cooling effect of the fluid has been shown to be significant [25] and this means that the choice of fluid is less straightforward.

Whilst lubricating ability has been associated with oil, and cooling associated with water based fluids, it should be noted that these two properties are not necessarily mutually exclusive as is commonly implied. The inverse solubility with temperature of non-ionic surfactants, and the finely dispersed oil phase and good wetting ability of semi-synthetics may mean that the manufacturers claims [38], that some water based fluids can be substituted for oils, are valid.

It has been stated that, for a particular operation with a particular material, there will be an optimum balance between workpiece quality and the achievable stock removal rates, and that the lubricating and cooling properties of fluids can affect these parameters and therefore the balance between them. Hence there will be an optimum choice of fluid, however the best fluid for a specific application may not be the one providing the most lubrication and the most cooling. For example, it may not necessarily be advantageous to have the best cooling action: some aerospace alloys are designed to work at very high temperatures but are damaged by quenching, and similarly, thermal shocking can crack thin coatings on materials [39]. Thus to identify the best fluid for a particular operation, the lubricating and cooling abilities of fluids need to be ranked separately. However, as will be explained in Chapter 2, the effects of these two properties are normally interdependent.

1.2.7. Summary of rationale for the work.

It has been demonstrated that creep feed grinding is an important and widely used process which is still undergoing new developments and finding new uses. It is normally essential to use a grinding fluid when creep feed grinding. The correct selection and application of grinding fluids is vital for a successful operation and they play an important role in determining the economics of the process. However, the action of the fluids is not fully understood and in consequence their selection and development is something of a 'black art' - so much so that fluids currently available are by no means ideal.

Whilst other properties of the fluid are important and may preclude its use, a grinding fluid has its major effect on the process by its cooling and lubricating action. Measurement of these two properties presents problems because under normal grinding conditions their effects are interdependent.

Different operations with different workpiece materials and geometries and different quality requirements will make different demands on the fluid in terms of the lubrication and cooling needed. They may therefore be best served by different fluids. Good cooling and good lubricating ability are not necessarily as mutually exclusive as they are in the two extremes of oil and water.

Independent measurement of the lubricating and cooling ability of fluids would be useful as a means of selecting the best fluid for a particular operation, and also as a tool for understanding how the constituents of a fluid act, so that more appropriate fluids can be developed. Hence the aim of this work is to investigate the independent measurement of these two properties.

2. THEORY

2.1. MECHANICS OF CREEP FEED GRINDING

Many have tried to simulate the action of a single abrasive grit in order to understand the cutting action of grinding wheels. The grinding wheel has been modelled as as array of single point cutting tools with negative rake angles (e.g. [40]) or as an array of rods of varying heights [41]. Whilst a wide range of mean rake angles have been calculated for grinding wheels [42,43], Rowe and Whetton suggest that they are probably always negative [44]. Rubenstein et al. [45] used high speed steel tools of varying rake angles to study the mechanism of metal removal. They concluded that the process was no different from other metalcutting operations, except that small depths of cut are used and the rake angles tend to be large and negative.

Kannapan and Malkin [46] have suggested a model of the grit cutting action, where three types of grit/workpiece interaction are considered. The energies associated with each of these are then summed to find the total grinding energy. These three mechanisms and the forces associated with them are illustrated in Figure 3. The 'sliding energy' is the term they used to describe the energy associated with the movement of the grit over the metal surface causing elastic deformation and removal of material only by attrition. The forces acting on such a grit are shown in Figure 3a. The grit does not penetrate the metal but the load between the wear flats and work, N_s, generates a frictional force, T_s, parallel to the direction of the grit motion, i.e. contributing to the measured tangential force. The tangential and normal forces generated by sliding are linked by the expression

$$T_s = \mu \times N_s$$

where μ is the friction coefficient for the particular wheel/work/fluid combination.

If the pressure between the work and grit is high enough the grit will penetrate the metal surface, generating a groove and throwing plastically deformed material sideways. This is an inefficient means of metal removal, called 'ploughing'. Figure 3b shows the force on the grit due to ploughing. The major movement of material is sideways, generating a load on the inclined grit side faces. As the grit moves through the material the unbalanced vertical portion of this resolved force, N_p, generates a tangential frictional force, T_p, opposing the motion of the grit. The magnitude of the frictional force depends upon the angle which the grit side faces make to the normal, and

$$T_p = \mu / \sin \theta \times N_p$$

so that the ratio of the tangential to normal forces is larger when ploughing takes place than when rubbing takes place.

The third part of the total energy is the 'chip formation energy'. Chip formation is the most efficient and therefore most desirable means of metal removal. It results from the shearing of metal ahead of the grit, represented schematically in Figure 3c, and occurs at a critical value of chip thickness. Besides the energy attributable to shearing metal, the chip formation energy includes a term, due to the friction between the grit rake face and the newly formed chip, called 'rake face friction'.

The 'cutting energy' is the term used for the sum of the chip formation and ploughing energies. Hence the total energy, according to Kannapan and Malkin, consists of the cutting energy and the sliding, or 'rubbing', energy. Malkin, working together with various other researchers (e.g. [28,35,47,48]), has studied the grinding process and proposed not only that the total grinding energy consists of these three parts but also that different proportions of the three energies

enter the workpiece as heat. This description of the energies in grinding will henceforth be referred to as "Malkin's model".

'Down-grinding', where the wheel and work move in the same direction at their interface (as shown in Figure 2), was used for the surface grinding operations described in this work. In down-grinding the grit first meets the workpiece at the top of the arc of cut, where the local normal infeed rate is at a maximum and, hence, where the grit depth of cut is highest. This geometry is conducive to chip formation. However, as the grit travels through the arc the local infeed rate of the material decreases to zero at the bottom of the arc. Thus towards the bottom of the arc of cut the grit will be more likely to plough and then to rub the surface. For a given grit geometry the likelihood of ploughing depends upon the grit depth of cut. There is a transition from ploughing to cutting at a critical geometry, which is a function of the rake angle of the grit and the depth of penetration of the grit.

The cutting geometry can alter the relative proportions of forces. For example, in up-grinding, where the grit depth of cut progressively increases as the grit move through the arc of cut, low initial forces discourage penetration and cutting of the metal and cause proportionally more rubbing and ploughing to occur than in down-grinding [49].

Whilst Rubenstein et al. [45] suggested that the metal removal process in grinding was similar to other types of metalcutting, conventional grinding grits are comparatively narrow cutting tools and hence have a tendency to displace metal sideways, causing ploughing and a departure from plane strain. However the wheels used for creep feed grinding are, in general, much coarser; the grits are larger, whilst the grit depths of cut are smaller than in conventional grinding. These together mean that the ratio of the width to the depth of cut, for individual grits, is larger than in conventional grinding, resulting in a less significant departure from plane strain in

creep feed grinding and less likelihood of ploughing. Thus, although the smaller grit depths of cut might be expected to produce more ploughing in creep feed grinding than in conventional grinding, the grit geometry means that ploughing may in fact be less likely.

2.2. THE EFFECT OF A FLUID ON THE MECHANICS OF GRINDING

The transitions between rubbing, ploughing, and cutting, and hence their relative proportions, will depend upon the cutting geometry, workpiece material properties, and the type of lubrication present.

For a given grit depth of cut, Rubenstein et al. have suggested that the critical rake angle for the transition from ploughing to cutting depends upon the ductility of the metal. A lubricant may alter the metal ductility by altering the local workpiece temperature.

More ductile materials are more inclined to adhere to the rake face, increasing rake face friction. A good lubricant may be able to reduce this rake face friction, reducing the critical rake angle and hence increasing the proportion of cutting to ploughing for a given wheel geometry.

For a given wheel speed, table feed, and workpiece depth of cut, the grit depth of cut will depend upon the relative amount of elastic deformation, both of the individual grit and of the whole system. This will be a function of the forces in the grinding zone and of the workpiece hardness. The grinding fluid can alter the cutting forces by its effect on interfacial friction and may alter workpiece hardness, both by affecting the temperature and by forming a low shear strength surface layer.

The grinding fluid has been shown to alter the rate at which the wheel wears, hence by altering the grit geometry it has an effect on the mechanics of grinding. This will be discussed more fully in the next section.

2.3. METHODS OF MEASURING THE LUBRICITY OF FLUIDS

2.3.1. Standardised tests.

Standard lubrication test methods exist: for example the Institute of Petroleum tests numbered IP241, IP240 and IP239, commonly known as the 'Falex', 'Timken', and 'Four Ball' test methods respectively. Details of novel test machines abound in the literature and this is evidence of the specificity of a measurement to a particular test method. Such tests simply compare relative performance under those particular test conditions; or, as Gonin et al. [50] expressed it, it is the combination of lubricant and machine that is tested. Indeed the Institute of Petroleum has called for care in interpreting the results of such tests because it states that the contact conditions are rarely reproduced in practice [51].

Metalcutting provides a different environment to that encountered in the above tests. These provide predominantly hydrodynamic or elasto-hydrodynamic lubricating conditions such as the sliding/rolling conditions encountered in the Four Ball test. However, metalcutting takes place under predominantly boundary lubrication conditions. Besides imposing the elevated temperatures and pressures commonly encountered at lubricated interfaces, metalcutting conditions in general also expose highly reactive nascent metal surfaces, requiring other properties of a successful lubricant. Carbon tetrachloride, for example, is only a good lubricant where new surfaces are formed; Shaw [52] has shown that it gives relatively high values of friction in sliding experiments but very low values of tool face friction in cutting experiments. Horne et al. [53] pointed out that the lubricant will require a finite time to penetrate the grinding interface, and that this time will depend on the exact cutting geometry. Duwell et al. [54] calculated that the rate of formation of the chemisorbed lubricant monolayer on the nascent metal surface was of approximately the same order as the rate at which the nascent surface was exposed under conventional grinding; therefore local pressures and diffusion rates could affect the

success of the lubricating operation. In addition, creep feed grinding in particular is associated with different temperature distributions and cutting geometries from other types of metalcutting. Thus creep feed grinding provides a specific lubrication environment which, for the above reasons, can only be reproduced by carrying out *actual* creep feed grinding tests and not by other measurements or by analogy to other types of metalcutting.

2.3.2. Grinding tests to measure lubrication.

The Department of Industry has evaluated metalcutting fluids recently [55]. They designed a test rig to investigate various practical aspects of the use of fluids, such as compatibility with machine tool elements, foaming resistance, stability, storage and swarf retention. However, their only assessment of performance was to measure lubricity using the Falex method.

Various criteria have been used to assess the lubricating action of metal working fluids. Bizeul [56], for example, measured the specific cutting energy during turning, milling, tapping, and drilling operations. He quantified the lubricating abilities of a selection of oils and soluble oils by interpolating from his results to find the energy owing to friction. Tool wear has also been used as a measure of lubricating ability (e.g. [57]). In grinding, wheel life and G-ratio are similarly used as measures of lubricating ability; Osman and Malkin [35], for example, used these criteria together with surface finish and the energy flux at burn. Lindsay [58] used the chatter limited volume of material removed as an overall measure of fluid performance and cost. Likewise, Peters and Aerens [34] used chatter limited ground volume, cost, surface finish, G-ratio, and metal removal rate as measures of overall performance.

Torrance [59] studied the effect of different grinding fluids on stainless steel under conventionally ground and dressed conditions at small depths of

cut. He mixed E.P. additives with two medicinal grades of oil of different viscosities in order to find their optimum concentration (in terms of the reduction in grinding forces and workpiece surface finish). He then formulated a microemulsion containing the better (more viscous) of these two oils and the E.P. additives. He varied the proportions of oil, surfactant, and water to find the region in which the microemulsion was stable. He compared the performance of microemulsions containing 5 and 19% oil fractions to the neat viscous oil with E.P. additives. Torrance found that there was little difference in the measured grinding forces between the three fluids, although the neat oil gave a slightly better surface finish.

This is interesting because it suggests that, under conventional grinding conditions, 5% of oil in the grinding fluid may confer the lubricating properties associated with neat oils. Torrance did not investigate lower oil concentrations than this with the optimum formulation, so it may be that less than 5% oil would have been sufficient.

However, from a commercial point of view this testing is not as exciting as it may appear, because microemulsions of this type (used undiluted) would be extremely expensive. The complexity of grinding fluid compositions and the balance between constituents was described in detail in Chapter 1. A typical commercially available microemulsion contains about 20 carefully balanced constituents and is more expensive to produce in its concentrated state than neat oils [7]. Dilution to about 2% with water reduces the cost of such systems to an acceptable level. In addition, the stability of the microemulsion formulated by Torrance is highly temperature dependent. Investigations carried out in the early stages of this work showed that a temperature rise of 12 K above ambient required 20% more emulsifier to be added to Torrance's microemulsion formulation for it to remain stable. This is a characteristic of such highly concentrated microemulsions.

In the early 1980s Ye and Pearce [60] compared oil and water based fluids in creep feed form grinding operations. They based their assessments on: the energy required to remove material; workpiece burn; surface finish; and profile wear. Their work showed that, immediately after the wheel was dressed, oil appeared to require less energy than water to remove unit volume of stock. However, this value, and the associated grinding forces rose rapidly as the removal of material progressively blunted the wheel when oil was used. Thus they concluded that water based fluids were preferable, in terms of energy requirements and of the likelihood of burn, when creep feed grinding Nimonic alloys.

Under conventional creep feed grinding, where the wheel is dressed prior to grinding, the forces at the wheel work interface increase as grinding progresses. Malkin and Cook [47] have shown that grinding forces increase linearly with the size of flat areas on active grinding grits at the wheel surface, and explained that this is due to rubbing between the flat areas and the workpiece. The rubbing forces cause attrition of the active grains, increasing the size of the wear flats and thus increasing the forces and attritious friction. This vicious circle continues until the grinding forces are large enough to cause the wheel grain or bond material to fracture and fall away, revealing new unworn grits beneath. This is the main cause of wheel wear [61]. Osman and Malkin [35] demonstrated that grinding fluids alter the rate at which the wear flat areas grow when these fluids lubricate at the grit/work interface, as described above. (To a lesser extent they also affect the wheel condition by chemically reacting with the wheel bond and grit material, changing their strength [9,10] and by their cooling effect influencing thermal stresses in the grits [62] and altering the rate at which the wheel blunts [16].) Thus the superior lubricating action of oil reduces the rate of wheel resharpening and causes the more rapid rise in forces, seen by Ye and Pearce, with volume of material removed. Similarly Yuen [63] investigated the build up of wear debris on grinding wheel grits (analogous to the built up edge on single point tools) and showed that the grinding

forces are directly proportional to the area of 'loading'; the term used for the wear debris. Sudholz et al. [64] have shown that the area of loading also depends on the grinding fluid.

Salmon [65] investigated a technique called 'continuous dressing', where the wheel is dressed at a given rate throughout the grinding operation rather than only prior to it. His results showed that in-process dressing can dramatically reduce the energy required to remove unit volume of Nimonic alloy. He also showed how the energy varied with increasing dresser infeed rate until a steady value was reached. This provides a possible means for comparing the lubricating abilities of fluids under the same geometrical conditions. By continuously dressing the wheel at a sufficiently high feed rate, dressing (and not the grinding forces) might be in control of the wheel condition and hence the process. This would enable the metal removal energy, surface finish, forces and other lubricity indicators to be compared. However, it would first be necessary to establish whether the dressing operation was indeed in control of the process.

2.3.3. Defining lubricity.

Having rejected other methods of measuring lubricity on standard test machines, in favour of performing creep feed grinding tests under specific controlled conditions, it is necessary to define the quality called 'lubricity'. On the shop floor the parameter most commonly observed is the power drawn by the operation; stock removal rates must be selected such that the machine is capable of delivering the power required. Therefore it is useful to define lubricity in terms of the energy required for the process. The 'specific energy' is a term used for the energy required to remove unit volume of stock and will be used as a measure of lubricity as defined in this work. Component quality is another important shopfloor consideration and, as explained in Section 1.2.3, surface finish is a major quality parameter. Hence it

would be useful to investigate the roughness of the surface generated as a measure of the lubricity of the fluid used.

Similarly, residual stresses, which affect quality by causing workpiece distortion, will be investigated. (Residual stresses are caused by the build up of stress, due to cold lower layers restricting expansion until the yield stress is exceeded and plastic flow occurs towards a free surface. On cooling the residual surface stress is then tensile. Residual stress has come under particular scrutiny in creep feed grinding because of its use on materials which have high temperature applications. Residual stresses in the material can relax at such high temperatures causing workpiece damage.)

2.4. METHODS OF MEASURING FLUID COOLING ABILITY.

2.4.1. Simulated grinding tests.

Various researchers have tried to assess the cooling ability of fluids in simulated machining operations. Ueno et al. [66] have compared the cooling abilities of cutting fluids by playing them on electrically heated simulated turning workpieces. They concluded that the cooling abilities can be considered as diminished functions of the difference in the heat transfer coefficients. Similarly Lee et al. [67] assessed the convective heat transfer coefficient of a fluid as a measure of its cooling ability. The workpiece was insulated at the sides and heated from beneath, whilst the surface which would normally be ground was cooled by the fluid. The wheel was brought in close to the workpiece without actually grinding.

Powell [31] wanted to compare the efficiency of different fluid application systems. Using a similar approach to Lee et al., he employed an electrically heated element, simulating a partially ground creep feed grinding specimen, and used the wheel to scrub the fluid past the workpiece without actually grinding. The current through the workpiece was gradually increased until the

element fused, indicating that the cooling mechanism had broken down. The heat flux at this limit (the 'critical heat flux' or 'burn-out heat flux'), which was believed to correspond to the onset of workpiece burn in grinding, was used to compare the different application systems. This method could be used to compare the burn-out heat flux values for different grinding fluids. Clewlow and Lewis [68] set out to find the properties of grinding fluids which affect the value of this critical heat flux. They compared fluids by quenching preheated mock grinding specimens and recording their temperatures during cooling. From the transient response they calculated the critical heat flux under simulated grinding conditions similar to those in references [31] and [67].

The disadvantage of simulated grinding conditions is that, in practice, the temperature distribution of a ground specimen is more complicated than the uniform heating provided in the references above. Malkin [69] suggests that the overall temperature distribution can be thought of as three types of temperature distribution superimposed. One type can be associated with each grit where a very localised high temperature field exists, due to shearing forces and deformation in the material. These high temperature fields are fast moving and short lived as each grit passes through the grinding zone. However their combined effect is to produce a high temperature 'interference zone' which Malkin calculates as extending typically 4 μm into the workpiece. The third type is the comparatively low bulk workpiece temperature distribution (analysed by Lee et al. [67]).

Mercier et al. [48] have shown, theoretically, that the convective heat transfer in metalcutting depends upon the size of the heat sources. Also, Kannapan and Malkin [46] have shown empirically that the critical heat flux (i.e. the heat flux at which the heat transfer mechanism breaks down) depends upon the source size. This cannot be accommodated in simulated grinding experiments. In addition Ueno et al. [66] note that the wetting ability of the fluid affects the removal of heat but

that this may only be apparent when the fluid path is complex. This may not be well reproduced in simulated grinding experiments where there is a clearance between wheel and work, even if some scrubbing action has been attempted. These factors therefore favour performing actual grinding operations in order to assess cooling ability.

2.4.2. Grinding tests to measure cooling

The work by Powell, previously described, to measure the heat flux at which burn-out occurs was based on a model of heat transfer first studied in boiler tubes. Figure 4 shows how the heat flux, by forced convection from a heated boiler tube surface, varies with the surface temperature. Initially the heat transfer from the tube wall is due to convection and takes place at a low rate. Once 100°C is reached however, nucleate boiling occurs and fluid movement, caused by rising vapour bubbles, improves the heat transfer rate until, if the value of heat flux is high, the vapour bubbles form a continuous vapour blanket. This 'film boiling' phenomenon has the effect of insulating the boiler tube wall and hence causes 'burn-out', so called because no significant heat transfer can occur until the wall is hot enough to radiate heat energy. At lower values of heat flux from the wall, the transition to a catastrophic break down in the heat transfer mechanism is slower and occurs with complete evaporation of the fluid, called 'dry-out', rather than vapour blanketing of the wall surface. This is reached via stages as the vapour content of the fluid increases, causing the liquid portion first to flow as 'slugs' and later only along the tube surface (annular flow).

Although the velocity of the fluid in boiler tubes has been shown to have little effect on the burn-out temperature, in grinding there is also a scrubbing effect of the grit past the workpiece, and in addition the cooling environment has already be discussed as being specific to the particular grinding operation. However Shafto found that, when Nimonic workpieces were creep feed ground using a water

based fluid, burn-out of the workpiece always occurred at approximately the same value of grinding power flux (32-36 W/mm^2). This suggested that a similar heat transfer mechanism to that in boiler tubes was occurring, such that a limiting grinding power flux and corresponding critical workpiece surface temperature existed at which 'burn-out' (or perhaps 'dry-out') occurred.

Assuming an adequate supply of fluid, the burn-out heat flux might be expected to depend upon the fluid type, workpiece material and also on the fluid pressure. Salmon showed experimentally that the limiting power flux could also be dependent upon coolant temperature, depth of cut, arc length, wheel grade and cutting geometry. Hence the critical power flux, being dependent on grinding geometry, would be expected to vary under different grinding conditions and therefore not necessarily be a good indicator of the cooling ability of the fluid. As an illustration of this, whilst the maximum burn-out heat flux measured by Shafto was 36 $W/mm^3/mm$, in this work values as high as 46 $W/mm^3/mm$ were obtained without burn. (The burn-out heat flux is also an awkward value to measure accurately, especially under continuous dressing conditions where power flux values remain constant throughout a test, rather than slowly increasing as the wheel wears under conventionally dressed grinding.)

Salter developed a method to determine the proportion of the grinding energy which enters the workpiece as heat. Shafto had proven that, for an easy to grind material where the local grinding forces are proportional to the local normal infeed rate, the creep feed grinding process could be modelled as a series of contiguous plunge grinding operations, each at a particular feed rate. Hence thermal modelling of creep feed grinding can be based on plunge grinding, and thus simplified to a one-dimensional heat flow. The calculated temperatures can then be compared to those measured in an insulated plunge ground specimen. Almost all of the energy generated in the grinding zone appears as heat [70] and, more importantly,

virtually all of the cutting energy becomes heat energy [71]. Thus a thermal analysis of the creep feed grinding operation is representative of the complete energy distribution. Most analyses of temperatures in grinding have been based on the model by Jaeger [72] of a heat source moving rapidly over a semi-infinite plane. Des Ruisseaux and Zerkle [73], basing their analysis on this model, showed that, although the heat sources in grinding are intense and localised, originating from individual grits, these temperature fields are short lived and can be considered to produce a uniform 'interference zone' temperature field at the ground surface. The depth of this zone is of the order of 4 μm. Salter therefore assumed a uniform surface temperature and used finite difference methods to calculate the temperature distribution through a workpiece with time. His model, modified by Fursden, was used for this work.

The model is based upon a second order differential equation, relating the variation of temperature with position in the pin and with time, derived using an energy balance approach. This is then solved using a finite difference approximation technique, to give the temperature in the future at a particular position in terms of the present temperature at the same position and also at neighbouring positions. Boundary conditions are set such that there is no heat flow from the bottom face of the workpiece and such that a fixed proportion of the energy enters at the top (ground) face. The flow of heat out through the side faces due to imperfect insulation (which causes a two-dimensional temperature field in reality) is dealt with by including a loss term in the original energy balance equations. In order to simulate the reduction in length of the pin as it is ground, the nodes at which temperatures are evaluated are moved closer together at each time step in the iteration. The proportion of the available energy which must enter the workpiece is then varied by trial and error until the nearest fit with the empirical temperature profile of the insulated plunge ground specimen is obtained. Appendix 2 describes the basis of this model in more detail.

Salter's tests, predominantly under conventional dressing conditions, indicated that about 2% of the grinding energy entered the workpiece when a water based fluid was used, but that about 13% entered the workpiece when oil was used as the grinding fluid. Similarly, the critical surface temperature associated with burn-out was about 130°C and 300°C for water and oil based fluids respectively. These values were shown to be dependent on the thermal properties of the workpiece.

2.4.3. Defining cooling ability.

In the same way as the lubricating ability has been defined for the propose of this analysis, it is also necessary to define an empirical measure which will be referred to as 'cooling ability'. The workpiece temperature and proportion of grinding energy entering the workpiece as heat under continuously dressed grinding conditions will be used as definitions of cooling ability. The workpiece temperature is a useful shopfloor measure, because it gives an indication of the likelihood of metallurgical damage and workpiece out-of-tolerance due to expansion. The proportion of the energy entering the workpiece is used in an attempt to find an empirical measurement which is independent of the effects of fluid lubricity, or at least where these are minimised.

According to Malkin's model, different proportions of each of the three types of energies associated with grinding enter the workpiece as heat. Malkin and Anderson [28] suggest that for conventional grinding, with no cutting fluid, all the sliding energy enters the workpiece as heat. They suggest in addition that in dry, conventional grinding virtually all of the ploughing energy and 55% of the chip formation energy enter the workpiece.

Continuous dressing, if it is able to maintain a constant wheel condition, would control the proportions of the three types of energy and hence help to control the partitioning of energy to the workpiece; i.e. it would control the

proportion of the total energy which enters the workpiece as heat. (However, it seems possible, from the foregoing discussion of the effect of lubrication on the mechanics of grinding that different fluids will alter the proportions of the three energies despite the constant wheel geometry.)

It is preferable to try to minimise the influence of the fluid lubricity when trying to assess cooling ability. We know from Salmon's measurements of wear flat area that this (and hence the sliding energy) can be reduced to a near zero value by continuously dressing at a high enough feed rate. This will then help to curtail the influence that the lubricity of the fluid has on the energy partitioning, if Malkin's model of grinding energies is accepted. The undeformed chip thickness decreases with increasing stock removal rate. Hence at high stock removal rates there is less ploughing taking place and another influence of fluid lubricity is reduced. The lubricity of the fluid might still affect the relative proportions of the three types of energy, and hence the partitioning value. However, under suitable grinding conditions and with continuous dressing, partitioning values would still seem useful as definitions of the cooling ability for ranking the performance of fluids. The relationship between fluid lubricating and cooling abilities, and the measured specific energy and workpiece temperature, is shown schematically in Figure 5.

2.5. METHODS OF STUDYING WHEEL SURFACES.

As the basis of much of the work was that the wheel surface condition was kept constant by continuous dressing, it was necessary to have a means of assessing the wheel surface to see whether this was being achieved.

There are many different ways of studying the geometry of surfaces (see Thomas [74]). However, three main methods which have been used in the context of grinding wheels are compared below.

2.5.1. Optical methods.

Suto et al. [75] have further developed the photoelectric method of Tsuwa [76] to determine the position, size, and subsequent cutting lives of cutting edges on a wheel. Light reflected by the cutting edges is then detected by a photomultiplier, modulated and digitized so that the signal can be handled by a computer. McAdams [77] studied the surface profile by projection of the specimens in a contour projector but found that the resolution was a limiting factor and he later resorted to stylus methods [78]. Peklenik [79] used microscopic photography of the surface. A similar method to this, which was tried, is described in Section 3.3.1.

2.5.2. Stylus methods.

Stylus methods are widely used for the study of surfaces and various researchers describe their use for the replication of grinding wheel surfaces. (See, for example, references [80], [81] and [82].) These are usually used in conjunction with powerful and expensive computational apparatus, some of which is described by Thomas [74]. The practical considerations of the stylus method will be described in more detail in Section 3.3.2.

2.5.3. Temperature and contact resistance probe methods.

Bhattacharyya and Hill [80] measured the active cutting grains in a grinding wheel using a contact resistance probe, which consisted of a miniature copper wire within, and insulated from, a fine stainless steel tube. When cutting takes place at the end of the probe, the cutting edge of an abrasive grain and the partially deformed chip produce an electrical contact between the two conductors. This is used to produce a voltage pulse every time an active grain passes the probe. The number of pulses and their duration thus give dynamic information about the cutting action of the wheel. A similar temperature probe, after Peklenik [83], which relies on the high temperature and mechanical stress produced when active grains

contact the probe to make an electrical contact, was also used by them. These probe methods have the advantage of being used in-process and have the added advantage that stylus and optical methods cannot distinguish between active and non-active cutting grains (i.e. without more complicated statistical analysis they cannot identify the parts of the profile able, due to their geometrical situation, to remove metal). The probe methods gave good correlation with measurements made by stylus methods. However, since suitable apparatus was readily available for the stylus and optical methods these were investigated in the first instance.

2.5.4. The analysis of profiles generated by styli

As long ago as 1946, Posey [84] suggested that the commonly used measure of surface roughness, the arithmetic average height from the centreline, was inadequate. This is because surfaces with the same *centreline average* value could have very different geometrical properties. Other common simple numerical measures, the *peak to valley height* and the *ten point height*, similarly do not uniquely describe a surface. Posey therefore characterised profiles by the *frequency distribution of their depths*, *slopes*, and *degree of curvature*. (See Appendix 3 for a definition of these terms and those in italics.) Based on this, Myers [85] suggested that a detailed description of the wheel surface geometry could be obtained using four related characteristics; these are the *standard r.m.s. of the profile* (a similar measure to the centreline average), together with the *r.m.s. of the first and second derivatives of the surface profile*, and a measure of the directional property of the surface, which is an *average value of the slope*. Since then, other researchers have used different (although often related) parameters to characterise grinding wheel surfaces. Bhateja et al. [82] were successful in distinguishing between coarsely and finely dressed wheels using the *cumulative distribution of peaks* above a specified height level in the wheel profile as a percentage of the total number of peaks in the profile. They also employed the *bearing area characteristic* and *degree of fullness*

successfully. The *cutting edge ratio*, *mean peak land area*, and *mean distance between successive peaks* were criteria used by Bhattacharyya and Hill [80] to compare the performance of experimental probes with a conventional stylus. McAdams [78] however computed the distribution of active cutting points by regarding the wheel profile as a two state (lands and voids), second order Markov chain, and analysing when the profile crossed an ordinate delineating these two states. (Some doubt has been cast [86], however, on the validity of this theory.) Baul et al. [81] showed that there was a measureable effect on the *probability density function (p.d.f.)*, and the *cumulative density function (c.d.f.)* of different dressing conditions. Peklenik [86] has used the more complicated random process analysis to distinguish between the periodic carrier profile and the random roughness of the profile. This leads to the *autocorrelation function* from which the *power spectrum* can be obtained by Fourier transformation. Following this approach, McAdams [77] advocated the use of autocorrelation, spectrum analysis, and of the *cross correlation function* between successive planes, because a measurement is needed which equates statistically all of the possible profile configurations which could lead to chip removal.

In respect of these different approaches, it was decided in this work to characterise the profile using the p.d.f. and c.d.f. which are more complete statistical measures than some of the more simple numerical standards described, and yet are straightforward to compute. Abbott and Firestone [87] had already described the usefulness of the c.d.f. (which is of the same form as the bearing area curve). The p.d.f. of a profile, which is of the same form as the frequency distribution of profile height, is in some respects a similar measure to the cumulative distribution of peaks of Bhateja et al. Indeed Radhakrishnan [88] found that there was a striking similarity between these two criteria. Although the major defect of these two parameters is that they do not provide any information about the frequency of irregularities, nor their shape, they do not require the elaborate and expensive equipment which is needed for the more sophisticated analysis used by Peklenik and McAdams and which

was not available for this work. In fact, Baul et al. [81] found that the autocorrelation function could not distinguish very well between coarsely and finely dressed wheels and Myers [85] implied that power spectrum analysis was unwieldy compared to his methods. Radhakrishnan suggests that until a simple quantitative value for autocorrelations is developed they are difficult to use practically. He has also pointed out however that methods which do not take into account the sequence of events will not uniquely describe the profile.

3. EXPERIMENTAL

This chapter is divided into three sections. The first section describes how the tests concerned with the measurement of lubrication were carried out. The second section describes the differences from this procedure when the tests to assess cooling performance were executed. Finally, the third section describes how the wheel surface condition was measured.

3.1. TESTS TO MEASURE LUBRICATION

3.1.1. The grinding machine.

Figure 2 showed the general arrangement of the grinding machine which was designed and built in the mid-seventies. The 35kW main spindle motor was capable of 3000 rpm, although 1060 rpm was the maximum speed used in this work and this speed was maintained at the selected value by a tacho generator. The wheel speed was only varied to take account of the changing wheel diameter in maintaining a constant surface speed of 30 m/s, which value was chosen to facilitate comparisons to earlier work in the Grinding Research Group. The same motor was used to drive the slideway at a constant proportion of the wheel rotational speed via a series of belts and gearboxes. The third and final gearbox had a reverse facility for withdrawing the slideway. Together these three gearboxes provided 83 choices of speed ratio which could be further increased by changing the pulley ratios on each box. A torque controlled electromagnetic clutch engaged this gear train with a recirculating ballscrew, (chosen for its stiffness), which provided for the slideway table motion. The traverse of the slideway was about 130 mm, defined by limit switches connected to the clutch. The wheel and slideway used hydrostatic bearings for maximum stiffness and were served by the same oil and pump system.

The dresser mechanism is shown in Figure 6. The dresser was fed into the wheel on a pivoted arm mechanism, the other end of which rolled up the incline

caused by a wedge on the slideway as the latter infed. Thus the dresser infeed rate was a function of the wheelspeed and of the slideway speed but could be altered additionally by selection of different wedge angles. Dresser infeed rates of between .15 and 3 μm/revolution (of the grinding wheel) were used. Whilst the dresser moves in an arc, for small displacements this can be considered to be a linear radial movement towards the wheel centre.

The dresser had 150 grits per carat synthetic diamonds hand set in a 100mm diameter roller. This was rotated at a surface speed of 80% of that of the wheel and in the same direction at their point of contact, a speed ratio which has been shown to be optimal [89] and allowed comparisons to be made to previous work. The dresser motor of 1.5 kW with its own tacho feedback system was independent of the main drive motor.

It had proved necessary to redesign the dresser housing because the operating speed could not be reached. This was caused by corrosion owing to fluid ingress which was cured by more complex labyrinth seals, positioning of v ring seals on the moving shaft and reducing their diameter, where possible, to reduce 'lift-off' at high shaft speeds. Figure 7 shows the redesigned shaft housing.

Down-grinding (i.e. where the wheel and work move in the same direction along their contact length, as in Figure 2) was used so that comparisons to previous work could be made. Similarly, the wheel grade used throughout the work allowed comparisons to be made to the previous work of Salmon. This was a WA 60 80 FP 2V, standard, fused alumina, vitrified bond, induced porosity creep feed grinding wheel.

3.1.2. Workpiece design and materials

The workpieces used on this machine were 130 mm long x 15 mm wide and were made in a variety of heights from 25 to 50 mm to fit under the range

of wheel diameters. They were held in position on the holder block, which located exactly in a dynamometer which, in turn, was bolted to the slideway. Two workpiece materials were studied, a carbon '55' steel, EN9, which is considered to be 'easy to grind' in its unhardened state, and a 'difficult to grind' Nimonic alloy, MARM002. Further details of these materials are given in Appendix 4. They were chosen because they represent a wide range of 'grindability' in terms of specific energy requirements, and because other researchers had used them previously so that comparisons across to their findings would be possible.

3.1.3. The grinding fluid and supply system.

Whilst there are many ways of applying fluid in conventional grinding, the requirements of creep feed grinding for a copious supply of fluid means that delivery by jets directed at the nip between wheel and work is usually the preferred method in industry. However, exact positioning of the jets is know to be critical [31,90]. Through-wheel application has also be recommended for creep feed grinding [91]. This can be achieved by supplying fluid through the bore, side or radially though the periphery. However the first two methods are inefficient, since they deliver fluid out of the full wheel periphery. Powell [31] compared jet and radial through-wheel fluid delivery and concluded that whilst jet application had potentially the same performance as the through-wheel method, the latter gave a more reliable fluid supply. This method was used throughout the research work and involved the delivery of fluid through a shoe fitting snugly against the wheel so that fluid was forced through the porous wheel and into the grinding zone. The consumable shoe was made of Tufnol and was ground by the wheel so that a close fit could be achieved as the wheel diameter varied.

There were two separate fluid delivery systems, one for water based fluids and one for oil. The oil system comprised of a 'Euroflow' pump, filter, and tank holding approximately 800 l of oil which could be delivered at 5 l/sec. The

water based system had a capacity of 1000 l and the 'Darenth' pump was capable of delivering 7 litres of fluid a second. After recovery from the grinding machine the fluid passed to a storage tank containing weirs and dams and a hydrocyclone filtration system for the removal of swarf down to a particle size of 10 μm. In total, 6 fluids were tested: an oil with E.P. additives; two soluble oils one with E.P. additives and one without (described in this text as the E.P. macroemulsion and the non-E.P. macroemulsion); a semi-synthetic microemulsion with E.P. additives; an oil-less synthetic fluid; and, in addition, as a control, pure tap water containing no additives or rust inhibitors. Details of these fluids are given in Appendix 5. The oil and the E.P. macroemulsion were selected in particular because they had been used previously in the Research Group, so comparisons would be possible with previous work.

Before the programme of testing could begin it was necessary to determine the rate of flow of fluid above which no additional benefits could be gained - in other words, the minimum flow necessary to ensure that the supply of fluid was not a controlling parameter. The approximate fluid pressure necessary could be determined from previous work [19,31]. Tests were carried out at the grinding conditions which nearly lead to burn at this pressure and then repeated at 75% of the pressure to ensure that there was still enough fluid to prevent burn occurring. The higher of these two pressures was then used for all tests. A pressure of 1 bar was found to be appropriate when using oil and 0.7 bar when using water based fluids. Before each test the shoe was moved into the rotating wheel, until it was ground, so that a close fit was achieved. It was found that the gate valve in the supply line needed to be opened by approximately the same amount to achieve the required fluid pressure. Hence, although it was not measured, the flow rate of the water based fluids must also have been kept approximately constant. Some tests were run with a pre-ground specimen in place to check the fluid forces without actually grinding. These were found to give a linear baseline, although fluid leakage from the base of the shoe could cause tensile forces on the left hand dynamometer strut.

3.1.4. Instrumentation and calibration.

Figure 8 is a diagram of the layout of the instrumentation used to measure the forces generated during grinding. As previously stated, the workpiece located in a dynamometer on the machine slideway. The dynamometer consisted of three I section struts which took the load and were necked to minimise the transmission of shear forces. Each of these had two pairs of temperature compensating strain gauges, one pair on each of its flat sides. Two of the struts took the vertical loading and the third supported horizontal loads. The output from each of these was fed to a wheatstone bridge arrangement and then amplified, filtered to suppress frequencies due to wheel vibration, and output to an ultra-violet (U.V.) recorder. Recorders of this type produce an analogue trace by exposing light sensitive paper to an ultra-violet beam reflected from the mirror of a galvanometer, and hence are current measuring devices. They have the advantages of a very fast response time due to the lack of inertia in the moving parts, the possibility of several signals being traced simultaneously without interference, and of a real time output.

This system was calibrated under purely vertical and purely horizontal loads using a Nene tensile testing machine. The magnitude and direction of the applied loads corresponded to those expected under grinding conditions. Hence the vertical struts were tested in compression and the horizontal strut in tension. Vertical loading was applied at discrete points along the length of the dynamometer via a ball bearing (to avoid bending) which was located in hemispherical hollows on a dummy workpiece, as shown in Figure 9a. The output on the U.V. recorder from all three struts is plotted in Figure 9b, which shows that the relationship is linear, that there is very little cross-coupling between struts, and that purely vertical loading had been applied. The left hand of the two struts gives a reduced output because it is constrained by the horizontal strut.

The dynamometer was similarly calibrated under horizontal loading by means of a pin coupled to a socket on the moving beam of the Nene. This psuedo-universal joint was intended to ensure the transmission of a pure load in one direction, but still required good alignment between the dynamometer and Nene. This was achieved by bolting the datum face of the dynamometer to an angle plate, bolting this to the machine bed and altering the relative positions of these until the U.V. recorder output was minimised. Great care was needed for this measurement and it was carried out several times to ensure repeatability. A calibration graph under tensile vertical loading at a variety of heights above the base is shown in Figure 10.

These calibration procedures were repeated six times at regular intervals during the testing programme but the outputs never varied by more than 2%. This procedure was followed because the electronic components in the amplifier, bridge and recorder circuits were operating under adverse, dirty conditions, so they could not be relied upon to give constant outputs; also, the strain gauges themselves were submerged by fluid during every test. The strain gauges on two struts had to be replaced during the testing programme owing to fluid ingress, so the opportunity was taken to test each strut in isolation, both through the test apparatus and using a direct reading strain measuring device. The values obtained were compared to the expected values from a knowledge of the Young's modulus, cross-sectional area and load. This showed that the system was behaving as expected, that the gauges were properly installed, and that the individual struts were equally sensitive when tested out of the dynamometer housing.

The slideway speed and dresser infeed rates were calibrated using a displacement transducer and stopwatch. The wheel and dresser rotational speeds were indicated by the voltage output from a tacho generator. This was calibrated using a hand-held tachometer and, in common with the rest of the electronic equipment, was

periodically recalibrated. As the hand-held tachometer was a delicate instrument it was checked approximately for signs of damage by comparison across to other tachometers and to the set spindle speeds on a number of lathes.

3.1.5. Experimental procedure for continuously dressed tests.

With a knowledge of the wheel diameter, the optimum choice of variables was computed before each test was run. Appendix 6 lists a programme written to do this. Priority was given in the computation to two of the four variables: slideway speed, depth of cut, dresser infeed rate and maximum normal infeed rate. The optimum values of the others were then selected within the constraints of the discreet values of gear reduction and dresser wedge available. All of these variables were affected by the need to alter the wheel rotational speed to compensate for the reducing wheel diameter as it was dressed away.

In addition, during the tests at low stock removal rates but high dresser infeed rates in particular, the diminishing wheel diameter altered the maximum normal infeed rate from the expected value; an effect apparently not corrected for by previous workers. The magnitude of this correction is demonstrated in Appendix 7.

The depth of cut made in the workpiece was selected by the use of spacers between the workpiece and holder, or between the dynamometer and the slideway. When continuous dressing is used the reducing wheel diameter causes the the depth of cut to decrease during a test unless a wedge is pre-ground on the specimen. This was not deemed to be necessary, but instead the reducing wheel diameter was allowed for, and the expected depth of cut was computed for the point when a full arc of cut was just achieved. However there was some variation in the depth of cut owing to the difficulty in reproducing the starting position of the work relative to the wheel and also due to limitations on spacer thickness.

The experimental sequence was as follows. The dresser was manually wound in until nearly in contact with the wheel. Both of these were then run up to their operating speeds. The recording equipment was activated and then the fluid was set to the required pressure so that the baseline fluid forces were recorded. Engaging the clutch then started the grinding operation which was stopped by a limit switch. The workpiece was wound back from the wheel by hand at the end of the test to provide a clearance. Each part of the equipment was then stopped in the reverse order.

The time taken for each test was recorded as a rough check of the feed rate. Similarly the change in diameter of the wheel gave a rough indication that the dressing had progressed as expected. The specimen was removed from the holder and the actual depth of cut measured; this value was used in the calculations that followed. The arc length was measured and compared across to the expected value from the depth of cut in order to ensure that a full arc of cut had been achieved. Without a full arc of cut the force and power distributions are unrepresentative, because the average normal infeed rate is higher than when there is a full arc of cut. In addition the flatness of the ground surface was used as a check for wheel breakdown. Signs of workpiece damage, such as burn, were recorded and the workpiece roughness was measured as soon as possible to avoid the effects of corrosion. The specimens were then covered in a protective layer of grease before storage. A Taylor-Hobson Tallysurf with a horizontal traverse was used for all specimen surface roughness measurements and the mean surface roughness value from five separate traces was used.

3.1.6. Calculation of results.

Figure 11 is a graph of the computed forces, in excess of the static forces, in the grinding zone versus elapsed time during a typical creep feed grinding test. The force seen on the right hand strut rises as the depth of cut increases until a

maximum is reached. It then falls because the depth of cut decreases as the wheel is dressed away and also because the point of action of the resultant force moves towards the left hand strut as the test progresses. Hence the force on the left hand strut increases through the test although the metal removal rate decreases. The total vertical force shows a peak as the full arc of cut is first reached, as does the horizontal force. Thus the forces and the depth of cut can be most easily determined at the moment a full arc of cut is first achieved, so it was these values that were used in the analysis.

If only cutting takes place then the forces and power flux would be expected to vary with the local depth of cut around the grinding arc, falling linearly from a maximum at the top of the arc to zero at the bottom. The centroid of this distribution would then occur 2/3 of the way around the grinding arc. Hence the force resultant can be expected to act in this position when pure cutting takes place. Shafto [32] investigated this experimentally on easy-to-grind steels, using oil as the grinding fluid, and showed that the approximation was reasonable. However, on difficult-to-grind materials, where some rubbing may be expected to occur, the force distribution will tend towards a constant rubbing force around the arc (a rectangular force and power distribution). In this limiting case the force resultant would act half-way around the arc of cut.

This leads to two possible methods of calculating the specific energy for the grinding process: either by assuming that the resultant acts at a particular position around the arc of cut or by calculating the torque at the wheelhead. Appendix 8 details a computer programme in 'Basic' to calculate the resolved and resultant forces, specific energy, power flux and stock removal rate by these two means.

3.2. TESTS TO MEASURE COOLING

3.2.1. The grinding machine.

Like the surface grinding rig, the machine used for these tests had been designed and built in the research group. However it allowed plunge and cylindrical grinding to be carried out. Only the plunge grinding facility was used in this work. The grinder, illustrated in Figure 12, was similar in many aspects to that already described, with a 37 kW main spindle motor driving the same specification induced porosity wheel. A diamond roller dresser, a coolant shoe for fluid delivery, and the same two fluid delivery systems and storage tanks were used as before. One difference, which simplified the setting up procedure, was that the work and dresser were both driven into the wheel via ballscrews from independent servomotors. A central unit operated to control servodrivers activating these servomotors. Hydrostatic spindle and slideway bearings had been used for the sake of stiffness.

The workpiece was mounted in a mandrel, held in a hydraulically loaded tailstock. This could then be plunged into the wheel radially at a preset rate. The work feed rate and start and stop positions, as well as resting positions between different stages of the grinding test, could be programmed into the control unit. This also controlled the dresser infeed rate, which was entered as a percentage of the work feed rate. The reduction in the work feed rate due to the reducing wheel diameter during continuous dressing was then easily allowed for. A digital indication of the position of the workpiece relative to a 'home' position, and hence to the wheel, was constantly displayed, and this proved very useful when monitoring the progress of a test as well as for setting-up purposes.

3.2.2. Workpiece design and materials.

EN9 and MARM002, the materials used for the surface grinding tests, were again used. They not only show different extremes of 'grindability', in terms of

the power consumed, but also their thermal conductivities vary by a factor of about four. This variation is useful for investigating the validity of a mathematical model.

For these tests, as continuous dressing was used throughout, the rate of wheel wear (and hence, according to Malkin's model, the energy partitioning to the workpiece) would not be altered by the use of larger specimens. Therefore 20 mm diameter pins were used rather than the 10 mm pins used by Salter. This increase in workpiece diameter reduced the heat losses by reducing the surface to volume ratio, with the intended aim of achieving a more one-dimensional heat flow. The sensitivity of specific energy measurements should also have been increased. The cylindrical pins were 25 mm long, which was the longest they could conveniently be to fit in the machine.

The four pins were clamped to a split holder made of Sindanyo, an asbestos cement chosen for its insulating properties together with its ease of grinding. It was however found to be porous, so workpiece holders were sealed with varnish before use in order to lessen the risk of cooling due to moisture in the holder.

In previous work only one thermocouple had been mounted in the specimen. The workpiece surface temperature was doubly extrapolated, via a calculated surface heat input, from this one temperature reading. Uncertainty in determining the position of this thermocouple and the possibility of a poor thermal contact due to the reliance on an adhesive bond between the workpiece and thermocouple compounded these errors. Therefore, in this work three thermocouples were used in an attempt to minimise these errors.

Figure 13 is a drawing of the pin design and of the Sindanyo holder. Comprehensive trials were undertaken, where steam was played onto the end of the pin whilst the other faces were insulated by the Sindanyo holder*. These showed that

* These trials, to find the best design of apparatus, and the steam calibration described in Section 3.2.4 were carried out with P.M.T. Fursden of Bristol

the most successful design of pin was one which was split along and parallel to its axis, with a hole machined slightly off centre - so that it just skimmed one of the halves - to accommodate thermocouple leads. The depth of the hole was determined by the required distance between the ground surface and the nearest thermocouple. The thermocouple junctions were spot welded directly to the slightly skimmed half of the pin. This enabled an accurate knowledge of the position of the thermocouple bead and ensured good thermal contact with the workpiece. It was also particularly advantageous for inserting more than one thermocouple into the workpiece. Further tests using steam showed that the individual responses of the thermocouples were not measureably altered by the presence of other thermocouples in the same workpiece, nor by the longer hole needed to accommodate them. To prevent any ingress of fluid into this hole, after the first thermocouple bead had been ground through, it was filled with silicon grease.

3.2.3. Instrumentation and its calibration.

The forces generated during grinding were measured, not by a workpiece dynamometer, but by recording pressure differences at three positions around the spindle. The signals from the pressure transducers used there were voltage and current amplified, filtered to remove wheel rotational frequencies, and then used to drive galvanometers in a U.V. recorder as before. Calibration was by means of loads applied vertically or horizontally to the spindle via a jig.

The slideway and dresser infeed rates were checked against the control unit settings by using a displacement transducer and stopwatch. The wheel and dresser spindle speeds were set using a hand-held tachometer before each test commenced.

University's Grinding Group. The objective of such collaboration was to establish a definitive, reproducible test method.

3.2.4. The temperature measuring equipment and its calibration.

Figure 14 shows the time-temperature traces of three thermocouples embedded in an insulated workpiece at varying distances down the central axis from the surface on which steam was being played. It was found that the corresponding curves generated using the finite difference model did not give a reasonable fit to these results, especially to the initial slopes of the curves. The model predicted higher temperatures than those recorded. This suggested that the boundary in contact with the steam was not reaching 100°C as assumed. In Figure 15 the time-temperature outputs from (1) a thermocouple welded to the surface, (2) one welded in a hole which just broke through the surface, and (3) a thermocouple which was positioned 10mm down into the workpiece are shown. Although the difference in height of the two top thermocouples was not measureable they gave different temperature responses. The thermocouple proud of the surface reached 100°C within 2 seconds whilst the thermocouple just flush with the surface did not reach 100°C within the two minutes duration of the test. This effect occurs because, whilst the thermocouple proud of the surface records the temperature of the steam, there is a heat transfer coefficient between the steam and the steel (a boundary layer effect due to the stagnant layer close to the surface). The temperature just under the surface would also be lower if the steam supply was inadequate. Therefore the surface temperature used in the model was unrealistic. Hence the time-temperature curve of the thermocouple which was flush with the surface was used as an empirical definition of the transient boundary temperature. From this the plausible heat loss values for this test could be found, by fitting the curve for the thermocouple 10 mm below the surface, as shown in the figure.

Repeated tests, on different days with new thermocouples and workpieces, were highly reproducible and therefore seemed to suggest that the steam supply remained nearly constant. Assuming this to be the case, the empirical

boundary temperatures were used to fit the temperature profiles from pins with three thermocouples. Figure 16 is an example showing a range of values of heat loss which give a fit to the experimental results. The figure is based on the same experimental data as that used in Figure 14 for comparison. From Figure 16, and the results of similar tests with thermocouples at a variety of depths down the workpiece, it seemed that a reasonable value of the heat loss coefficient, C_L, probably lay in the range 180 to 310 $W/m^2/K$. Salter had determined the value to be 300 $W/m^2/K$.

In addition to this the temperature gradient was measured across the width of a pin, both as another method of investigating the loss term, and to assess the validity of the approximation to a one-dimensional temperature field. Figure 17 shows how the temperature varied across the pin with time at a depth of 10mm from the steam heated surface. The temperature gradient across the central 16 mm portion of the pin decreases with increasing time, as the Sindanyo insulation heats up. Whilst the thermocouple at the interface may be unreliable, because it may measure an average temperature of the pin and insulation, the temperature gradient between the thermocouples 1 and 2 mm from the outside of the pin shows this effect more markedly. Figure 18 shows how the heat loss coefficient from the central portion of the pin varies with time and with the temperature of the point 8mm from the pin centre. From these graphs it can be seen that the coefficient has a high value initially but rapidly tends to a value of approximately 175 $W/m^2/K$, which agrees with the value associated with Figure 16. This initial variation occurs while a stable temperature gradient is established in the Sindanyo at the pin interface.

3.2.5. Experimental procedure.

At least a half hour before the test commenced the cold junction for the thermocouples was made up so that the ice and water mixture had time to equilibrate. The chromel leads, being of lower thermal E.M.F., were used as the outer wires between the recording equipment and the hot and cold junctions, so that

any voltages produced due to temperature differences at the recording equipment would be minimised.

It had been found that cooling by the fluid was adversely affected unless a full grinding nip was formed between the wheel and Sindanyo workpiece holder. Therefore specimen holders were designed to be proud of the workpiece and, before a test progressed, each holder and workpiece was ground to fit the shape of the wheel. The workpiece then had to be retracted whilst it was allowed to cool back to room temperature. This initial grinding gave a value for the specific grinding energy of the Sindanyo and also enabled accurate setting up of the test, because the position at which grinding would commence was identified. The dresser was jogged in to within 50 μm of the wheel before each test. The first feed point of the workpiece was then set such that an adequate depth would be dressed from the wheel before grinding commenced. All tests were carried out under continuous dressing conditions at a feed rate of 2 μm/rev, in order to minimise the influence of fluid lubricity on the proportion of energy entering the workpiece (as rationalised in Section 2.4.3).

The force measuring equipment was enabled before the flow of coolant was set, so that a force baseline with coolant flow was recorded. The temperature recording equipment was then switched on and the plunge feed initiated so that continuously dressed grinding took place, until the lowest thermocouple had been ground through. All instrument settings and other test conditions and observations were noted on a sheet designed for the purpose. The specific grinding energy for the specimens was calculated from the forces measured at the wheelhead (by subtracting those due to the insulation). This value, together with the pin dimensions and thermal properties and the plunge feed rate, was entered into the computer model, already described, in order to obtain a fit for the experimental temperature profiles.

3.3. EXPERIMENTAL METHODS TO STUDY THE WHEEL SURFACE CONDITION

3.3.1. Optical methods tried.

The area of flat surfaces on abrasive grains ('wear flats') has been shown to affect the forces generated in grinding [47]. Following the approach of Suto et al. [75], a Joyce Lobel 'Magiscan 1' image analyser could be used to look at these flats by sensing the light reflected from them; thus providing a quick and simple method of measuring their size, distribution etc.. However, difficulties were encountered in reproducing the illumination and measuring conditions from sample to sample, and individual features on the grinding wheel surface were also difficult to distinguish. Similar problems with reproducibility would have existed if photographic or imprint (where a inked roller is used to find the wear flats on the very surface of the wheel) methods of reproducing the grinding wheel surface for evaluation had been used. (Later the same technique was investigated using a 'Magiscan 11', on which measurements would have been feasible had this apparatus been available.)

3.3.2. Stylus method used.

In the light of the successes in using stylus methods, described in Section 2.8, this method was the main one employed.

3.3.2.1. General description of profile measuring apparatus.

Taylor-Hobson 'Tallymin' equipment was used. This consisted of an electromagnetic head which measured the displacement of a stylus fitted into it as the stylus traversed a surface. An amplifier magnified the signal from the stylus; it was also used to drive a rectilinear recorder which reproduced the profile on 'Teledeltos' paper. The equipment is shown schematically in Figure 19a. This output could be calibrated in both directions and was modified to provide a changing voltage signal

for a Gould Storage Oscilloscope. The oscilloscope converted the signal from analogue to digital form and could digitise and store 4100 points from the trace.

3.3.2.2. Stylus design.

The stylus was chisel shaped, after Bhateja [92], because a standard pointed stylus may record the wheel porosity (see Figure 19b). This was manufactured from a segment of hard steel razor blade such that it would have a small radius at the edge. The radius of 10 μm and included shank angle of 60° fit the British Standard requirement [93]. The length of the stylus was determined by the theoretical distance between average independent profiles on the grinding wheel, α,

where $\alpha = \sqrt{3}.(u-r)$ see ref [94]

and $r =$ grit radius

$u =$ grit separation

where $u = 1.8\ r.\sqrt[3]{s}$

and $s =$ grinding wheel structure factor

Three different values for r, within the range covered by the 60/80 grit size specification of the wheel, were used to compute three different stylus lengths and three styli were then manufactured. Each stylus was checked for consistency of output over the same profile for ten traces and the traces from the different styli were compared. If the stylus is too wide then the area under the profile will be integrated, leading to a loss of information. If, however, it is too narrow, it will be deflected from a straight course by the porosity of the wheel. The stylus whose length had been calculated from the average grit radius was found to give the most detailed and consistent trace. This stylus had a length of 0.88 mm.

3.3.2.3. Experimental procedure.

The creep feed, induced porosity, grinding wheel was dressed in the usual manner using one of two infeed rates, fast (1.9 μm/rev), or slow (0.26 μm/rev), until about 2 mm had been dressed, which is sufficient to remove any surface history. The dresser was then wound quickly away to prevent any 'sparking out'. Grinding fluid (either the oil or the macroemulsion), was provided at the usual pressure both in the shoe and at the dressing interface in order to mimic the conditions under grinding as closely as possible. No grinding, or other conditioning of the wheel, was undertaken. Due to the difficulty in providing a traversing mechanism for a stylus within the grinding rig, the wheel was removed to lie on the table of a milling machine. The stylus, held in the chuck of the miller, could then traverse the wheel surface axially as it was driven vertically upwards at a speed of about 12 mm/min. Two different machines were used and, unfortunately, on one of these the spectrum of speeds was continuous, but could be controlled to within 5% of this value and was calibrated using the record on 'Teledeltos' paper. Figure 19c shows a typical trace obtained in this way on 'Teledeltos' paper.

This method for studying the wheel surface geometry was also used after the wheel had ground metal. The high dresser infeed rate of 1.9 μm/rev was used to continually dress the wheel whilst a Nimonic specimen was ground, using a 3 mm depth of cut and 8 mm/min maximum normal infeed rate. The same oil and macroemulsion as before were used. The slideway was withdrawn as quickly as possible before the endstops were reached, to reduce any sparking out or dwell. The wheel was examined as before except that the transverse traces were taken every 5 cm around the circumference.

3.3.2.4. Treatment of data.

The programme written to compute the p.d.f. and c.d.f. of the profiles is given in Appendix 9. This enables the computer to transfer data from the oscilloscope and manipulate it into the form required for graphical output. Intervals of $1/50^{th}$ of the profile height were used to calculate the frequency distribution of the heights as this interval had been used satisfactorily by Brettell and Richardson [95]. The stylus could easily penetrate to a depth of 200 μm but only the upper 80 μm of the profile were studied. The work of Bhattacharyya and Hill [80] suggests that this will include all of the cutting edges which could become engaged with the workpiece.

3.3.3. Tests where dressing took place with one fluid and conventional grinding followed with another.

Of necessity, these tests were spread through the grinding programme because of the practical difficulties of changing between fluids and of avoiding wheel contamination with the wrong fluid. A Nimonic specimen was ground to remove some of the material which has to be ground before a full arc can be achieved. Then the wheel was dressed without grinding at a feed rate of 2 μm/rev until about 5 mm had been removed from the radius. Either oil or macroemulsion was used in the dressing nip and the dresser was wound out rapidly before the infeed mechanism had stopped, in order to prevent dwell. The other fluid was then used to grind the pre-shaped specimen without further dressing.

4. RESULTS

4.1. LUBRICATION MEASUREMENTS

Three types of test to investigate lubrication are described in this section. Conventional dressing conditions, but combined with low stock removal rates to maintain wheel sharpness, were first studied. The effect of continuous dressing on wheel condition was then examined. Finally, various tests were carried out under continuous dressing conditions.

4.1.1. Tests without continuous dressing.

A few tests were carried out at low stock removal rates without continuous dressing in order to see whether the results of Ye and Pearce could be reproduced; viz., shortly after dressing, oil leads to a lower specific energy requirement than water does. Figures 20 and 21 show how the specific energy varies with the volume of stock removed for Nimonic at a depth of cut of 1 mm, and for steel at a 3 mm depth of cut. These values were chosen to reproduce approximately the test conditions of Ye and Pearce [60] and of Morgan and Salter [96] respectively.

In both cases the forces rose during each test with increasing volume of stock removed, as the wheel became blunter. In addition a lower specific energy was generated when oil was used than when a macroemulsion was the grinding fluid. The total volume of metal removed was less than that in the tests by Ye and Pearce and hence the wheel may have remained sharper. Therefore these tests appear to confirm their hypothesis of the efficacy of oil, compared to a macroemulsion, when the wheel is sharp.

The difference in the specific energy with the two fluids was smaller when the steel was ground than when the workpiece was Nimonic, and the specific energy was considerably lower with the easy to grind material, as expected.

Morgan and Salter carried out tests using the macroemulsion on EN9 under identical conditions on the same grinding machine; it is therefore encouraging that these results are comparable with theirs.

4.1.2. Preliminary tests to ensure that the grinding conditions are kept constant.

Malkin and Cook [47] have shown that the measured force in grinding is proportional to the wear flat area, and we know that the wear flat area depends upon the dresser infeed rate. This is demonstrated in Figure 22 where some of the results of Salmon [65] have been replotted. As has already been described, as grinding progresses, without some means for regulating the wheel condition, the grinding forces on each grit cause attrition. This increases the wear flat area and hence the forces generated, until the forces are large enough to cause grit or bond fracture, revealing a new sharp grit underneath. The cycle then begins again. Grinding fluids alter this cycle by influencing the rate at which the wear flats grow. They do this by modifying the forces between the wheel and work. The basis of the experimental work to compare the lubricating ability of fluids depends upon keeping the grinding conditions constant by continuously dressing the wheel during grinding. However, it is necessary to show that this constant wheel condition is truly being achieved. Firstly, it must be determined whether (or not) the fluid used in the dressing nip significantly alters the wheel surface generated. Secondly, the range of grinding conditions for which dressing at a specified rate controls the process must be identified.

4.1.2.1. Results of tests to assess whether the fluid used affects dressing.

4.1.2.1.1. Stylus tests.

Examples of typical results from tests using oil and water based fluids at two different infeed rates are given in Figures 23 to 26 for comparison. From these it can be seen that for both fluids there is a greater concentration of material at

the extreme surface of the wheel when a slower dresser infeed rate is used. On the c.d.f. curves the cumulative number of points does not pass through the origin because a proportion of the profile lies more than 80 μm below the highest points on the surface. The value of this intercept is much lower for the finely dressed wheels, indicating that more of the profile lies in the top 80 μm of the surface than in a coarsely dressed wheel. The p.d.f. curve shows more clearly that within this 80 μm the material is concentrated more towards the surface in a finely dressed than in a coarsely dressed wheel. Although this analysis is sensitive to differences in the dressing rate, it does not seem to distinguish so markedly between surfaces produced using different dressing fluids. Therefore, from this analysis we can conclude that the fluid used for dressing does not seem to alter the profile significantly.

4.1.2.1.2. Tests where grinding with one fluid follows dressing with another.

The results of tests where steel was conventionally creep feed ground using oil or water, after dressing with the other of the two fluids are presented in Table 2. Steel was used for these tests because it is known to cause the wheel to wear more slowly than Nimonic does, and hence the effects of the wheel surface produced by prior dressing might be expected to show for longer. These results show that the forces generated by grinding in this way are those associated with the fluid used in grinding rather than in dressing. This corroborates the previous tests of wheel surface measurements and indicates that the fluid alters the grinding forces by its influence in the grinding nip, rather than in the dressing nip.

4.1.2.2. Results of tests to see whether dressing is in control of the wheel condition.

Measurements of specific energy at the beginning and end of grinding tests with continuous dressing were compared. These showed no apparent differences in specific energy as a test progressed, even under the conditions considered most likely to cause wheel wear, i.e. low dresser infeed rate, a Nimonic workpiece and oil

grinding fluid. This suggests that dressing can control the wheel condition on a comparatively long-term basis (i.e. that dressing, rather than grinding, controls wheel breakdown and hence the forces generated). Salmon [65] has examined the relationship between dresser infeed rate and specific energy. He said that, at a particular dresser infeed rate, the grinding wheel reaches a state of maximum sharpness, and hence the specific energy remains constant, suggesting that dressing controls the wheel condition. However, it has not been shown whether the wheel grits are significantly altered during a single sweep through the arc of cut, prior to their next contact with the dresser. Dressing could prevent any build up of such an effect over more than one wheel rotation, thus maintaining a stable degree of wheel sharpness (for a particular dresser infeed rate).

4.1.2.2.1. Results of tests to examine the wheel surface in the grinding arc.

In order to investigate circumferential variations in the wheel surface conditions, the slideway and dresser were rapidly retracted during continuously dressed grinding of a Nimonic workpiece. No such variation in the surface topography could be detected in tests with either type of grinding fluid. It is perhaps not surprising that the part of the wheel which had been through the grinding arc at the moment of retraction could not be identified, given the elastic deflection of the system during grinding.

4.1.2.2.2. Results examining the overall wheel profile when it grinds metal under continuous dressing.

Whilst circumferential variations in the wheel condition could not be detected, comparisons could be made between a wheel which had been subjected to continuously dressed grinding and one which had simply been dressed. Figures 27 and 28 show typical c.d.f. and p.d.f. curves from random positions around a wheel after grinding Nimonic with oil and water based fluids respectively. These are

equivalent to Figures 24 and 26 except that no grinding took place with the latter. There seems to be no appreciable difference between the curves obtained. This implies that grinding does not significantly affect the wheel topography in the grinding arc when continuous dressing at a high enough feed rate takes place. It must be assumed for this analysis that the wheel/dresser interface is not more elastic than the wheel/workpiece interface, as the method requires that dressing should stop at the same moment as (or before) grinding.

4.1.2.2.3. Change in the workpiece surface roughness around the grinding arc.

As the above investigation was not wholly reliable further tests were carried out. Whilst it had not proven possible to measure the condition of the wheel surface in the arc of cut, it was possible to measure the surface roughness of the workpiece at different positions along the arc of cut and hence infer the nature of changes in the wheel condition as it moves through the arc. In order to obtain a reasonable picture, the wheel was retracted as quickly as possible from the workpiece. A series of stylus generated traces, perpendicular to the cutting direction, were taken at intervals of 2.5 mm around the arc of cut. The specimen was Nimonic, the fluid water based, and the wheel was coarsely dressed - conditions which were expected to be conducive to producing the maximum change in the specimen roughness within the grinding arc. However, at a maximum normal infeed rate of 8 mm/min there was very little visible evidence of a change in profile though the length of the arc, and the same surface features could be identified in the stylus traces at the beginning and end of the arc. A similar series of traces was taken around the arc on a specimen ground at a maximum normal infeed rate of 100 mm/min and again very little variation was seen. However, when the roughness average values of these profiles are plotted against position around the arc of cut, as in Figure 29, there is a trend of decreasing roughness average towards the end of the arc of cut at the high feed rate but not at the low feed rate. Similar results are plotted on this figure for

an intermediate feed rate. One implication of this is that a dresser infeed rate of 2 μm/rev is sufficient at a table speed of 60 mm/min and 150 mm/min (which are equivalent to values of V_n of 8 mm/min and 20 mm/min), but not at a table feed of 790 mm/min (equivalent to V_n = 100 mm/min). Alternatively, at the high table feed rate a change in the metal removal mechanism may have caused the change in surface roughness around the arc. If more rubbing was taking place at the bottom of the arc of cut (where V_n is smallest) this might cause a smoother surface. The variation of surface roughness around the arc at a low dresser infeed rate (0.2 μm/rev) is also plotted on this figure and shows that there is no significant progressive change in roughness at a maximum normal infeed rate of 8 mm/min.

4.1.3. Grinding tests using continuous dressing.

4.1.3.1. Tangential force and specific energy.

Figure 30 is a graph of tangential force versus dresser infeed rate when Nimonic is ground at constant depth of cut and constant stock removal rate. It shows that with all the fluids used the force decreases with increasing dresser infeed rate, although above an infeed rate of about 1 μm/rev little reduction is achieved. The implication is that dressing controls the process, at this stock removal rate and depth of cut, if the dressing rate is at least 1 μm/rev.

A graph after the results of Salmon, showing wear flat area versus dresser infeed rate, was presented in Figure 22 and took the same form as this force curve. Kannapan and Malkin [46] explained that the sliding force is proportional to the wear flat area, hence as the dresser infeed rate increases the forces due to sliding decrease.

The graph shows that oil significantly lowers the tangential force over a macroemulsion which, surprisingly perhaps, appears to offer no advantage, in terms

of the tangential force, over plain tap water with no additives. The microemulsion, however, exhibits a performance intermediate between that of the oil and water.

If the proportion of rubbing taking place at a particular feed rate is the same for all the fluids then a graph of specific energy at constant stock removal rate will take the same form as the tangential force curve. A histogram comparing the specific energy when Nimonic and steel are ground using oil, the microemulsion, and the macroemulsion at a high dresser infeed rate is presented in Figure 31. The results correspond to a region of the variable parameters where, from the foregoing evidence, we can be reasonably confident that dressing is in control of the process. At a low maximum normal infeed rate of 8 mm/min the oil reduces the energy requirement to one half of that of the macroemulsion when steel is ground, and to one third when Nimonic is ground. The microemulsion generates a lower tangential force than the macroemulsion and hence is associated with a lower specific energy. However, this effect is only significant with the Nimonic; on steel the differences between the specific energies is of the same order as the experimental error. The histogram also shows that with the water based fluids Nimonic has a higher specific energy than steel, but that there is no difference in the specific energy needed for the two different workpiece materials when oil is the grinding fluid. At a higher maximum normal infeed rate of 50 mm/min the differences between the microemulsion and the oil are less significant, on either material, than at the lower feed rate. However, differences between the micro- and the macroemulsion show more clearly, with the microemulsion being associated with about two-thirds of the equivalent specific energy for the macroemulsion on either material.

In Figure 32 the specific energy variation with dresser infeed rate is compared for steel and Nimonic with the macroemulsion grinding fluid. The specific energy decreases until a near constant value is reached and this seems to occur at a lower dresser infeed rate with steel than with Nimonic. Salmon suggested

that the specific energy approaches a minimum value in this way when the wheel surface geometry reaches maximum sharpness. In Figure 22 the wheel sharpness variation with dresser infeed rate was shown to take the same form as the specific energy does in Figure 32. Also presented in Figure 32 are the results of Salmon when the same Nimonic alloy was ground under the same conditions and with a similar macroemulsion, showing that these results are consistent with his. In Figure 33 the normal and tangential forces are shown at varying dresser infeed rates when Nimonic and steel are ground with the macroemulsion. Both forces settle to a near constant value at a lower dresser infeed rate on steel than on the Nimonic.

Continuing to look at the effect of using the macroemulsion when grinding the two different materials, the specific energy variation with stock removal rate, whilst the dresser infeed rate is kept high, is shown in Figure 34. Lines 'A-A' drawn on this and Figure 32 show equivalent conditions. No wheel breakdown was observed during these tests even at the highest stock removal rate and when grinding Nimonic. From Figure 34 it can be seen that the specific energy decreases with stock removal rate until a steady value is reached and that a lower specific energy is required when steel is ground than when Nimonic is ground at all values of stock removal rate investigated. Grinding becomes more efficient with increasing stock removal rate because the grit depth of cut increases, promoting chip formation, so that there is proportionally less ploughing and rubbing. Morgan and Salter [96] found no variation in the specific energy when EN9 was ground at high and low feed rates, using the same conditions and fluid as in Figure 34. However their low feed rates correspond approximately to the position marked by the line 'A-A' and their high feed rate was four times faster, so (from Figure 34) little variation in specific energy would be expected.

The corresponding increase in forces with stock removal rate is presented in Figure 35, from which it can be seen that, whilst the tangential force is

lower with steel than with Nimonic, the differences in the normal forces are more marked. At a given feed rate, the normal force is about 50% higher when Nimonic is ground than when steel is ground.

The water based fluid appears to require a lower specific energy when steel is ground than when Nimonic is ground at all values of stock removal rate. However, at a low value of stock removal rate and high dresser infeed rate, oil required approximately the same specific energy independent of whether the material was easy or difficult to grind (Figure 31). In Figure 36 the variation of specific energy with stock removal rate is plotted for these fluid/work combinations. It shows that, with oil, steel only appears to require a lower value of specific energy at the higher values of stock removal rate. Surprisingly, at low stock removal rates steel, was associated with higher values of specific energy. The curves cross at a value of maximum normal infeed rate corresponding approximately to that to which Figure 31 relates.

In Figure 37 a graph of specific energy versus stock removal rate, at a low dresser infeed rate on steel to match the conditions used by Liverton [97], shows that the results obtained are consistent with his. However, compared to the results presented for a higher dresser infeed rate in the previous figure, the specific energy appears to vary with all values of the feed rate. No wheel breakdown was apparent in the tests by the author, and Liverton saw wheel breakdown only at twice the highest maximum normal infeed rate illustrated in this figure. Dressing may not be in control of the wheel sharpness at this low feed rate, although the forces do not seem high enough to cause wheel breakdown.

Although at low dresser infeed rates oil seems to produce a higher normal force than the water based fluids, the normal force generated when steel is ground seems to be very similar for the different grinding fluids at dresser infeed rates sufficiently high to control the process (see Figure 38). The equivalent results

for Nimonic are shown in Figure 39. In contrast to steel, the difficult to grind material is associated with a wider spread of normal forces with the different fluids. Water and the macroemulsion give the highest normal force, and oil the lowest, with the microemulsion showing intermediate behaviour. This result conflicts with the findings of Ye and Pearce [60] who found that, under conventional dressing, oil produced higher normal forces than a macroemulsion when a Nimonic alloy was ground. Comparing Figures 39 and 38, the curves seem to flatten out at a higher dresser infeed rate with Nimonic than with steel.

The differences between the micro- and macroemulsions on the difficult to grind material at varying stock removal rates were investigated. Figure 40 shows that although the normal forces are approximately the same, the microemulsion generates a lower tangential force than the macroemulsion. This is then reflected in the graph of specific energy with stock removal rate, Figure 41, which reveals a lower value of specific energy when the microemulsion is used for all values of stock removal rate studied. (The tests at varying dresser infeed rate (Figure 32) also showed lower values of specific energy with the microemulsion at all values.) At higher stock removal rates, where the curve in Figure 41 has levelled out, the microemulsion is associated with about two-thirds the value of specific energy for the macroemulsion. At lower stock removal rates the difference is less marked (see Figure 31). In Figure 41, at the value of stock removal rate used for the tests at varying dresser infeed rate (e.g. Figure 32), the specific energy is sensitive to small variations in the stock removal rate.

When EN9 is ground, the most significant differences in performance are between oil and the macroemulsion. In Figure 42 the variation of the normal and tangential forces with stock removal rate is shown for these two fluids. Whilst the normal force with oil appears to be lower than with the macroemulsion, the tangential force is significantly lower with oil than with the macroemulsion at all values of stock

removal rate. Figure 43 shows how the specific energy varies with stock removal rate under the same conditions. The graph appears to level out at about the same stock removal rate as in the previous graph for Nimonic (about 6 $mm^3/mm/min$ for both fluids). The difference in specific energy between oil and the macroemulsion on EN9 appears more marked at high stock removal rates than at the lower stock removal rate used in the tests where the dresser infeed rate was varied.

The forces were also measured when the pins were plunge ground in the cylindrical grinder and these are presented versus plunge feed rate in Figure 44 for the steel pins. For all water based fluids these results appear to take the form of straight line graphs through the origin: the normal forces were very similar for all the fluids tested; there was slightly more variation in the tangential forces. Oil is the exception, showing higher normal forces than the water based fluids and little variation with feed rate. This contrasts with the surface grinding tests, where oil produced lower normal forces than the water based fluids at this dresser infeed rate. An increase in the forces at the onset of burn was only apparent with pure tap water.

The effects on the specific energy of varying the depth of cut, at high stock removal and dresser infeed rates, are presented in Figures 45 and 46 for the grinding of Nimonic and steel respectively. They reveal that, when oil is the grinding fluid on a Nimonic workpiece, the specific energy appears to increase with increasing depth of cut whereas it appears to remain constant when steel is ground. No dependence on the depth of cut was found with the water based fluids.

4.1.3.2. Roughness averages.

The appearance of the ground surface was assessed by eye before being measured in order to identify redeposited swarf. No redeposition was seen in the grinding arc, as long as burn did not occur. Roughness averages provide another means for assessing lubricity. In Figure 47 the roughness averages of an EN9

workpiece are plotted against dresser infeed rate for three fluids. The oil and water based fluids give approximately the same value of workpiece surface roughness at values of dresser infeed rate which are high enough to be in control of the process. However it is interesting that, at low values of dresser infeed rate, whilst the water based fluids still perform approximately equivalently to each other, the oil produces a significantly rougher surface.

The roughness average versus stock removal rate graph for EN9, corresponding to the specific energy results in Figure 43, is presented in Figure 48. Again oil is, surprisingly, shown to produce a rougher surface under some circumstances. The form of the curves differs, depending on the fluid used. Morgan and Salter [96] found no dependence on feed rate of the surface roughness of steel specimens using the macroemulsion grinding fluid, but the feed rates which they used correspond to the flat portion of the graph in Figure 48.

Roughness average measurements were also taken for the plunge ground pins. Figure 49, for Nimonic and steel specimens with the full range of fluids, shows a decrease in surface roughness with increasing plunge feed rate which is not as marked as the decrease seen on the surface ground specimens. The individual values correlate approximately when specimens ground at the same maximum normal infeed rate or plunge feed rate are compared. It is interesting to note that those water based fluids giving the best finish with Nimonic give the worst finish with steel, whilst oil and the microemulsion give very similar surface finishes on either material.

Figure 50 is a graph of roughness average versus stock removal rate for EN9 and Nimonic when the macroemulsion was used as the grinding fluid, showing a smoother finish on Nimonic at all values of stock removal rate investigated.

4.1.3.3. Force ratios.

The force ratio is the ratio of the tangential to the normal grinding force, and the effect that different metal removal mechanisms might have on the force ratio was described in Chapter 2. This ratio may therefore provide some clues to how a fluid influences the metal removal process and indeed has been considered to be equivalent to the coefficient of friction with a particular fluid [60]. Force ratios for the different fluids and materials, under both high dresser infeed and stock removal rate conditions and also under low dresser infeed and stock removal rate conditions, are compared in Table 5. The latter conditions would be expected to generate a higher proportion of rubbing, because the wheel would have a larger area of wear flats on it and because the equivalent chip thickness would be smaller. Table 5 shows that the force ratios are lower for both materials when oil is the grinding fluid and that they are also lower on Nimonic than on steel, i.e. it indicates that there is more rubbing taking place under these conditions. The micro- and macroemulsion appear to perform equivalently (in terms of the measured force ratios) on steel, but the microemulsion gives a lower force ratio than the macroemulsion on Nimonic. The general trends under the two sets of conditions are of the same order, and the conditions conducive to rubbing appear to give lower force ratios, as expected from the assessment in Chapter 2 of the forces operating. A graph (Figure 51) of force ratio versus plunge feed rate is given for the plunge ground pins, and shows how the ratio decreases with increasing feed rate with the water based fluids.

Osman and Malkin [35] argue that the specific cutting energy can be calculated from the intercept on a graph of tangential force versus wear flat area. According to their model the specific energy is only equal to the specific cutting energy when the wear flat area is zero, because then there is no rubbing taking place. Such a graph is presented in Figure 52 for Nimonic workpieces ground whilst using four different fluids. The values of wear flat area were based on the dresser infeed

rate used and were obtained from Salmon's measurements which were given in Figure 22. (It seems reasonable to use these measures, as the same wheel grade and workpiece material were used in both cases; the tests in Section 4.1.2.1 have indicated that dressing is independent of the fluid used, in terms of the distribution of grit heights on the grinding wheel.) The specific cutting energies indicated by this analysis are presented in Table 3 which also presents the friction coefficient, μ, between the wear flats and the workpiece. The friction coefficients are obtained from the ratio of the gradients of the graphs of tangential force versus wear flat area to the gradients of similar graphs of the vertical force versus wear flat area. From Figure 52 it would appear that the specific cutting energy for oil and the microemulsion are about the same and, at 15 J/mm^3, approximately half of the value with the macroemulsion and a third of the value with water. However, there is a large uncertainty in the determination of such intercepts. The value obtained from the macroemulsion seems the most reliable as there is the least deviation from a straight line by the data points. The values of friction coefficient are similar for all the fluids, although perhaps highest with the microemulsion. An equivalent analysis was carried out for steel workpieces and the values for the specific cutting energy and friction coefficient are presented in Table 4. Specific cutting energies are approximately the same as for Nimonic (although possibly slightly higher) but the friction coefficients appear to be larger with steel.

4.1.3.4. Residual stress analysis.

A few residual stress measurements were arranged on steel specimens ground using oil and water based fluids under the same machining conditions. These were necessarily limited because they depended upon the goodwill of equipment suppliers. The x-ray diffraction method was used, as this is regarded as the most suitable for machined surfaces (Littmann [98]).

The results showed that with the water based coolant tensile stresses, which are undesirable, are only apparent on the outer surfaces of the specimen (as expected) in areas which discoloured, showing 'burn'. Figure 53 illustrates this and shows how the tensile stresses are worst on the side wall of the specimen, indicating that it was perhaps not cooled adequately; alternatively, damaged material on the ground surface could have been subsequently ground away. These results suggest that very abusive grinding is necessary before undesirable tensile stresses are generated and that these correlate with visible signs of burn on the specimen.

Comparisons with oil as the grinding fluid revealed smaller compressive stresses under unburnt conditions and smaller tensile stresses when burn did occur, compared to the water based fluid. However these results, presented in Table 6, were more qualitative and no actual values could be attached to them. The implication from this scant information is that oil is advantageous in terms of reducing residual stresses during the creep feed grinding of steel.

4.1.4. Summary of results of the lubrication tests.

The wheel profile generated does not appear to depend on the dressing fluid. At an infeed rate of 2 μm/rev dressing appears to be in control of the grinding process up to a stock removal rate of at least 20 $mm^3/mm/min$, under the experimental conditions used in this work. A higher dresser infeed rate is needed to control the wheel condition when Nimonic is ground than when steel is ground.

When continuous dressing is used, and grinding conditions are limited to those within which dressing controls the process, oil shows itself to be advantageous in terms of the specific energy and grinding forces; although at very low stock removal rates it may be detrimental on easy to grind materials in terms of surface roughness and specific energy. Hence a definition of lubricity, in terms of the specific energy under continuous dressing conditions, classifies oil as a better

lubricant than a microemulsion, which is in turn better than a macroemulsion. The macroemulsion appears to offer no advantages in terms of lubricity, so defined, over pure tap water with no additives. These differences in lubricity were more marked on the difficult to grind material than on the easy to grind material. The differences between the water based fluids are more marked at high stock removal rates.

At low stock removal rates, some anomalous specific energies and surfaces roughnesses were measured (compared to those at higher stock removal rates). At medium or higher stock removal rates Nimonic was always associated with higher specific energies and smoother workpiece finishes than steel.

On the whole the results appear to be consistent with those of other researchers where they are comparable.

Force ratios, a measure of the amount of rubbing taking place, indicated that there was more rubbing taking place when the oil grinding fluid was used than with the microemulsion, which itself showed more rubbing than the macroemulsion (on a Nimonic workpiece). Friction coefficients, assessed according to a method by Osman and Malkin, did not distinguish between the fluids. Values for the specific cutting energy (according to their model) increased in the order: oil, microemulsion, macroemulsion.

4.2. COOLING MEASUREMENTS

4.2.1. Observations based on recorded temperatures.

Figure 54 shows a trace of the output from three thermocouples embedded in a steel workpiece versus elapsed time since the start of grinding with a non-E.P. macroemulsion. Each trace ended when the thermocouple was ground through. The feed rate of the work into the wheel was comparatively slow and was chosen to mimic the maximum normal infeed rate used for the majority of tests on

the surface grinding machine. The three thermocouples each registered approximately the same temperature of about 17 K* above ambient as they were ground through which suggests that at this feed rate and with this fluid the surface temperature reached a constant value.

The tests reported by Salter [19] using continuous dressing were both at feed rates of 15 mm/min. Figure 55 shows the results of several tests at feed rates of 15 mm/min, all with the same water based fluid. It appears that a constant, but higher, surface temperature was also attained at this feed rate and that this value of surface temperature was reproducible from test to test. It seems likely that the major variations between the traces were due to variations in the positioning of the thermocouples down the axis of the pin; the traces of the thermocouples which were ground through first have the steepest initial gradient.

Figure 56 is a similar plot, where the results of tests with three further water based fluids are compared to one of the traces from the previous figure. The variations between three of the traces are within the error bound, found previously, owing to variations in thermocouple positioning. However the synthetic fluid allowed the workpiece to reach significantly higher temperatures. The surface temperature indicated was again constant at about 30 K, with four of the water based fluids, but about 48 K above ambient temperature with the synthetic fluid.

This type of analysis was carried out using the five water based fluids at increasing feed rates on steel workpieces, until burning of the workpieces occurred. As the feed rate was increased differences in the performances of the fluids became apparent. To summarise these: the synthetic fluid performed worst, causing the highest workpiece surface temperatures and causing burning to occur at the lowest feed rate; conversely, the microemulsion gave the best performance, slightly better

* To avoid any confusion, temperature differences have been quoted in Kelvin (K); otherwise, the Celsius (°C) scale has been used for fixed temperatures.

than the two macroemulsions and pure tap water. In Figure 57 the results of this analysis are summarised graphically, in terms of the apparently stable surface temperatures of the steel workpieces at different feed rates: they would seem to be nearly linear relationships, until immediately before burn. The microemulsion not only seemed to cause slightly lower surface temperatures than the macroemulsion and tap water but also allowed grinding to continue successfully, without burn up to a higher feed rate. The feed rate at which burn occurred was between 80 and 85 mm/min with the E.P. macroemulsion and water, but between 90 and 95 mm/min with the microemulsion. (The non-E.P. macroemulsion caused burn between 85 and 90 mm/min and the synthetic below 70 mm/min.)

Most testing was carried out near the burn limit, in an attempt to identify the conditions which lead to burn. The surface temperature appeared to remain constant throughout a test at all feed rates with all the water based fluids unless burn occurred. In this case burn seemed to occur from the onset of the test, rather than developing as the test progressed. Some interesting results, apparently near the burn limit, are presented in Figures 58 and 59 which are graphs of thermocouple temperature outputs versus time at a feed rate of 80 mm/min. Water and the microemulsion appear to give stable surface temperature increases of about 114 and 110 K respectively whilst the E.P. macroemulsion gave a surface temperature nearer 120 K above the ambient temperature (of 19°C). This actual temperature was therefore above the 130°C figure which has been mentioned by other workers as a critical surface temperature for the breakdown of the heat transfer mechanism. Figure 59 represents the results from a previous test at this feed rate where, due to the design of workpiece holder used, it seems likely that a full nip was not achieved at the start of grinding and hence cooling was inefficient. It shows that a higher surface temperature was initially reached but that later (presumably once enough of the holder had been ground through to provide a full nip) the surface temperature was apparently stable at about 140 K above the ambient temperature. The initial

high heat input may have caused this higher final surface temperature but, it is very interesting to note that, with an ambient temperature of 19°C, the actual temperature of the surface was about 160°C. At a feed rate of 85 mm/min with this fluid the workpiece burned.

With the microemulsion at a feed rate of 90 mm/min, steady workpiece temperatures were also recorded at a temperature of 157°C (135 K above ambient), as shown in Figure 60. This fluid did not prevent burn when used at a feed rate of 95 mm/min. Hence it would seem that, under these particular test conditions, if the surface temperature has a critical value then this is near to 160°C, rather than the value of 130°C suggested by other researchers [19,32].

Similar tests on steel using oil as the grinding fluid showed different behaviour from the water based fluids insofar as the surface temperature appeared to rise slowly during the test rather than remain constant. (The forces generated remained constant in tests where burn did not occur.) The rate of temperature rise was not constant but increased through the test and this was more marked at higher feed rates. For a given feed rate the temperatures reached were considerably higher than (about five times) those attained when using the water based fluids. For example, surface temperatures increasing from 150 to 200 K above ambient were recorded at a feed rate of 15 mm/min when oil was the grinding fluid, whereas 30 K was a typical surface temperature rise with water based fluids; at a feed rate of 8 mm/min the surface temperature recorded with oil was in the range 100 to 115 K, whereas, with the water based fluids, it was about 17 K above ambient. Breakdown of the heat transfer mechanism occurred at much lower feed rates, but higher surface temperatures, than with the water based fluids. Burn occurred at a feed rate of 22.5 mm/min with oil, although it is believed that this was near the borderline, as signs of burn on the workpiece were very faint. At 25 mm/min signs of burn damage were also slight although burn occurred more rapidly - within 5 seconds of the start of

grinding, as opposed to within 8 seconds at 22.5 mm/min. Typical force and temperature versus time traces, when burn occurred with oil, are presented in Figure 61. Dramatic surges, both in the temperature and force traces, occurred simultaneously, although the forces reached a constant final value. Note also that the surface temperature reached appears to have been hot enough to have rewelded the (ground-through) thermocouples, such that they continued to give a reading after the test had ended. Neither, this nor a breakdown in heat transfer after successful grinding for a time, occurred with the water based fluids.

It was thought that the apparent differences in performance between the fluids, in maintaining the workpiece temperature, might be echoed in a 'Linefrost' test. In this the temperature of a flat steel hotplate is indicated by the tendency of liquids to form balls, which shoot off the hot surface on a layer of vapour and therefore have little cooling effect. However, when the temperature of a hotplate was slowly raised from 95 to 150°C the performances of the five water based fluids could not be distinguished. At 100°C all five started to boil on the hot plate and at 133°C they all began to form balls, the mobility of which increased with the hotplate temperature. The oil, however, showed behaviour reminiscent of the first stages of boiling in water (i.e. corresponding to a surface temperature of 100°C) at 230°C. At 265°C, the maximum attainable by the hotplate, the oil spread over the surface more rapidly but did not form the vapour cushioned droplets.

When the fluids were heated in bulk, in a distillation set with a condenser attached, all of the water based fluids boiled at 100.5°C, as indicated by a mercury in glass thermometer just above the liquid surface. There was, however, some variation in the appearance of this boiling, with the synthetic fluid and water forming large vapour bubbles (showing more tendency to 'bump'), whilst the macro- and microemulsions boiled foamily. Thus the vapour bubbles were smaller than those

in the water and synthetic fluid. This is indicative of more nucleation sites being available for bubble formation in the fluids containing oil.

The oil was heated slowly in the distillation set and gave off vapour in increasing amounts from 110°C on. At 230°C sufficient vapour was produced for it to condense. Vapour did not appear to distill over in distinct fractions, and the temperature of the fluid in the flask rose steadily, indicating that there was a mixture of a spread of molecular weight fractions present.

It was suspected that the poor performance of the synthetic fluid might be connected with the way in which it appeared to be more opaque and foamy than the other fluids immediately after a grinding test. This foaming had the appearance of air bubbles, evenly distributed throughout the volume of the fluid, rather than forming a foamy head. A simple test was performed in which a parallel sided beaker was placed under the workpiece during a test in order to catch fluid as it left the grinding zone. Two minutes after the end of each test the volume of fluid in the beaker was measured. The synthetic fluid then filled the beaker to about 90% of its volume on average, whereas the other water based fluids filled it to at least 98% of its volume. This implied that the synthetic fluid contained 8 to 10% of temporarily entrained air during a test whereas the others contained a maximum of 2%. (They would also all be expected to contain dissolved gases.)

The thermal properties of MARM002 are compared with those of EN9 in Appendix 10. When pins of MARM002 were ground under the same conditions as EN9 the temperature profiles with time were a different shape, as expected from their different thermal conductivities. At low feed rates the surface temperature, registered as a thermocouple was ground through, was about the same as when EN9 was ground; i.e. it remained constant at about 30 K above ambient, at a feed rate of 15 mm/min with all the water based fluids except the synthetic, and it varied between approximately the same non-constant values from 150 to 200 K with the oil.

However the temperature in the body of the pin rose more slowly initially, but increased more rapidly as the thermocouple approached the ground face. These two types of temperature profile are illustrated in Figures 62 and 63 for Nimonic and steel pins, with water based and oil fluids respectively.

The shapes of the temperature profiles also altered with time. Although a point on the surface of the pin appears to remain at a constant temperature (from soon after the start of grinding), points below the surface become hotter with time. This is illustrated in Figure 64 where it can be seen that a point which is 2 mm below the surface increases in temperature though a test. The effect is more marked with Nimonic than with steel, at high rather than at low feed rates, and with oil rather than with water based fluids. It seems likely that this is due to the Sindanyo heating up during a test until a stable temperature gradient is established. The surface temperature is little affected by the heat sink below, but at levels below the surface the loss of heat to the insulation decreases during a test, as the insulation warms up, so that the temperature on the central axis of the pin increases with time at positions which are a constant distance from the surface.

Some difficulty was experienced in obtaining reliable temperature profiles from Nimonic workpieces at higher feed rates, as though the welds between thermocouple and pin were less mechanically secure than with EN9. However, all the water based fluids caused the Nimonic workpieces to burn at a feed rate of 70 mm/min, which was lower than for steel workpieces. The worst workpiece damage appeared to occur when the synthetic fluid was used. In the same way it seemed that higher feed rates could be sustained with the steel than with Nimonic when oil grinding fluid was used. For example, at 25 mm/min the Nimonic pins burnt immediately, whereas the steel pins appeared to have been ground successfully for a while.

4.2.2. Specific energy, forces, and surface roughness.

The pin tests rely on modelling creep feed surface grinding as a series of contiguous plunge ground grinding tests. The specific energies obtained with steel and water based fluids in the pin tests are presented in Figure 65. They are shown to be roughly comparable to those from the surface grinding tests at equivalent maximum normal infeed rates. There was no measurable difference between the specific energies associated with the different water based fluids. However, contrary to the results of the surface grinding tests, oil was associated with higher specific energies than the water based fluids. Indeed, the results obtained with oil in the plunge tests are less comparable to those obtained in the surface creep feed grinding tests at low feed rates. However, in this region the specific energy appears to vary rapidly with feed rate - hence errors in matching the feed rates would cause a larger difference in the specific energy than at higher feed rates. When Nimonic pins were plunge ground the measured specific energies were always found to be within 10% of the values obtained at comparable feed rates under surface grinding, both for oil and for water based fluids.

The forces and roughness averages generated in these tests were presented in Section 4.1. There was no significant difference in performance between the water based fluids, except that tap water alone produced higher forces (than would be expected from a linear extrapolation of the force versus feed rate graph) when burn occurred. Although the cooling performance of the synthetic was below the average for water based fluids, it performed as well as them in terms of lubricity indicators.

Whilst inaccuracies in measuring specific energies were likely to be larger in the plunge grinding tests than in the surface grinding tests, due to the relative sizes of the workpieces, the actual values measured during the plunge

grinding tests were used in the finite difference model (rather than extrapolating from the surface grinding tests).

4.2.3. Comparison between experimental results and the thermal model.

Salter found that when a steel workpiece was ground the proportion of energy entering the workpiece was of the order of 2% with water based fluids. Experimental traces from three thermocouples in a steel workpiece, ground at one of the feed rates studied by Salter and using the same fluid, are shown in Figure 66. Superimposed on these are attempts to fit computer generated curves obtained by the finite difference method. None of the generated curves, obtained using either Salter's or Fursden's programmes, appears to be a convincing fit for the experimental data if the proportion of energy entering the workpiece is set at 2%. In Figure 67 it is shown that a partitioning fraction of 8% can provide a better fit for the results of Salter than the 2.5% value he presented. However it is not intended to suggest that 8% provides the best fit to the data; this figure was selected at random. Partitioning fractions from 2 to 40% were investigated and, in Figure 68, the same experimental data from Figure 66 are shown plotted against a range of partitioning values, Q_w, from 10 to 25%. The rate of decrease of the proportion of energy entering the workpiece, Q_v, can be arranged to compensate for the increasing fraction of the energy entering the workpiece, Q_w, so that a constant surface temperature is obtained. The major effect of changing the partitioning is then to change the initial slopes of the curves. On the basis of this, and on the assumption that as a test proceeds additional, undetermined, factors come into play, it was considered most important to fit the initial slopes of the thermocouple outputs to the computer modelling.

If Figure 55, showing the range of experimentally measured temperatures under nominally the same conditions, is again referred to it will be seen that the experimental uncertainty is of the same order as the variation due to altering the partitioning values in the model between 10 and 25%. In Figures 69 to 72 the

effect on the modelled output of the uncertainties in such parameters as specific energy, thermal properties (these are temperature dependent), thermocouple positions and loss factor, respectively, are shown. Hence there is a large degree of uncertainty in the proportion of energy entering the workpiece, as determined by this iterative fitting method, owing to the degree of inaccuracy in measuring temperatures in the workpiece. However an estimate of the partitioning fraction of say 15% would not seem unreasonable.

When oil was the grinding fluid a range of fits to the experimental data were again plausible and values between 5 and 45% were attempted. A 'best' estimate around 30% is shown in Figure 73.

Within the constraints of the uncertainty in determining the partitioning fraction, no significant change in the fraction with feed rate was found. This agrees with the results of Salter, who found no dependence on feed rate if the wheel was continuously dressed.

Fitting data for the proportion of the energy entering a Nimonic workpiece was more problematic and no value attempted between 3.5 and 24% gave a convincing fit when oil was the grinding fluid. The curvature of the calculated graphs from the model did not correspond well with the experimental graphs. A range of 'best fits' for partitioning fractions between 6 and 18% with oil as the grinding fluid are shown in Figure 74. An equally broad spread was found with water based fluids, but possibly with values between 5 and 20% providing a better fit than those outside this range.

4.2.4. Summary of the results of plunge grinding tests.

Measurements of specific energy at varying plunge feed rates correlate well with those measured at equivalent maximum normal infeed rates under surface grinding conditions with water based fluids. This is important because it suggests

that it reasonable to model grinding energies in surface creep feed grinding as a series of contiguous plunge grinding operations when water based fluids are used. At low feed rates with oil there is a less strong correlation between the plunge and surface grinding tests.

With the water based fluids the surface temperatures appear to remain constant throughout each test. The temperature reached increases approximately linearly with plunge feed rate and, except for the synthetic, is similar for all the water based fluids. The microemulsion appeared to generate the lowest surface temperatures and allowed grinding without burn at the highest feed rate. The synthetic appeared to contain a proportion of entrained air which may have contributed to its poor performance in terms of these criteria. Grinding was achieved, without any evidence of burn occurring, at stable surface temperatures up to about 160 °C. Nimonic workpieces burned at lower feed rates than steel workpieces. Much higher surface temperatures were observed with oil and these appeared to rise during a test rather than remaining constant. Burn also occurred at a lower feed rate on Nimonic with oil than on steel.

Data fitting appears to suggest that between 10 and 25% of the grinding energy enters a steel workpiece with water based fluids. A large degree of uncertainty, owing to temperature measuring inaccuracies, may have masked any variation of the partitioning with feed rate. With oil the partitioning to a steel workpiece would appear to be approximately 30%.

5. DISCUSSION

5.1. LUBRICATION

5.1.1. Control of the wheel surface geometry by continuous dressing.

Direct comparisons of the grinding forces, and hence specific energies, generated with different fluids and workpiece materials would appear reasonable in this work, because initial experiments seem to show that it has been possible to maintain a constant wheel cutting geometry. These experiments have demonstrated the apparent independence of the wheel profile on the fluid used in the dressing nip. They also indicate that, within a particular range of grinding conditions, dressing controls wheel attrition over more than one revolution and that the geometry of the active grits on the wheel is not significantly altered whilst in the grinding arc.

5.1.2. Higher forces and specific energies with Nimonic.

5.1.2.1. Comparisons of material properties in relation to grinding.

When forces are compared under identical grinding conditions, within the range controlled by continuous dressing, they appear always to be higher with Nimonic than with steel (see Figures 33 and 35). In addition, a higher dresser infeed rate appears to be necessary to control the wheel condition with Nimonic (see Figure 32, where a macroemulsion is the grinding fluid). This effect could be owing to the higher forces experienced with Nimonic causing the wheel to wear at a higher rate.

Nimonic has a higher Vickers hardness number than steel. (The Vickers Hardness number is a measurement based on penetration and plastic deformation of the surface, which is not dissimilar to the action of a grinding grit.) This was measured with a pyramidal indenter as 700 for MARM002 and 200 for EN9. This higher hardness could cause more rubbing to take place with Nimonic before the grit is able to penetrate and cut, because Nimonic can support larger

stresses before plastically deforming (based on the yield stresses quoted in Appendix 4). The values of the force ratios given in Table 5 appear to be consistent with more rubbing taking place with Nimonic than with steel under the same conditions, i.e. that the normal forces are proportionally higher (compared to the tangential forces). A comparison of the relative values of the force ratios with the two materials (from Table 5) reveals that the value for Nimonic is about 60% of the value for steel, irrespective of the fluid used.

Morgan and Salter [96] investigated the effect of workpiece hardness under conventional and continuously dressed creep feed grinding and found higher forces with harder steels than with softer steels, even when the wheel was continuously dressed. They explained that this difference was due to the rate of wheel wear under conventionally dressed conditions but did not explain the reasons for the differences they found under continuously dressed conditions.

Rubenstein et al. [45] discussed a number of factors, including ductility and hardness, which affect the grindability of a metal. They showed that the critical rake angle for the transition to cutting depends upon the ductility of the metal. Whilst at higher dresser infeed rates there may be little rubbing taking place on steel, the ductility of steel may worsen rake face friction, encouraging proportionally more ploughing. The brittleness of Nimonic may discourage plastic flow sideways, causing less likelihood of ploughing. Therefore overall, the brittleness of Nimonic might be expected to be beneficial in terms of ploughing and rake face friction, reducing, rather than increasing, the measured forces and specific energies.

5.1.2.2. Malkin's model and its inferences for different workpieces.

The model according to Malkin superposes the energies associated with each of the metal removal mechanisms in grinding. Malkin suggested that the limit to the total energy was the melting energy of the material, because this limits the

shearing energy and hence the cutting energy. The melting energy of both steel and Nimonic is about 10 J/mm^3.

The lowest value of specific energy measured for EN9 was 12 J/mm^3 (see Figure 34); a value obtained under high dresser infeed rate and high stock removal rate conditions with oil. These conditions would be expected to be conducive to minimum sliding and ploughing energies in Malkin's model and hence to approach conditions where the total specific energy is equal to the specific cutting energy. The specific cutting energy for EN9 extrapolated from a specific energy value at zero wear flat area was 16 J/mm^3 (Table 4), but this was not measured at a low stock removal rate. Hence the energy due to ploughing may not have been minimised.

Salmon [65] obtained a minimum specific energy of 13 J/mm^3 when grinding MARM002, but the minimum value obtained in this work (see Figure 36) was 16 J/mm^3 (under minimum ploughing and sliding conditions). The specific cutting energy, measured at a low stock removal rate, was also 16 J/mm^3 (see Figure 52 and Table 3).

These energy values are not incompatible with Malkin's model of grinding energies. As the shearing energies are similar for both materials, Malkin's model would attribute the differences in forces and specific energy between them to increased sliding energy under the grits, increased ploughing, or increased rake face friction. It has already been suggested that ploughing and rake face friction may be greater with the steel, than with the Nimonic, because they may be dependent upon ductility. In addition, Malkin and Cook [47] showed that there was no correlation between hardness and specific cutting energy, which implies that the difference in the total specific energies for the two materials may be owing to different sliding (rubbing) energies.

5.1.3. The differences in lubricity between the fluids.

5.1.3.1. Forces and specific energies as measures of lubricity.

From the values for force ratios given in Table 5, it might appear that there is more rubbing with oil than with water based fluids on either material. However both normal and tangential forces measured were lower with oil, and hence it was associated with lower specific energies. The ratio of normal to tangential forces is simply proportionately higher (the force ratio is lower). Others who have measured higher normal forces with oil than with water based fluids were not using continuous dressing, and therefore may not have had the wear flat area under control.

Osman and Malkin [35] also found increased sliding friction with oil which they ascribed to lower temperatures under the wear flats, requiring larger stresses for sub-surface deformation.

When the insulated steel pins were plunge ground, however, the specific energy with oil was higher than with the water based fluids (Figure 65). (The values for water based fluids were comparable to those in the surface grinding tests.) This may have been owing to the higher bulk temperatures measured in the insulated pins with the oil fluid, increasing ductility and hence rake face friction. When insulated Nimonic specimens were ground the specific energy was lower with oil than with water based fluids, as expected, and was comparable to the surface grinding tests. Although Nimonic specimens became hotter than steel specimens at the same feed rate, Nimonic does not show the same high temperature ductility as steel.

Chu Boyi [99] has suggested that higher normal forces with oil are owing to hydrodynamic pressure from a wedge of oil immediately ahead of the grinding arc.

Osman and Malkin [35] showed how lubrication reduces the chip formation energy by reducing rake face friction. This would, in addition, decrease the critical undeformed chip thickness for the transition from ploughing to cutting, encouraging cutting and so reducing the ploughing energy. Hence the reduced specific energy in the surface grinding tests on both materials when oil is the grinding fluid (see Figure 31) could be attributed to lubrication of the rake face. Indeed the specific cutting energies, measured according to the Malkin method, were reduced by oil to about half their value with water based fluids (Tables 3 and 4).

5.1.3.2. Surface roughnesses with the different fluids.

It has been suggested that, under the conditions used, there is little rubbing taking place under wheel grits on the easy-to-penetrate steel. In this case, if the balance of mechanisms for the ductile steel specimens is between cutting and ploughing, then a good lubricant would be expected to reduce the amount of ploughing. As ploughing throws metal up and out sideways, this reduction in ploughing should improve the surface finish. This is the case in Figure 49 and in Figure 48 (except at low stock removal rates).

In addition, oil may reduce the likelihood of redeposition of ground metal swarf onto the ground face. No redeposition was seen with the oil. (As continuous dressing was in use, there should be no danger of loading patches redepositing onto the workpiece, as there would be under conventionally dressed conditions.)

Looking at Figure 48, the surface roughness is worse with both fluids at very low stock removal rates (than at high stock removal rates). If on steel, as suggested previously, a balance exists between cutting and ploughing, then at very low stock removal rates the geometrical requirements for the transition in metal removal mechanism from ploughing to cutting may not have been attained.

In Figure 48, the surface roughness continues decreasing to a higher value of stock removal rate with the oil than with the macroemulsion. Following the previous line of argument, this suggests that once the geometrical conditions for the optimum transitions from ploughing to chip removal have been reached by increasing the stock removal rate, the macroemulsion cannot influence the surface roughness further. The oil, however, appears to be able to reduce the rake face friction and hence further reduce the proportion of ploughing as chip formation is made easier. This would then tend to improve the surface finish. Figure 43 is the equivalent specific energy graph to the roughness graph, Figure 48. In Figure 43 the disparity in specific energy values between the fluids increases with increasing stock removal rate. If, as argued, oil is able to reduce rake face friction and hence reduce the amount of ploughing up to higher stock removal rates than the macroemulsion, then this would also explain the increasing disparity in measured specific energies. It has been suggested that there is still some sliding energy associated with grinding Nimonic, owing to its high yield stress, even when the grits are sharp and that the brittleness of Nimonic discourages ploughing. Therefore, on Nimonic a good lubricant might be expected to favour cutting over rubbing, worsening the surface finish but reducing the energy requirement. Rowe et al. [44] described how a poor lubricant smears the surface so that it appears smoother, whereas a good lubricant allows 'clean' cutting which appears rougher. Whilst a 'balance' in the metal removal mechanisms, which can be altered by the conditions or by the fluid used, has been suggested, the evidence in Figure 29 appears to be to the contrary. It would seem from this figure that, at the feed rates commonly used the surface roughness generated did not vary around the arc of cut. This implies that there was no change in the metal removal mechanism.

5.1.3.3. Intrinsic properties of the fluids.

Figure 41 showed how, when grinding Nimonic at high stock removal rates, the microemulsion reduced the specific energy to about two-thirds that associated with the macroemulsion. It is particularly interesting that the microemulsion showed a better lubricating ability than the other water based fluids, because it suggests that lubricating ability need not necessarily be sacrificed for the sake of cooling. The microemulsion showed improved performance over the macroemulsion although it contains less oil than the latter. The oil and E.P. additives are more finely dispersed through the microemulsion. This may make the microemulsion more effective, by enabling the reactive components of the fluid to be distributed into the geometrically intricate grinding zone more effectively. Under boundary lubrication conditions chemical lubrication is of major importance, hence the availability of the chemical additives for reaction could be critical.

The differences in the physical properties of the fluids have already been discussed, but to summarise these: water based fluids have little or no inherent physical lubricity whereas oils are more able to interpose between surfaces and have higher load bearing abilities. In addition, oils are able to dissolve more oxygen and E.P. additives than water based fluids are. The viscosity of oils may also play a part by encouraging the coating of the exposed surfaces rather than rapidly running from them.

It should be noted as an aside here that, since the mode of lubrication is predominantly chemical in nature, it is specific to the conditions. Coes [100] showed that fluid performance is directly dependent on abrasive type because of chemical reactions between the abrasive and bond. (The shape, hardness and thermal conductivity of the grits and the porosity of the wheel may also have an effect which is fluid dependent.) Therefore the results obtained here should be considered to be specific to this abrasive.

Researchers have shown that water gives a detrimental performance compared to grinding in air (e.g. [54]), and it has been suggested that the reason for this is that the presence of water tends to exclude atmospheric oxygen from the grinding zone. Torrance [59] ground in a Nitrogen atmosphere with water through which he had bubbled nitrogen for 24 hours to displace the oxygen and he found no difference in performance between this and oxygenated water used in an atmosphere of air. This appears to suggest that the levels of oxygen in water are not sufficient to have a beneficial effect, although the conclusion depends upon all of the oxygen having been removed from the deaerated water.

Water can dissolve up to 13 mg/l of oxygen (although tap water commonly contains about 70% of this amount [101]). Rowe and Smart [102] have shown that 10^{-3} Torr is a sufficient pressure of gaseous oxygen to improve dry grinding performance. However, Appendix 12 shows that, although there is 5000 times more oxygen dissolved in tap water than the gaseous amount that Rowe showed was necessary, the rate of diffusion of oxygen in water into the grinding zone would be about 10 orders of magnitude slower than in a gaseous form at 10^{-3} Torr. Creep feed grinding is, however, a process where the fluid is well aerated and kept under pressure, which will tend to aid the transport of macroscopic bubbles of air into the grinding zone, as well as the absorption and subsequent retention of oxygen. In addition, tap water contains typically 1 mg/l of chlorine and 0.3 mg/l of fluoride ions, species which are more reactive than oxygen. This seems to suggest that the exclusion of oxygen may not be entirely responsible for the deleterious effect of water; but some other effect, such as the way in which it keeps the workpiece cool, preventing thermal softening, has an influence. The exclusion of oxygen would not explain the differences found between the different types of fluids in this work.

5.1.3.4. Larger differences between the fluids seen on Nimonic.

In Section 4.2.2. it was suggested that the increase in specific energy, seen when an insulated steel pin was ground with oil, was caused by an increase in ductility at elevated temperatures. This would also provide an explanation for the larger differences in performance between the fluids when Nimonic is ground. On steel an increase in friction on the rake face, and hence also the amount of ploughing, owing to higher temperatures with oil, may negate some of the benefits of this fluid.

Lindsay [58] has suggested that nickel based alloys are relatively inert to reactions with cutting fluid additives, which could also help to explain the differences in performance between the fluids. In addition to chemical lubricity oils have their own intrinsic physical lubricity, as perhaps demonstrated in their higher normal forces; the less viscous water based fluids rely on chemical effects, however, and hence this may contribute to their comparatively poor performance on the relatively inert Nimonic.

On an easy to grind material like steel, even under adverse lubrication conditions, the proportion of cutting should be higher (than on a difficult to grind material like Nimonic). Thus the influence of a good lubricant would tend to be less significant.

5.1.3.5. Residual stress measurements.

Residual stress analysis indicated that these were smaller with the oil than with the water based fluids. Although scant these results are consistent with the findings of Letner [103], who suggested as early as 1957 that lubrication is the most important function of a grinding fluid relative to the control of residual stresses because this reduces the heat input. He found under conventional grinding conditions that water was no better than air at reducing residual stresses and thought that the

workpiece absorbs heat so quickly that subsequent cooling is of minor importance. Fletcher and Price [104] have investigated the residual stresses due to quenching in oil and water of equally hot plates of steel. They showed that the residual stress levels are lower with oil because the quenching is less severe. Lenning [105] investigated different types of grinding fluid and methods of their application under cylindrical grinding of AISI 4340 steel and found that only the use of sulphurised oil grinding fluids was beneficial in producing compressive residual stresses.

5.1.4. Influence of chip thickness.

The increase in the specific energy with increasing depth of cut, on Nimonic with the oil grinding fluid, is partially explicable in terms of the equivalent chip thickness. The proportion of cutting taking place and hence the specific energy depends upon the thickness of chips produced. The chip thickness (h), depends upon the depth of cut (a), table speed (V_w), the ratio of the width to the depth of cut for individual grits (R) and other wheel parameters (W_p), and can be approximately described by the relation

$$h = \sqrt{(V_w/W_p.R.\sqrt{a})} \qquad [106]$$

The wheel parameters include, the wheel diameter, the wheel speed and the number of active grits on the wheel. Under the conditions used these and the grit width to depth ratio should be constant. For a constant stock removal rate the product of the depth of cut and the table speed is a constant, hence under these conditions the chip thickness and specific energy have a small dependence on table speed. However, this effect appears to be surprisingly large in Figure 45, and it is interesting to note that it is not apparent on the easy to grind material in Figure 46. This is perhaps because of a higher proportion of chip formation with EN9 and hence reduced dependence on reaching a particular chip thickness for chip removal. Larger

elastic deflections of the wheel, owing to larger normal forces with Nimonic than with steel, may reduce individual grit depths of cut and hence chip thicknesses.

The variation in the specific energy with maximum normal infeed rate at low dresser infeed rates can also be understood in terms of the above relationship. Whereas there was little dependence on the infeed rate when higher dresser infeed rates were used, Figure 37, which corroborated the findings of Liverton [97], showed that there was a dependence at low dresser infeed rates. Under these conditions the wheel will be comparatively blunt, so that the width to depth of cut ratio for the individual grits will be larger, causing a corresponding decrease in h. Hence the proportion of chip formation at a given feed rate will be lower than for a more coarsely dressed wheel, so that there is more scope for the increasing feed rate to have some influence.

It has already been suggested, in Section 5.1.3.2, that a transition in the cutting mechanism may occur at low stock removal rates, because the equivalent chip thickness depends upon feed rate and there is a critical value above which cutting can take place.

5.1.5. Drawbacks of surface roughness measurements as a lubricity indicator.

Surface roughness measurements can give some clues to the metal removal process although, as will be illustrated, they should be interpreted with care. The drawbacks of roughness measurements based on the centreline average, which does not uniquely describe geometrically different surfaces although it does provide a rapid shop floor measurement of roughness, were explained in Chapter 2.

In Figure 47 the surface roughness is shown to increase up to a dresser infeed rate of 2.4 μm/rev, whereas in Figure 38, under the same conditions, the normal forces were shown to have levelled out at a dresser infeed rate below 1 μm/rev. This effect is consistent with the results of Salmon (see Figure 75). The

meter-cut-off (filtering level) of 0.8 mm used is the value recommended for ground surfaces and, in Appendix 11, is shown to be a reasonable value to use in this case. Figure 76 shows the measured surface roughness versus dresser infeed rate when three different values of meter-cut-off are used. The normal force curve is shown for comparison. At a meter-cut-off of 0.8 mm the roughness measurement does not correlate with the force curve but, as the longer wavelengths are filtered out, the value of the dresser infeed rate at which the surface roughness appears to reach a constant value reduces. Thus it seems that, at the commonly used value of meter-cut-off for ground surfaces, longer wavelength irregularities (probably due to wheel eccentricities) obscure those which correlate with the measured forces and wear flat area on the wheel.

Hence, from the above discussion it can be seen that, the workpiece surface roughness at a meter-cut-off of 0.8 mm provides a differently defined measure of lubricity from that of the specific energy measurement. In addition the roughness average measurement has shown itself to be specific to the workpiece material ground when ranking fluids, whereas the specific energy measurement has not revealed this disadvantage.

It is interesting to note, aside from this, the implication that for a particular stock removal rate there will be an optimum dresser infeed rate. Not only does increasing the dresser infeed rate above the value necessary to maintain the specific energy consume the wheel faster than is necessary, but it also causes a rougher surface finish.

5.1.6. The change in lubricity with volume of oil.

As a sequel to the work of Torrance [59], which seemed to indicate that a comparatively small amount of oil is necessary to impart the lubricity associated with neat oil grinding fluids, it might have seemed sensible to investigate

the relationship between the percentage composition of oil and the lubricating performance. However, on the advice of the sponsoring company, fluids were only studied at their correct formulation. The influence of additives in the fluid can be shown from the work of Torrance. Consider Figure 77 of the variation of forces versus number of passes; this shows that a sulphur containing additive reduces the forces by a factor varying between 4 and 5. By comparison, the difference in performance due to varying the proportion of oil is small. In addition, for this particular system, the microemulsion containing varying proportions of oil and E.P. additive gives lower forces than the neat oil with E.P. additive; an effect which is presumably owing to the surface active agents contained in the microemulsion rather than to the oil content. Indeed, Furuichi et al. [107] have shown that varying the concentration of surface active agents significantly alters the wheel wear in plunge grinding operations. Torrance also found that, in a system where the oil contained both sulphur and chlorine E.P. additives, the neat oil with additives performed as well as it did when diluted to a 6% or 20% oil in water microemulsion.

Peters and Aerens [34] studied the effect of varying the oil concentration in a soluble oil emulsion. They concluded that increasing the concentration of oil yields only a slight improvement in the specific energy, which they attributed to changes in the fluid viscosity. They found that the influence of the concentration on such parameters as surface roughness, G-ratio, and the chatter limited volume was 'dubious'.

The lubrication tests of this work have shown that the commercially available microemulsion performed better than the macroemulsion although the macroemulsion contained between six and ten times more oil, (1.25 to 2% c.f. 0.2%). Thus it has been demonstrated that, whilst it may be possible to formulate fluids containing only small proportions of oil which are as lubricative as oil, the proportion of oil is not the only determining factor and may play a minor part. Indeed it seems

that the lubricity could depend upon the complex mixture of the many constituents of some fluids. (Contrary to these findings, Nicholson [108] has suggested that the lubricating influence of oil in an emulsion decreases proportionally with the fineness of the droplet size and with the emulsion stability.)

Rezaei [109] has taken a commercial microemulsion and diluted it to 5% rather than the recommended 2%. He found that this fluid showed a performance between those of a macroemulsion and a neat oil, in terms of specific energy and surface roughness when grinding a Nimonic (C1023) workpiece with continuous dressing. (This work showed the same type of behaviour at a 2% dilution.) However the 5% microemulsion appeared to require a lower dresser infeed rate for the avoidance of burn than the other two fluids. It is not known how a 2% dilution would have performed in direct comparison to the 5% dilution.

5.2. COOLING

5.2.1. Validity of the steam calibration.

The assumption has been made that the heat loss from a plunge ground pin obeys a simple convective law. However, this does not seem to give a reasonable account for the temperature profiles seen during the steam calibration tests. The heat loss coefficient has been shown (in Figures 16 and 18) to vary during tests such that a range of values between 180 and 320 W/mm^3 were equally acceptable. During these tests some of the temperature rise in the body of the Sindanyo was due to the steam heating the Sindanyo surface; Figure 78 shows temperature-time curves for Sindanyo heated by steam. However Sindanyo has a thermal conductivity equal to about 2% that of EN9 and 10% that of MARM002. Therefore most of the heat in the Sindanyo in the vicinity of the pin is likely to have come from the pin rather than the steam heated surface (except in positions very near this surface). This means that during grinding tests, although the specific grinding energy of Sindanyo is only

approximately 20% that of the workpiece materials and hence proportionately less energy will be available to enter the Sindanyo at the surface than in the steam tests, the loss characteristics of the Sindanyo would not be expected to be significantly altered. Figure 17 showed how the heat loss coefficient varied with time as the Sindanyo was heated near the pin interface until a steady temperature gradient was achieved. Therefore, assuming from the above discussion that the results are applicable to actual grinding conditions, the value of C_L would be expected to decrease as grinding progresses. It would also be expected to vary with depth from the ground surface.

The measured value of the heat loss term is only valid where the boundary temperature is 100°C. For grinding tests where more energy is available than in the steam simulation the loss coefficient will initially and ultimately be higher than the value measured in the steam tests; conversely, where less energy enters the workpiece the loss coefficient would be expected to be lower.

5.2.2. The importance of cooling in creep feed and conventional grinding.

The most striking feature of the plunge grinding tests was that oil was associated with significantly higher workpiece temperatures than the water based fluids, at a given feed rate, and also that sustainable feed rates (without burn occurring) were much lower, at about 20 mm/min with oil compared to 90 mm/min with the microemulsion on steel workpieces.

Under conventional grinding conditions, with alumina wheels, cooling has been considered to be less important than lubrication (Mercier et al. [48]). Des Ruisseaux and Zerkle [73] have shown theoretically that very high convective heat transfer coefficients are needed to reduce conventional grinding temperatures. This has been confirmed experimentally by Mayer and Shaw [110], who used infra red radiation measurements to compare the temperatures generated when various water

based fluids and oil were used. They showed that the maximum temperatures observed were lower with oil than with water based fluids or with dry grinding. Hence, it has been suggested that lubrication, to reduce the cutting energy, is the best way to reduce the maximum workpiece temperature in conventional grinding.

However, Shaw et al. [111], who measured tool chip interface temperatures, found that, as the depth of cut and workpiece speed were increased, a water based fluid became less effective such that the same temperatures were generated as in dry grinding. They suggested that this occurred either because the fluid could not reach the grinding interface at higher depths of cut, or because there was insufficient reaction time to produce a low shear strength film. Further evidence of this transition in the cooling ability of water based fluids under conventional grinding conditions comes from the work of Yasui and Tsukuda [112]. They have shown that, as the depth of cut is increased, water based fluids suddenly go from producing lower temperatures under the grit than oil to causing temperatures nearly as high as those in dry grinding, as shown in Figure 79. They suggest that this is due to a film boiling effect. Hence, Yasui and Tsukuda have shown that, under some conventional grinding conditions, water based fluids can produce lower surface temperatures than oil, as occurred in this work under creep feed grinding conditions. It may be, therefore, that other researchers (e.g. [110]), who reported lower temperatures with oil than with water, were working under that particular regime where water based fluids are ineffective (owing either to film boiling, or inability to reach the grinding zone).

In contrast, under creep feed grinding conditions, where large volumes of fluid are forced into the grinding zone, the fluid has been shown to have a significant cooling effect (e.g. Shafto [32] and Salter [19]).

The differences between the temperature performances of the two types of fluid, under the conditions usually used for conventional and creep feed

grinding, could be owing to the use of denser wheel structures for conventional grinding. Hassell [113], who used a dense wheel for creep feed grinding, found that oil was superior to water in terms of metal removal rates and power fluxes at burn. Other workers, who have used the induced porosity wheel commonly specified for creep feed grinding, have found that water based fluids were superior in terms of the burn limit (Ye and Pearce [60] and Salter [19]) which is in agreement with the findings of this work. Denser wheel structures could inhibit the transport of sufficient water based fluids for cooling to the cutting zone whereas more viscous oils might cling to the wheel and work surfaces. Hence they would be able to confer some lubrication (and possibly cooling) to reduce the temperatures generated compared to those in dry grinding.

5.2.3. Surface temperatures attained with water based fluids on steel.

The constant surface temperatures recorded when steel was ground with a water based fluid suggest that some sort of equilibrium is established, which is in agreement with the findings of Lee et al. [67] who showed that, when cylindrically grinding with water based fluids the surface temperature rapidly reached an equilibrium value. This suggests that very little heat enters the steel pins. From Figure 18 it can be seen that, at low workpiece temperatures the loss coefficient is high, i.e. that the Sindanyo acts as a large heat sink. This may explain the constant surface temperatures achieved at low plunge feed rates (low workpiece temperatures). At higher feed rates less of the heat energy would be expected to enter the workpiece, because the plunge direction is the same as the major direction of heat flow. Hence more heat energy is removed in the chips before it can be conducted down the workpiece. (This is the basis of the abrasive cut-off method, which relies on ablation.) Such a means of heat removal may counter the effect that a smaller loss coefficient (owing to more rapid heating of the insulation) has at higher feed rates.

The poor performance of the synthetic fluid, in terms of workpiece temperature, seems explicable in terms of entrained air bubbles, preventing sufficient liquid from reaching the grinding zone. Dry grinding, i.e. with air, has been shown to produce higher surface temperatures than with water based fluids. However it is interesting to note that there seems to have been sufficient liquid present for the lubricating effects of this fluid to have been unaffected; it did not appear to cause higher forces or worse surface roughnesses than the other water based fluids.

With water based fluids constant forces and workpiece surface temperatures were achieved, unless the workpiece burned. In such cases burn occurred immediately the test started. These results suggest that:

(1). continuous dressing was in control of the process;

(2). the fluid could remove enough of the heat generated to maintain a temperature equilibrium (unless burn occurred);

(3). when burn occurred, the breakdown in the heat transfer mechanism was rapid, i.e. it occurred over a narrow range of grinding conditions.

However, with oil the surface temperature was found to rise during a test at all feed rates and the rise became more rapid as the test progressed. This suggests that the oil was not able to remove heat at a sufficient rate to maintain thermal equilibrium. It is assumed that this temperature rise was not owing to a change in grit geometry, as all other evidence has suggested that dressing was in control of the process. If burn occurred it was accompanied by a significant increase in forces which then tended to stable (but increased) values. Other researchers have described force and temperature surging on burn and suggested that this is caused by loading patches which are cyclically removed, as the forces increase, and then grow again [114]. However, the use of continuous dressing at a high rate, the absence of

wheel breakdown, and the stability of the increased forces, suggest that loading is unlikely to be a factor in these tests. No loading was seen on the wheel at the end of a test. The most likely explanation would seem to be that the forces generated are those associated with dry grinding at this feed rate, i.e. that some form of film boiling is occurring. Shafto [32] suggested that, in conventionally dressed grinding, these raised temperatures and forces due to film boiling would accelerate wheel wear, causing resharpening and a return to stable grinding conditions. The gradual increase in the forces before burn on such tests may be owing to increasing grit depths of cut, connected with workpiece expansion from surface heating. Such rising forces were not evident at lower feed rates where burn did not occur.

Whereas with water based fluids the delineation between the tests where burn either did or did not occur seemed sharp, it was not so clear with oil. Grinding at a higher feed rate than was known to cause burn could take place successfully for a while before burn occurred when oil was the grinding fluid. If the breakdown in the heat transfer mechanism is assumed to correspond to a critical workpiece surface temperature being attained, then this finding is consistent with the observation that surface temperatures rose as the tests progressed with the oil grinding fluid but that it remained constant with water based fluids.

Heating the oil in a distillation set had indicated that there was a distribution of molecular weight fractions and hence that, at the lower range of boiling temperatures, only a proportion of the oil would be hot enough to vapourise. Hence it seems possible that improved heat transfer might occur as these lower molecular weight fractions reached their boiling temperature but that, owing to the presence of higher molecular weight fractions, the tendency to film boiling might be reduced. Hence it is suggested that the region of enhanced heat transfer may be extended with the oil. The breakdown in heat transfer would still be expected to be catastrophic, as before with the water based fluids.

The Linefrost test suffers from the same drawbacks as other non-grinding tests of cooling, as outlined in Section 2.4.1. However it provided evidence towards the idea that 130°C is a critical temperature for the quenching of steel workpieces by these fluids at atmospheric pressure. Salter calculated from his measured workpiece temperatures that burnout occurred when the surface reached a temperature between 120 and 140°C for steel workpieces and water based fluids. However, in this work, surface temperatures near 160°C were recorded (rather than being extrapolated from temperatures measured lower in the workpiece as Salter's were). The boiling temperatures of fluids are dependent on pressure. Chu Boyi [99] has recorded maximum hydrodynamic pressures of 17 bar in the grinding arc, although this was with oil and a non porous wheel. Even the pressure of the fluid in the shoe (0.5 bar) would raise the boiling point of water to 113°C. It is assumed that if the boiling point of the liquid is raised then the temperature at which burn-out occurs is also raised. In addition, raising the pressure decreases the surface tension of a fluid and this has the effect of increasing the heat flux to the fluid for a given temperature difference (fluid superheat) [115].

From Table 1 it can be seen that the microemulsion contains the highest proportion of emulsifier. This lowers the interfacial surface tension between the oil and water phases allowing smaller oil droplet to be stable. In addition the emulsifier would be expected to lower the surface tension between the fluid and the metal surface, and between the fluid and vapour, encouraging the formation of vapour bubbles at lower fluid superheat. This should promote better cooling and less likelihood of bumping arising from the formation of the large vapour bubbles. Hence microemulsions may reduce the likelihood of the formation of a vapour blanket at a given superheat. This corresponds to the behaviour of the microemulsion in the distillation set, where many small vapour bubbles were formed rather than the bumping which occurred with tap water. This may therefore be one of the contributing factors for the ability of the microemulsion to sustain grinding at higher

feed rates than the other fluids could. Ueno et al. [66] have shown that good wetting ability (achieved using high emulsifier content, causing low surface tension) is associated with effective heat removal.

Surface roughness can affect bubble formation by altering the interfacial surface tension between the surface and the fluid and also by its effect on the availability of nucleation sites for bubble formation. (Hence, on very smooth surfaces and using pure, gas free water, it is possible to superheat water to 150°C before vapour bubbles are formed [115].) Nimonic was shown to produce a smoother surface finish than steel in these tests. This smoother surface finish with Nimonic than with steel may therefore have contributed to the higher surface temperatures measured on Nimonic. However, it is not known whether the differences in sizes of the surface irregularities would be of the order which would affect vapour bubble formation and hence heat flux from the surfaces.

5.2.4. Comparison between experimental results and the thermal model.

The results of this analysis appear to show that higher proportions of the energy enter the workpiece (about 15%) when steel is ground using water based fluids than the 2% values suggested by Salter and Shafto. However, Ohishi and Furukawa [116] added a cooling effect to the Jaeger [72] model and hence calculated that 10% of the grinding energy enters the workpiece under creep feed grinding conditions. Lee et al. [67] showed that, under conventional cylindrical plunge grinding with water and a semi-synthetic, 25 to 35% of the energy entered the steel workpiece and that this value appeared to be independent of the dressing rate used. Hence 15% partitioning with water based fluids on steel would not seem to be an unreasonable value when compared with those of other researchers.

With oil as the grinding fluid the proportion of the grinding energy entering the workpiece (about 30%) was again higher than Salter's values (about 13%).

A lower, rather than higher, value of partitioning might have been anticipated in these continuously dressed tests owing to less friction under the grits. (According to Malkin's model of grinding energies, almost all of this friction energy enters the workpiece, whereas only a portion of the energies associated with the other metal removal mechanisms is able to enter.) However, higher partitioning values with oil than with water based fluids are in agreement with the findings of Salter, even if there is a discrepancy between the actual values.

Results of lubrication measurements suggest that the specific energies, under the same grinding conditions with steel, are in the ratio 1:2 for oil and water based fluids respectively. The workpiece temperatures recorded appeared to be about five times higher with the oil than with the water based fluids. Were the temperature profiles independent of the fluid, the partitioning values might be expected to be approximately in the ratio 10:1. From the modelled results, however, they appear to be in the ratio 2:1 (30%:15%). Despite the differing forms of the temperature profiles for the two fluids (see Figures 62 and 63), there is a discrepancy between model and experiment, and this re-emphasises the degree of uncertainty in the partitioning values obtained by comparison with the thermal model.

A smaller proportion of the energy appeared to enter a Nimonic than a steel workpiece. This might be expected from the lower thermal conductivity of Nimonic. Salter found that roughly two thirds the proportion of energy entering a steel workpiece entered Nimonic under the same conditions. This is broadly born out in this work, although the actual values seem higher than Salter's.

The large error bound associated with this technique by comparison makes further analysis of the partitioning values difficult. There are two separate causes for this error: one arises from the errors from uncertainties in the input parameters for the model which have already been discussed; the other is caused by the difficulty in matching the shapes of the measured and modelled curves. The

latter may partly stem from the temperature dependence of the loss term, and hence the fact that this will vary down the length of the pin. This effect would be more marked on the Nimonic specimens, owing to their lower thermal conductivity causing slower attainment of equilibrium across the Sindanyo interface. The heat capacity is not so different from that of steel. In Appendix 13 it is shown that the range of possible values for the energy entering the chips, fluid, and wheel grits is too large to allow the partitioning to the workpiece to be calculated by subtraction with any accuracy.

Burn was not achieved in the surface grinding tests on Nimonic, even at a maximum normal infeed rate of 100 mm/min, whereas it occurred below 70 mm/min on the insulated plunge ground Nimonic pins. This suggests that the pins were not long enough to provide as good a heat sink as the larger surface ground specimens where the amount of heat available to enter the workpiece reduces around the arc of cut to a minimum at the bottom. This effect may therefore have contributed to the poor correlation between measured and modelled temperatures. However the effect would be expected to be more significant on steel specimens, owing to their higher thermal conductivity, whilst in practice the model proved to be a better fit with steel, than with Nimonic, workpieces. Difficulties in recording temperatures were experienced with Nimonic workpieces and it is possible that poor thermal contacts caused unrealistic recording of workpiece temperatures, and hence later difficulties with data fitting. However, the thermocouple responses had seemed reasonable when checked by playing steam on the face to be ground.

One of the aims of this work was to categorise the cooling abilities of fluids in terms of the percentage of grinding energy which entered the bulk of the workpiece. This seemed useful because the product of this, together with the specific energy, a measure of the lubricating ability, gives a value for the total energy entering the workpiece, and hence the likelihood of workpiece damage. Although it

has been possible to put approximate values to the percentage of the energy which enters the workpiece, inaccuracies in the method were too large to allow comparison between similar water based fluids. However, from these and the surface grinding tests, the water based fluids all appear to be associated with the same specific energy when steel is ground. Therefore the temperature of the workpieces should mirror the relative percentages of energy entering them if the temperature distributions are the same. The interdependence of these parameters was represented pictorially in Figure 5. Hence it would appear that, according to the definitions used for this work, the microemulsion can be said to have a superior cooling ability, i.e. it allows a smaller proportion of the grinding energy to enter the workpiece. The synthetic had a markedly lower cooling ability than the other fluids, although its lubricating ability was comparable with them. One explanation of the lower temperatures recorded when the microemulsion was used would be a superior lubricating action, reducing the total grinding energy. The microemulsion did not, however, appear to reduce the specific energy, and the experimental uncertainty in determining specific energies would not seem large enough to account for the temperature differences recorded.

5.3. DISADVANTAGES OF THE METHODS USED

Whilst the basis of the experimental method is to reproduce grinding conditions but keep the wheel geometry constant there are drawbacks worthy of consideration.

Although the geometry of the wheel has been kept constant, the results of these tests must be considered to be specific to the conditions used. The complexity of the metal removal process in terms of pressure, temperature, stress and chemical reactivity has been outlined; but by way of an additional example, Mathewson [117] has shown that different chemical reactions take place with different grinding wheel grits (e.g. alumina, diamond, silicon carbide, cubic boron nitride). In addition the high dresser infeed rate used may not produce a wheel

surface which is representative of real situations. It is possible that at high dresser infeed rates the distribution of rake angles on the grits may be unrealistic and, hence, so will the proportions of chip formation to ploughing taking place. We know that the local temperature and stress distributions will be specific to the material and thermal characteristics of the workpiece. Although two workpiece materials with quite different thermal and mechanical properties were studied, the results obtained should be considered to be specific to these two materials with their particular combinations of properties. Hence, whilst in these tests the specific energy has proved a reliable means of ranking fluids used when grinding two very different workpiece materials, it should not be assumed that this method of comparing lubricity will rank fluids in the same way independent of the particular wheel/workpiece combination.

Different methods of applying the fluid affect its efficacy and may therefore change the ranking order. Powell [31] has shown that shoes and jets can be equally effective if the flow rate is sufficient, but that differences in fluid properties (e.g. viscosity) may have an effect under other methods of application. For example, whilst the shoe method of application seems highly effective it had the disadvantage of aerating the synthetic fluid studied.

Most importantly it is impossible to isolate entirely the lubricating from the cooling effects of a fluid. Continuous dressing was used in the plunge ground tests in order to try to minimise the influence of fluid lubricity when assessing cooling ability. The proportion of the total energy entering the workpiece was then used as a definition of cooling ability (rather than using workpiece temperatures). However, the nature of the lubrication may affect the way in which heat travels into the workpiece, grits, chips, and the fluid. The quality of the lubrication may affect the proportions of the three types of metal removal mechanism and, if Malkin's model is assumed to hold, therefore affect the partitioning of energy

to the workpiece. Hence the cooling ability would appear to be a function of the lubricating ability.

In the same way, the fluid cooling ability will alter the environment for lubrication by its effect on temperatures in the grinding zone. Ductility is temperature dependent - at high temperatures strain softening, rather than strain hardening, occurs. Temperature also affects fluid viscosity, altering the load bearing capability and possibly the ease with which interfaces can be penetrated. The rates of the chemical reactions necessary to provide lubricative species may be altered within the range of temperatures experienced in the grinding arc. Hence, although the cooling and lubrication effects of a fluid have been isolated to a greater degree than in previous work by the use of continuous dressing, they will always remain interdependent to some extent.

5.4 RECOMMENDATIONS FOR FURTHER WORK

Investigations of the boiling mechanism in grinding when oil is used would seem useful to determine whether parallels exist with the occurrence of 'burn-out' when water based fluids are used.

The Finite Difference model does not appear to reproduce the empirical temperature curves accurately, perhaps because of variations in the loss term as the temperature of the insulation increases. Therefore, more extensive tests should be conducted to determine the variation of the loss coefficient with temperature under transient conditions. A comprehensive axisymmetric Finite Difference (or Finite Element) model, incorporating realistic thermal properties for the Sindanyo should be developed.

A study of the size, shape, and appearance of grinding swarf under continuous dress creep feed grinding may give some indication of the mode of chip formation and hence the degree of lubrication taking place.

6. CONCLUSIONS

The use of continuous dressing for the elimination of the feedback of wheel wear in the grinding process has been investigated. The change in wheel condition, both within the grinding arc during each wheel revolution and on a long term basis, has been shown to be under the control of dressing for a range of parameters used in this work. Also the fluid used in the dressing nip has been shown not to have a significant influence over the geometry (measured in terms of the p.d.f. and c.d.f. curves) of the wheel surface generated.

Under such controlled grinding geometry conditions, measurements of workpiece roughness have been shown not to rank fluids independently of workpiece hardness; measurements of force ratio give an indication of the mode of cutting but are influenced by the work speed and have been shown not to directly correlate with grinding efficiency; measurements of specific energy, however, have been shown to give useful practical values for determining the power input necessary and appear to rank fluids consistently, independent of other grinding parameters. Thus, the specific energies associated with creep feed grinding under constant wheel cutting geometries have been compared for a variety of fluids. The values so obtained have been used as definitions of fluid lubricity. These have clearly indicated that oil is a better lubricant than water based fluids but that, of the water based fluids, a microemulsion appears to be a better lubricant than a macroemulsion which performed no better than plain tap water.

It has also been found that there is an optimum dresser infeed rate, above which the surface roughness becomes worse for no improvement in specific energy.

The technique of maintaining wheel cutting geometry by continuous dressing has been extended to assess an empirical definition of a fluid's cooling

ability. Using continuous dressing at a high infeed rate, to create a sharp wheel, the influence of fluid lubricating ability has been minimised. Then, with a knowledge of the grinding energy available, the proportion of this which enters an insulated pin workpiece under plunge grinding conditions has been used as a definition of fluid cooling ability. This energy partitioning has been investigated using an extant model of temperatures in grinding. It has been demonstrated that there is a good correlation between the energy associated with plunge grinding at a particular feed rate and surface grinding at the same value of maximum normal infeed rate. Thus it seemed reasonable to model creep feed grinding as a series of contiguous plunge grinding operations.

Previous experimental technique has been improved upon by the use of several thermocouples and larger workpieces. However, calibration and error analysis of the model have shown that the experimental procedure used still creates a large degree of uncertainty in the calculated partitioning values. However, the technique still showed clear differences between the water based fluids and oil. The partitioning values obtained appear to be larger than those found by some previous researchers in creep feed grinding (although broadly similar to others), being about 30% for oil and about 15% for water based fluids with steel workpieces. The technique was not sensitive enough to distinguish between the partitioning values for different water based fluids. However, workpiece temperature comparisons, when the same amount of grinding energy was available, seemed to indicate that a microemulsion showed a better cooling ability than other water based fluids. In addition a synthetic fluid performed particularly badly in terms of cooling ability. The critical surface burn-out temperature at which heat transfer broke down was about 160°C with water based fluids and above 240 °C with oil. Whereas this transition was sudden with water based fluids it was less sudden with oil. Oil generated workpiece temperatures which were significantly higher than those with

water based fluids and the burn limit occurred at lower feed rates (20 mm/min compared with 90 mm/min for the microemulsion).

Overall the microemulsion has been shown to have favourable properties when compared to other fluids. It appears to show slightly improved cooling ability, even over other water based fluids, and also to have significantly improved lubricating ability. Despite the low concentration of oil contained in the microemulsion, it appears to perform midway between the superior lubricating ability of oil and that of other water based fluids.

APPENDIX 1.

Some of the typical tests carried out on fluids by the manufacturer.

1. Corrosion tests.

e.g. (a). IP287 - *"Rust prevention characteristics of soluble oil emulsions; chip/filter paper method."*

This method is used to investigate the range of concentrations within which emulsions are effective in preventing rust, and so to rank oils in order of expected performance. However, as it is unreproducible, it is not intended to be used to define safe working dilutions. The water hardness and test temperature are specified.

(b). IP 125 - *"Aqueous cutting fluid, corrosion of cast iron."*

This test assesses the area and intensity of staining and degree of corrosion when steel millings are left in contact with a cast iron plate in the presence of the fluid under evaluation. The reagent quantities, environmental conditions, and time for the test are specified.

(c). Test for free sulphur in neat oils.

This test classifies the level of staining (by comparison to ASTM standards) when a copper strip is immersed in a given volume of the oil for 3 hours at 100°C.

2. Skin sensitivity tests.

Skin irritation/sensitivity tests are carried out on rabbits.

3. Emulsion stability/shelf life.

The concentrate is assessed for stability by cycling the temperature and checking for separation or gelling after a set number of cycles.

The emulsion is made up to a set dilution with very hard water and is visually checked for the degree of separation between the oil and water fractions after standing for a set length of time.

4. Foaming.

The emulsion is made up to a standard concentration using soft water and the volume of foam produced is assessed after shaking (alternatively, air may be blown through the sample at a constant rate) and then leaving to stand for set periods of time.

5. Misting.

There is no standard test for misting. Suppliers, users, and trade associations appear to have designed their own rigs for the visual comparison of misting propensity between fluids. However, the degree of misting in use will depend on the operating conditions. The maximum statutory limit is 5 mg/kg (5 ppm).

6. Chlorinated degradation products.

Mist from oils containing HCl can settle out onto surfaces in the vicinity of the operation and cause corrosion. The test commonly involves placing a mild steel plate over a beaker of the fluid, which is then heated to 160°C for 2 hours. After 24 hours at ambient temperature the plate is checked for signs of corrosion.

7. Wetability.

The propensity of graphite fines to float, sink, or wet is used as a measure of this property.

APPENDIX 2.

The basis for the thermal model.

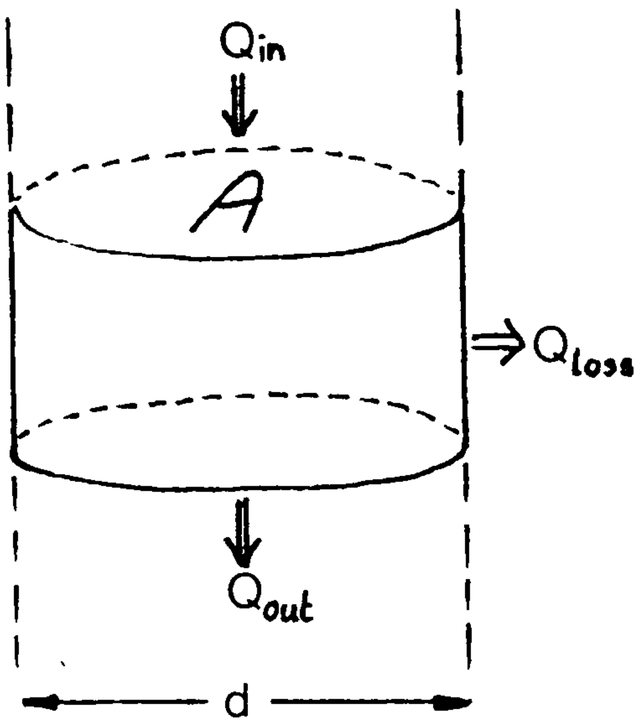

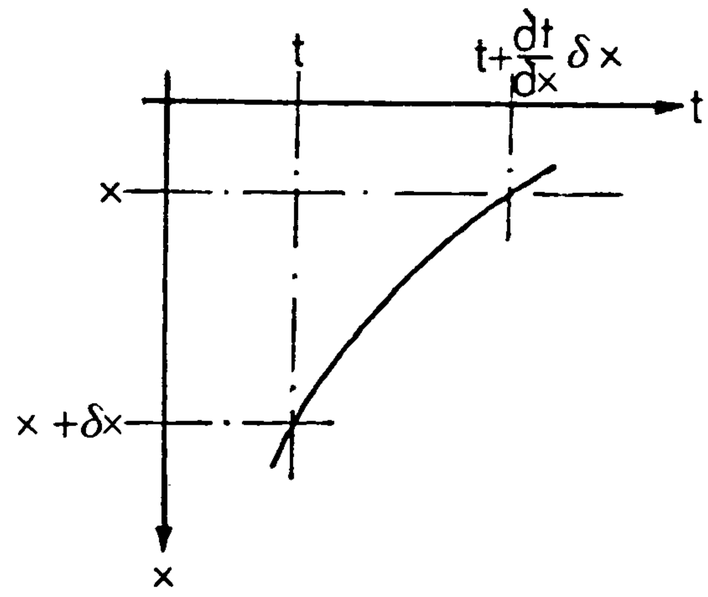

Heat flow equations

Energy approach equates, in a time δT,

heat rise in pin, Q = heat flow in, Q_{in} - flow out, Q_{out} - heat loss, Q_{loss}

Fourier's law for heat flow gives

$$Q_{in} = - kA \frac{\partial t}{\partial x} \delta T$$

and

$$Q_{out} = - kA \frac{\partial}{\partial x} \left[t + \frac{\partial t}{\partial x} \delta x \right] \delta T$$

where k is the thermal conductivity. In reality it is temperature dependent but assumed here not to be. The heat loss term used is an approximation to a one-dimensional convective loss. It depends upon the average boundary temperature and boundary area:

$$Q_{loss} = \pi d C_L \delta x \left[t + \frac{\partial t \delta x}{\partial x \; 2} \right] \delta T$$

where C_L is the convective heat loss coefficient.

The increase in energy of the element is the product of the heat capacity, temperature rise, and time

$$Q = \rho C_p A\, \delta x\, \frac{\partial t}{\partial T}\, \delta T$$

Substituting these into the energy balance equation and simplifying produces a second order differential equation:

$$k \frac{\partial^2 t}{\partial x^2} - 2 \frac{C_L \delta x}{d} \frac{\partial t}{\partial x} - 4 C_L \frac{t}{d} = \rho C_P \frac{\partial t}{\partial T}$$

This can be solved by a numerical approximation, using McLauren's theorem and the finite difference method. At a fixed time, if the temperature varies continuously with position x then, using McLauren's theorem, it can be expressed as a power series

$$t = t_n + \left[\frac{\partial t}{\partial x}\right]_n \frac{x}{L} + \left[\frac{\partial^2 t}{\partial x^2}\right]_n \frac{x^2}{L^2} + \left[\frac{\partial^3 t}{\partial x^3}\right]_n \frac{x^3}{L^3} + \ldots.$$

At 2 positions, n - 1 and n + 1, at distances - Δx and + Δx from n

$$t_{n+1} = t_n + \left[\frac{\partial t}{\partial x}\right]_n \Delta x + \left[\frac{\partial^2 t}{\partial x^2}\right]_n \frac{\Delta x^2}{2} + \ldots.$$

$$t_{n-1} = t_n - \left[\frac{\partial t}{\partial x}\right]_n \Delta x + \left[\frac{\partial^2 t}{\partial x^2}\right]_n \frac{\Delta x^2}{2} - \ldots.$$

$$t_{n-1} + t_{n+1} = 2t_n + \left[\frac{\partial^2 t}{\partial x^2}\right]_n \frac{\Delta x^2}{2} + \left[\frac{\partial^4 t}{\partial x^4}\right]_n \frac{\Delta x^4}{4} + \ldots.$$

Neglecting higher powers (for small Δx)

$$\left[\frac{\partial^2 t}{\partial x^2}\right]_n \simeq \frac{t_{n+1} + t_{n-1} - 2t_n}{\Delta x^2}$$

Similarly, at a fixed position

$$\left[\frac{\partial t}{\partial T}\right]_p \simeq \frac{t_{p+1} - t_p}{\Delta T}$$

Hence, substituting into the energy balance equation with an expression relating the temperature in the future at a point n to the temperature in the past at n, n+1, and n-1 separated by distances Δx

$$t_{n,p+1} = F_o t_{n-1,p} + (F_o - W)t_{n+1,p} + (1 - W - 2F_o)t_{n,p}$$

where F_o is the Fourier number

$$F_o = \frac{k\Delta T}{\rho C_P \Delta x^2}$$

and W is a non-dimensional term for the heat loss

$$W = \frac{2C_L \Delta T}{\rho d C_P}$$

In order to solve this equation it is necessary to specify the boundary conditions. The top face is assumed to be a convective boundary, where the convective heat transfer to the coolant is proportional to the temperature.

The position of the top boundary moves as material is ground away. This is achieved in the model by reducing the distance between nodes at which the temperature is evaluated. These calculations are performed in Fursden's computer program, the logic of which is summarised overleaf.

Computing sequence

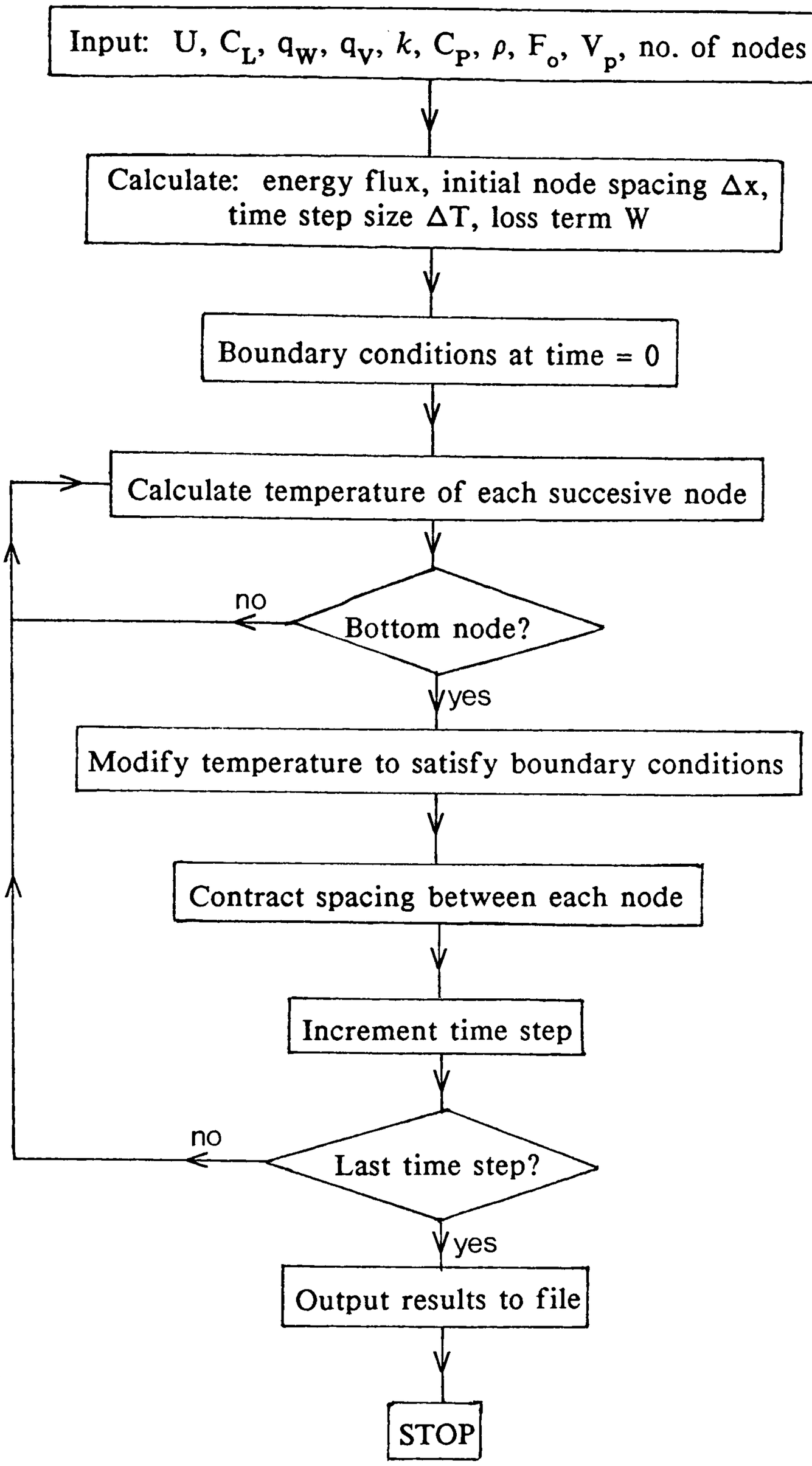

APPENDIX 3.

Definition of surface measurement terms.

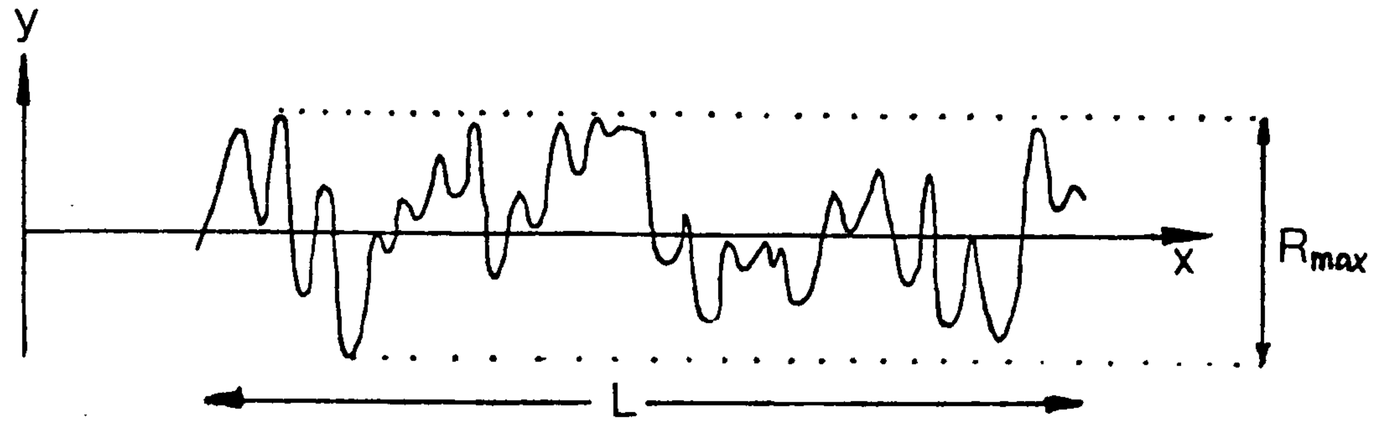

1. **Average arithmetic deviation from centre line (centreline average), R_a.**

$$R_a = 1/L \int_0^L |y|\,dx$$

2. **Peak to valley height, R_{max}.**

This is the vertical distance between the highest peak and the lowest valley within the sample length.

3. **Ten point height, R_z.**

The average height between the 5 highest peaks and the 5 lowest valleys in the sample length.

4. **The frequency distributions of the depths, slopes and degree of curvature.**

These are the histograms of the frequency distribution of y, y' and y".

5a. **R.M.S. deviation from centre line, Z_1.**

$$Z_1 = 1/L \int_0^L y^2 dx$$

5b. **R.M.S. of slope, Z_2.**

$$Z_2 = 1/L \int_0^L y'^2 dx$$

5c. **R.M.S. of curvature, Z_3.**

$$Z_3 = 1/L \int_0^L y''^2 dx$$

5d. Measure of average slope of profile, Z_4.

$$Z_4 = \frac{\sum(\Delta x_i)_{positive} - \sum(\Delta x_i)_{negative}}{L}$$

Where $\sum(\Delta x_i)_{positive}$ is the sum of the lengths for which the slope is positive.

6. Cumulative distribution of peaks.

The percentage of peaks above a particular height (where a peak is an ordinate value which is higher than the neighbouring ones).

7. Probability density function (p.d.f.)

The function representing the probability that a point on the profile lies within a particular height range.

i.e. probability of $a < x < b = \int_a^b pdf(x)\, dx$

8. Cumulative density function (c.d.f.)

The integral of the probability density function.

i.e. $cdf = \int_{-\infty}^{x} pdf(x)\, dx$

This is equivalent to the bearing area characteristic.

9. Degree of fullness.

The ratio of the shaded to the unshaded area.

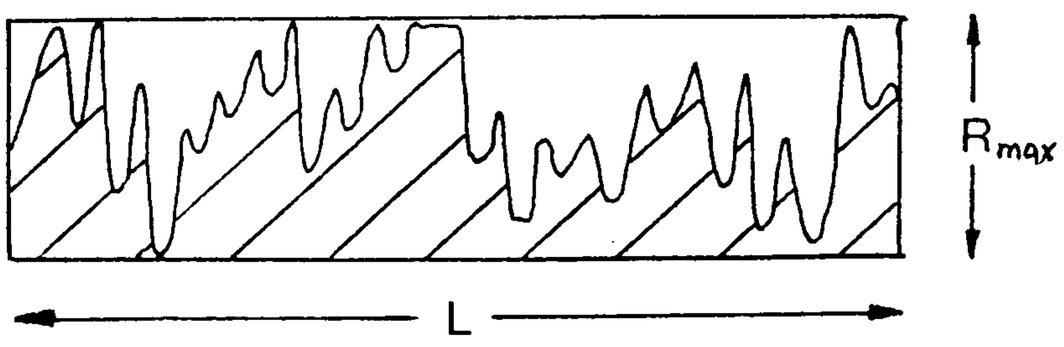

10. Cutting edge ratio, e_L

$$e_L = \frac{\text{area of wheel in contact with workpiece}}{\text{total area}}$$

11. Mean distance between successive peaks, M_L.

This is the mean distance between neighbouring peaks at a particular height.

12. Mean peak land area, M_A.

The average area of each of the peaks at a particular height, assuming that these are circular in cross section. It says nothing about the distribution of the peaks.

13. Autocorrelation function, R_{yy}.

A measure of the similarity of a signal to a lagged form of itself.

$$R_{yy}(\beta) = \lim_{L\to\infty} 1/L \int_{-L/2}^{L/2} y(x)y(x+\beta)\,dx$$

where β is the correlation interval.

14. Power spectrum, S_y.

The Fourier transform of the autocorrelation function.

$$S_y(\omega) = 2/\pi \int_0^{\infty} R_{yy}(\beta)\cos\omega\,d\beta$$

where ω is the frequency.

15. Correlation length.

The distance at which two points on the surface can be considered independent. This has been defined as the value of β when R_{yy} has decayed to 10% of its initial value, i.e. when $\beta = 0$.

16. Cross correlation function, R_{yz}.

A measure of the similarity between two signals, one of which is lagged with respect to the other.

$$R_{yz}(\beta) = \lim_{L\to\infty} 1/L \int_{-L/2}^{L/2} y(x-\beta)z(x)dx$$

APPENDIX 4.

Details of test materials.

1) EN9 - a '55' carbon steel.

a) Composition

Carbon	Silicon	Manganese	Sulphur	Phosphorus	balance
.5-.6%	.05-.35%	.5-.6%	.06% max.	.06% max	Iron

(after Woolman and Mottram [120]).

b) Uses

EN9 is used for moderately wear resistant machined parts where toughness is not important. However it can be heat treated to improve these properties. It was used in its unhardened state for the tests described in this thesis.

c) Mechanical properties

Yield stress 350 MPa [121 (quoted in tons/in^2)].

Hardness 200 VPN (approx.) in the unhardened state.

2) MARM002 - a high temperature "super alloy" developed by Martin Metals, a division of M Marietta Corporation.

a) Composition

Maximum values:

Aluminium	Cobalt	Chromium	Hafnium	Tantalum	Titanium
5.5%	10%	9%	1.5%	2.5%	1.5%

Silicon	Copper	Iron	Manganese	Molybdenum	Boron
.2%	.1%	.5%	.2%	.5%	.02%

balance in Nickel.

b) Uses

MARM002 is used in the manufacture of gas turbine blades, owing to its ability to withstand high temperatures.

c) Mechanical properties

Hardness: 700 VPN approx.

0.1% proof stress at 20°C approximately 811 MPa (this is the value for MARM246 with 1.5% Hafnium, to increase the ductility, making it very similar to MARM002 [122]).

APPENDIX 5.

Details of the six grinding fluids used.

	dilution
oil	
Duckhams Adformal EP7	used neat
macroemulsions	
Castrol Clearedge EP284 (primarily)	50:1 with tap water
Castrol Clearedge E (a few tests)	50:1 with tap water
microemulsion	
ESSO Kutwell 82	50:1 with tap water
synthetic	
Universal - Van Straaten 951N	50:1 with tap water
water	
plain Bristol tap water with no additives (hardness approximately 250 ppm).	

Program listing: determination of grinding variables.

```
70  DIM WH(4)
80  DIM WA(4)
90  DIM S(23)
100  GOSUB 130: REM   INPUT DATA
110  GOSUB 282: REM   CALCULATION
120  GOSUB 670: REM     PRINT DATA
125  END
130  REM  ****** INPUT ROUTINE
135  INPUT "PRINTER SLOT? ";X
140  IF X < 0 OR X > 7 THEN 130
150  PRINT "TEST NUMBER? ";
160  INPUT "";Y
170 D$ =  CHR$ (4)
180  POKE 33,33
190  PRINT D$;"PR£";X
200  PRINT "TEST NUMBER "Y
210  PRINT "WHEEL DIAMETER IN MM ?"
220  INPUT DI
230  PRINT "EXPECTED DEPTH OF CUT (MM)  ?"
240  INPUT DC
250  PRINT "DESIRED MNIR IN MM/MIN ?"
260  INPUT M1
265  PRINT "4 WEDGE HEIGHTS STARTING AT .5 DEGREE WEDGE ?"
266  INPUT WH(1),WH(2),WH(3),WH(4)
270  PRINT "DESIRED DRESSER INFEED RATE IN MICRONS PER REV?"
280  INPUT DFR
281  RETURN
282  REM  *****CALCULATIONS
283 WR = DI / 2
284 W1 = WR + 50
285 C1 = (WR - DC) / WR
286 S1 =  SQR (1 - C1 ^ 2)
287 R1 = 572957.8 / DI
288 Q = R1 * 3 * .1162 * S1
289 G = M1 / Q
290  PRINT "GEAR RATIO REQUIRED ="G
300  PRINT "GEAR RATIO TO BE USED ?"
301  INPUT GU
310 WA(1) = .45
311 WA(2) = 1
312 WA(3) = 2
313 WA(4) = 4.3
320 S(1) =  - .03
321 S(2) =  - .025
322 S(3) =  - .02
323 S(4) =  - .017
324 S(5) =  - .015
325 S(6) =  - .012
326 S(7) =  - .010
327 S(8) =  - .007
328 S(9) =  - .005
329 S(10) =  - .004
330 S(11) =  - .002
331 S(12) = 0
332 S(13) = .002
333 S(14) = .004
334 S(15) = .005
335 S(16) = .007
336 S(17) = .01
337 S(18) = .012
338 S(19) = .015
339 S(20) = .017
340 S(21) = .02
341 S(22) = .025
342 S(23) = .03
343 X = 99
360 CA =  (W1 ^ 2 + 386 ^ 2 - 105 ^ 2) / (2 * 386 * W1)
370 L =  SQR (WR ^ 2 + 386 ^ 2 - 2 * WR * 386 * CA)
380 SA =  SQR (1 - CA ^ 2)
390 SF = SA * 386 / L
400 CF =  SQR (1 - SF ^ 2)
410 F =  ATN (SF / CF)
420 PI = 3.142
430 G = PI / 2 - F
440 CT =  (105 ^ 2 + 386 ^ 2 - W1 ^ 2) / (2 * 386 * 105)
450 S =  SQR (1 - CT ^ 2)
460 T =  ATN (S / CT)
470 T1 = PI / 2 - .4822 - T
480 T2 = PI / 6 - T1
490 T3 = T1 - (13 * 2 * PI / 360)
491  FOR M = 1 TO 4
492 WH = WH(M)
500 B = 305 *  COS (T2) + (307 - WH - 305 *  SIN (T2))
510 TE =  (307 - WH) / B                          *  TAN (T3)
520 E =  ATN (TE)
530 Y = B /  COS (E)
531  FOR N = 1 TO 23
532 WA = WA(M) + (S(N) * 7.2667)
540 WA = WA * PI / 180
550 DX =  TAN (WA) / ( COS (E) +  SIN (E) *  TAN (WA))
560 DD = L *  COS (G) * DX / Y
570 D = R1 * 3 * .1162 * DD * GU
580  IF  ABS (DFR - D) > X THEN  GOTO 620
590 X =  ABS (DFR - D)
600 ANG = WA(M)
605 SHI = S(N)
610 DRES = D
620  NEXT N
630  NEXT M
645 S3 =  SQR (1 - C3 ^ 2)
655 M3 = M1 * S3 / S1
660  RETURN
670  REM  ****** OUTPUT RESULTS
675  PRINT "DRESSER TO SLIDEWAY SPEED RATIO="DD
680  PRINT "WHEEL SPEED ="R1"RPM"
715  PRINT "USE "ANG" DEG WEDGE & "SHI" MM SHIM"
765  PRINT "INFEED RATE = ";DRES" MIC/REV"
770  PRINT D$;"PR£0"
780  RETURN
```

APPENDIX 7.

Correction to the value of V_n due to diminishing wheel diameter.

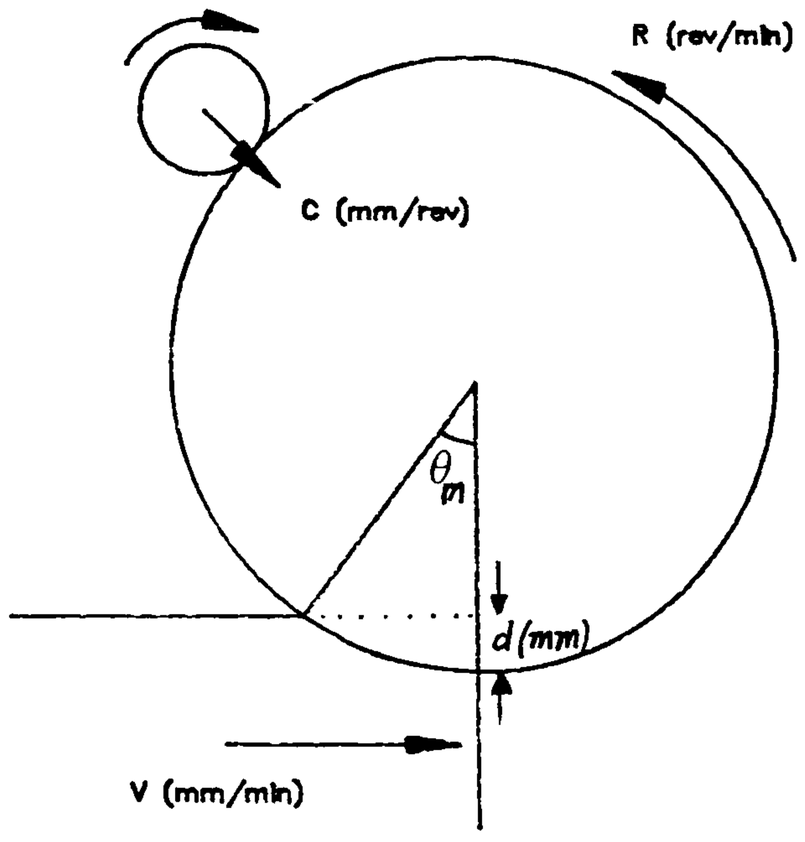

At any point in the grinding arc, the normal infeed rate is $V\sin\theta$ - CR (mm/min)

where θ is the angle subtended between that point and the bottom of the arc.

Hence the maximum normal infeed rate is $V\sin\theta_m$ - CR

Since CR is a constant around the arc, and $V\sin\theta$ decrease towards the bottom of this arc, this reduction due to dressing has a proportionally larger effect on the normal infeed rate as θ decreases (i.e. towards the bottom of the arc).

From the figure overleaf, where the wheel radius reduces from r_1 to r_2 in time t and γ is the net taper ground on the workpiece,

$$r_2 = r_1\cos^2\gamma \quad \text{and} \quad \sin\gamma = CR/V$$

$$\cos\theta_m = \frac{r_1\cos\gamma - d}{r_2} = \frac{r_1\cos\gamma - d}{r_1\cos^2\gamma}$$

The stock removal rate can be written as

$$r_2 \int_{\gamma}^{\theta_m} (V\sin\theta - CR)\, d\theta$$

$$= r_2 \left[-V\cos\theta - CR\theta\right]_{\gamma}^{\theta_m}$$

$$= r_1\cos^2\gamma \left[V(\cos\gamma - \cos\theta_m) - CR(\theta_m - \gamma)\right]$$

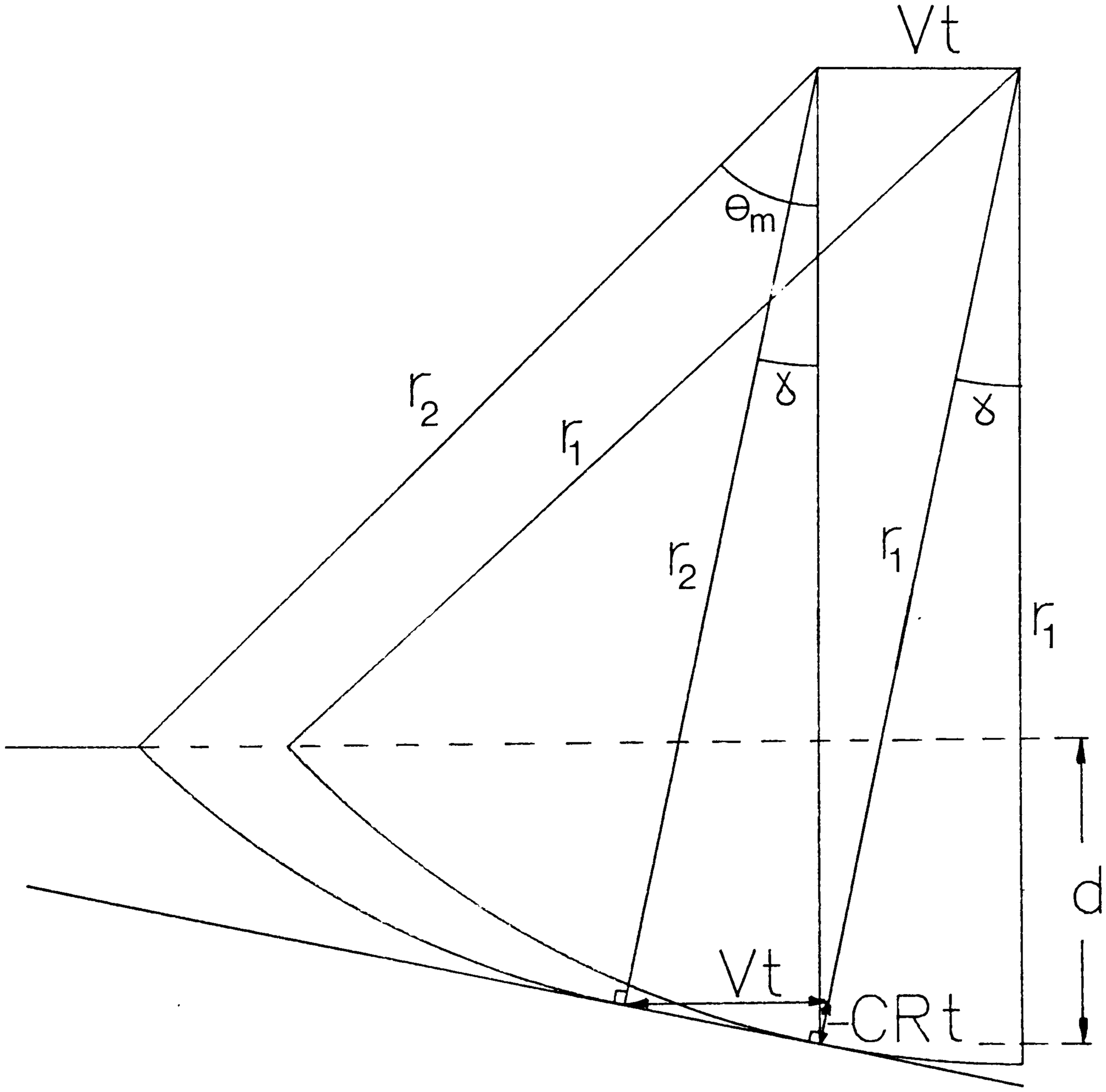
Vt
θm
r2
r1
γ
γ
r2
r1
r1
d
Vt
CRt

Program listing: calculation of forces, power flux, and stock removal rate.

```
360  REM  CALCULATIONS SUBROUTINE
370 C = .0169 + .000951 * (H - DC / 2)
380 D =  - (.0326 + .00216 * (H - DC / 2))
390 E = .209 + .000155 * (H - DC / 2)
400 PI = 3.142
410 WR = DI / 2
420 C1 = (WR - DC) / WR
430 S1 =  SQR (1 - C1 ^ 2)
440 A1 =  ATN (S1 / C1)
450 A2 = A1 * 2 / 3
460 S6 = S5 * PI * DI: REM  SURFACE SPEED
470 S4 = S5 * .1162 * GF * 3.175
482 CD = DR * 3.175 / 3
484 K = CD * S5 / 1000: REM  WHEEL LOSS MM/MIN
485 SG = K / S4
486 CG =  SQR (1 - SG ^ 2)
487 AG =  ATN (SG / CG)
489 CT = (WR * CG - DC) / (WR * CG ^ 2)
489 ST =  SQR (1 - CT ^ 2)
490 AN =  ATN (ST / CT)
491 R2 = WR * CG ^ 2 * S4 * ((CG - CT) - SG * (AN - AG))
492 R3 = R2 / 60
495 M2 = S4 * S1 - K
500 L1 = A1 * WR
510 A(1,1) = .209
520 A(1,2) = 0.003
530 A(1,3) = C
540 A(2,1) = .006
550 A(2,2) = .333
560 A(2,3) = D
570 A(3,1) = 0.009
580 A(3,2) = 0.003
590 A(3,3) = E
```

Results for surface grinding tests

```
100  DIM A(3,3),B(3,3),C(2,2)
110  GOSUB 140: REM   INPUT DATA
120  GOSUB 360: REM   . CALCULATIONS
130  GOSUB 1080: REM   PRINT DATA
135  END
140  INPUT "PRINTER SLOT? ";X
150  IF X < 0 OR X > 7 THEN 140
160  INPUT "TEST NUMBER? ";Y
170 D$ =  CHR$ (4)
180  POKE 33,33
190  PRINT D$;"PR£";X
200  PRINT "TEST NUMBER "Y
205  PRINT "**************"
210  PRINT "DEPTH OF CUT (MM)?"
220  INPUT DC
230  PRINT "WHEEL DIAMETER (MM)?"
240  INPUT DI
250  PRINT "WIDTH OF SPECIMEN (MM)?"
260  INPUT W
270  PRINT "WHEEL SPEED (REV/MIN)?"
280  INPUT S5
290  PRINT "GEAR REDUCTION ?"
300  INPUT GF
310  PRINT "U.V. TRACE DEFLECTIONS DL,DR,DH?"
320  INPUT K1,K2,K3
330  PRINT "HEIGHT OF WORKPIECE AND PACKING?"
335  INPUT H
340  PRINT "OLD DIR ?"
345  INPUT DR
346  PRINT ""
348  PRINT "DEFLECTION MATRIX"
350  RETURN
```

```
600  FOR J = 1 TO 3
610 B(J,J) = 1
620  NEXT J
630  FOR J = 1 TO 3
640  FOR I = J TO 3
650  IF A(I,J) <  > 0 THEN 690
660  NEXT I
670  PRINT "SINGULAR MATRIX"
680  GOTO 1240
690  FOR K = 1 TO 3
700 S = A(J,K)
710 A(J,K) = A(I,K)
720 A(I,K) = S
730 S = B(J,K)
740 B(J,K) = B(I,K)
750 B(I,K) = S
760  NEXT K
770 T = 1 / A(J,J)
780  FOR K = 1 TO 3
790 A(J,K) = T * A(J,K)
800 B(J,K) = T * B(J,K)
810  NEXT K
820  FOR L = 1 TO 3
830  IF L = J THEN 890
840 T =  - A(L,J)
850  FOR K = 1 TO 3
860 A(L,K) = A(L,K) + T * A(J,K)
870 B(L,K) = B(L,K) + T * B(J,K)
880  NEXT K
890  NEXT L
900  NEXT J
902  FOR I = 1 TO 3
904  FOR J = 1 TO 3
906  PRINT  INT (B(I,J) * 1000 + 0.5) / 1000;"   ";
908  NEXT
909  PRINT : NEXT
910 F1 = B(1,1) * K1 + B(1,2) * K2 + B(1,3) * K3
920 F2 = B(2,1) * K1 + B(2,2) * K2 + B(2,3) * K3
930 F3 = B(3,1) * K1 + B(3,2) * K2 + B(3,3) * K3
940 F4 = F1 + F2
945 HZTLF = F3 / W: REM  HORIZONTAL FORCE
950 VERF = F4 / W: REM  TOTAL VERTICAL FORCE
952 F9 = HZTLF / VERF
954 F3 =  - F3
955  REM  TORQUE BASED CALCULATIONS
956 HC = H + 12 + WR - DC: REM  CENTRE TO STRUT DISTANCE
958 TQ = F1 * 122 - F2 * 11 + F3 * HC: REM  TORQUE
960 TF = TQ / WR
962 TA = TF / W
966 SQ = TA * S6 * .001 / R2
967 PQ = SQ * M2 / 60
968 NF =  SQR (F4 ^ 2 + F3 ^ 2 - TF ^ 2)
970 RTHETA =  ATN (TF / NF) -  ATN (F3 / F4)
972 NO = NF / W
974 PR = RTHETA / A1
976  REM  END OF TORQUE BASED CALCULATIONS
980 F5 = F3 *  COS (A2) + F4 *  SIN (A2): REM TANGENTIAL FORCE
990 F6 = F4 *  COS (A2) - F3 *  SIN (A2): REM  RADIAL FORCE
1000 R = F5 / F6: REM  FORCE RATIO
1004 K6 = K3 + F3 * E: REM  DEFL.ON H DUE TO VERF
1005 K4 = K1 + F3 * C: REM  DEFLECTION ON LEFT
1006 K5 = K2 + F3 * D
1007 N1 = K4 * B(1,1) + K5 * B(1,2) + K6 * B(1,3)
1008 N2 = K4 * B(2,1) + K5 * B(2,2) + K6 * B(2,3)
1009 RL = K5 / K4
1010 F7 = F5 / W
1011 N4 = (N1 + N2) / W
1020 F8 = F6 / W
1030 E1 = F7 * S6
1045 SP = F7 * S6 * .001 / R2
```

```
1055 PL = SP * M2 / 60
1060  IF Z = 1 GOTO 1080
1070  RETURN
1080  REM  PRINT SUBROUTINE
1085  PRINT ""
1086  PRINT "DRESSER INFEED RATE="CD"MIC/REV"
1087  PRINT "SLIDEWAY SPEED ="S4"MM/MIN"
1088  PRINT "RIGHT/LEFT FORCE="RL
1089  PRINT "RIGHT +LEFT ="N4"N/MM"
1090  PRINT "HORIZONTAL FORCE ="HZTLF"N/MM"
1100  PRINT "VERTICAL FORCE ="VERF"N/MM"
1110  PRINT "FORCE RATIO="F9
1112  PRINT "ARC LENGTH="L1"MM"
1114  PRINT ""
1116  PRINT "FROM 2/3 ARC ANGLE"
1120  PRINT "TANGENTIAL FORCE="F7"N/MM"
1130  PRINT "NORMAL FORCE="F8"N/MM"
1140  PRINT "FORCE RATIO="R
1145  PRINT ""
1235  PRINT "FROM TORQUE CALCULATION"
1240  PRINT "TANGENTIAL FORCE="TA
1250  PRINT "NORMAL FORCE="NO"N/MM
1260  PRINT "FORCE RATIO="TA / NO
1270  PRINT "RESULTANT THETA="RTHETA"RADIANS"
1280  PRINT "ARC ANGLE ="A1"RADIANS"
1290  PRINT "RATIO OF ANGLES="PR
1300  PRINT ""
1310  PRINT "SRR="R3"MM^3/MM/SEC"
1320  PRINT "MNTR="M2"MM/MIN"
1330  PRINT "SE ,2/3 ARC="SP"J/MM^3"
1335  PRINT "PF, 2/3 ARC="PL"W/MM^2"
1340  PRINT "SE FROM TORQUE="SO"J/MM^3"
1350  PRINT "PF FROM TORQUE="PO"W/MM^2"
1389  PRINT ""
1400  PRINT D$;"PR£0"
1410  RETURN
```

Results for plunge grinding tests

```
95 PI = 3.142
100  INPUT "PRINTER SLOT ?";X
110  IF X < 0 OR X > 7 THEN 100
120  INPUT "TEST NO ?";Y
130 D$ =  CHR$ (4)
140  POKE 33,33
150  PRINT D$;"PR£";X
160  PRINT "TEST NO. "Y
170  PRINT "**********"
180  PRINT "MATERIAL ?"
185  INPUT M$
190  PRINT "WHEEL DIA?'
195  INPUT WD
200  PRINT "RPM?"
205  INPUT RPM
210  PRINT "DEFLECTIONS?"
215  INPUT D1,D2,D3
220  PRINT "GAIN?"
225  INPUT GN
226  PRINT "PLUNGE SPEED(MM/MIN)?"
227  INPUT PS
228  PRINT "WORK DIA?"
229  INPUT DI
230 K1 = 11.628
232 K2 = 11.03
234 K3 = 11.75
240 FH =  SQR (3) / 2 * (K3 * D3 + K2 * D2) / GN
250 FV = ((K1 * D1) + .5 * (K3 * D3 - K2 * D2)) / GN
260 SRR = PS * (DI / 2) ^ 2 * PI
270 FR =  SQR (FH ^ 2 + FV ^ 2)
280 RA =  ATN (FV / FH)
290 SE = FV * PI * WD * RPM / (SRR * 1000)
300 PF = SE * PS / 60
310  PRINT "HOR. FORCE= "FH
320  PRINT "VER. FORCE= "FV
330  PRINT "RES. FORCE= "FR
340  PRINT "RES. ANG.= "RA
350  PRINT "SRR= "SRR
360  PRINT "SE= "SE
370  PRINT "PF= "PF
380  PRINT D$;"PR£0"
390  END
```

Program listing: computation of p.d.f. and c.d.f

```
 10 ! FINDING PDF
 20 ! BINARY DATA
 30 ! TRANSFER ROUTINE
 40 CLEAR
 45 OPTION BASE 0
 50 DIM B$[4100]
 60 B$=""
 65 SHORT H(4100)
 70 FOR N=1 TO 4100
 71 H(N)=0
 72 NEXT N
 80 SEND 7 ; MTA LISTEN 7 SCG 1
 90 SEND 7 ; DATA "C3F3Y120%0D2R
    4T0.1E0B"
100 SEND 7 ; DATA "IF3"
110 SEND 7 ; UNT UNL
120 SEND 7 ; MLA TALK 7 SCG 0
130 ENTER 7 USING "#%,#%K" ; B$
135 ! FINDING GREATEST
136 ! HEIGHT OF PROFILE
140 GCLEAR
141 SCALE 5,4094,0,250
142 XAXIS 0,500 @ YAXIS 0,50
143 FOR N=5 TO 4094
144 PLOT N,NUM(B$[N,N])
145 NEXT N
146 COPY
150 X=NUM(B$[5,5])
155 FOR N=6 TO 4094
160 IF NUM(B$[N,N])>X THEN X=NUM
    (B$[N,N])
164 NEXT N
166 Y=X-133
167 GCLEAR
168 SCALE 5,4094,0,250
169 XAXIS 0,500 @ YAXIS 0,50
170 FOR N=5 TO 4094
171 IF NUM(B$[N,N])<Y THEN GOTO
    176
172 H(N)=(NUM(B$[N,N])-Y)*250/13
173 GOTO 177
174 GOTO 177
176 H(N)=0
177 PLOT N,H(N)
178 NEXT N
179 COPY
182 INTEGER A(51),C(51)
183 FOR N=0 TO 51
186 A(N),C(N)=0
188 NEXT N
200 FOR N=5 TO 4094
210 D=INT(H(N)/5)
220 A(D)=A(D)+1
230 NEXT N
240 C(0)=0
250 B=0
260 FOR N=1 TO 51
270 C(N)=A(N)+B
280 B=C(N)
290 NEXT N
300 GRAPH @ GCLEAR
310 SCALE 0,51,0,250
315 XAXIS 0,10 @ YAXIS 0,50
320 X,Y=0
330 PLOT X,Y
340 FOR N=1 TO 51
350 X=X+1
360 Y=A(N)
370 PLOT X,Y
380 NEXT N
385 COPY
400 GCLEAR
410 SCALE 0,51,0,4500
411 XAXIS 0,10 @ YAXIS 0,1000
420 X=0
430 FOR N=1 TO 51
440 X=X+1
450 Y=C(N)
460 PLOT X,Y          473 COPY
470 NEXT N            480 END
```

APPENDIX 10.

Comparison of the thermal properties of MARM002 with those of EN9.

MARM002

thermal conductivity	9.6	W/m/K
specific heat capacity	422	J/kg/K
density	8560	kg/m^3

EN9

thermal conductivity	41.0 to 46.7	W/m/K
specific heat capacity	418 to 490	J/kg/K
density	7800	kg/m^3

APPENDIX 11.

The validity of 0.8 mm as a meter-cut-off value for the surface roughness measurements.

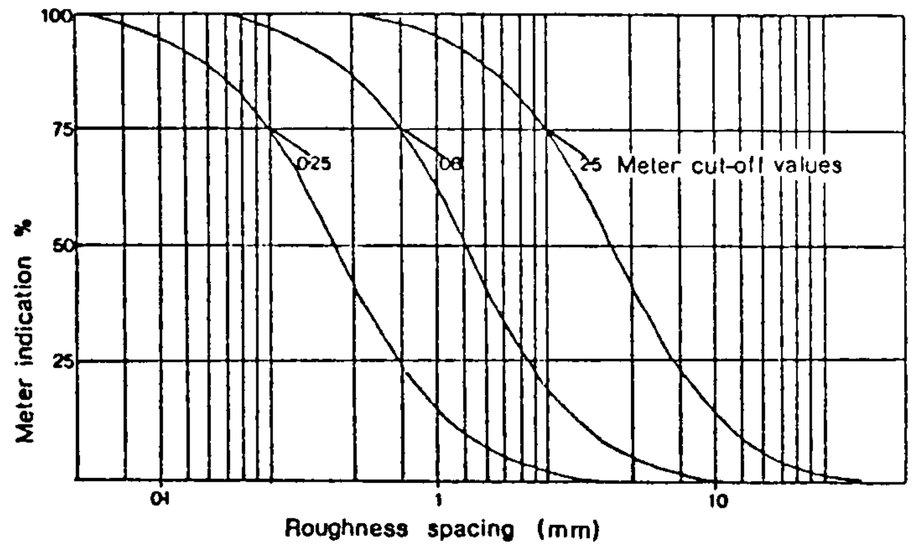

From the above graph it can be seen that a meter cut-off of 0.8 mm will give prominence to features with spacings between 270 and 800 μm when the roughness average is calculated. The average grit diameter for the wheel used is of the order of 250 μm. The grit centre separation can be calculated as

$$u = 1.8\ r\ s^{0.3}$$

where r = grit radius

s = grinding wheel structure factor

giving a value for u of about 660 μm. The wheel profile separation, α, is 923 μm ($\alpha = \sqrt{3}\ \{u-r\}$). These together suggest that 0.8 is indeed the optimum value of the meter-cut-off.

Peklenik [86] suggests however that cutting elements with dimensions smaller than one grit diameter can be produced. Indeed Baul et al. [81] and Sayles and Thomas [94] have found experimental evidence of this when analysing wheel profiles. The results of Sayles and Thomas imply that, in one pass creep feed grinding where the ratio of wheel to work speeds is particularly high, the surface finish is dependent only upon the wheel structure. Hence, whilst the sizes of chips appear from Figure 32 to reach a constant value once a dresser infeed rate of about 1

μm/rev is reached, the surface roughness of the specimen measured at the usual meter-cut-off continues to increase above this value.

APPENDIX 12.

The availability of oxygen in grinding.

The molar volume of oxygen (v_1) at 1 atmosphere pressure (p_1) and 273 K (t_1) is 22.414 litres. Assuming oxygen to be an ideal gas

$$\frac{p_1 v_1}{t_1} = \frac{p_2 v_2}{t_2}$$

Therefore the molar volume of O_2 (v_2) at a pressure of 10^{-3} Torr (p_2) and a temperature of 293 K (t_2) will be

$$v_2 = 1.8 \times 10^7 \text{ l}$$

1 mole of O_2 weighs 32 g
Hence at 10^{-3} Torr, 1 litre of O_2 contains 1.8 μg.

1 litre of water at atmospheric pressure and ambient temperature commonly contains 9 mg dissolved O_2 [99].
Therefore the ratio of gaseous O_2 necessary for beneficial effect in dry grinding [44] to the O_2 available in tap water

$$= 1.8 \times 10^{-3} : 9 = 1 : 5 \times 10^{+3}$$

However, the diffusion coefficient D_g for gaseous O_2 is

$$D_g = (3/16)\lambda c = 6.56 \text{ m}^2/\text{s}$$

where c = average molecular speed = 443 m/s

λ = mean free path of a molecule = $\dfrac{kt}{\sqrt{2}\,\sigma p}$

k = Boltzmann constant = 1.38×10^{-23} J/K

t = temperature = 293 K

p = pressure = 0.13333 Nm^{-2}

σ = collision cross-section = 2.7×10^{-19} m^2

The diffusion coefficient for oxygen in water D_{H_2O} is approximately 3×10^{-9} m^2/s [123], hence

$$D_g : D_{H_2O} = 2 \times 10^9 : 1$$

Therefore, overall, although there is 5000 times more oxygen in water than the amount shown to be beneficial [44] the transport properties in water are such that the

availability of water-born oxygen is approximately 1/1000000th of that shown to be necessary in the grinding zone.

APPENDIX 13.

Energy partitioning in grinding.

The energy in grinding is known to be converted almost entirely to heat. This heat energy is then divided between the workpiece, the grinding chips, the wheel grits and the fluid (or, in dry grinding, the environment). Therefore it may be possible to determine the proportion of energy entering the pin by subtracting the energies entering the other three items from the total.

Energy entering the fluid

Lee et al [67] showed that under conventional cylindrical plunge grinding conditions with water and a semi-synthetic 25 to 35% of the energy entered a steel workpiece. They also found that 75 to 85% entered the workpiece under dry grinding and hence concluded that 50% of the energy is taken away by the coolant. This was based on the assumption that the proportion of the heat energy entering the chips and the wheel is little affected by the fluid used and the interface temperature - Des Ruisseaux and Zerkle showed that the convective cooling coefficient of such fluids is too small to affect the peak grinding temperatures in conventional grinding, hence the assumption seems reasonable.

Energy entering the chips

Geisweid and Gärtner [118] recorded peak temperatures of 500°C under creep feed grinding condition and at this temperature chips could carry away about 2.5 J/mm^3. Malkin [61] measured local peak temperatures in conventional grinding to be near the melting energy of the workpiece and several investigators have calculated that localised peak chip shear plane temperatures are of this order [73]. If chips leave the workpiece at these temperatures they could carry away a maximum of 9.5 J/mm^3 (heat capacity plus melting energy). Juchem and Cooley [13]

claim that chips can carry away up to 80% of the total heat generated in creep feed grinding.

It has already been suggested that the peak grinding temperatures under a grit are unaffected by the fluid, and that therefore the energy entering the chips and wheel will be independent of the fluid.

Energy entering the grits

This can be calculated if the heat flux to the grits is assumed to depend upon the mean temperature gradient for a given contact time.

Heat flux to the grit, $q = 2T_0 \sqrt{(k\rho C_P/\pi t)}$

where, contact time, $t = 2l/V_W = 1.5x10^{-3}$ seconds.

and l = contact length

Assuming that the grit temperature, T_0, is approximately 1500°C gives a value for q of $2.6x10^8$ J/m^2s. However, this value of heat flux should be reduced by the contact area of the grits $\simeq$ 0.025% of the total surface area (from Figure).

This gives a value of heat flux to the grit of $6.5x10^4$ $J/m^2/s$.

Energy fluxes on steel workpieces with oil or with water based fluids at dresser infeed rates giving wear flat areas of 0.025% were measured in the range 14 to 35 W/mm^2 (20 to 50 times greater than this heat flux value). This suggests that 2 to 5% of the grinding energy enters the wheel grits.

However, the uncertainty in determining these three energies does not make it possible to specify the energy entering the workpiece by subtraction with enough accuracy to be of value.

REFERENCES.

1. **Doyle, E.D., & Turley, D.M.,** *"The nature of surface finish produced by grinding."* Proc. 4th North American Metal Working Research Conf., May 1976, pp346-350.

2. **Duwell, E.J., & McDonald, W.J.,** *"The effect of active gases on the dry grinding of steel with aluminium coated abrasives."* Wear **4** pp384-386 (1961).

3. **Anon.** *"A stream of development."* Mach.Prod.Eng., pp143-147, 3rd Sept., 1986.

4. **Gannon, J.E., Bennett, E.O., Onyekwelu, I.U., & Izzat, I.N.,** *"Benzylamines in cutting fluids: inhibitory properties."* Trib.Int. 13(1), Feb. 1980.

5. **Kilbourne, L.W.,** *"The refining of waste lubricating oils."* I.Mech.E. Conf.Pubn. C235/76. (1976)

6. **Shintaku, J., Noda, H., Hirose, M., & Fujimaki, H.,** *"On biodegradation of metal cutting emulsions."* Int. Symp. on Metalworking Lubn., San Francisco Ca., Aug. 1980.

7. **Russell, J.,** Esso, Private communication.

8. **Ishibashi, A., & Katsuki, A.,** *"Effects of rust preventatives in cutting fluids on tool wear."* Bull.Jap.Soc.Prec.Eng., 5(3), Sept. 1971.

9. **Ellendman, M.,** *"How coolants affect the performance of resin-bonded abrasive wheels."* Mach.Prod.Eng., Nov. 19th, 1969.

10. **Imanaka, O., Fujino, S., & Shinohara, K.,** *"Effect of environment on the fracture strength of aluminium oxide grains."* Bull.Jap.Soc.Prec.Eng. 2(1), 1966.

11. **Tripathi, K.C.,** *"Contradictions and gaps in present theory of lubrication: main challenge to newer developments."* Int. Symp. on Metalworking Lubn., San Francisco Ca., Aug., 1980.

12. **Anon.** *"Creep feed grinding - the answer to a production engineer's dream ?"* Prod.Engr. **58**(12) pp20-24, Dec. 1979.

13. **Juchem, H.O., & Cooley, B.A.** *"Creep feed grinding - a review."* Ind. Dia. Rev. **6** pp313-319, 1984.

14. **Peters, J., & Vansevenant, E.,** *"A thermal model covering pendulum grinding and creep feed grinding."* Annals of the CIRP **32** pp491-494, Jan. 1983.

15. **Andrew, C., Howes, T.D., & Pearce, T.R.A.,** *"Creep feed grinding."* Holt, Rinehart & Winston 1985.

16. **Trmal, G.J.,** *"Comparison of creep feed and conventional grinding."* Proc. 21st MTDR Conf., 1980.

17. **Morgan, J.E.,** *"The grinding of glass fibre reinforced plastics."* 5th Poly.Symp.Manuf.Eng., May 1986, pp290-297.

18. **Davidson, T.N.,** *"Creeping to higher grinding productivity."* Mod.Mach.Shop, Dec. 1982, pp50-57.

19. **Salter, N.D.,** *"Creep feed cylindrical grinding of deep forms."* PhD thesis, University of Bristol, 1985.

20. **Anon.** *"Creep feed grinding lifts quality and cuts costs."* Mach.Prod.Eng., 6th Feb., 1985.

21. **Morgan, J.E.,** *"Filament wound pipes - machining and finishing."* 6th Int.Conf., "Plastic Pipes", University of York 1985. Proc. published by the Plastics and Rubber Institute.

22. **Sprow, E.E.,** *"Continuous dress creep feed grinding - should we be taking it more seriously ?"* Tooling & Prod., June 1984, pp53-59.

23. **Astrop, A.,** *"CNC complements operator skills."* Mach.Prod.Eng., 18th Sep., 1985.

24. **Hahn, R.,** *"Grinding wheel wear, fluids and chatter limited grind time, a leverage for reduction of grinding costs."* Int.Comm. to CIRP STC"G", Jan. 1976.

25. **Shafto, G.R., Howes, T.D., & Andrew, C.,** *"Thermal aspects of creep feed grinding."* 16th MTDR Conf., 1975.

26. **Torrance, A.A.,** *"Metallurgical effects associated with grinding."* Proc. 19th MTDR Conf., 1978.

27. **Sato, K.,** *"Grinding temperature."* Bull. Jap. Soc. of Grinding No. 1, 1961.

28. **Malkin, S., & Anderson, R.B.,** *"Thermal aspects of grinding. Part 1: Energy partition"* ASME Trans., J. Eng. Ind., p1177. (1974).

29. **Torrance, A.A., Stokes, R.J., & Howes, T.D.,** *"The effect of grinding conditions on the rolling contact fatigue life of bearing steel."* Mechanical Engineering, pp68-73, Oct. 1983.

30. **Ambrose, P.,** Rolls-Royce, Private communication.

31. **Powell, J.W.,** *"The application of grinding fluids in creep feed grinding."* PhD thesis, University of Bristol, 1979.

32. **Shafto, G.R.,** *"Creep feed grinding."* PhD thesis, University of Bristol, 1974.

33. **Hill, E.C., & Al-Zubaidy, T.,** *"Some health aspects of infections in oils and emulsions."* Trib.Int. **12** pp161-164, Aug. 1979.

34. **Peters, J., & Aerens, R.,** *"An objective method for evaluating grinding coolants."* CIRP(25), 1976.

35. **Osman, M., & Malkin, S.,** *"Lubrication by grinding fluids at normal and high wheel speeds."* ASLE paper no.72AM5, pp261-268, 1972.

36. **Mueller** *"How much do grinding fluids affect wheel performance ?"* Nat. Metalworking Weekly, March 7, 1957.

37. **Chandrasekar, S., & Shaw, M.C.,** *"Cutting fluid performance in fine grinding."* Wear **86** pp139-149 (1983).

38. **Anon.** *"Cutting Fluid Specification Chart"* Mach.Prod.Eng., 3rd Sep., 1986.

39. **Howes, T. D.,** University of Bristol, Private communication.

40. **Graham, D., & Baul, R.M.,** *"An investigation into the mode of metal removal in the grinding process."* Wear19 pp301-314 (1972).

41. **Baul, R.M.,** *"Mechanics of metal grinding with particular reference to Monte Carlo simulation."* Proc. 8th MTDR Conf., 1967.

42. **Backer, W.R., & Merchant, M.E.,** *"On the basic mechanics of the grinding process."* ASME Trans., Jan. 1958, pp141-146.

43. **Backer, W.R., Marshall, E.R., & Shaw, M.C.,** *"The size effect in metal cutting."* ASME Trans. 74(61) pp61-72, 1952.

44. **Rowe, G.W., & Wetton, A.G.,** *"Theoretical considerations in the grinding of metals."* J.Inst.Metals 97 pp193-200, 1969.

45. **Rubenstein, C., Groszman, F.K., & Koenigsberger, F.,** *"Force measurements during cutting tests with single point tools simulating the action of a single abrasive grit."* Science & Technology of Industrial Diamonds, Proc. of the Industrial Diamond Conf., Oxford, 1966.

46. **Kannapan, S., & Malkin, S.,** *"Effect of grain size and operating parameters on the mechanics of grinding."* ASME Trans., J.Eng.Ind. 93(103) pp833-842, 1972.

47. **Malkin, S., & Cook N.H.,** *"The wear of grinding wheels. Part1: Attritious wear."* ASME Trans., J.Eng.Ind., Nov. 1971, pp1120-1128.

48. **Mercier, R.J., Malkin, S., & Mollendorf, J.C.,** *"Thermal stresses from a moving band source of heat on the surface of a semi-infinite solid."* ASME Trans. 100(1) pp43-48, Feb. 1978.

49. **Furukawa, Y., Ohishi, S., & Shiozaki, S.,** *"Selection of creep feed grinding conditions in view of workpiece burn."* Annals of CIRP 28 pp213-218, 1979.

50. **Gonin, A., Berger, A., & Neyron, J.,** *"Lubricant testing: a new type of machine."* Trib.Int., Feb. 1980, p25.

51. **Institute of Petroleum** *Standards for petroleum and its products. I. Methods for analysis and testing.* IP239, 1977.

52. **Shaw, M.C.,** *"On the action of metal cutting fluids at low speeds."* Wear 2 pp217-227, 1958.

53. **Horne, J.G., Tabor, D., & Williams, J.A.,** *"Action of gaseous and liquid lubricants in metal cutting."* Int. Symp. on Metalworking Lubn., San Francisco Ca., Aug., 1980.

54. **Duwell, E.J., Hong, I.S., & McDonald, W.J.,** *"The effect of oxygen and water on the dynamics of chip formation during grinding."* ASLE Trans. 12 pp86-93, 1969.

55. **PERA & MTIRA** survey for DTI *"Metal cutting fluids and machine lubricants for automated small batch production."* 1982.

56. **Bizeul, D., & Le Maitre, F.,** *"Qualification of lubricants by energy measures."* Annals of CIRP **28**, 1979.

57. **Kurimoto, T., & Barrow, G.,** *"The wear of high speed cutting tools under the action of several different cutting fluids."* 22nd MTDR Conf., 1981.

58. **Lindsay, R.P.,** *"Evaluating grinding fluid performance."* Man. Eng. Trans., Soc. of Manu. Eng., 1975/6.

59. **Torrance, A.C.,** *"An investigation of the mode of action of fluids used in the grinding of stainless steel."* PhD thesis, University of Bristol, 1981.

60. **Ye, N.E., & Pearce, T.R.A.,** *"A comparison of oil and water as grinding fluids in the creep feed grinding process."* Proc.I.Mech.E, Nov. 1984.

61. **Malkin, S., & Cook N.H.,** *"The wear of grinding wheels. Part2: Fracture wear."* ASME Trans., J.Eng.Ind., Nov. 1971, pp1129-1136.

62. **Tarasov, L.P.,** *"The theory of grinding."* Grinding and Finishing, Sep/Nov. 1967.

63. **Yuen, M.,** *"Dynamics of grinding."* PhD thesis, University of Bristol, 1977.

64. **Sudholz, L.H., Manilych, S., & Mapes, G.S.,** *"Grinding fluids - a method of measuring the metallic wheel loading characteristics."* Mech.Eng., Dec. 1950, pp963-965.

65. **Salmon, S.C.,** *"Creep feed surface grinding."* PhD thesis, University of Bristol, 1979.

66. **Ueno, T., Ishibashi, A., & Katsuki, A.,** *"Experiments on the cooling ability of cutting fluids."* Bull.Jap.Soc.Mech.Eng. 13(59) p729, 1970.

67. **Lee, D.G., Zerkle, R.D., & Des Ruisseaux, N.R.,** *"An experimental study of thermal aspects of cylindrical plunge grinding."* ASME Trans, J.Eng.Ind., p1206, Nov., 1972.

68. **Clewlow, B.A., & Lewis, M.R.,** *"Transient boiling heat transfer in simulated grinding."* B.Sc. thesis, University of Bristol, 1979.

69. **Malkin, S.,** Discussion section of reference 62.

70. **Outwater, J.O., & Shaw, M.C.,** *"Surface temperatures in grinding."* ASME Trans., Jan. 1952., pp73-86.

71. **Von Turkovich, B.F.,** *"Dislocation theory of shear stress and strain rate in metal cutting."* Proc. 8th MTDR Conf., 1967, pp531-542.

72. **Jaeger, J.C.,** *"Moving sources of heat and the temperature at sliding contacts."* Proc. Roy. Soc. of New South Wales 76 pp263-274, 1942.

73. **Des Ruisseaux, N.R., & Zerkle, R.D.,** *"Thermal analysis of the grinding process."* J. Heat Transfer, ASME Trans. 92(B) pp428-434, 1970.

74. **Thomas, T.R.,** *"Recent advances in the measurement and analysis of surface microgeometry."* Wear 33 pp205-233, 1975.

75. **Suto, T., Waida, T., & Sata, T.,** *"In-process measurement of wheel surface in grinding operations."* Proc. 10th. MTDR Conf., Sep. 1969.

76. **Tsuwa, H.,** *"An investigation of grinding wheel cutting edges."* ASME Trans. 86(B) p371, Nov. 1964.

77. **McAdams, H.T.,** *"The role of topography in the cutting performance of abrasive tools."* J.Eng.Ind. 86, 1964.?

78. **McAdams, H.T.,** *"Markov chain models of grinding profiles."* Proc. ASME, 1964, pp383-388.

79. **Peklenik, J.,** *"Untersuchungen uber das Verschleisskriterium beim Schleifen."* Ind. Anz. 80(27) p397, 1958.

80. **Bhattacharyya, S.K., & Hill, C.G.,** *"Characterisation of grinding wheel topography and wear."* 17th MTDR Conf., 1978.

81. **Baul, R.M., Graham,D., & Scott, W.,** *"Characterisation of the working surface of abrasive wheels."* Tribology, Aug. 1972, p169.

82. **Bhateja, C.P., Chisholm, A.W.J., & Pattinson, E.J.,** *"A computer-aided study of the texture of the working surfaces of grinding wheels."* Proc. 12th MTDR Conf., 1971.

83. **Peklenik, J.,** *"Contribution to the theory of grinding."* Stojniski Vestnic, Ljubjana, 1959.

84. **Posey, C.J.,** *"Measurement of Roughness."* Mech.Eng. (68) p305, 1946.

85. **Myers, N.O.,** *"Characterisation of surface roughness."* Wear **5** pp182-189, 1962.

86. **Peklenik, J.,** *"Contribution to the correlation theory for the grinding process."* J.Eng.Ind., May 1964, pp85-94.

87. **Abbott, E.J., & Firestone, F.A.,** *"Specifying surface quality."* Mech.Eng. 55(9) pp569-572, 1933.

88. **Radhakrishnan, V.,** *"Statistical behaviour of surface profiles."* Wear **17** pp259-267, (1971).

89. **Meyer, H.R., & Weimann, H.J.,** *"Diamond roller dressers: their design and application considerations in Europe."* Ind.Dia.Rev., March 1975 pp89-95.

90. **Parrott, E.,** Rolls-Royce, Private communication.

91. **Graham, W., & Whiston, M.G.,** *"Some observations of through wheel coolant application in grinding."* Int. J. Mach. Tool Des.Res. **18** pp9-18, 1978.

92. **Bhateja, C.P.,** *"On dressing of grinding wheels."* Presentation paper for the S.R.C. grinding research meeting at Salford on July 5th, 1973.

93. British Standard 1134. *"Method for the assessment of surface texture."* 1972, parts 1 & 2.

94. **Sayles, R.S., & Thomas, T.R.,** *"A stochastic explanation of some structural properties of a ground surface."* Int. J. Prod. Res. 14(6) pp644-655, 1976.

95. **Brettell, C.R., & Richardson, M.R.,** *"The prediction of surface finish in grinding."* B.Sc. thesis, University of Bristol, 1979.

96. **Morgan, J.E., & Salter, N.D.,** *"The creep feed grinding of hard and soft steels."* ASME Trans. 106, 1984.

97. **Liverton, J.W.,** *"Creep rotation plunge cylindrical grinding."* PhD thesis, University of Bristol, 1980.

98. **Littmann, W.E.,** *"Control of residual stress in metal surfaces."* Proc. CIRP. Int. Conf. Man. Tech., Sept.25-28, 1967.

99. **Chu Boyi** Unpublished work, Wuhan University of Technology, Peoples Republic of China, 1986.

100. **Coes, L., Jnr.,** *"Knowledge of the scientific principles of grinding is basis for recent progress in abrasives... "* Ind. & Eng. Chemistry 47(12), 1955.

101. Private enquiry to the Bristol Waterworks Co..

102. **Rowe, G.W., & Smart, E.F.,** *"The importance of oxygen indry machining of metal on a lathe."* Brit. J. App. Phys. 14 pp924-926, 1963.

103. **Letner, H.R.,** *"Influence of grinding fluids upon residual stresses in hardened steel."* ASME Trans. 79 pp 149-153, 1957.

104. **Fletcher, A.J., & Price, R.F.,** *"Generation of thermal stress and strain during quenching of low-alloy steel plates."* Metals Technology pp427-446, Nov. 1981.

105. **Lenning, R.L.,** *"Controlling residual stresses in cylindrical grinding."* Abrasive Engineering, Dec. 1968, pp24-30.

106. **Reichenbach, G.S., Mayer, J.E., Kalpakcioglu, S., & Shaw, M.C.** *"The role of chip thickness in grinding."* ASME Trans. 78 pp847-859, 1956.

107. **Furuichi, R., Nakayama, M., & Tsunetsugu, T.,** *"Effects of grinding fluids on grinding performances in forced infeed plunge grinding."* Memoirs of Fac. of Eng. **8**, Osaka City University, Dec. 1966.

108. **Nicholson, R.A.,** *"Soluble cutting oil developments."* Ind. Lub. & Trib. May/June 1983.

109. **Rezaei, S.M.,** *"Investigation of in-process dressing in creep feed grinding."* PhD thesis, University of Bristol, 1987.

110. **Mayer, J.E., Jnr., & Shaw, M.C.,** *"Grinding temperatures."* ASLE Trans., 1957.

111. **Shaw, M.C., Pigott, J.D., & Richardson, L.P.,** *"The effect of cutting fluid on tool chip interface temperature."* ASME Trans, 1951, pp45-56.

112. **Yasui, H., & Tsukuda, S.,** *"Influence of fluid type on wet grinding temperature."* Bull. Jap. Soc. Prec. Eng. 17(2) pp133-134 (1983).

113. **Hassell, B.,** *"A grinding fluid comparison."* MAI thesis, Trinity College Dublin, 1979.

114. **Werner, P.G., Younis, M.A., & Schlingensiepen, R.,** *"Creep feed - an effective method to reduce work surface temperatures in high-efficiency grinding processes."* wt - Z. Ind. Fertig. **69** pp613-620 (1979).

115. **Rogers, G.F.C., & Mayhew, Y.R.,** *"Engineering thermodynamics - work and heat transfer. "* Longmans, 2nd Ed., 1967.

116. **Ohishi, S., & Furakawa, Y.,** *"Analysis of workpiece temperature and grinding burn in creep feed grinding."* Bull. Jap. Soc. Mech. Eng. **28** p1775, 1985.

117. **Mathewson, W.F., Jnr.,** *"The role of lubricants in diamond grinding."* Seminar of Ind. Dia. Ass. of America, April 7th, 1965.

118. **Geisweid, G., & Gärtner, W.,** *"Deep and oscillation grinding - temperatures and power requirements."* Ind. Dia. Review, Aug. 1978, p285.

119. **Stuart, T.V.,** *"High speed creep feed grinding."* PhD thesis, University of Bristol, 1977.

120. **Woolman, J., & Mottram, R.A.,** *"The mechanical and physical properties of of the British Standard EN steels (BS970 1955) volume 1."* Pergamon, 1964.

121. British Standard 970, Volume 1, 1955

122. **Betteridge, W., & Heslop, J.,** *"The Nimonic alloys and other nickel-base high-temperature alloys."* Arnold, 1974.

123. **Atkins, P.W.,** *"Physical Chemistry."* Oxford University Press, p836 (1st ed.), 1978.

Fluid	% composition of concentrate					
	mineral oil	E.P. & lubricity additives	emulsifiers	coupling agents	corrosion inhibitors	dilution with water
soluble oils (oil in water macro -emulsions, 'suds', 'mystic', 'slurry')	50-80	0-10	10-40	0.5-3	0-10	1:40 to 1:80
semi-synthetics (microemulsions)	5-30	0-10	up to 50	0.5-3	0-10	1:50 to 1:80
synthetic fluids (chemical fluids)	<5		0-40	0.5-3	up to 40 to 1:200	1:10

Table 1: Summary of typical compositions of water based fluids.

Specific energies measured after 200 mm^3/mm of workpiece removed:

grinding and dressing with oil	27 J/mm^3
grinding and dressing with macroemulsion	35 J/mm^3
grinding with oil, dressing with macroemulsion	26 J/mm^3
grinding with macroemulsion, dressing with oil	36 J/mm^3

Note.

Conditions: conventional dressing, EN9 workpieces, 3 mm depth of cut, 8 mm/min maximum normal infeed rate.

Table 2: The results of grinding tests to investigate the influence of the type of fluid used in the dressing nip.

grinding fluid	u_c (J/mm^3)	μ
water	52	0.27
macroemulsion	29	0.27
microemulsion	15	0.32
oil	15	0.28

Table 3: The specific cutting energies, u_c, and friction coefficients, μ, for Nimonic.

grinding fluid	u_c (J/mm^3)	μ
macroemulsion	30.5	0.57
microemulsion	24	0.57
oil	16	0.57

Table 4: The specific cutting energies, u_c, and friction coefficients, μ, for steel.

	v_d = 2 ± 0.2 μm/rev z' = 16 ± 0.8 mm^3/mm/s		v_d = 0.3 ± 0.03 μm/rev z' = 2.85 ± 0.14 mm^3/mm/s	
	EN9	MARM002	EN9	MARM002
microemulsion	0.51	0.32	0.43	0.27
macroemulsion	0.51	0.45	0.43	0.26
oil	0.39	0.23	0.30	0.18

Table 5: Comparison of force ratios obtained under a range of grinding conditions.

Residual stresses measured transverse to the grinding direction

Fluid used	undamaged specimen	visual signs of burn
E.P. macroemulsion	-25	+45
oil	-20	+40

Note that the residual stress values are for relative comparison only, as the probe used could not be calibrated to give values in MPa. Positive values denote tensile stresses.

Table 6: Comparison of residual stresses with oil and an E.P. macroemulsion on specimens with and without visual signs of burn.

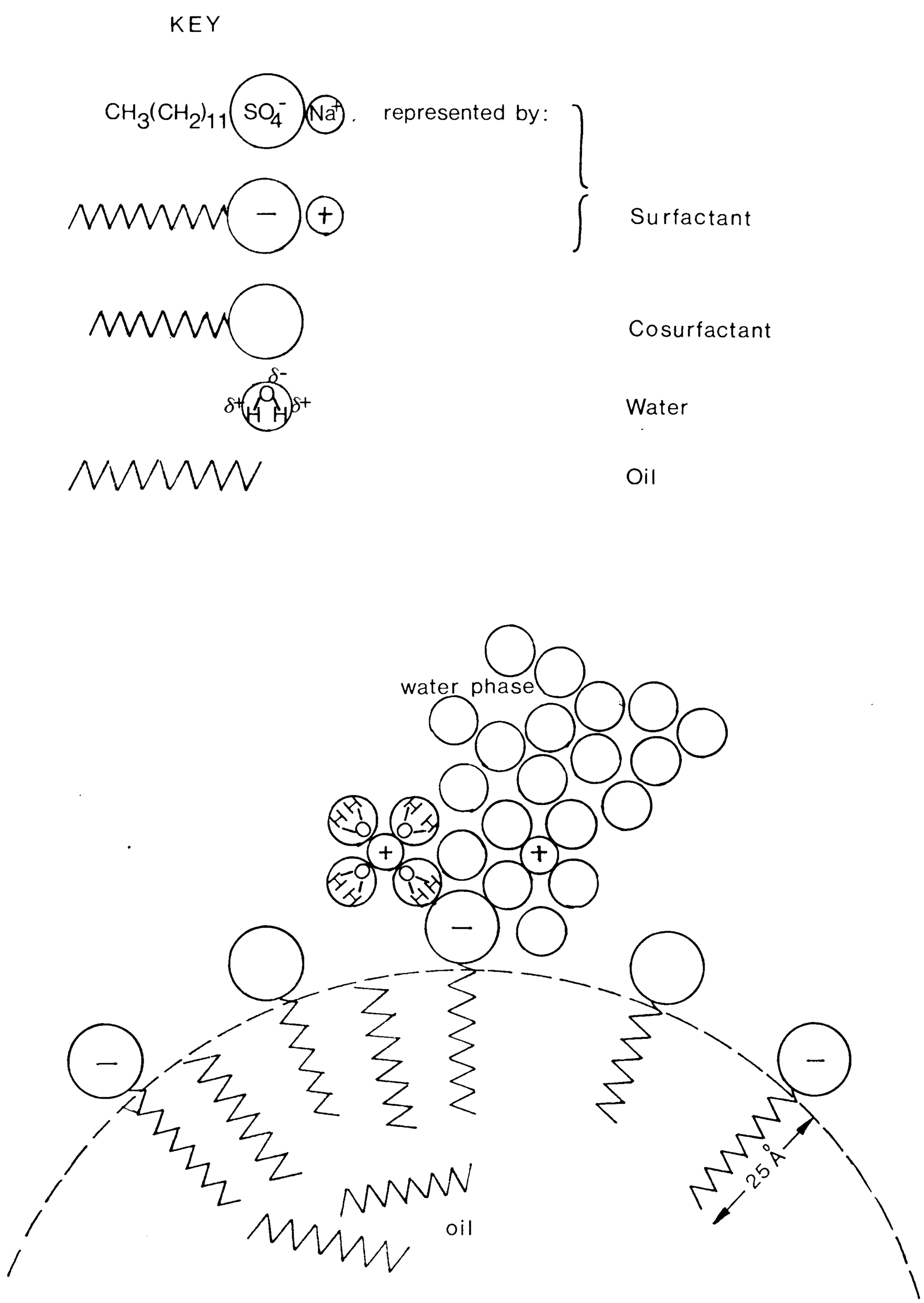

Figure 1. Schematic two dimensional diagram of the interface between an emulsified oil droplet and water.

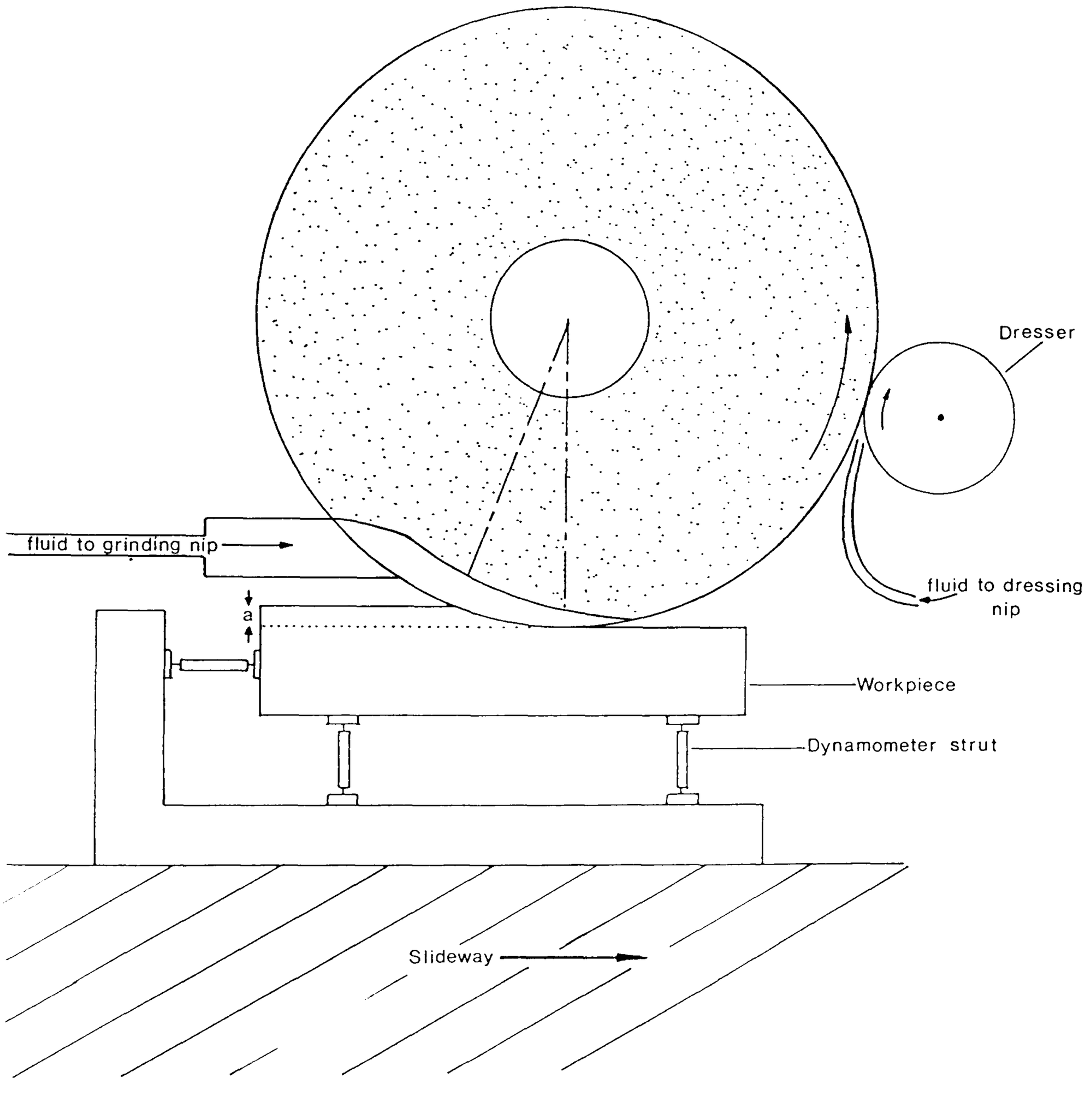

Figure 2. Schematic diagram of the creep feed surface grinding machine (showing relative directions for down-grinding)

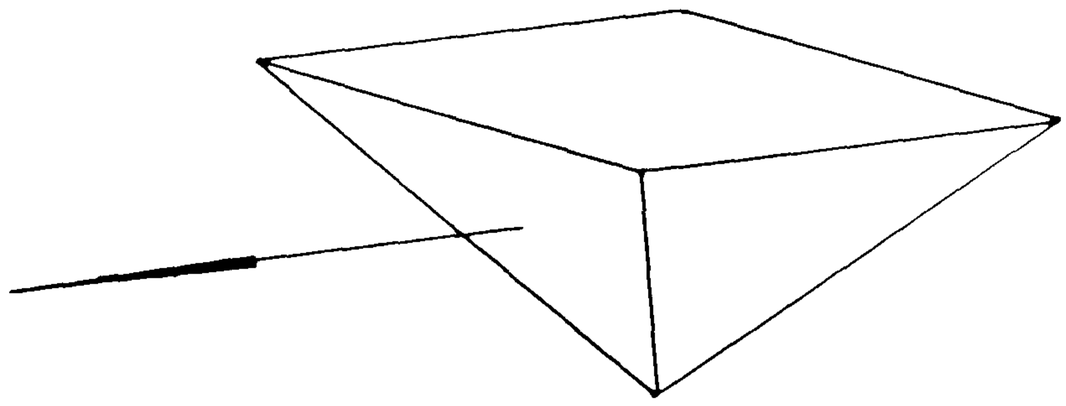

(a)

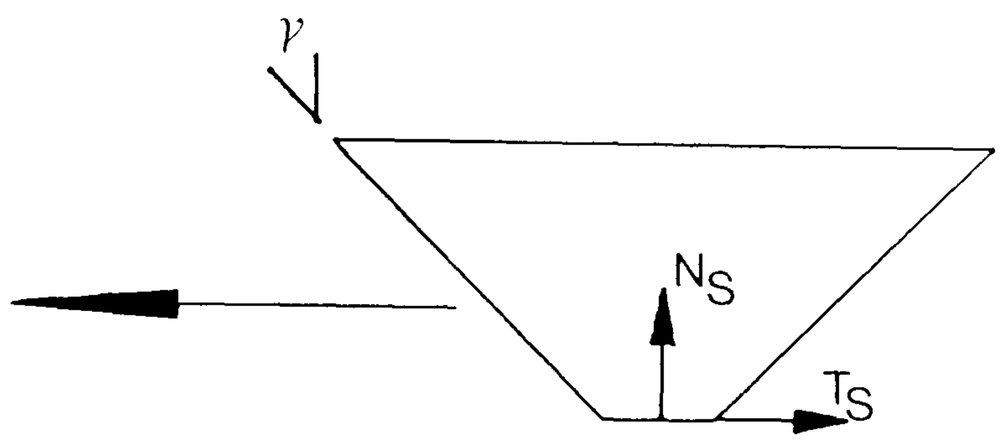

$$T_S = \mu N_S$$

(b)

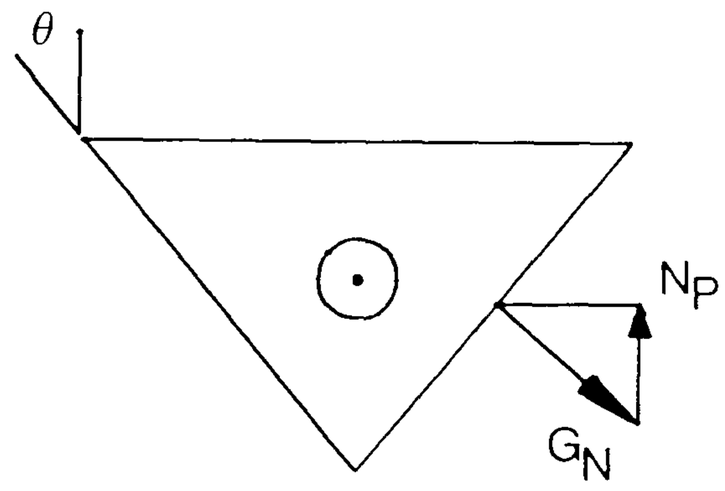

$$N_P = G_N \sin \theta$$

$$T_P = \mu G_N$$

$$\frac{T_P}{N_P} = \frac{\mu}{\sin \theta}$$

(c)

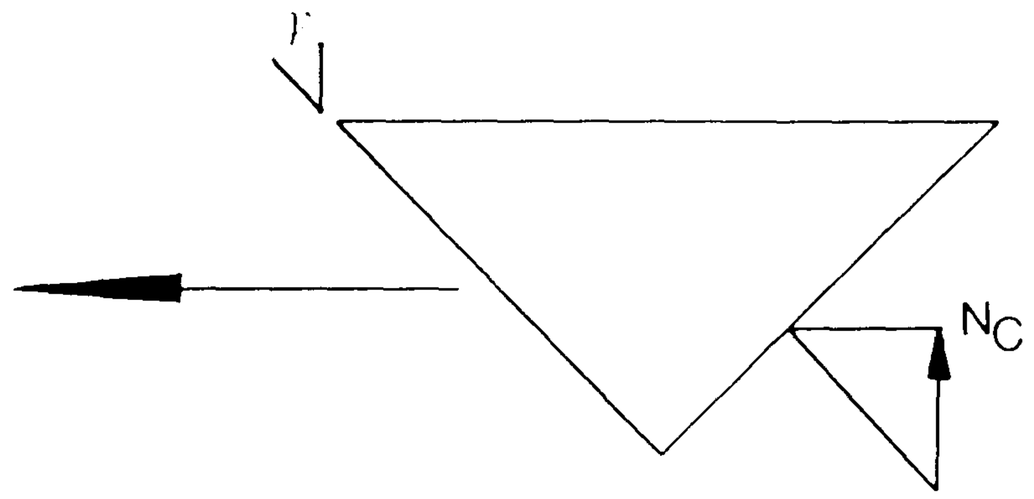

$$\frac{T_C}{N_C} = \frac{\mu}{\sin \gamma}$$

Figure 3. The forces associated with the three types of metal removal mechanism: (a) sliding (b) ploughing (c) chip formation.

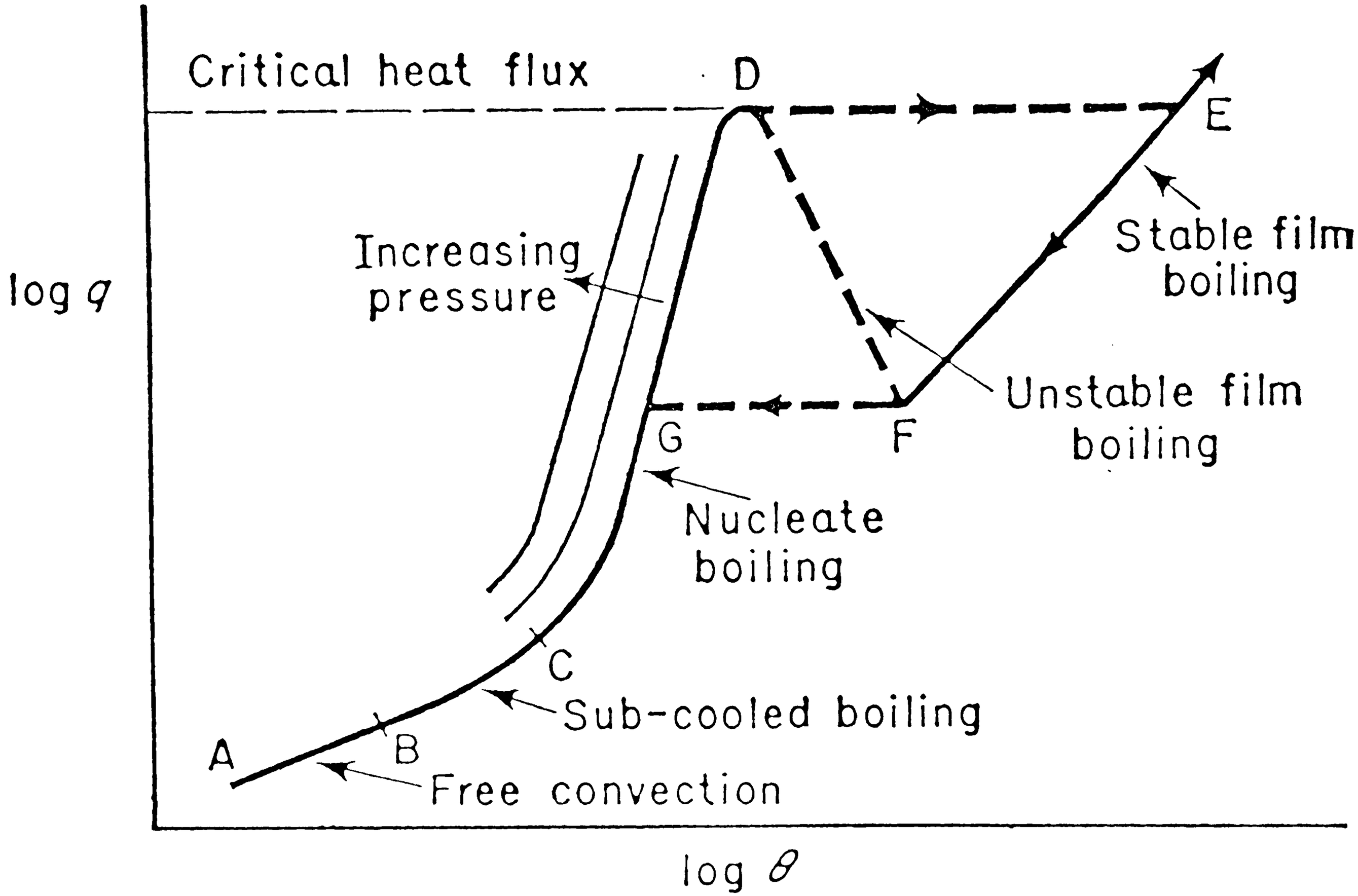

Figure 4. The heat flux from a heated boiler tube surface versus surface temperature (after [ ]).

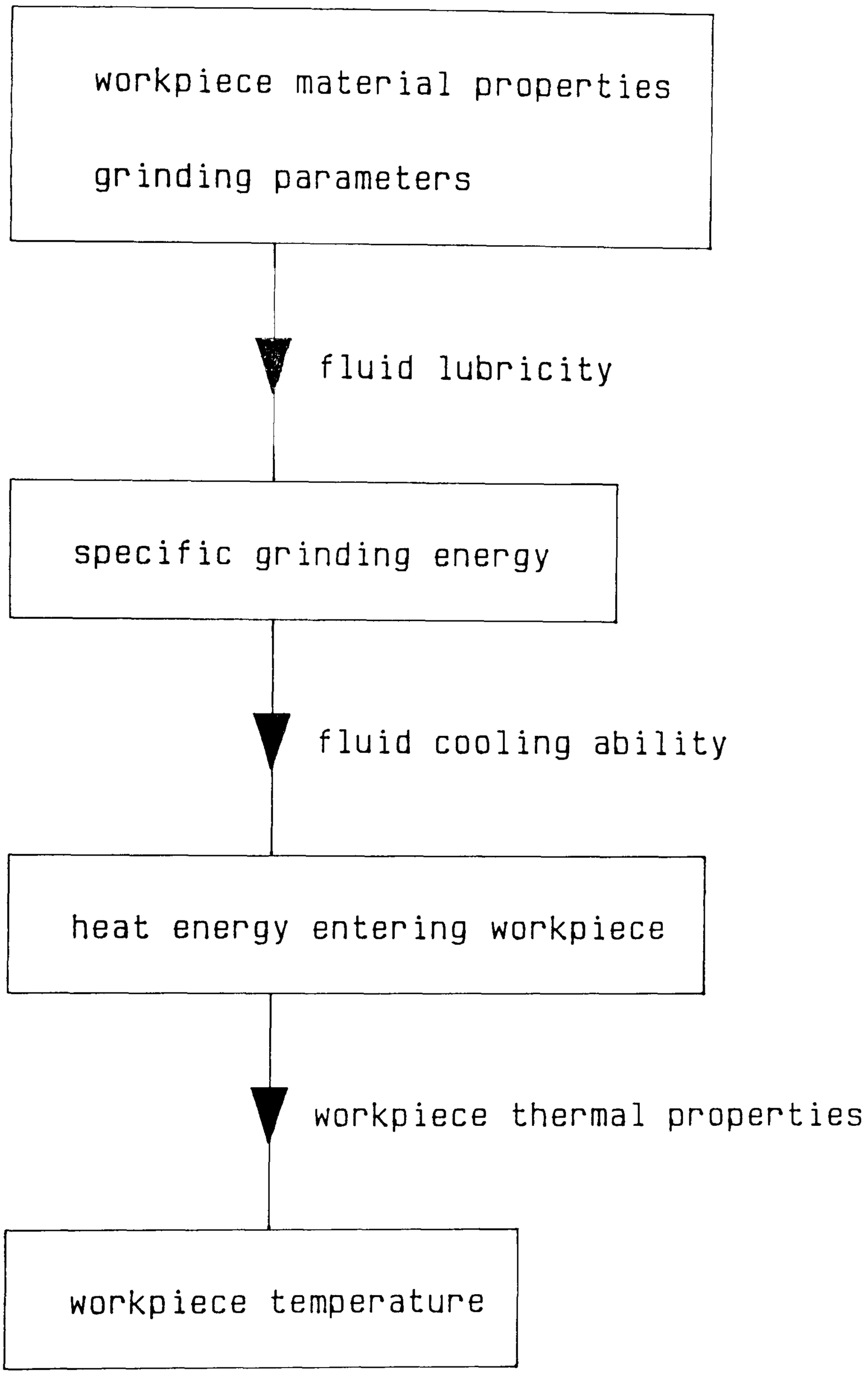

Figure 5. Pictorial representation of the relationship between lubrication and cooling under continuous dressing conditions.

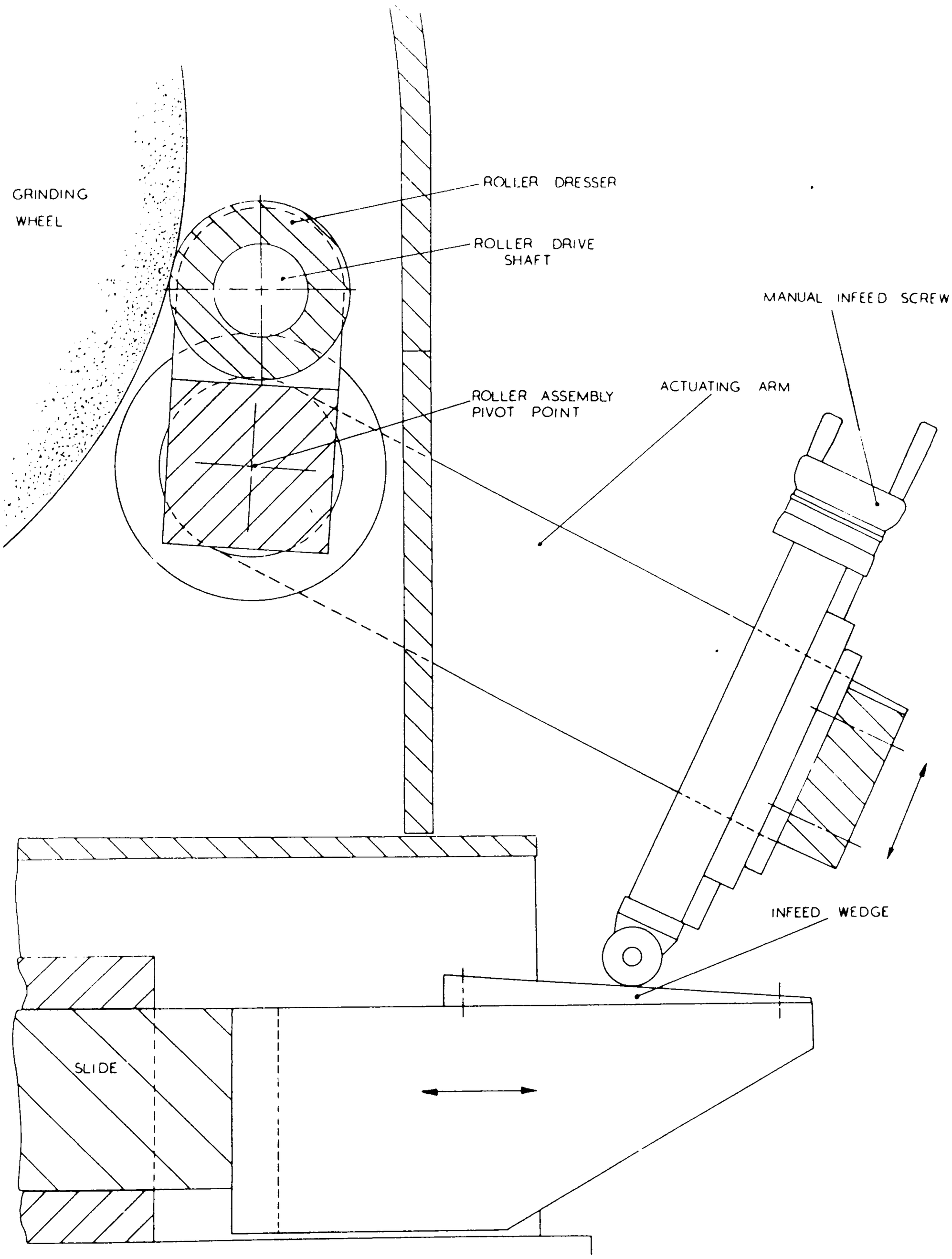

Figure 6. The dresser mechanism (after Stuart [119]).

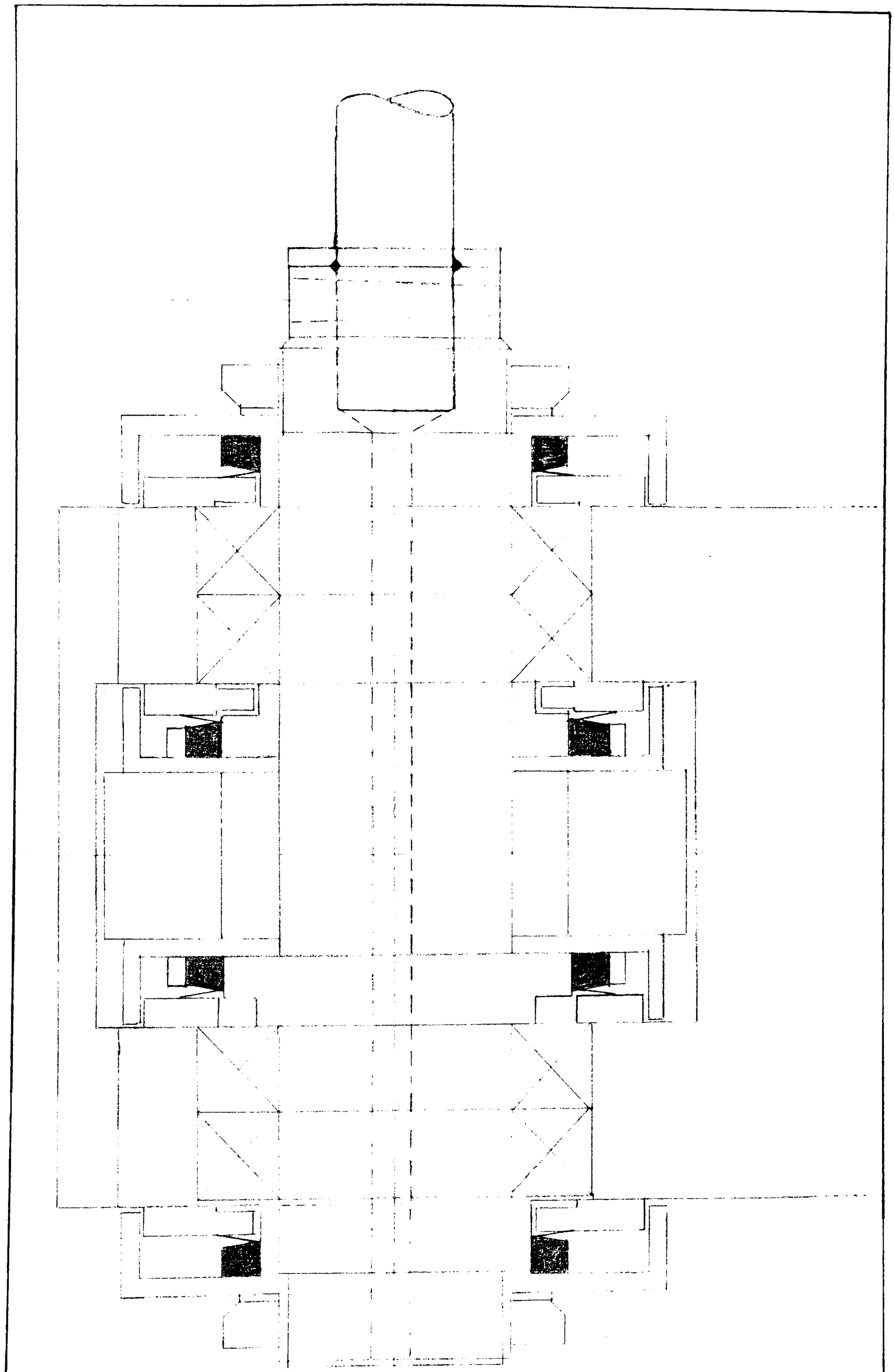

Figure 7. General assembly of the redesigned dresser housing.

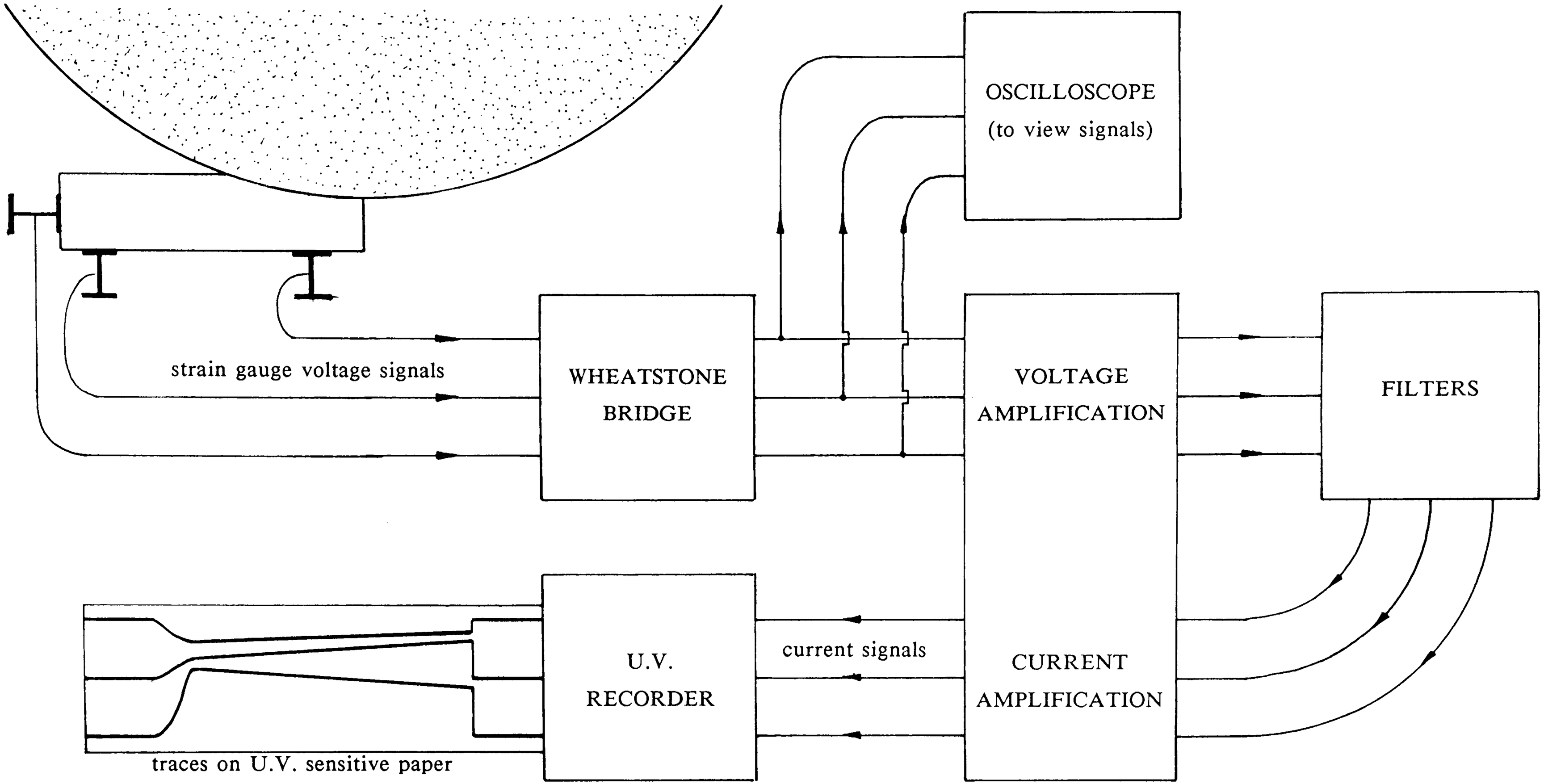

Figure 8. Arrangement of the instrumentation used to capture the forces generated during grinding.

(a)

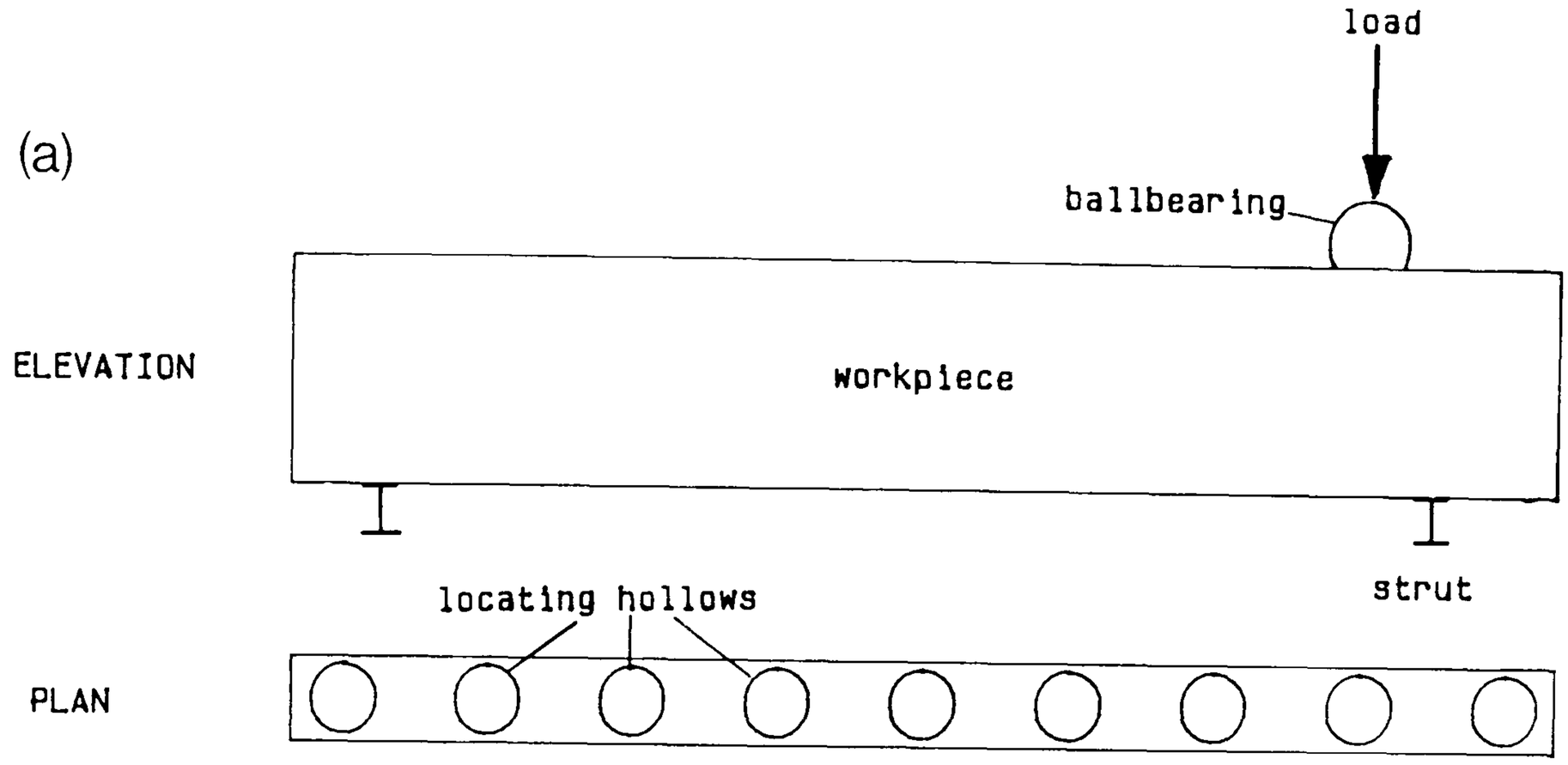

(b)

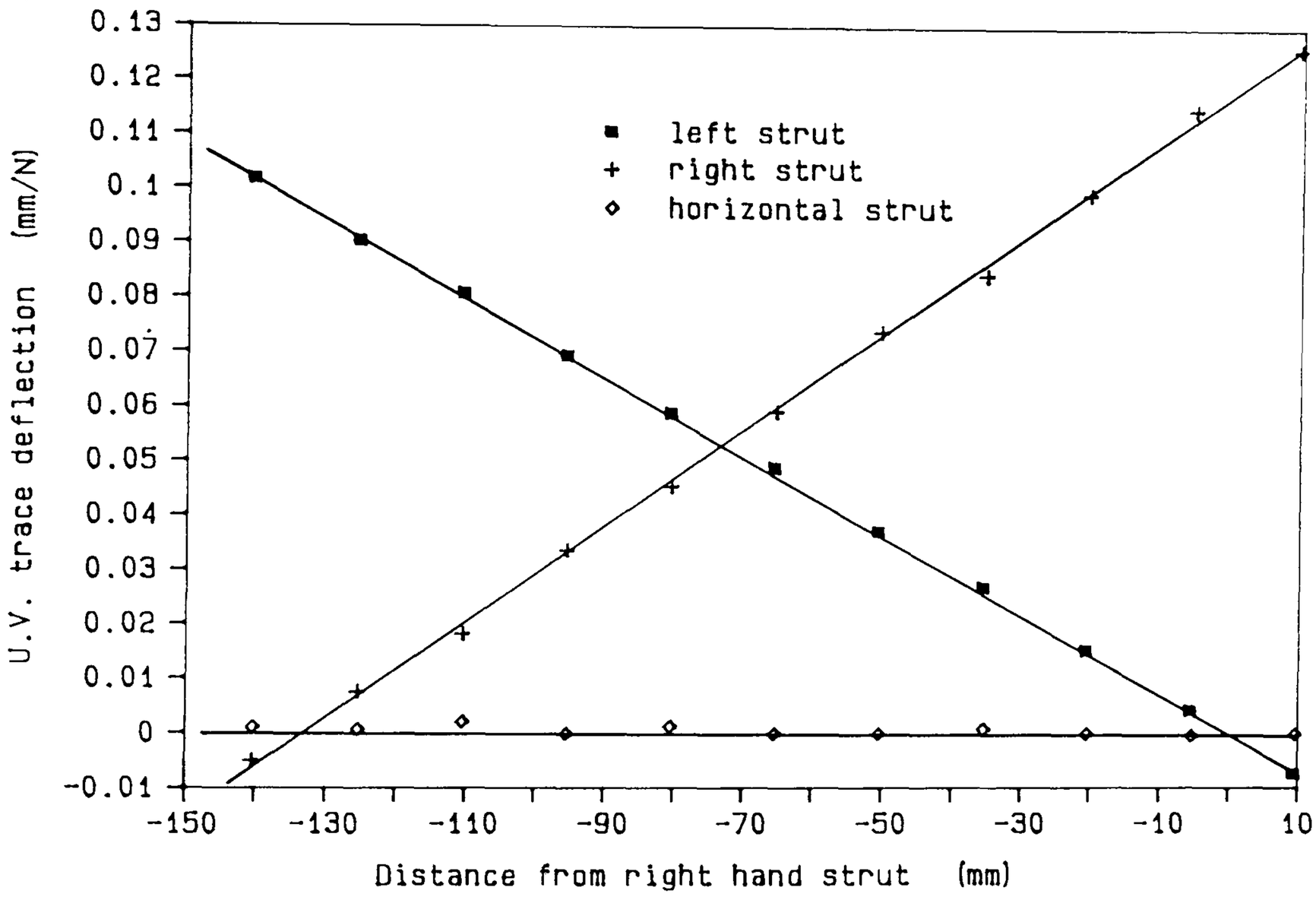

Figure 9. Calibration of the dynamometer struts under compressive loading: (a) arrangement (b) graph of U.V. trace deflections for each strut.

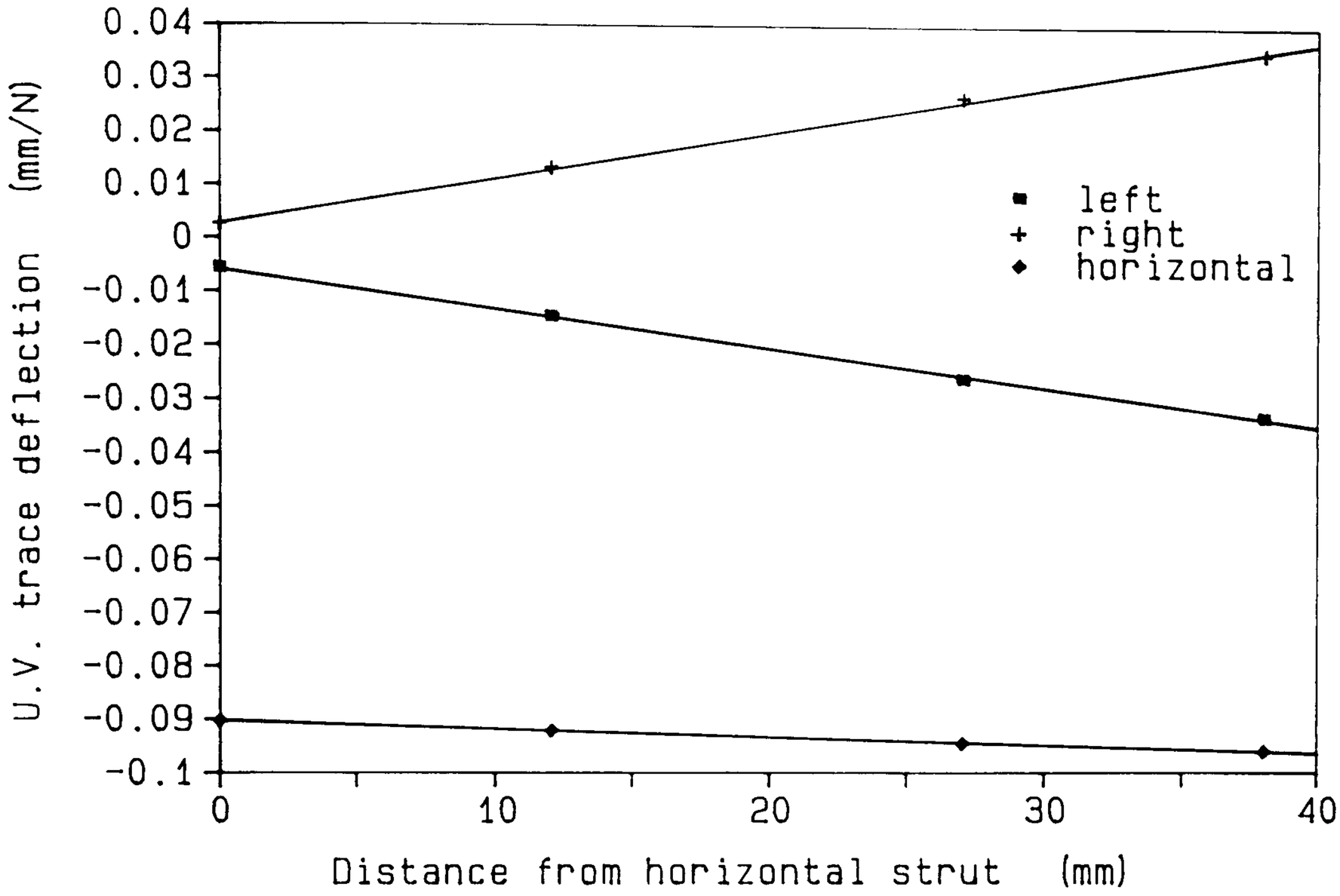

Figure 10. Calibration graph of the dynamometer under tensile loading.

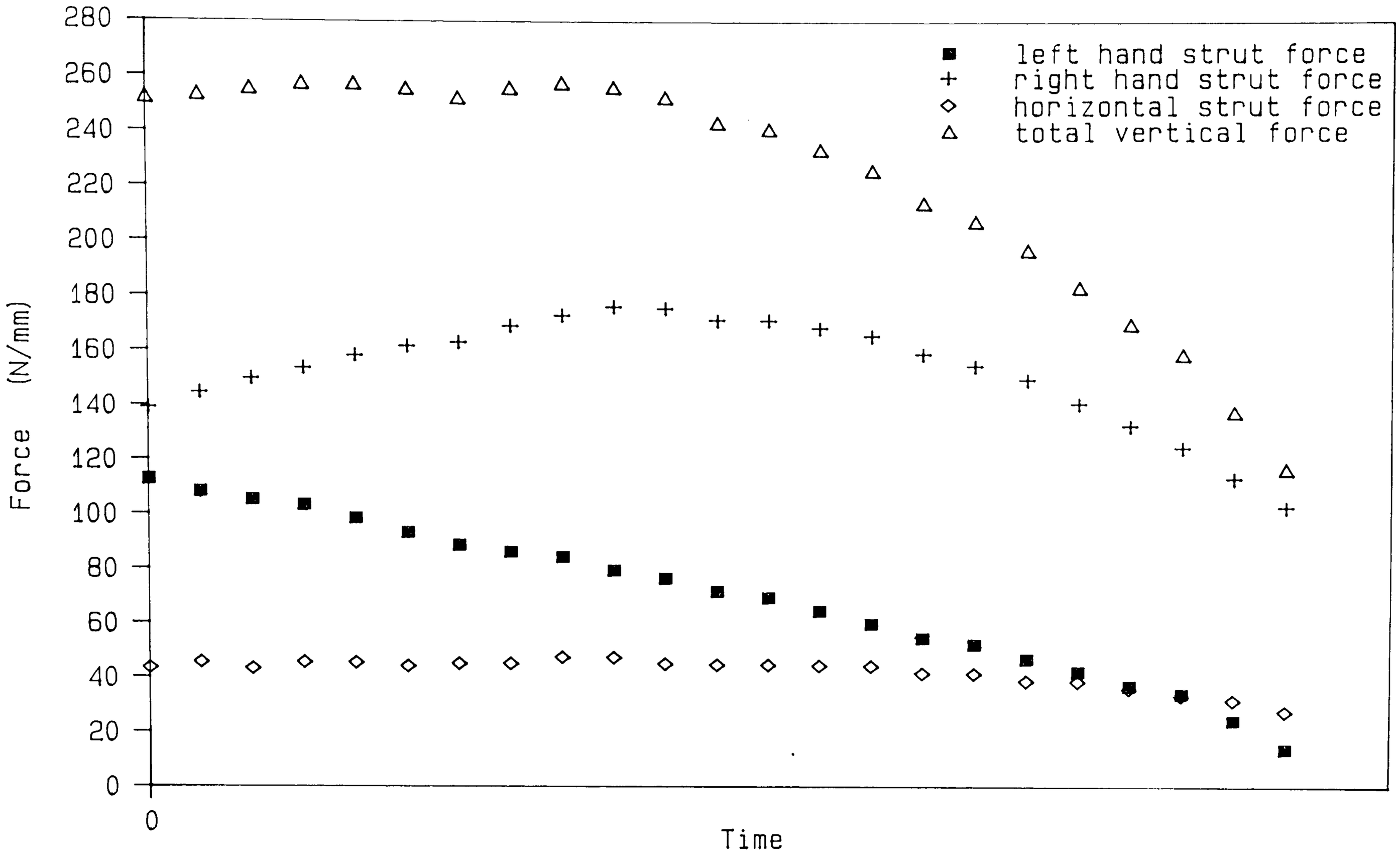

Figure 11. Graph of computed forces (in excess of the static forces) in the grinding zone versus elapsed time.

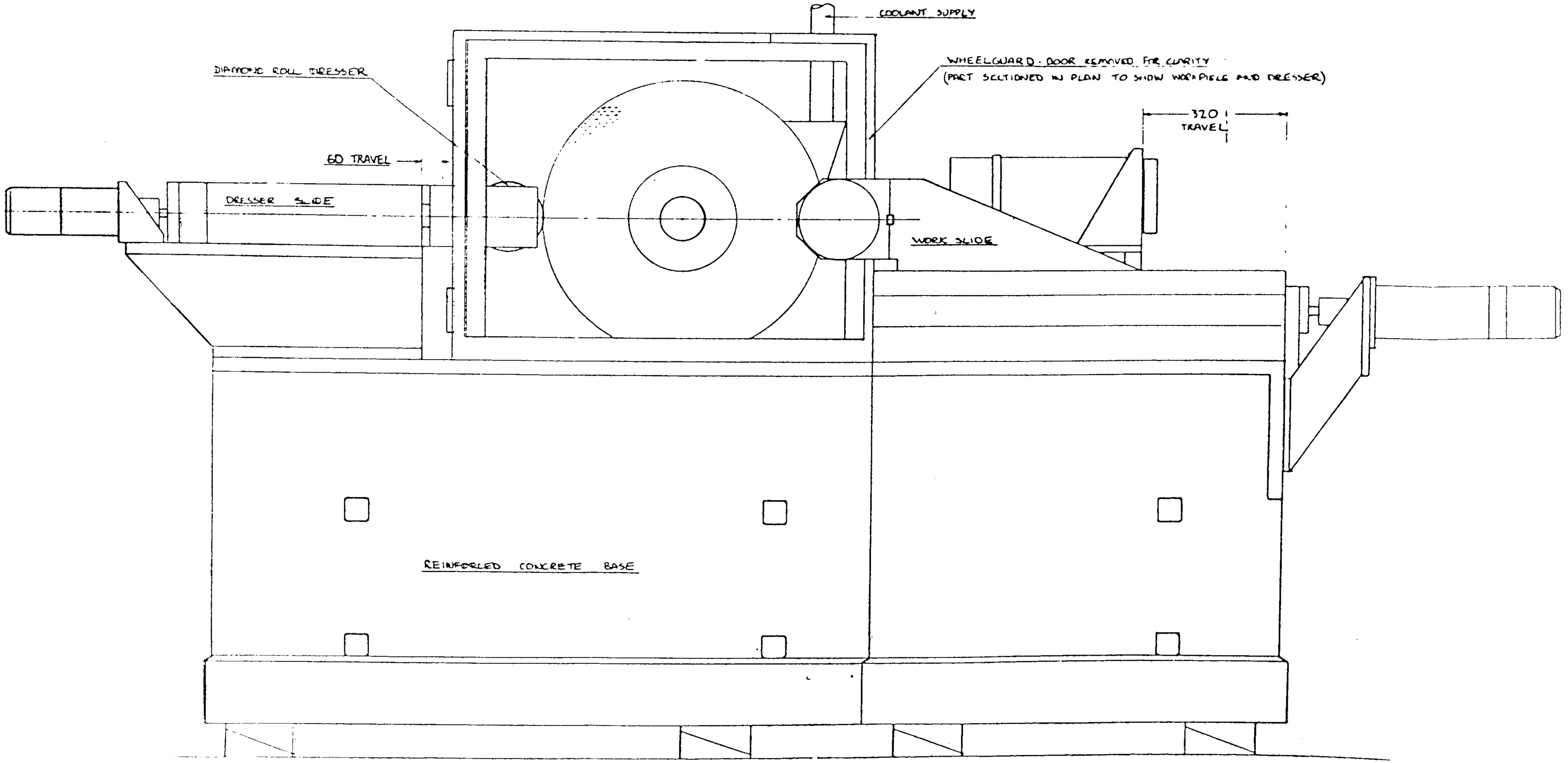

Figure 12. **The plunge grinding machine.** (after [97]).

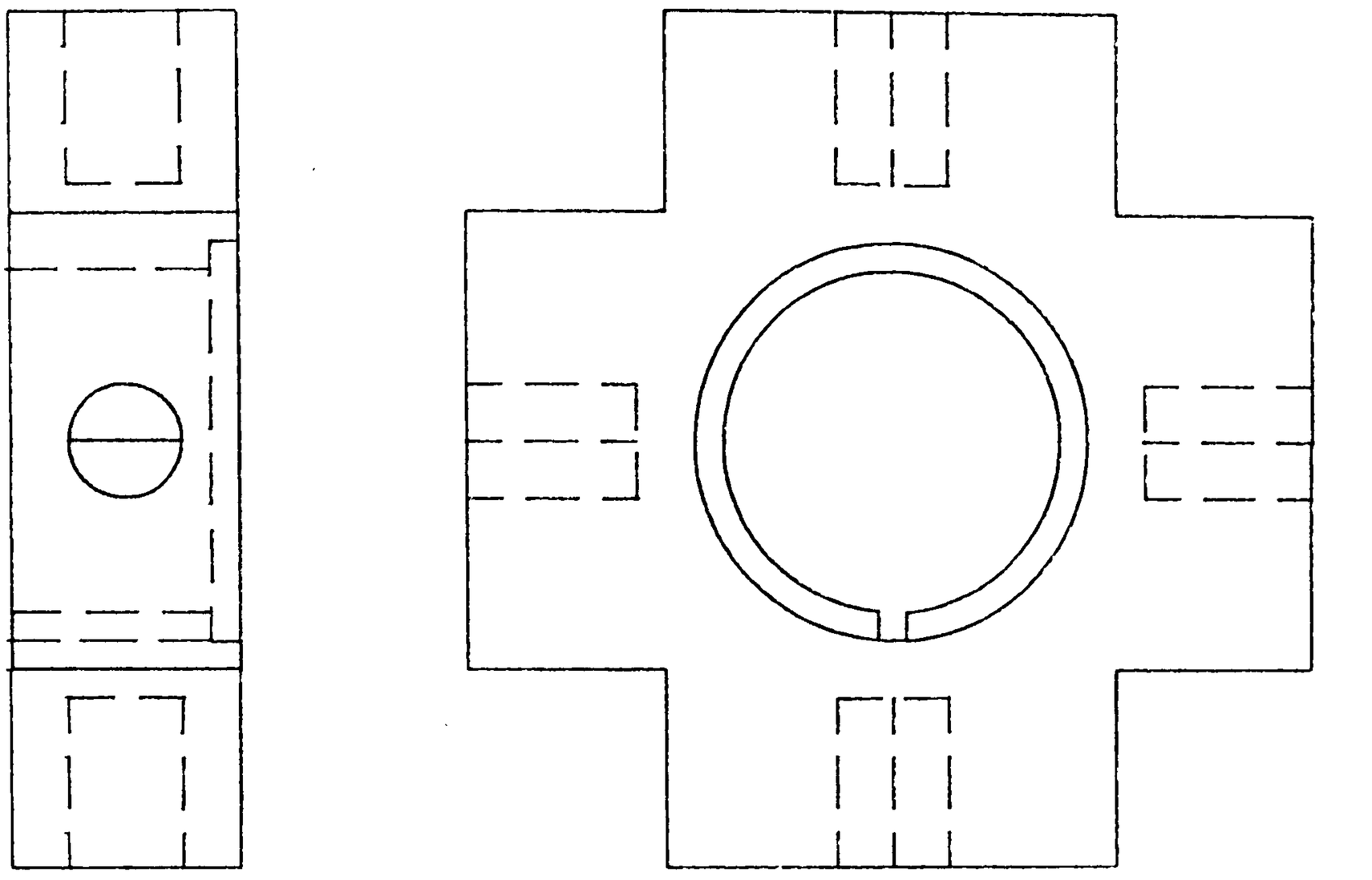

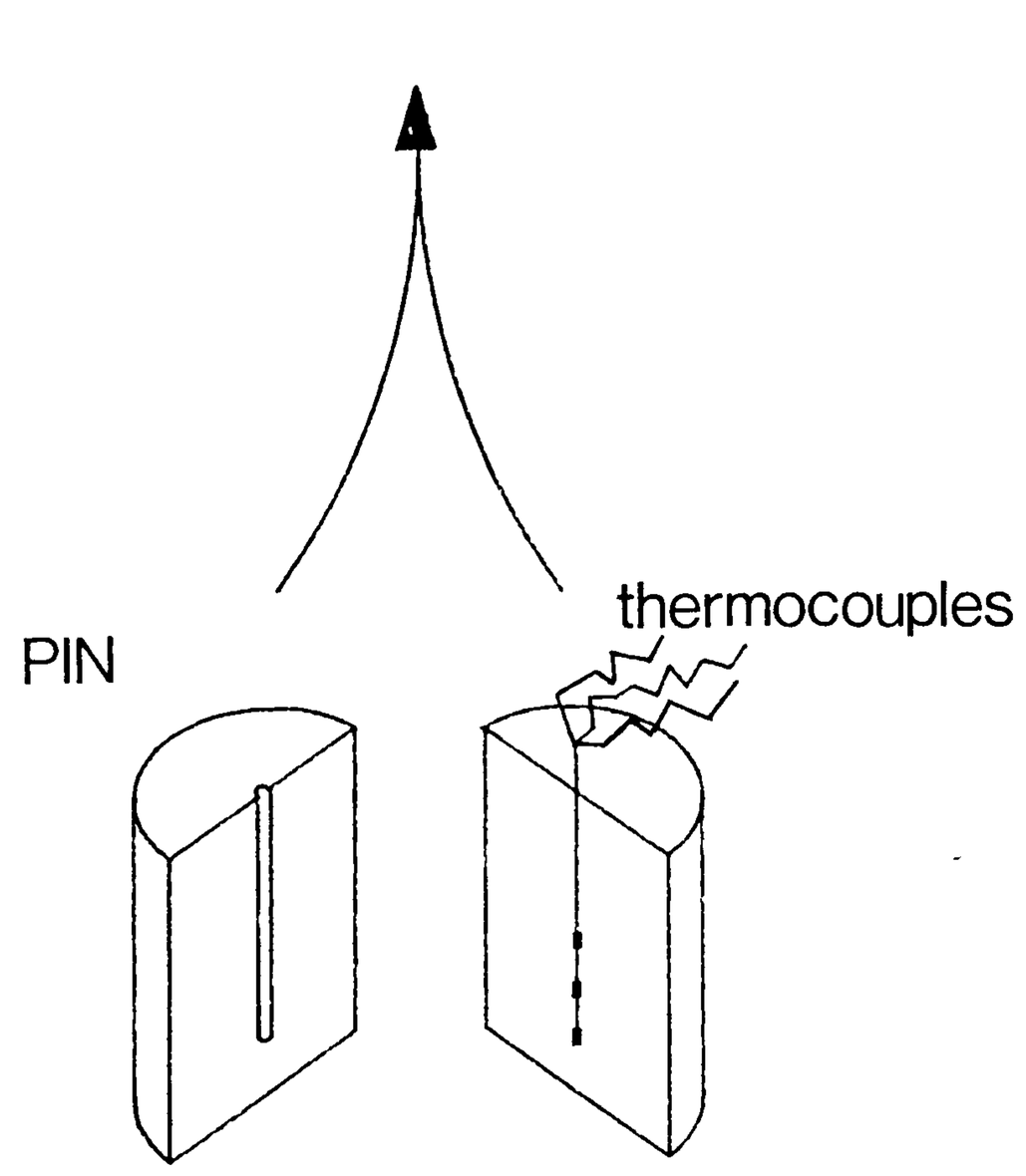

Figure 13. The pin design and the sindanyo holder.

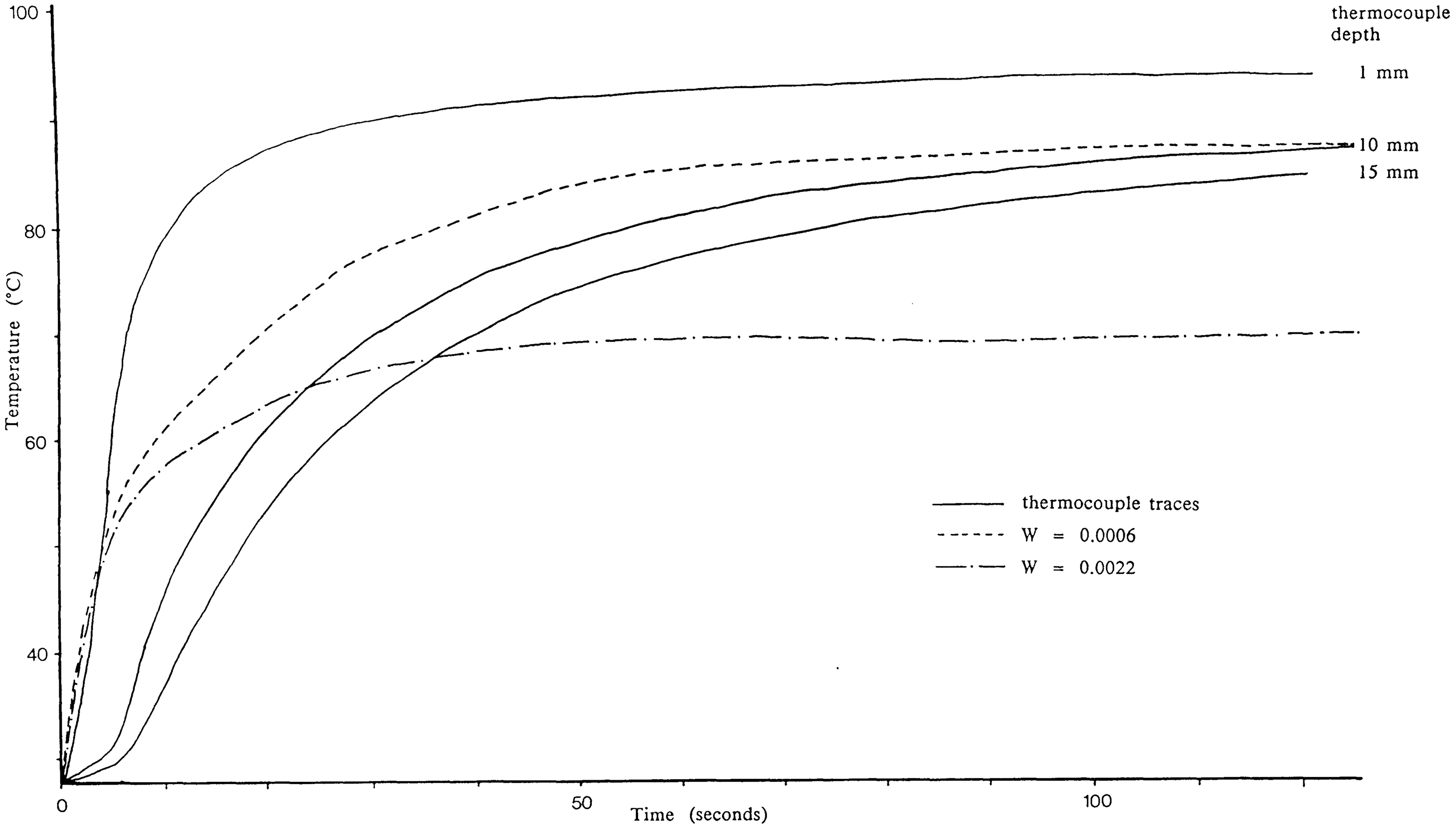

Figure 14. Time-temperature graphs for three thermocouples at varying distances below the steam heated surface of an insulated pin.

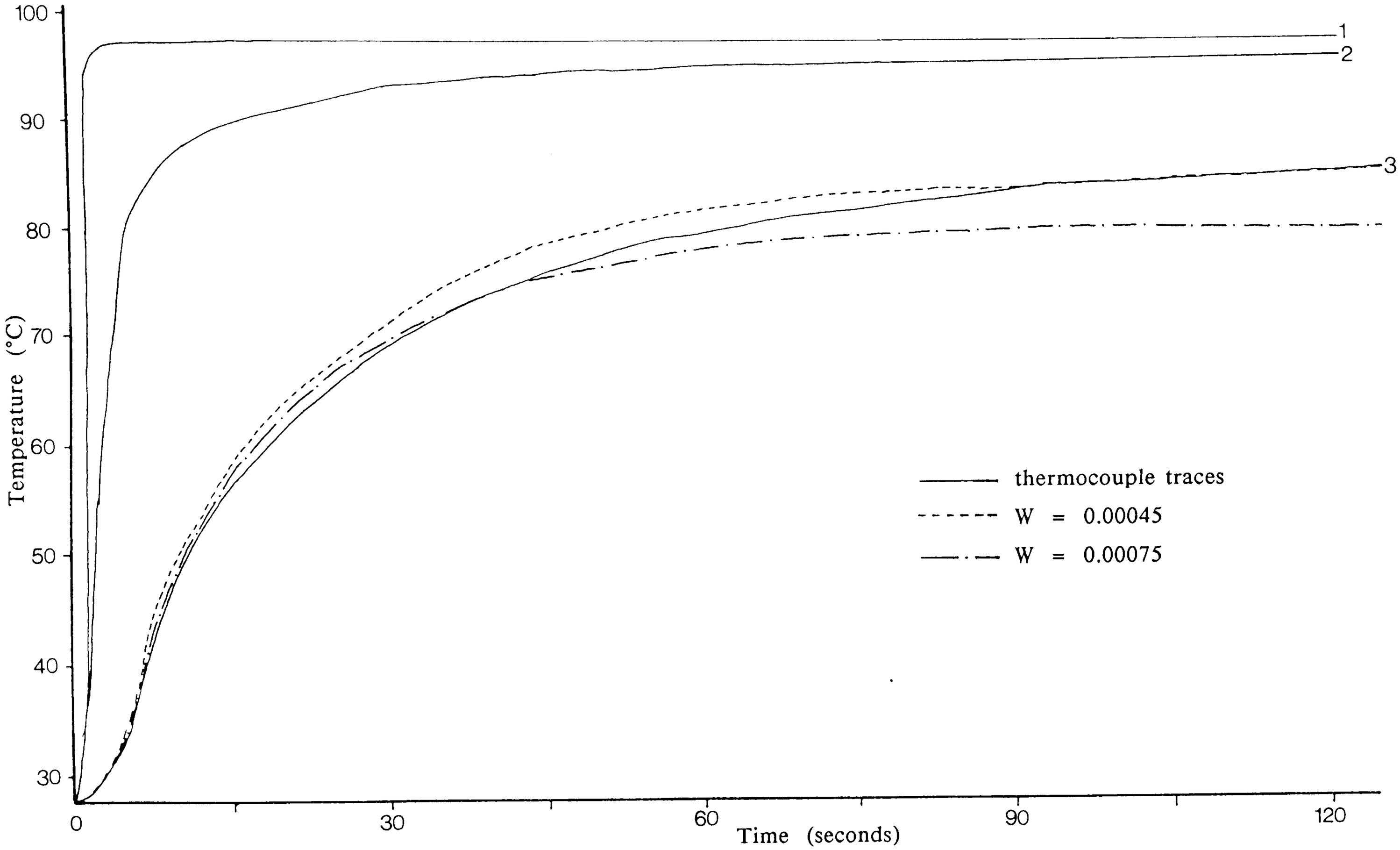

Figure 15. Time-temperature outputs from (1) a surface thermocouple, (2) one just under the surface, and (3) a thermocouple at a depth of 10 mm.

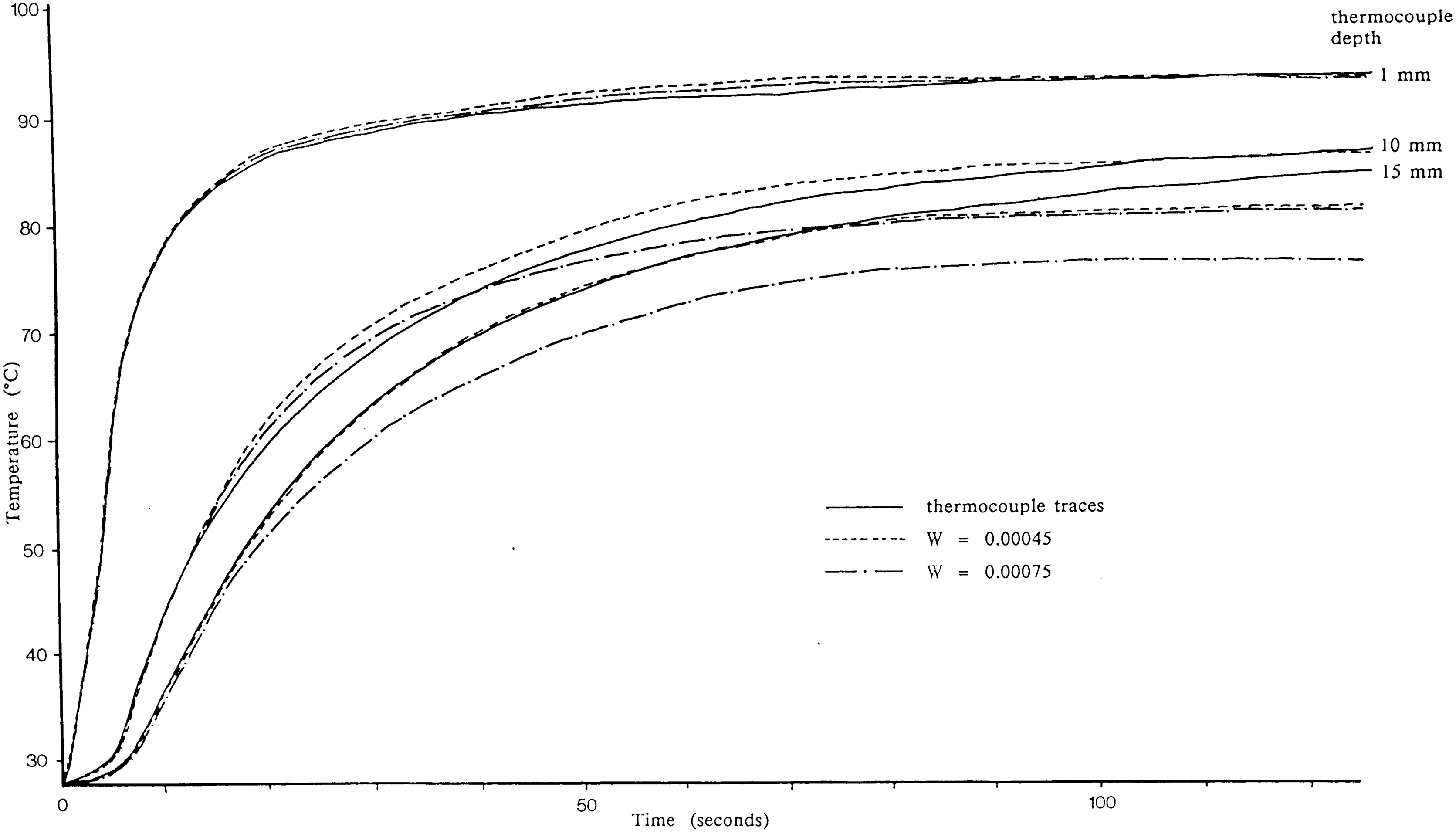

Figure 16. The range of values of heat loss which give a fit to the experimental results using the finite difference model.

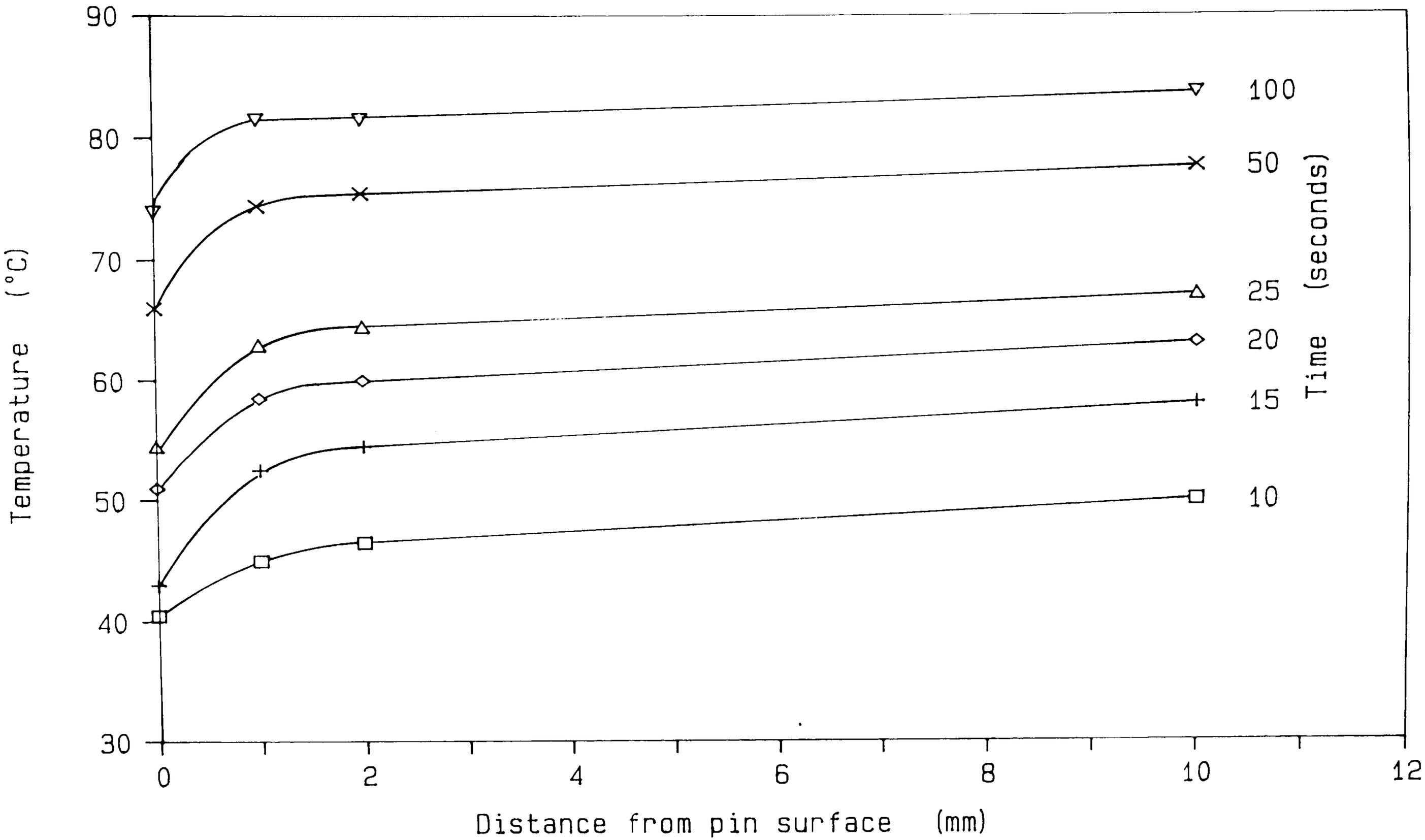

Figure 17. Temperature variation across the pin with time at a depth of 10 mm from the steam heated surface.

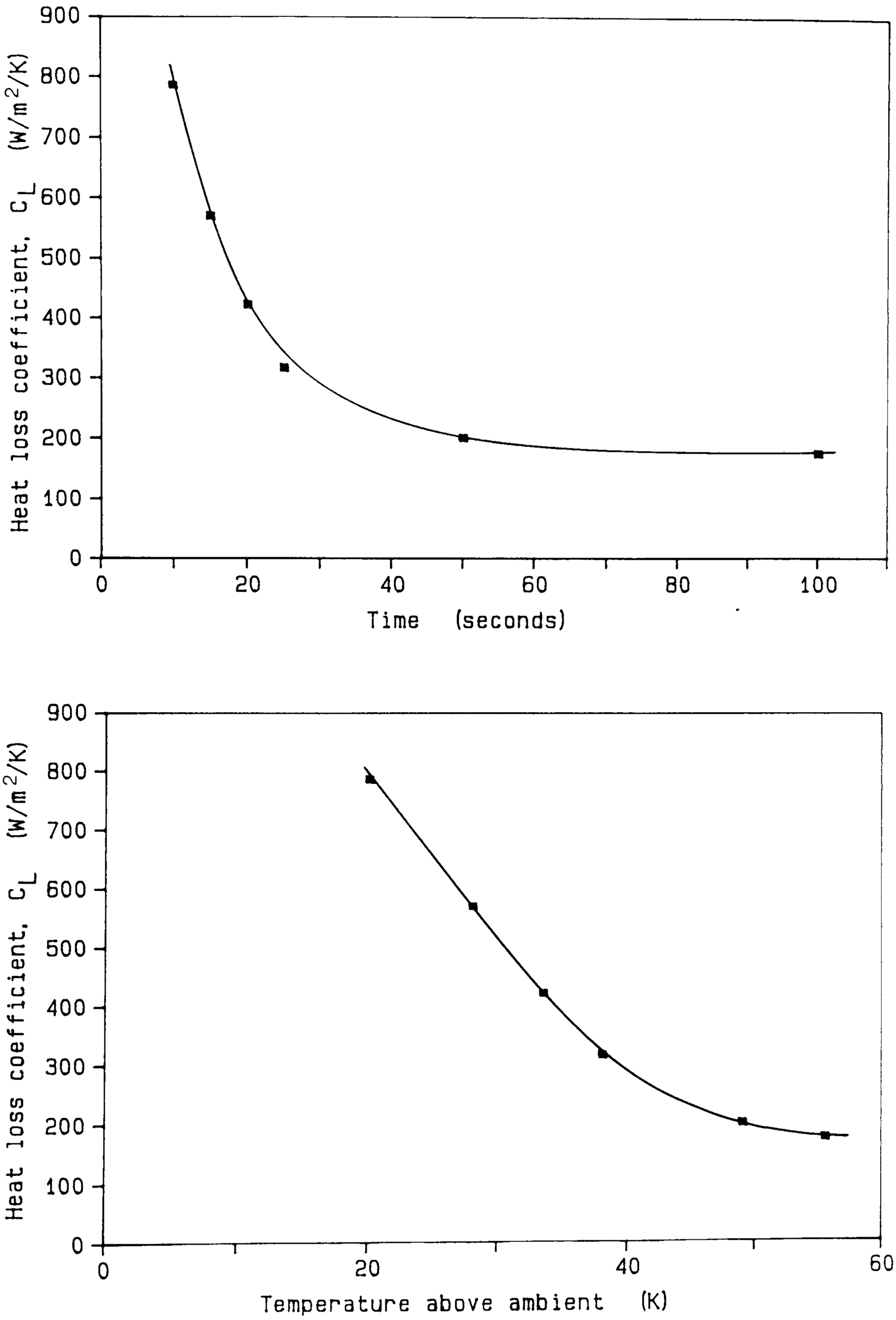

Figure 18. Variation of the heat loss coefficient with time and with the temperature of the point 8 mm from the pin centre.

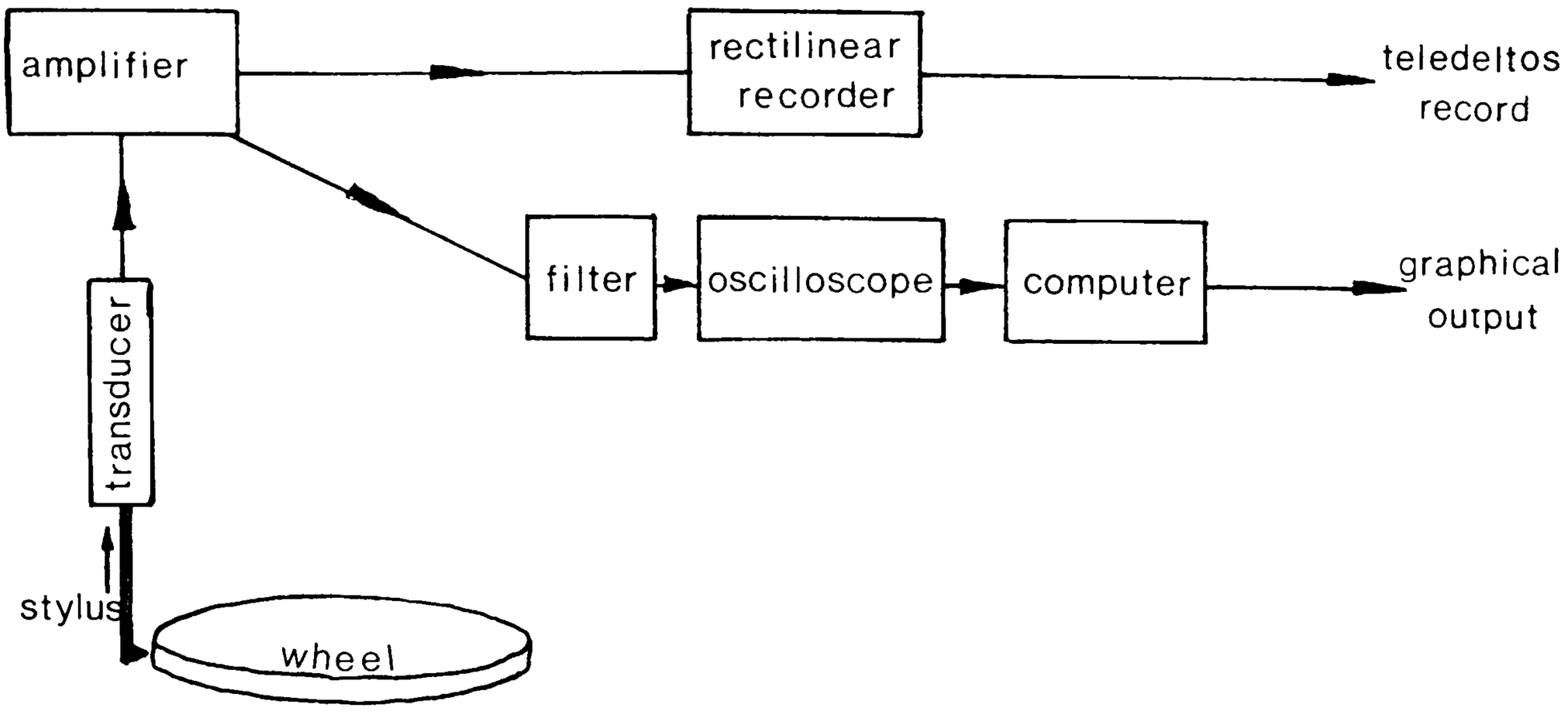

(a)

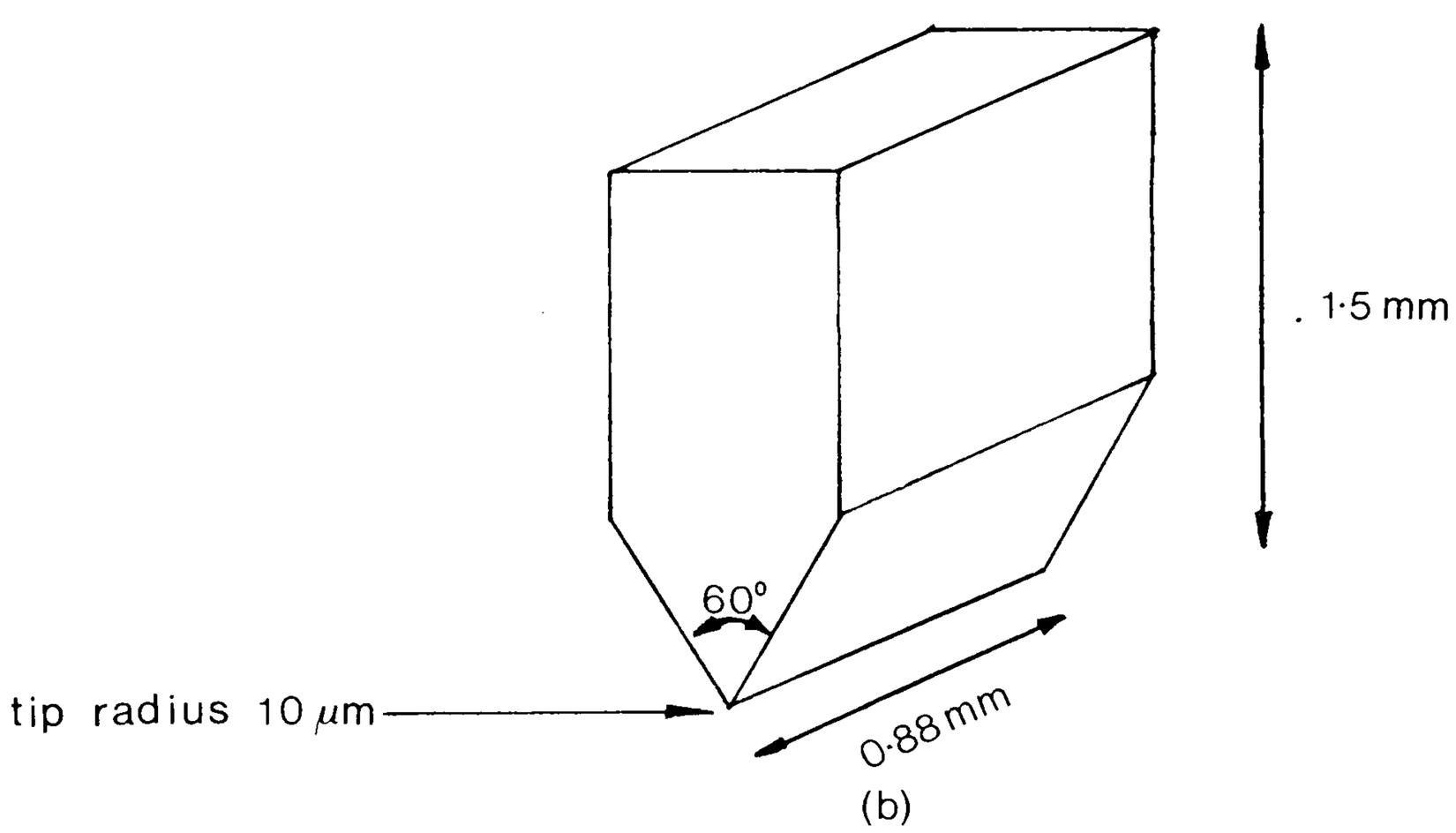

(b)

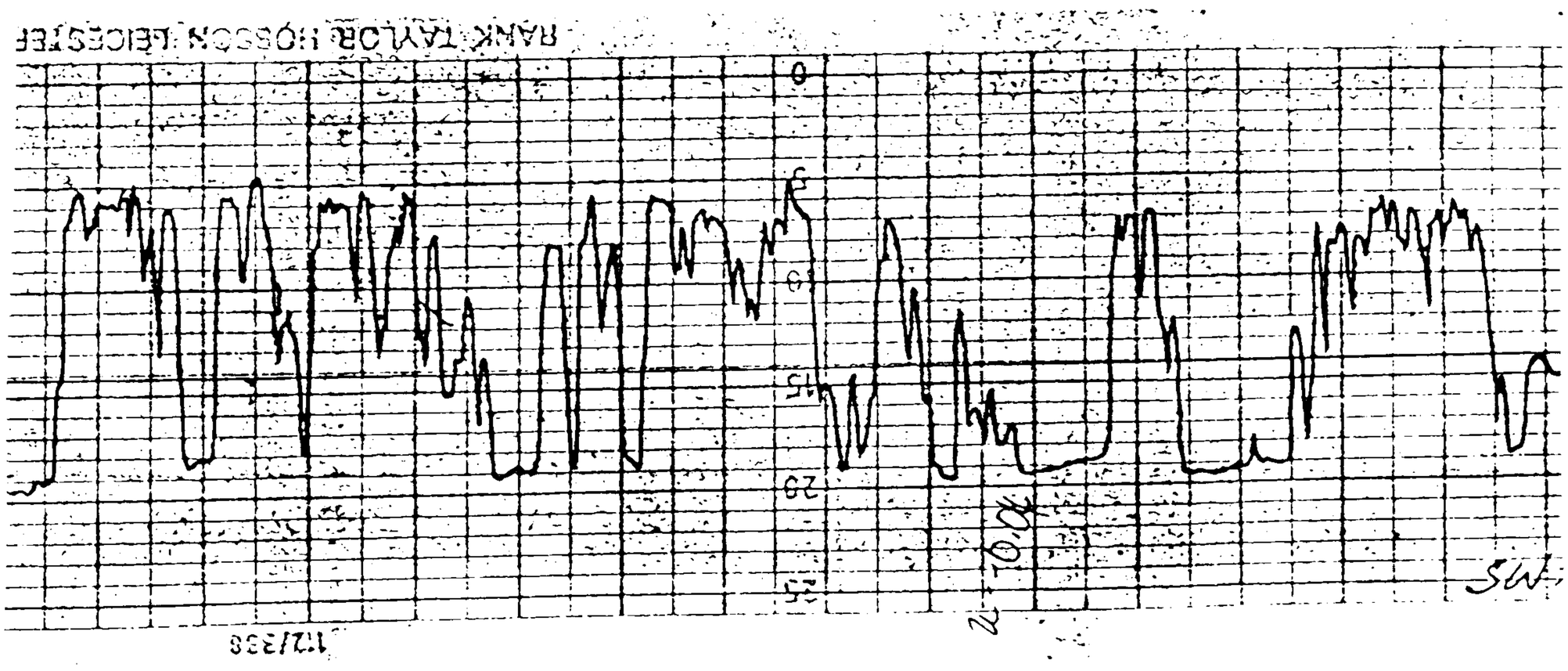

(c)

Figure 19. Surface measurement: (a) schematic diagram of the surface measuring equipment; (b) the stylus dimensions; (c) a typical profile trace on 'Teledeltos' paper.

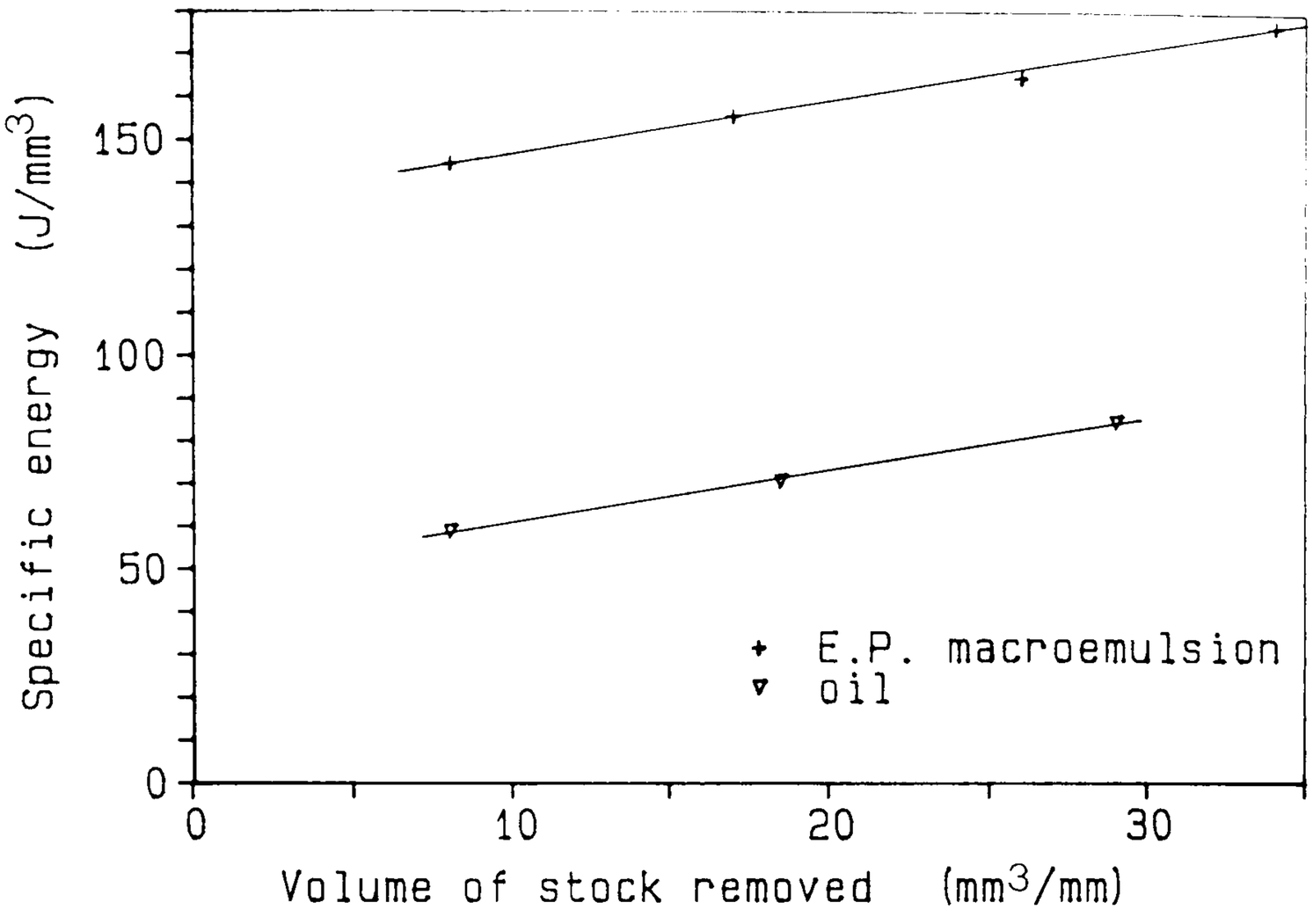

Figure 20. Specific energy variation with the volume of stock removed for Nimonic at a depth of cut of 1 mm under conventional dressing conditions.

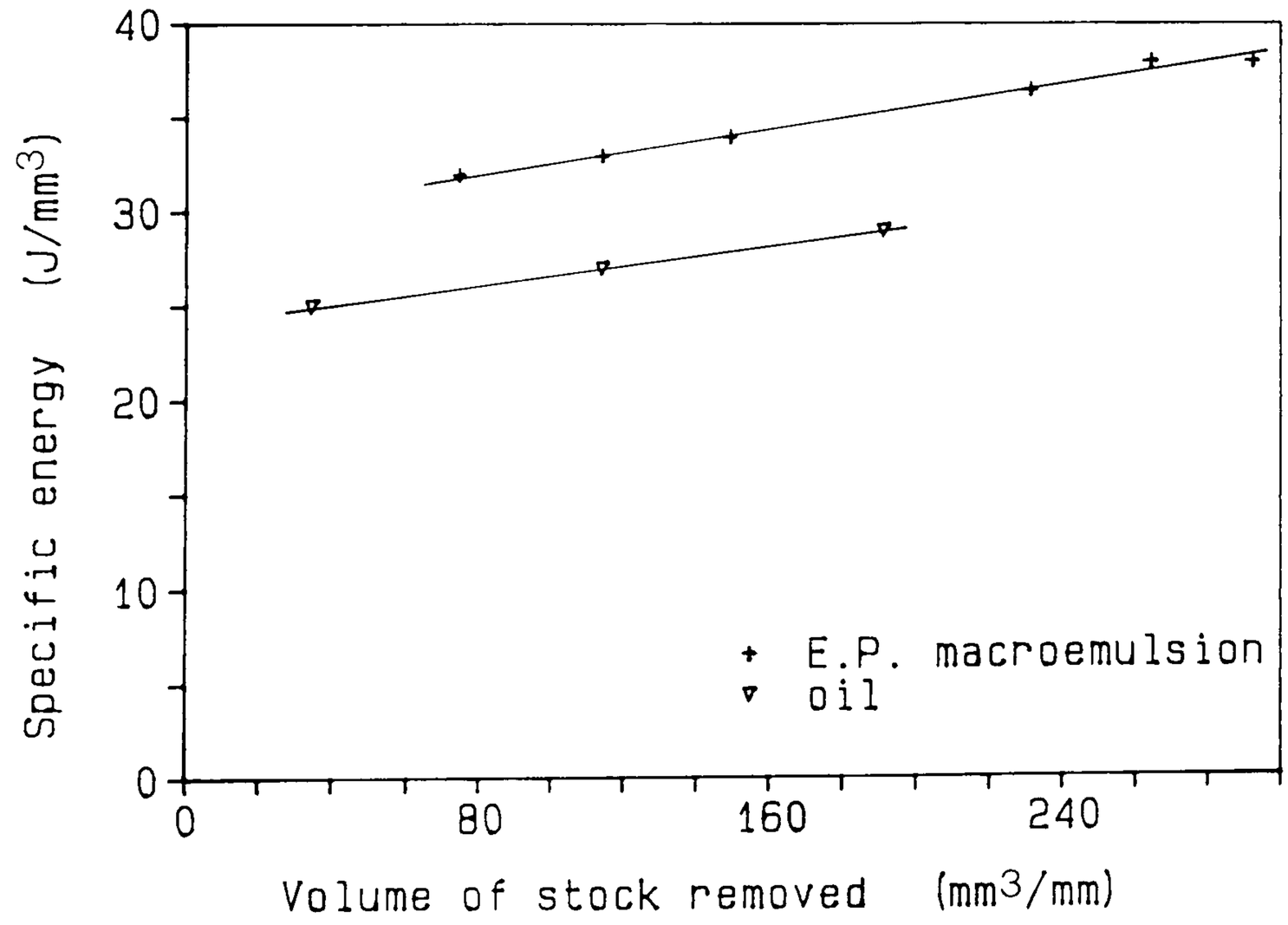

Figure 21. Specific energy variation with the volume of stock removed for steel at a 3 mm depth of cut under conventional dressing conditions.

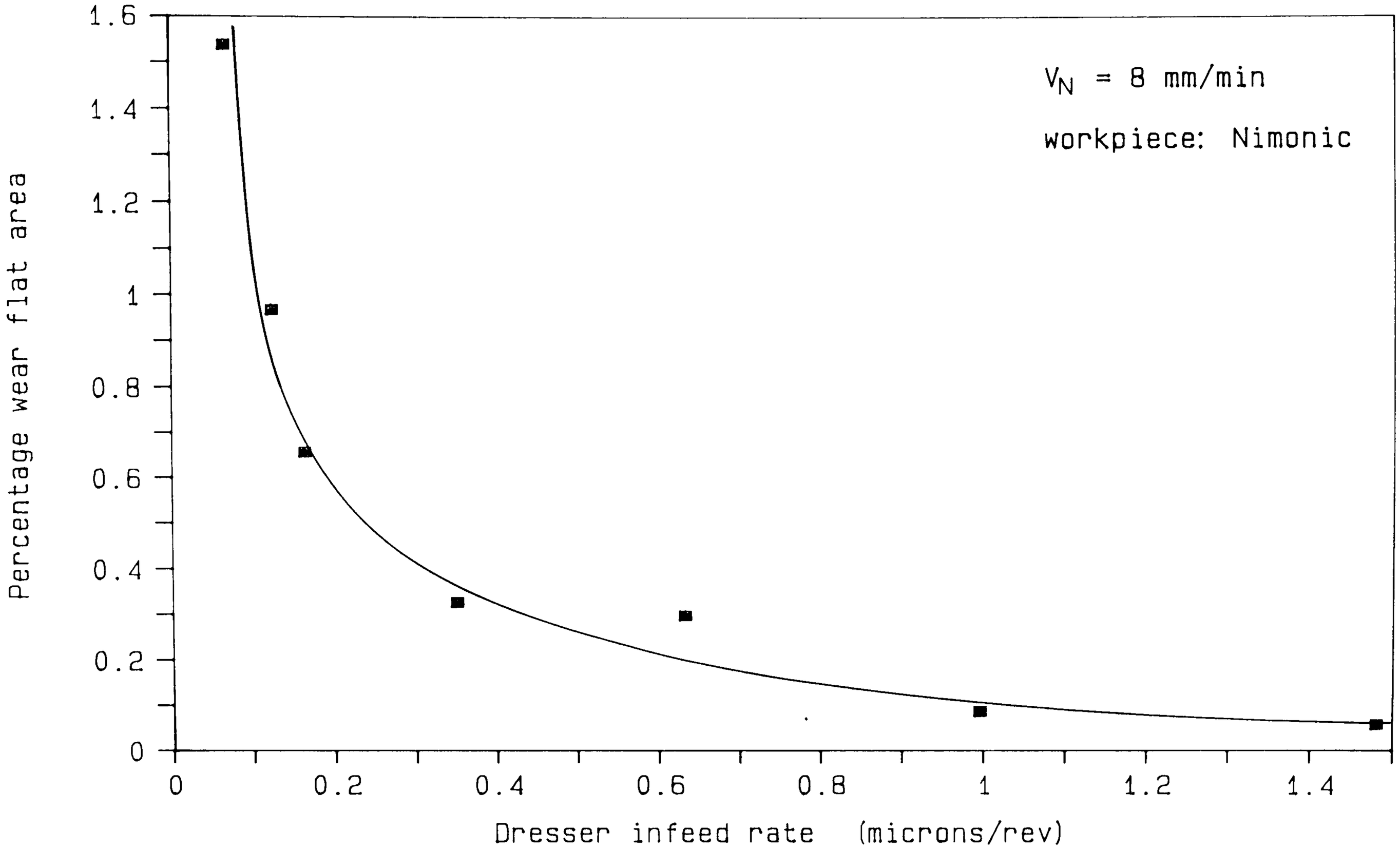

Figure 22. Wear flat area versus dresser infeed rate (replotted from Salmon [65]).

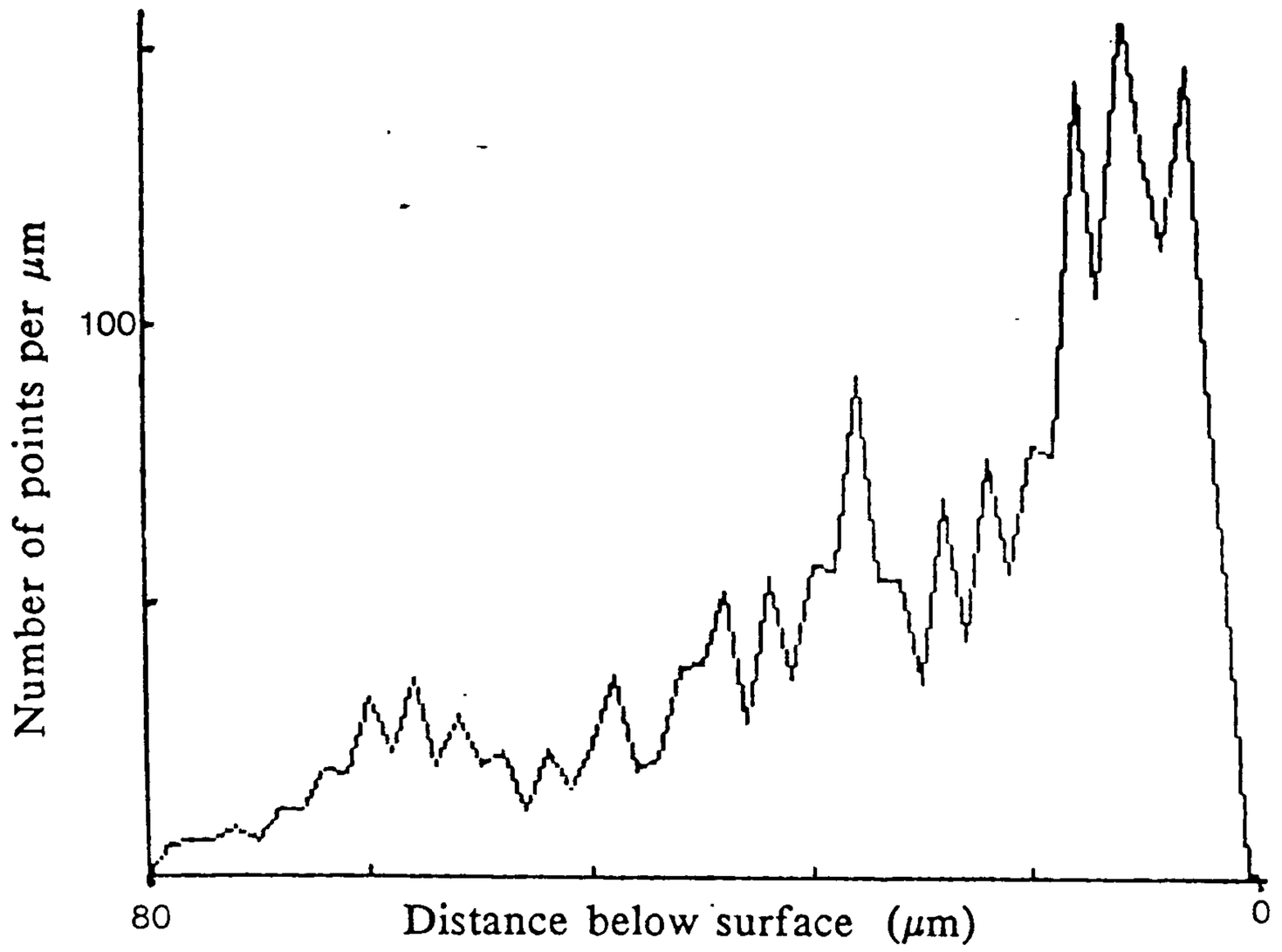

(a) Probability density function

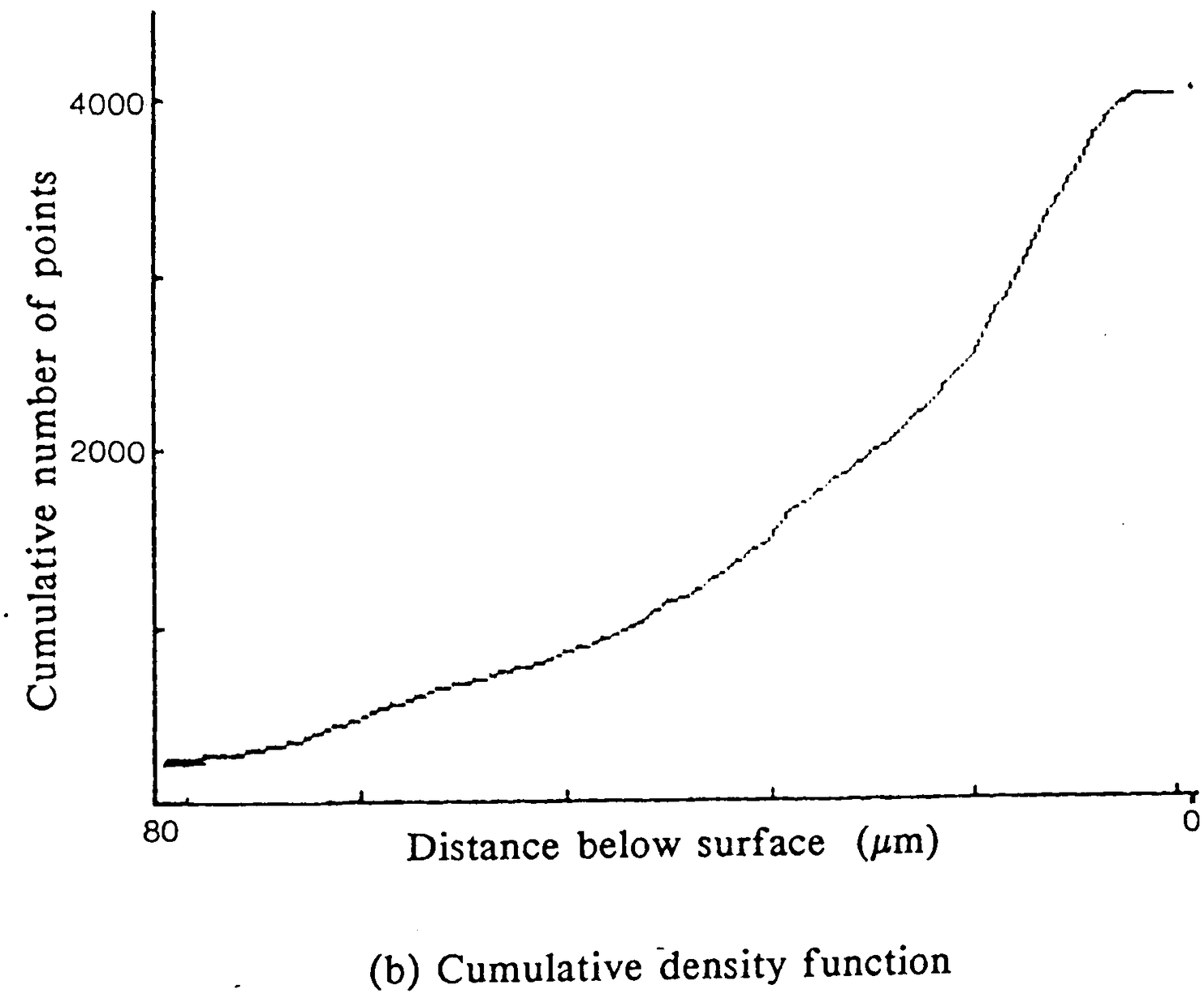

(b) Cumulative density function

Figure 23. Typical wheel surface generated by dressing at 0.25 μm/rev with the macroemulsion.

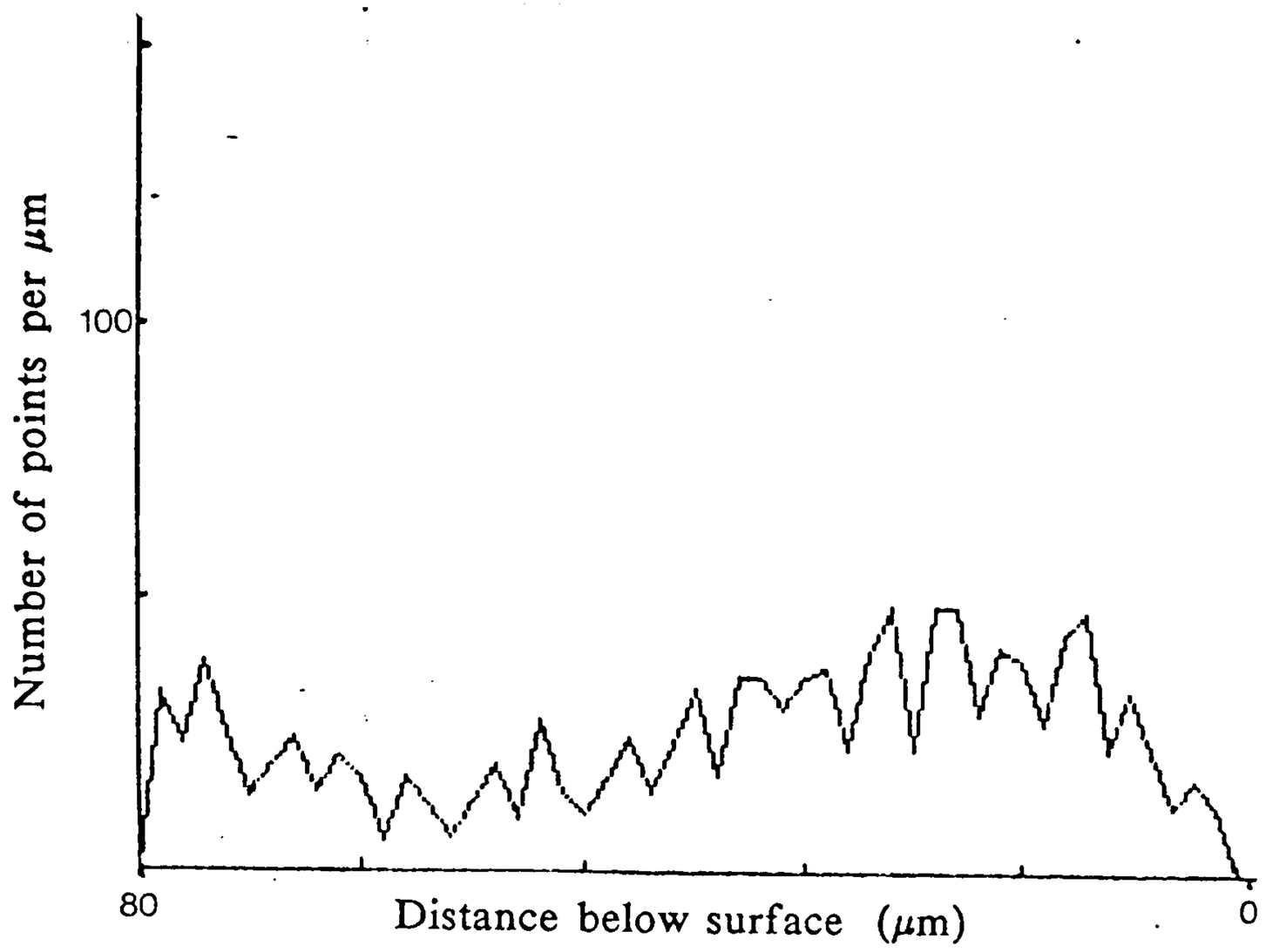

(a) Probability density function

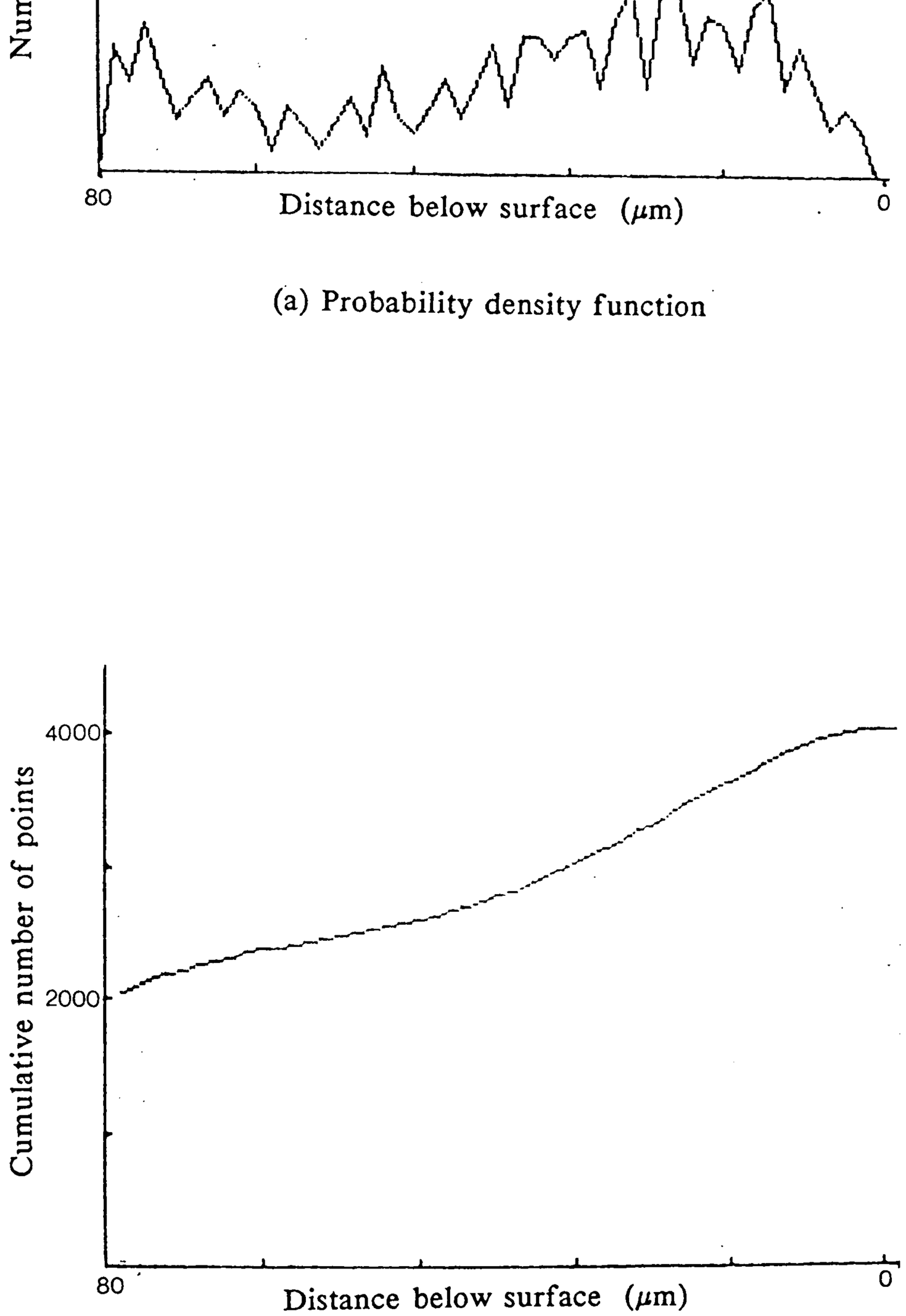

(b) Cumulative density function

Figure 24. Typical wheel surface generated by dressing at 1.8 μm/rev with the macroemulsion.

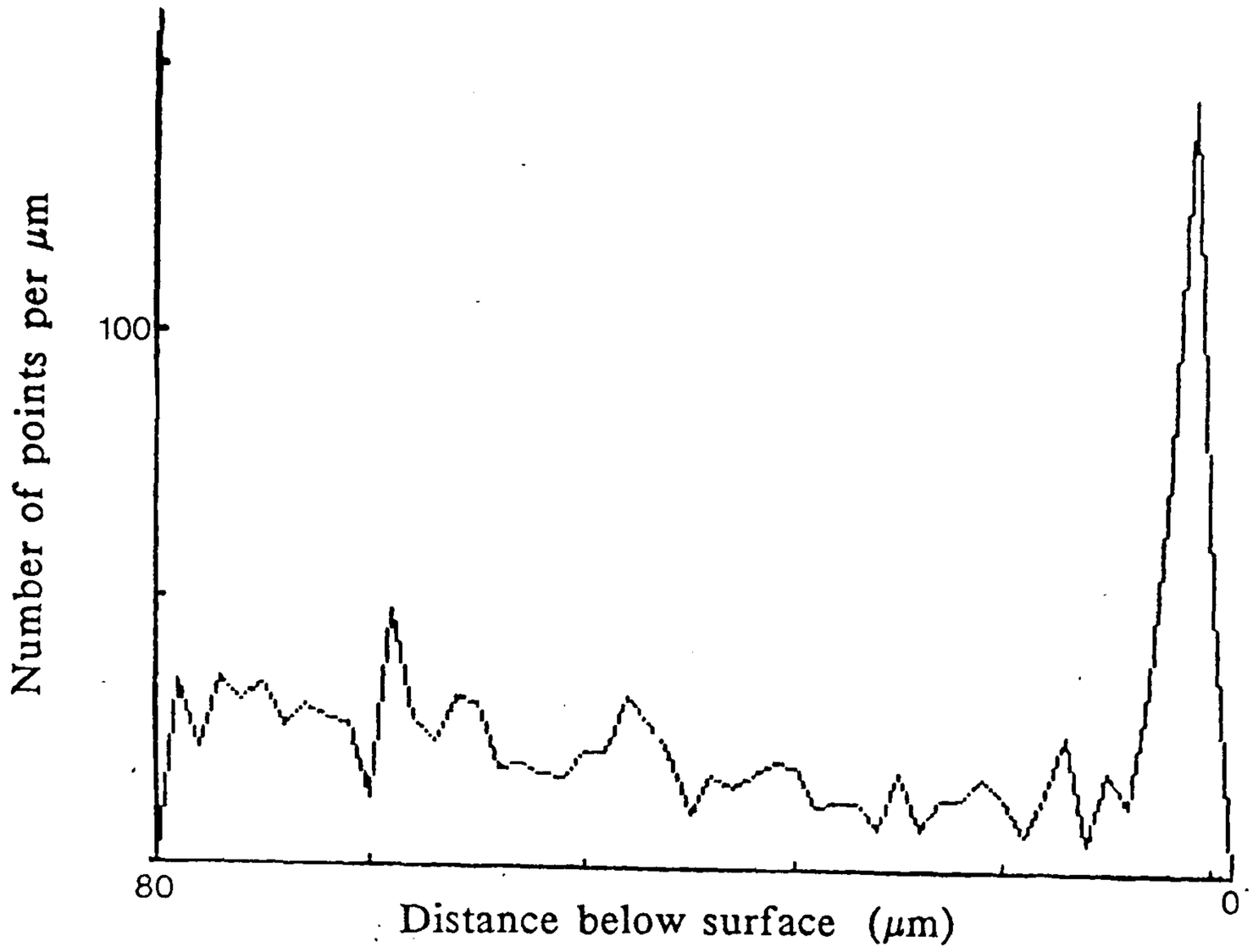

(a) Probability density function

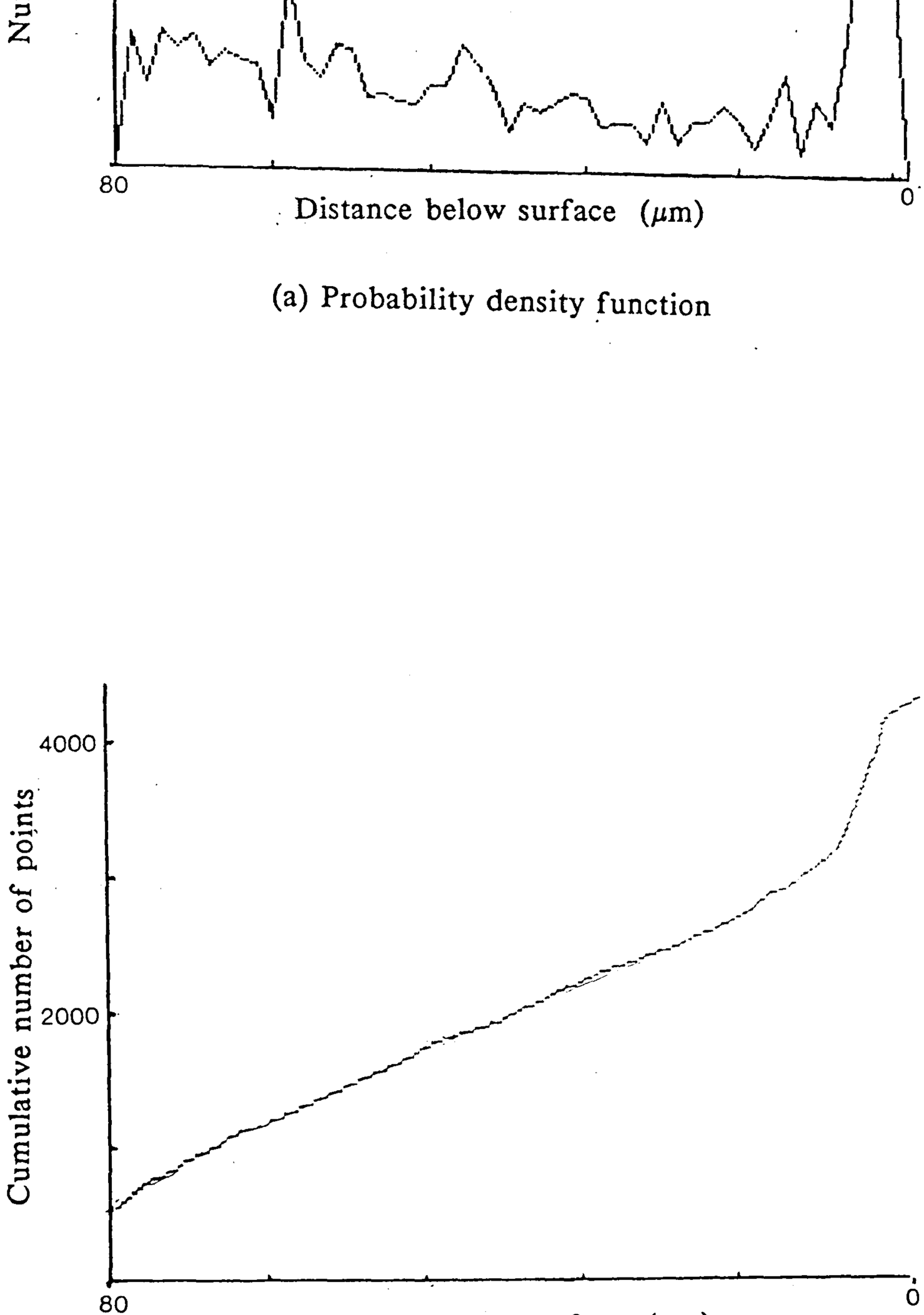

(b) Cumulative density function

Figure 25. Typical wheel surface generated by dressing at 0.25 μm/rev with oil.

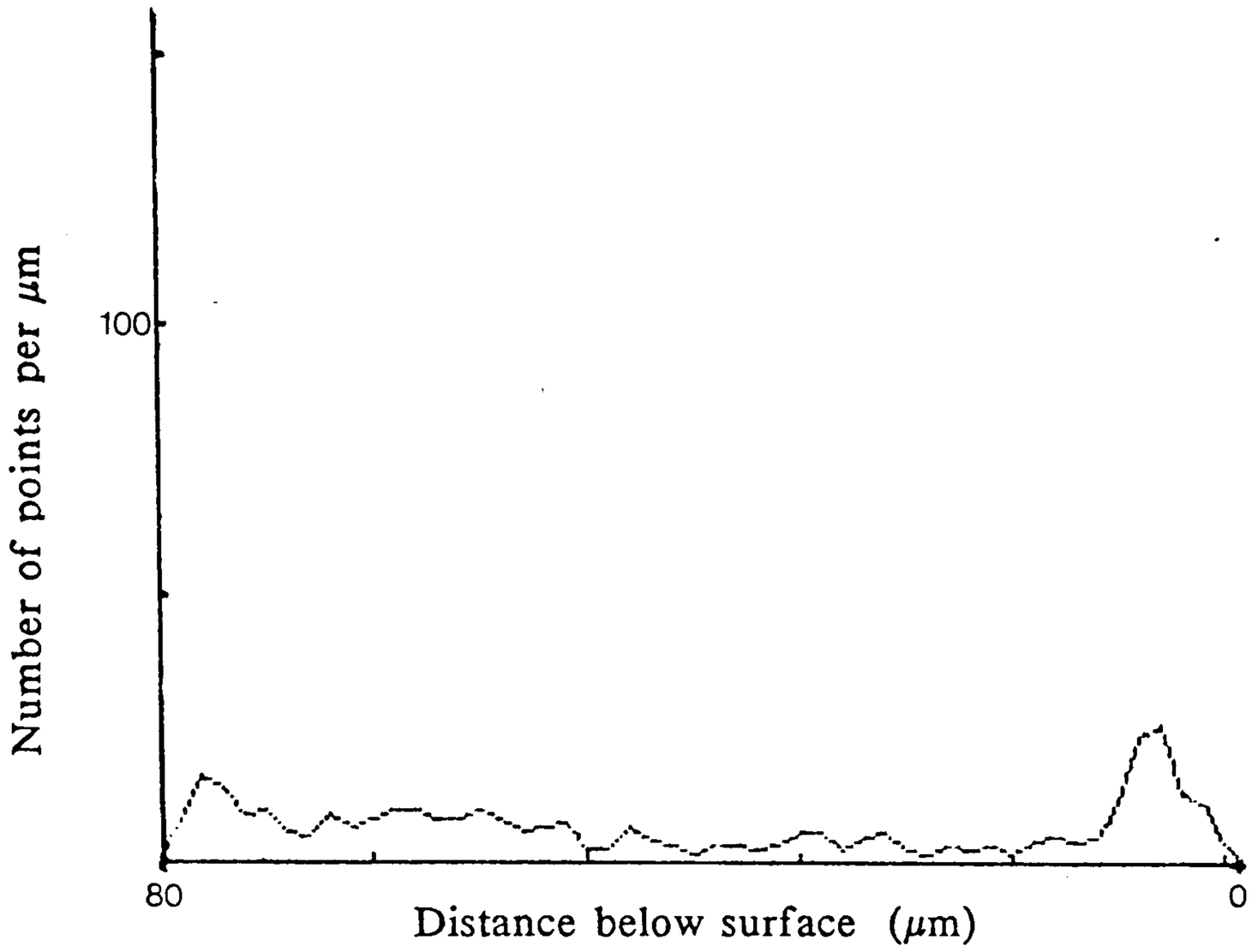

(a) Probability density function

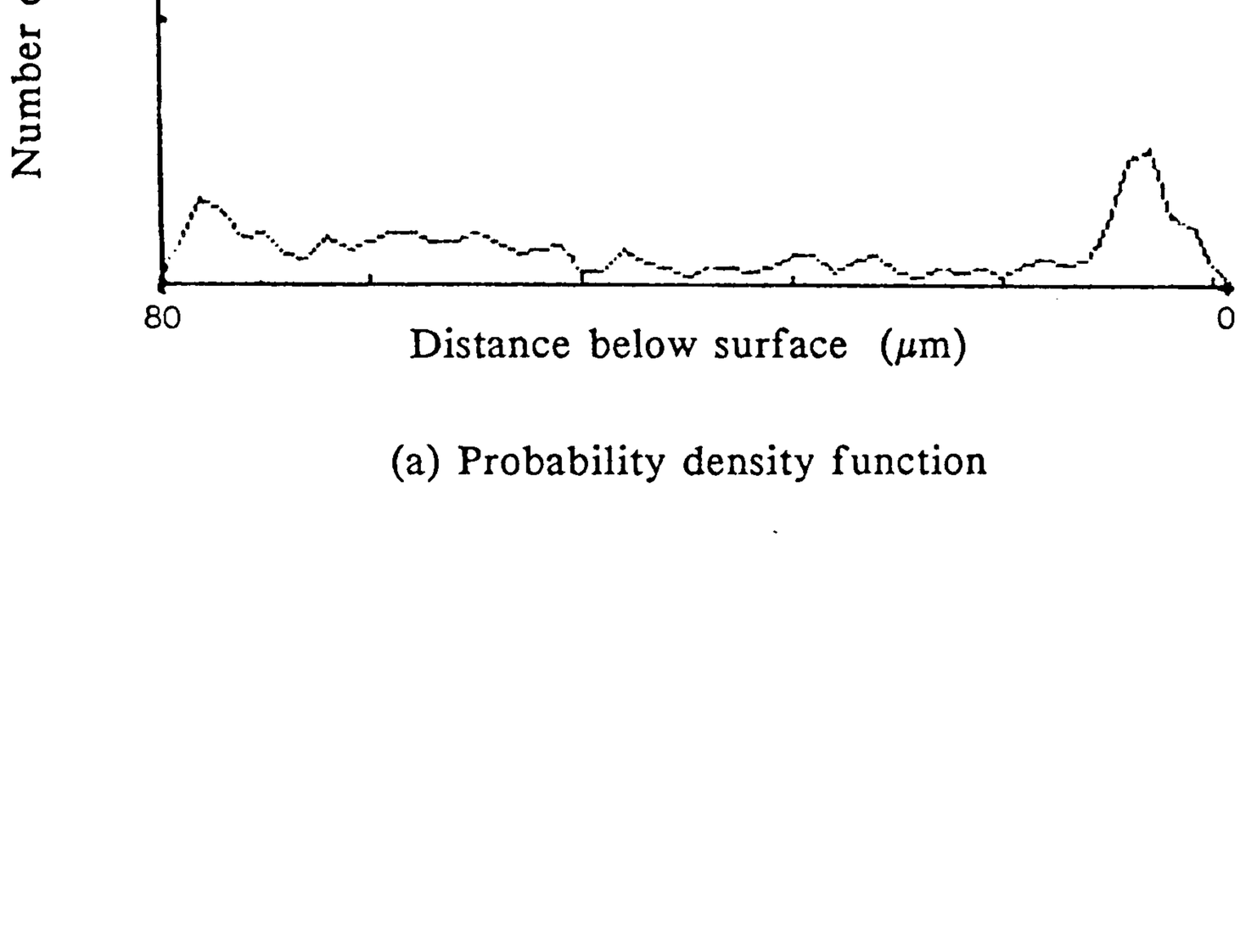

(b) Cumulative density function

Figure 26. Typical wheel surface generated by dressing at 1.8 μm/rev with oil.

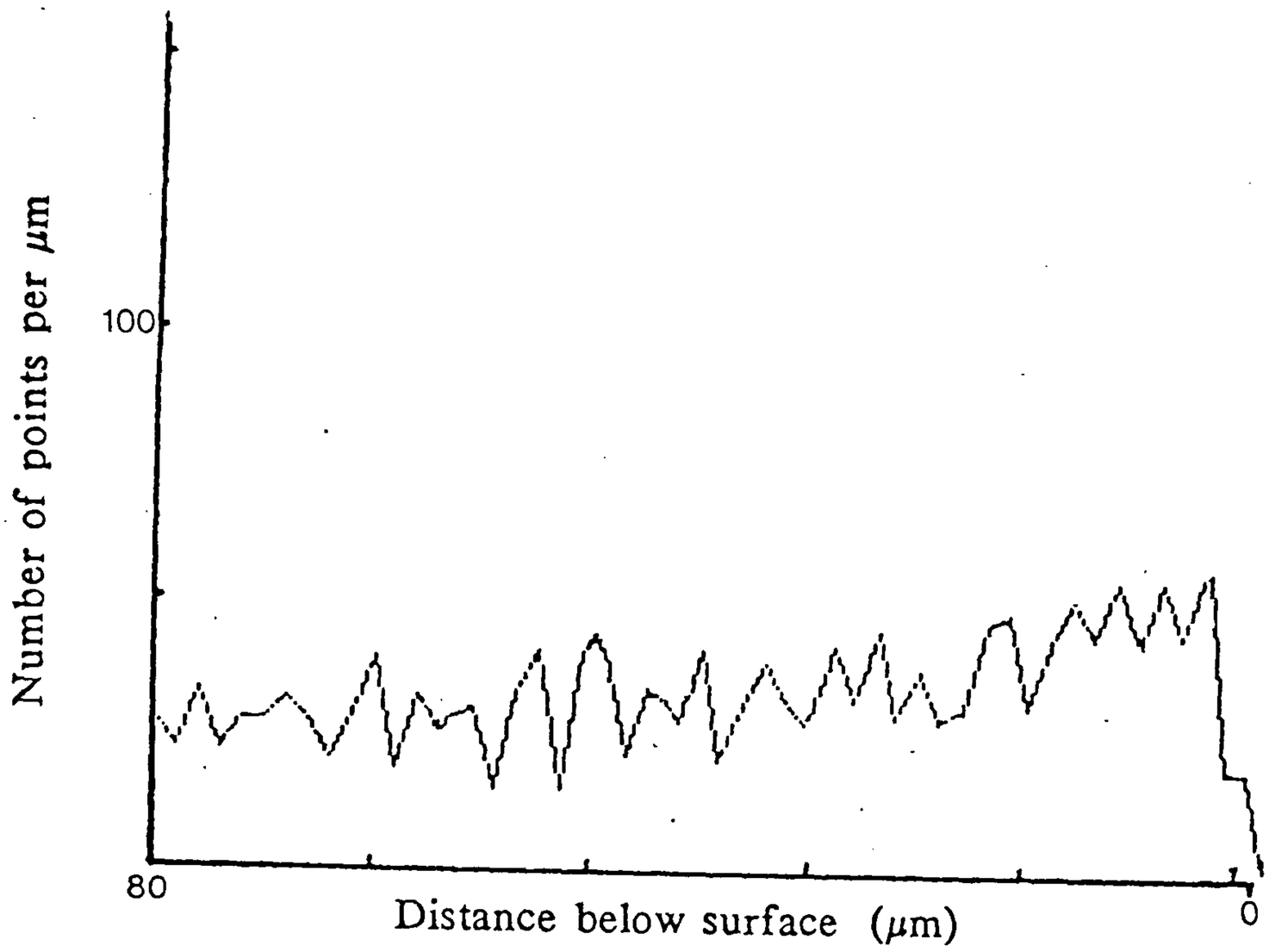

(a) Probability density function

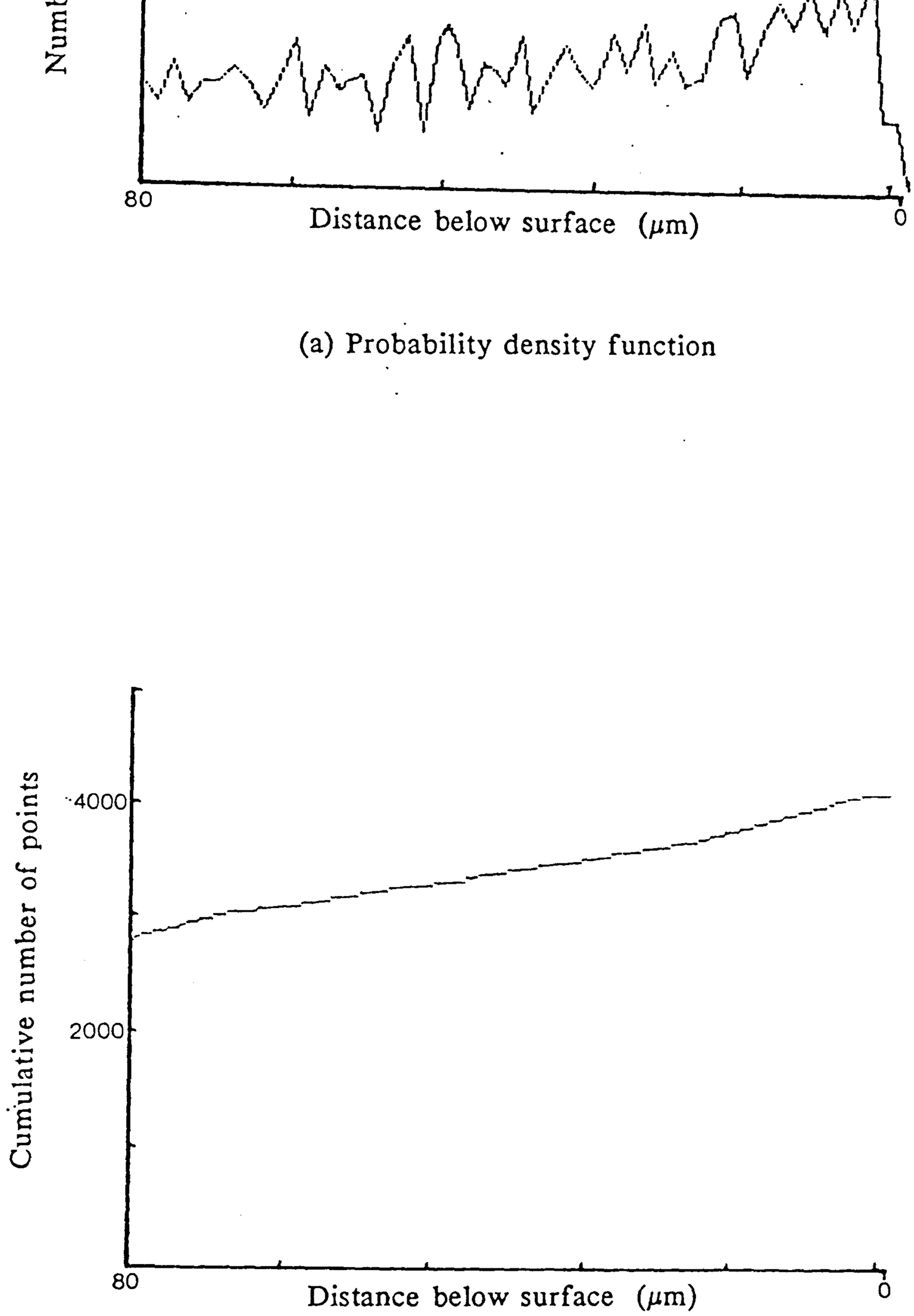

(b) Cumulative density function

Figure 27. Typical wheel surface generated when Nimonic is ground with the macroemulsion (dressing at 1.8 μm/rev).

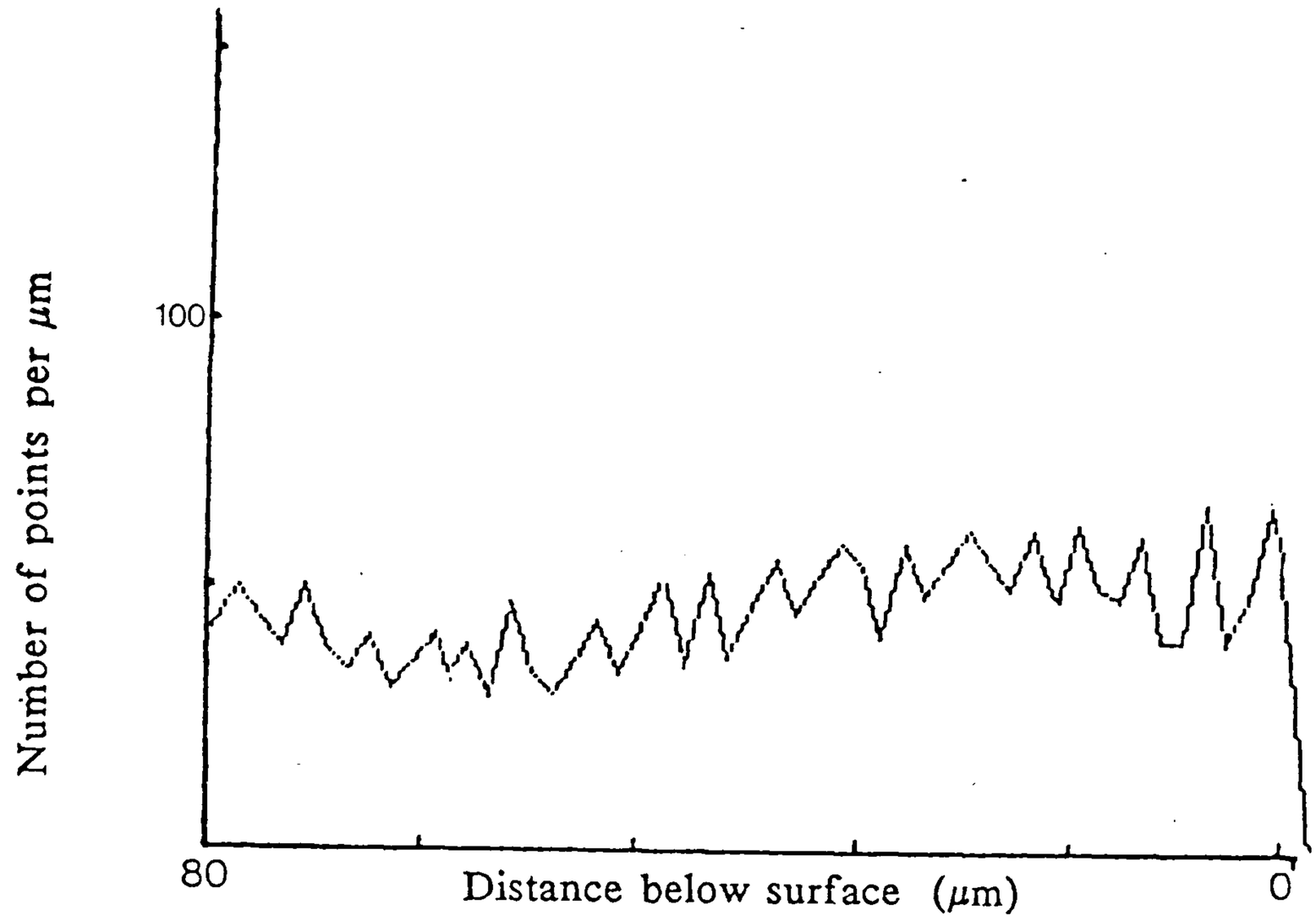

(a) Probability density function

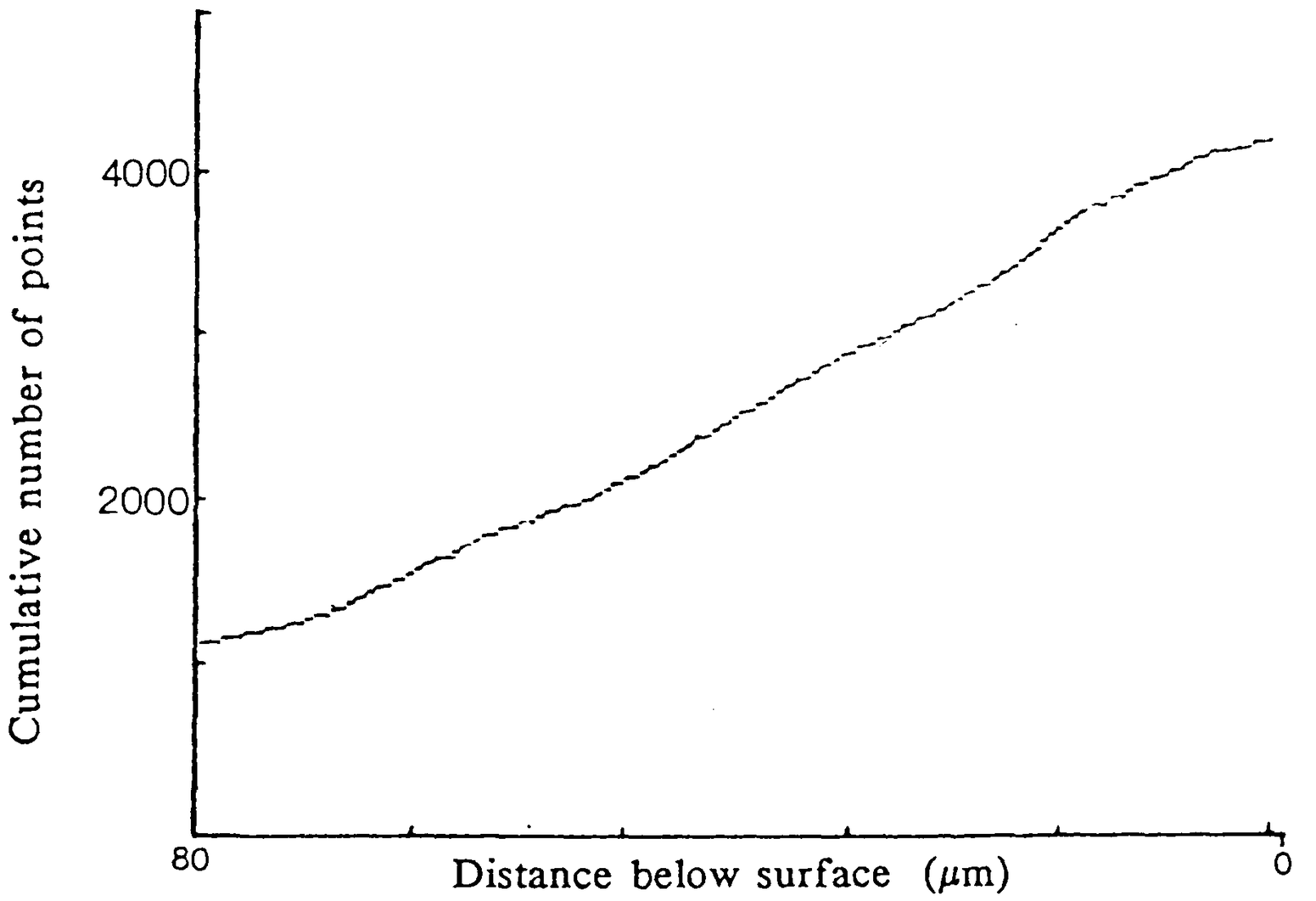

(b) Cumulative density function

Figure 28. Typical wheel surface generated when Nimonic is ground with oil (dressing at 1.8 μm/rev).

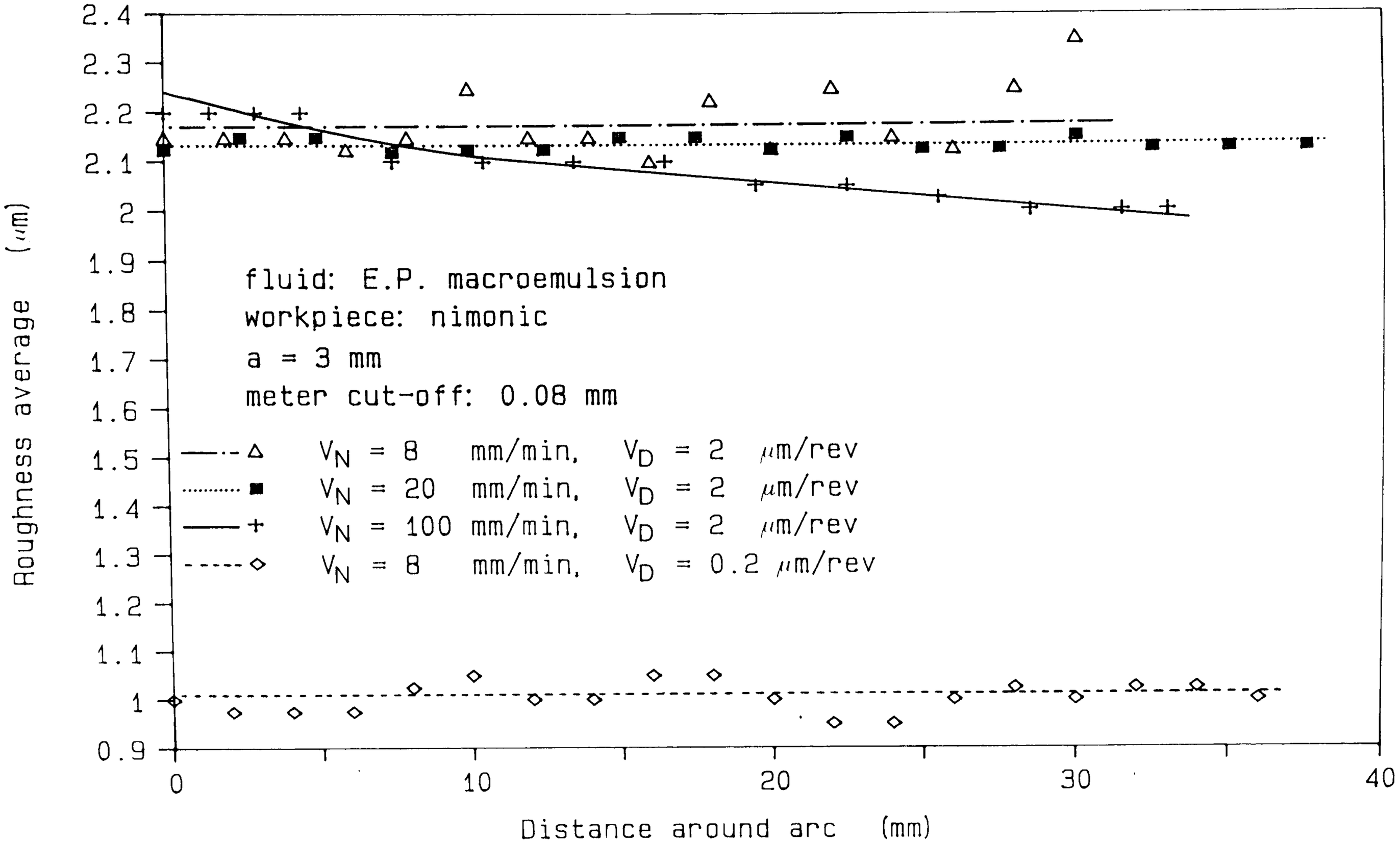

Figure 29. Workpiece roughness averages plotted against position around the arc of cut.

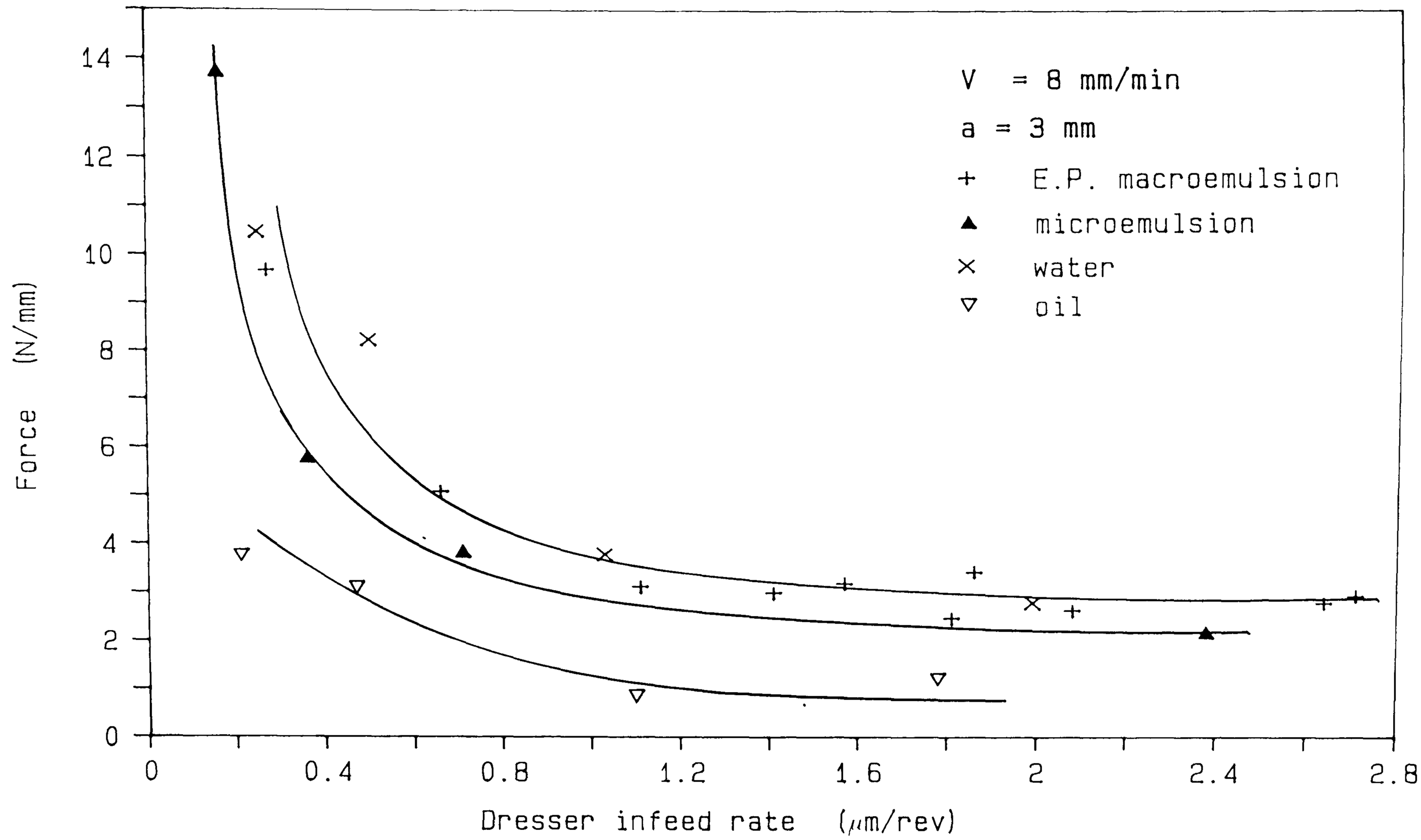

Figure 30. Comparison of the tangential force generated versus dresser infeed rate with a range of fluids on Nimonic.

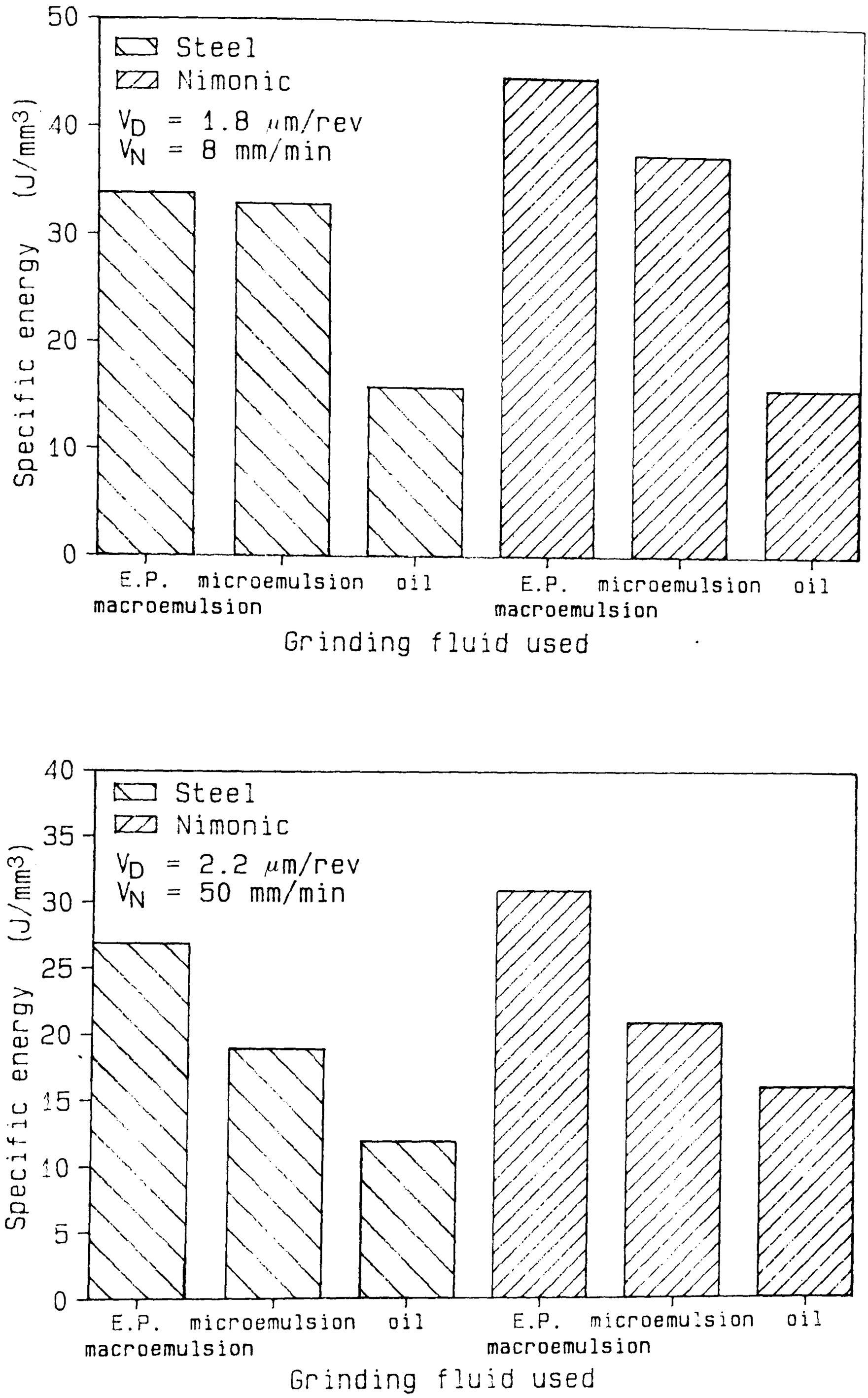

Figure 31. Histogram of specific energies for a range of fluids on Nimonic and steel.

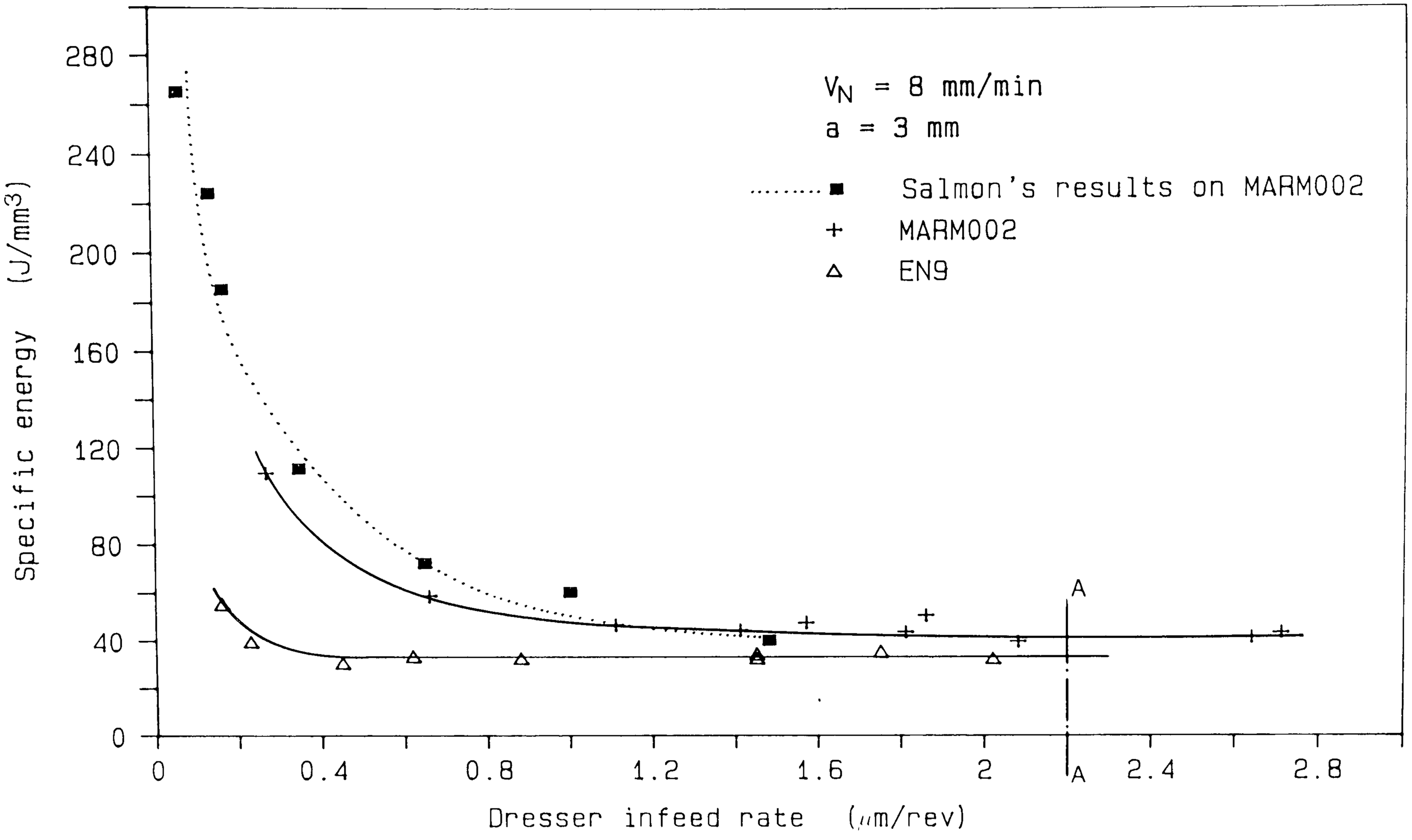

Figure 32. Specific energy versus dresser infeed rate for steel and Nimonic.

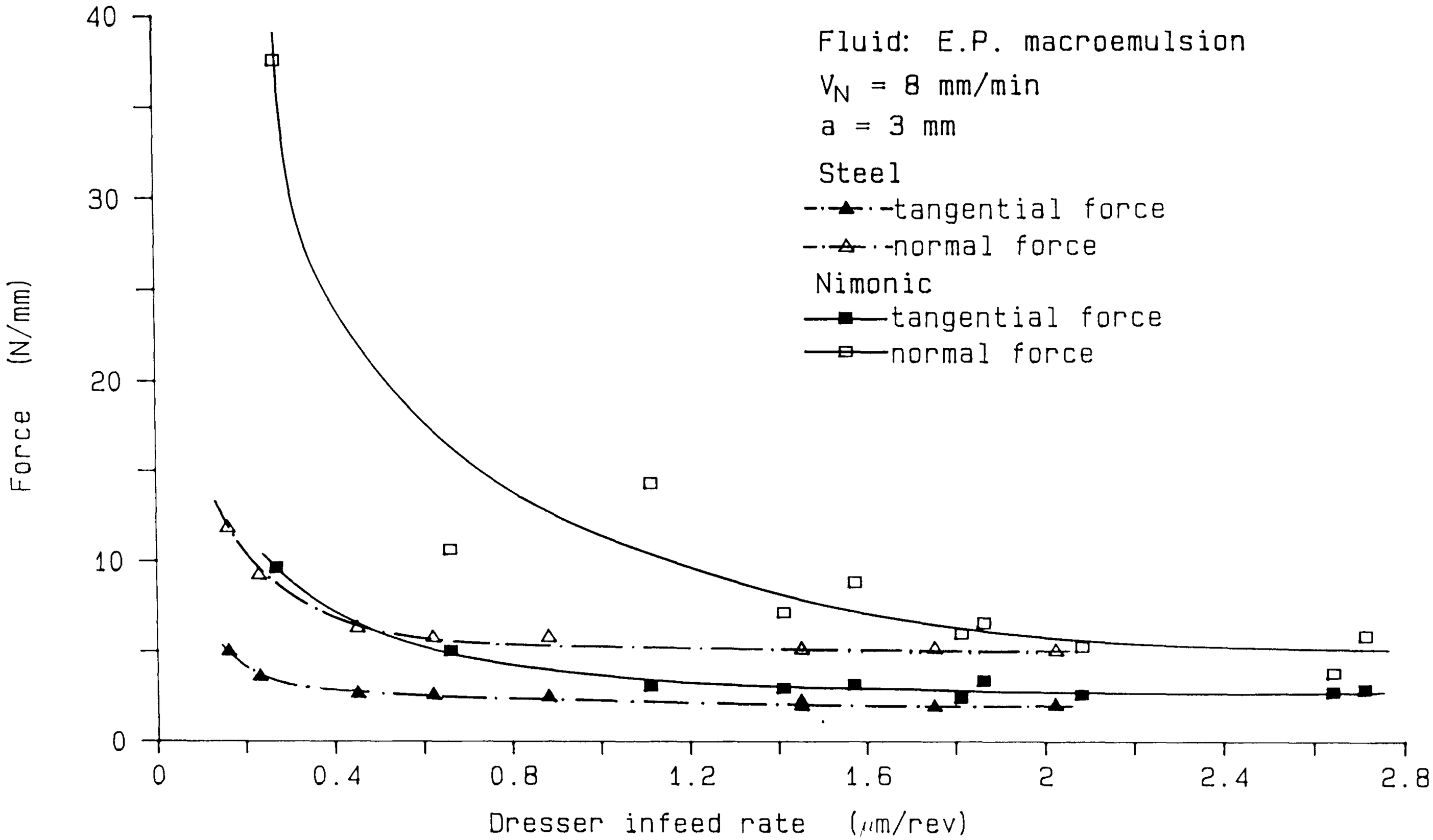

Figure 33. Variation of forces with dresser infeed rate (a replot of Figures 23, 29 & 30).

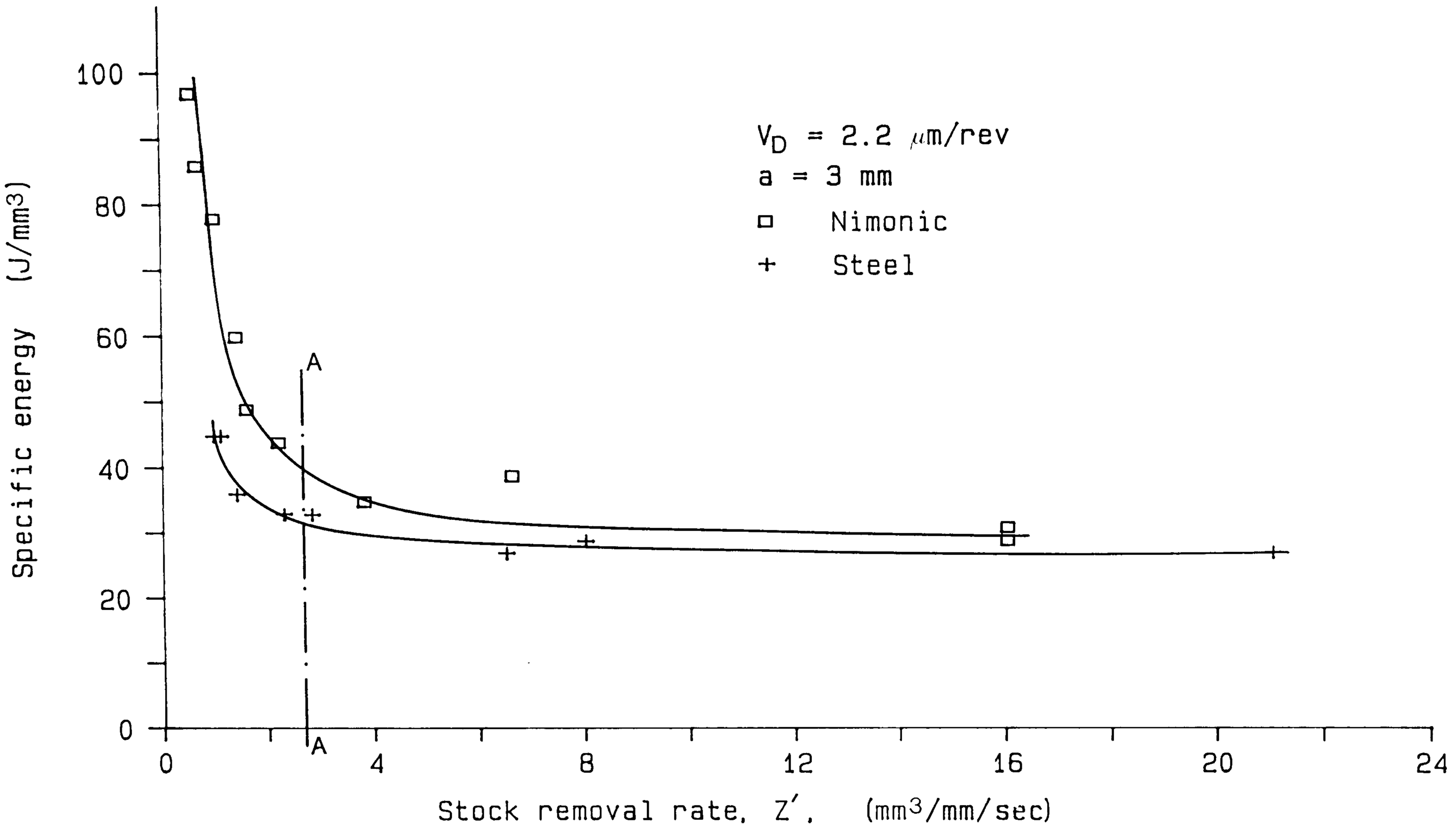

Figure 34. Specific energy variation when the stock removal rate is altered whilst keeping the dresser infeed rate high.

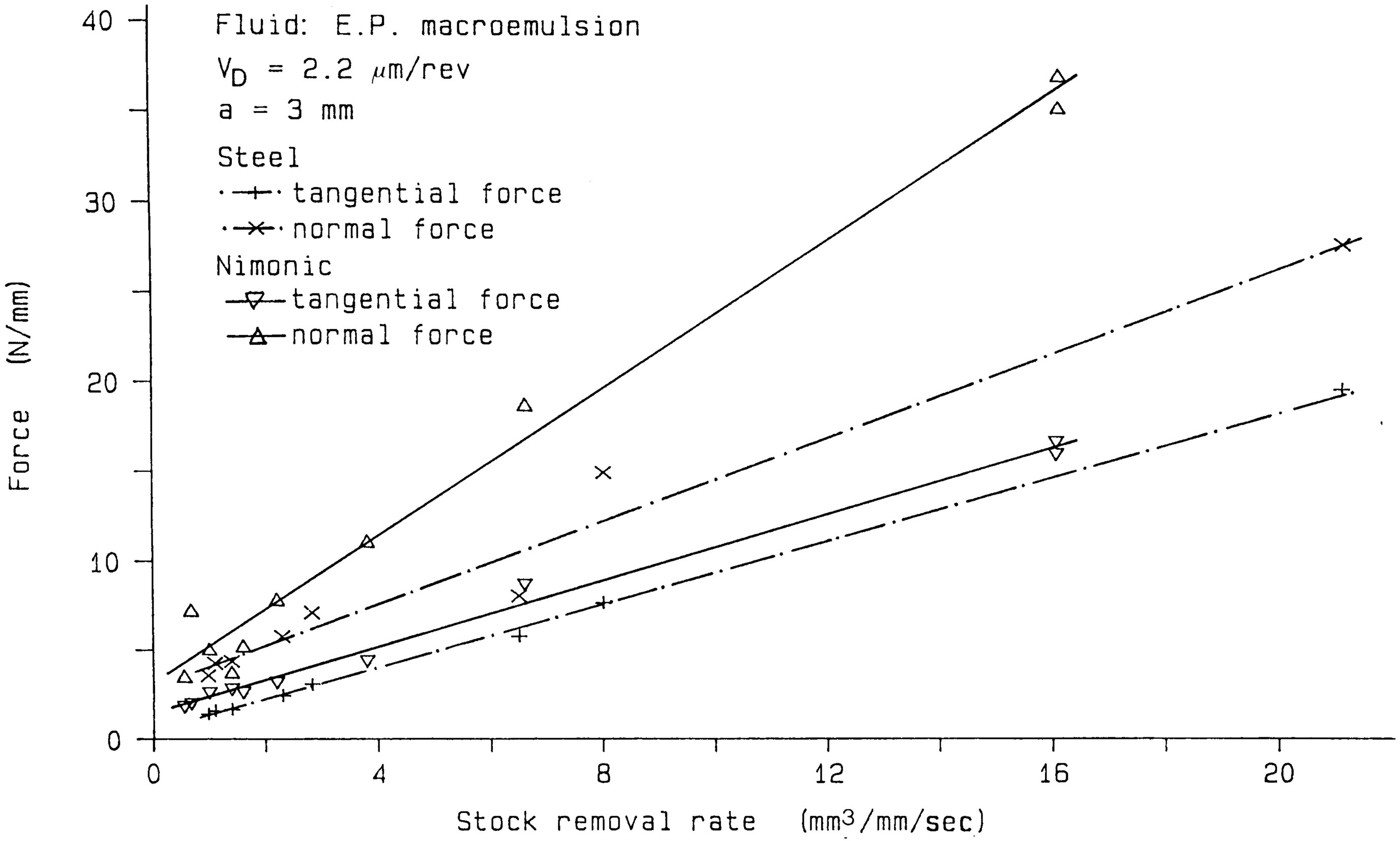

Figure 35. Graph of forces versus stock removal rate using the E.P. macroemulsion.

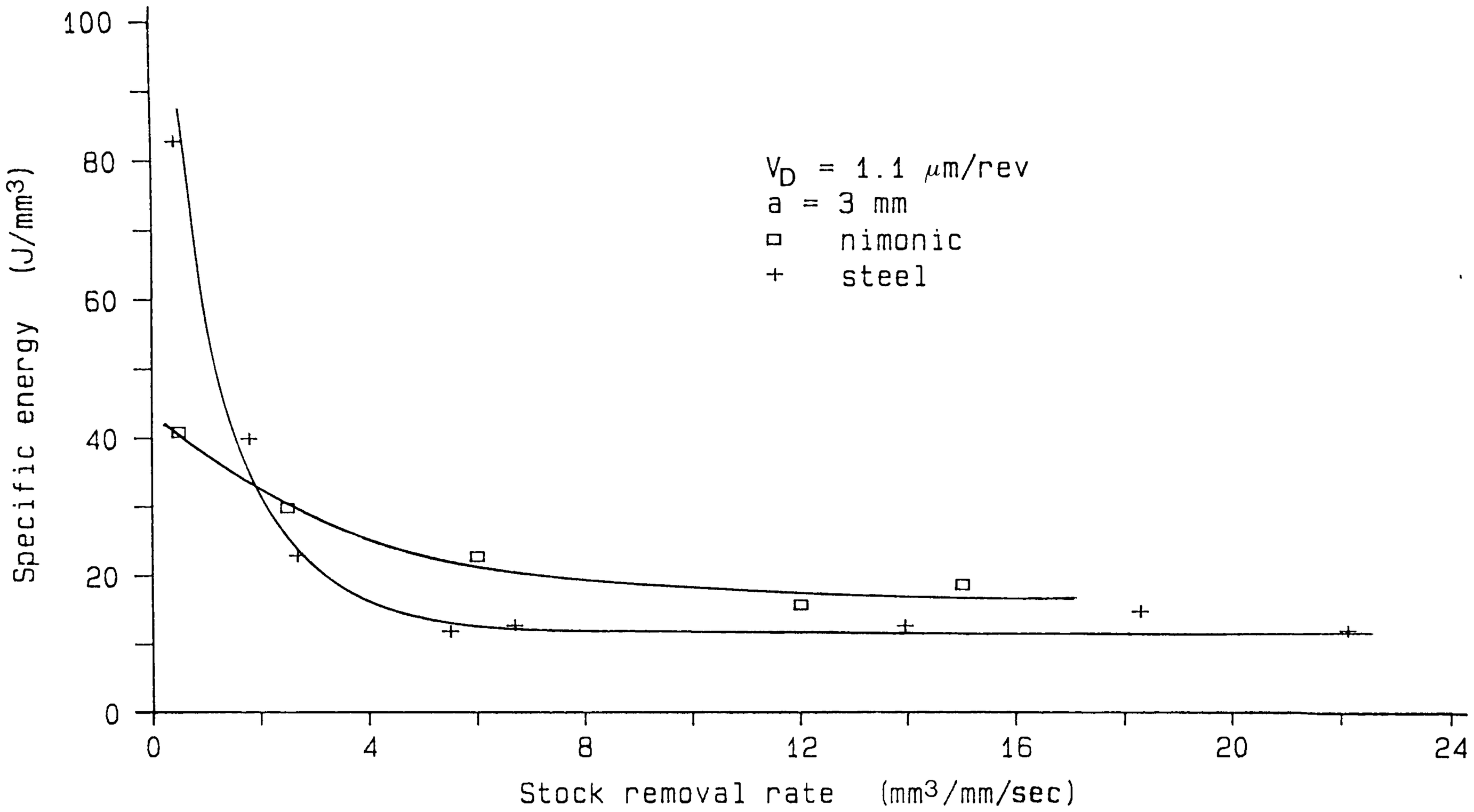

Figure 36. Variation of specific energy with stock removal rate using oil.

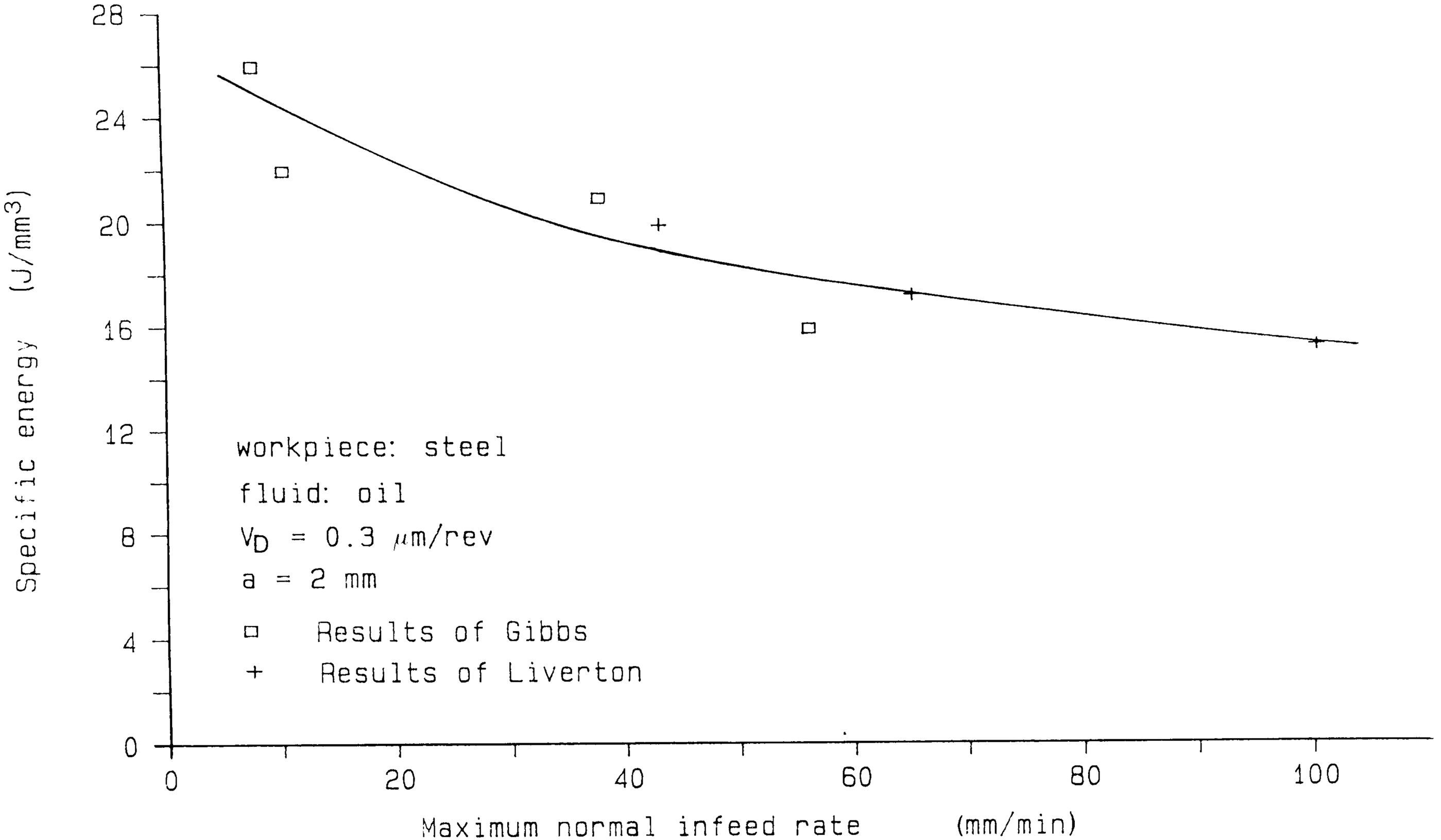

Figure 37. A graph of specific energy versus stock removal rate, as a comparison with the results of Liverton [97].

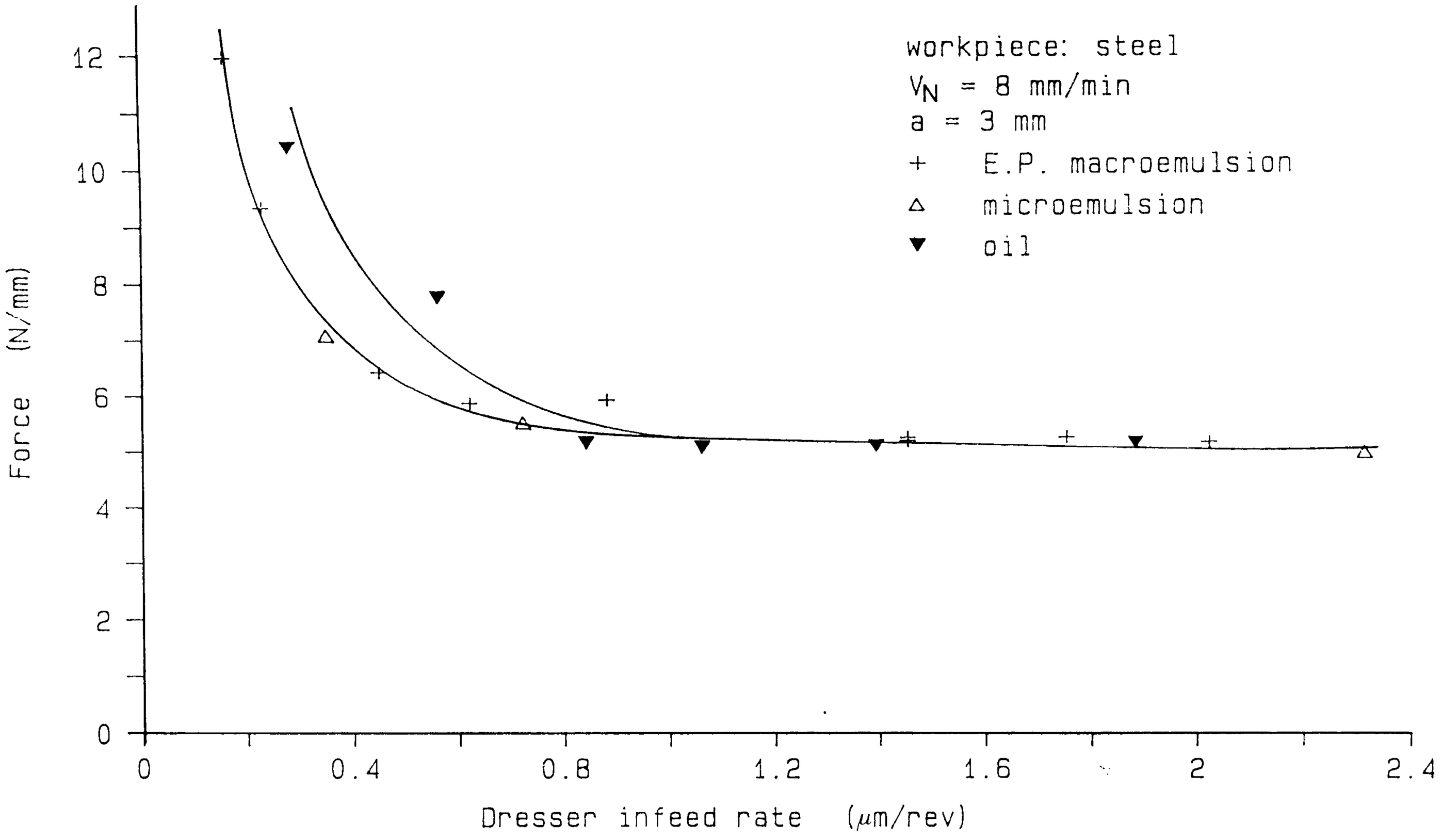

Figure 38. Graph of the normal force versus dresser infeed rate when steel is ground.

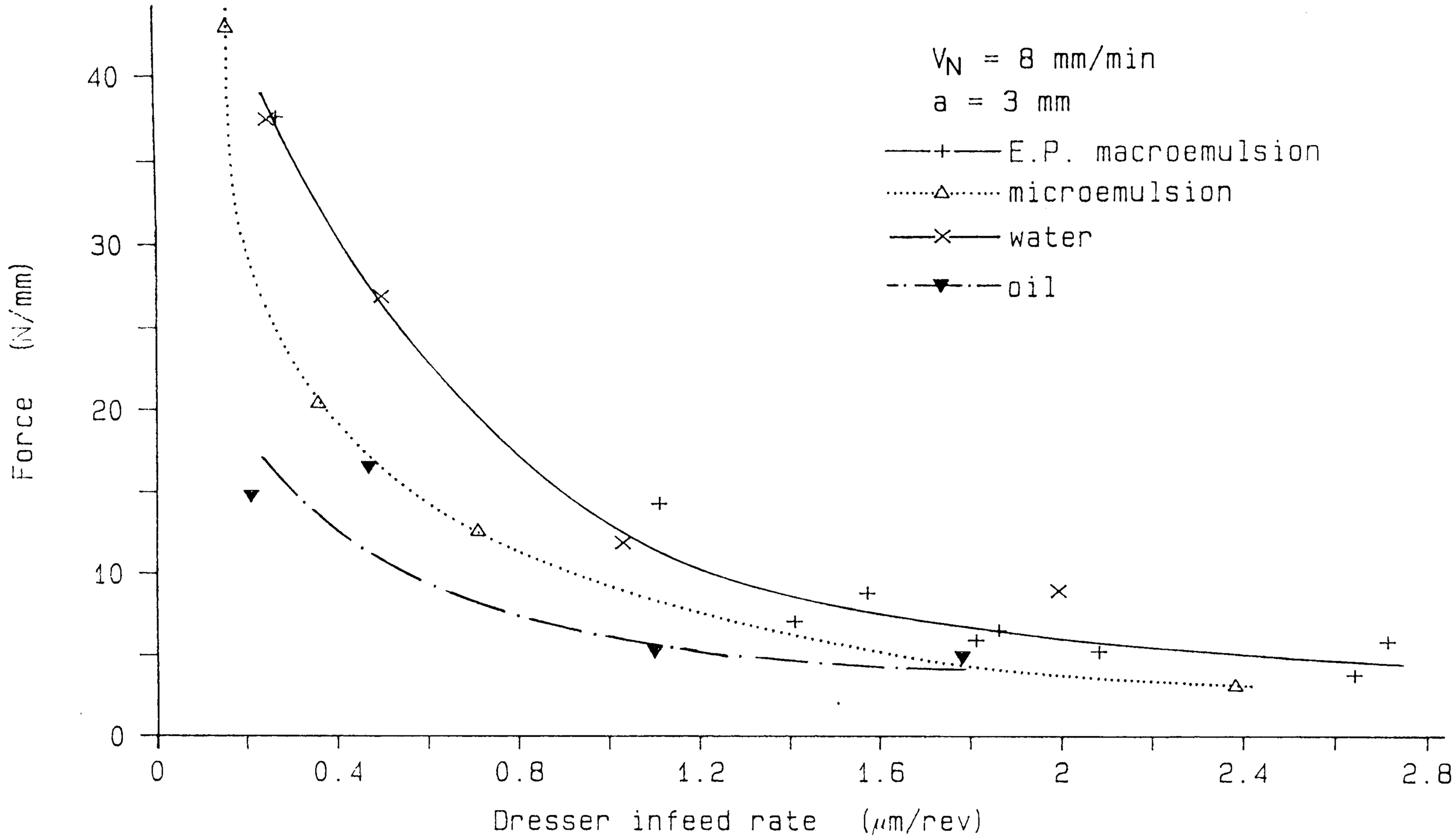

Figure 39. Graph of the normal force versus dresser infeed rate when Nimonic is ground.

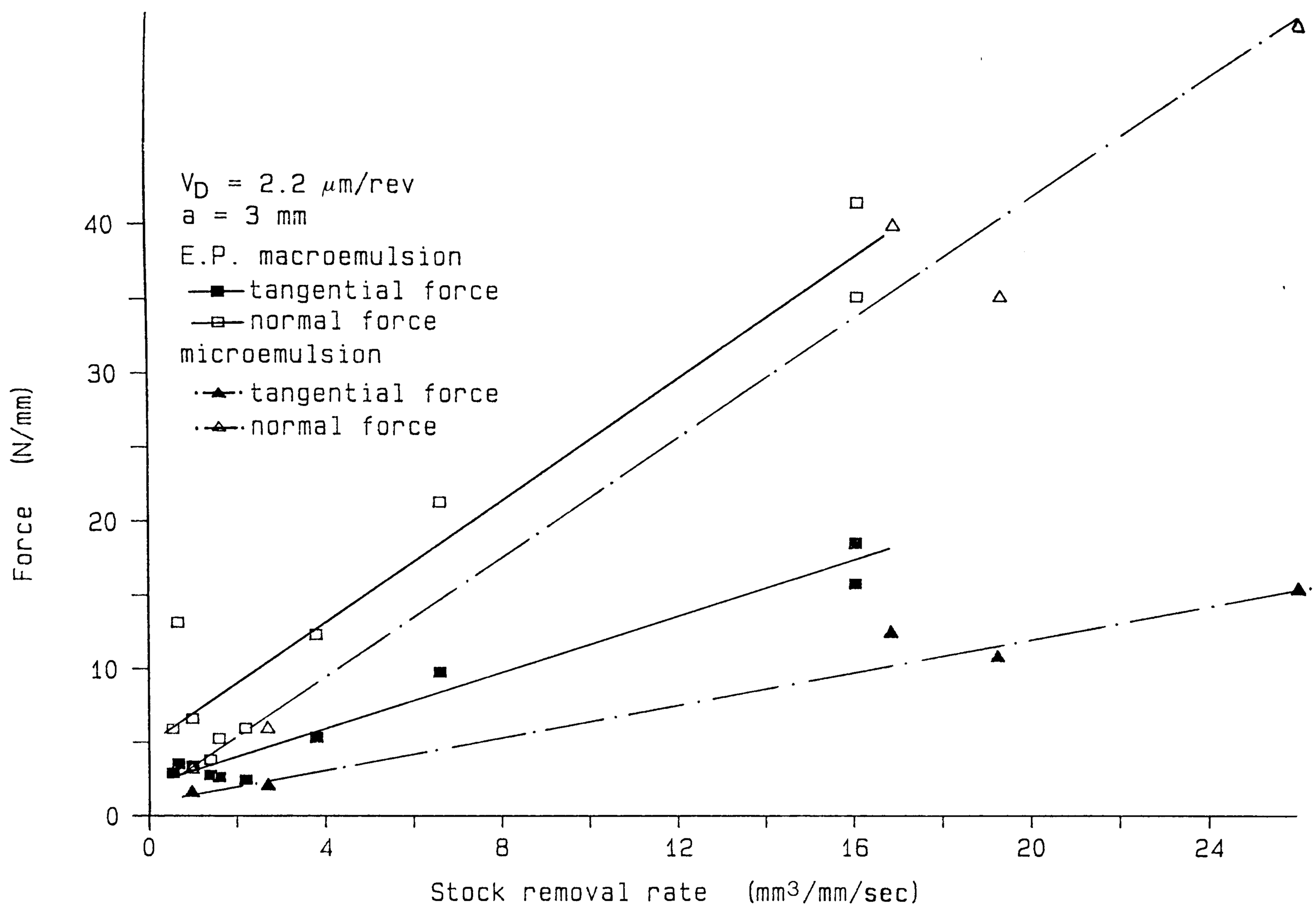

Figure 40. Graph of forces versus stock removal rate of Nimonic with water based fluids.

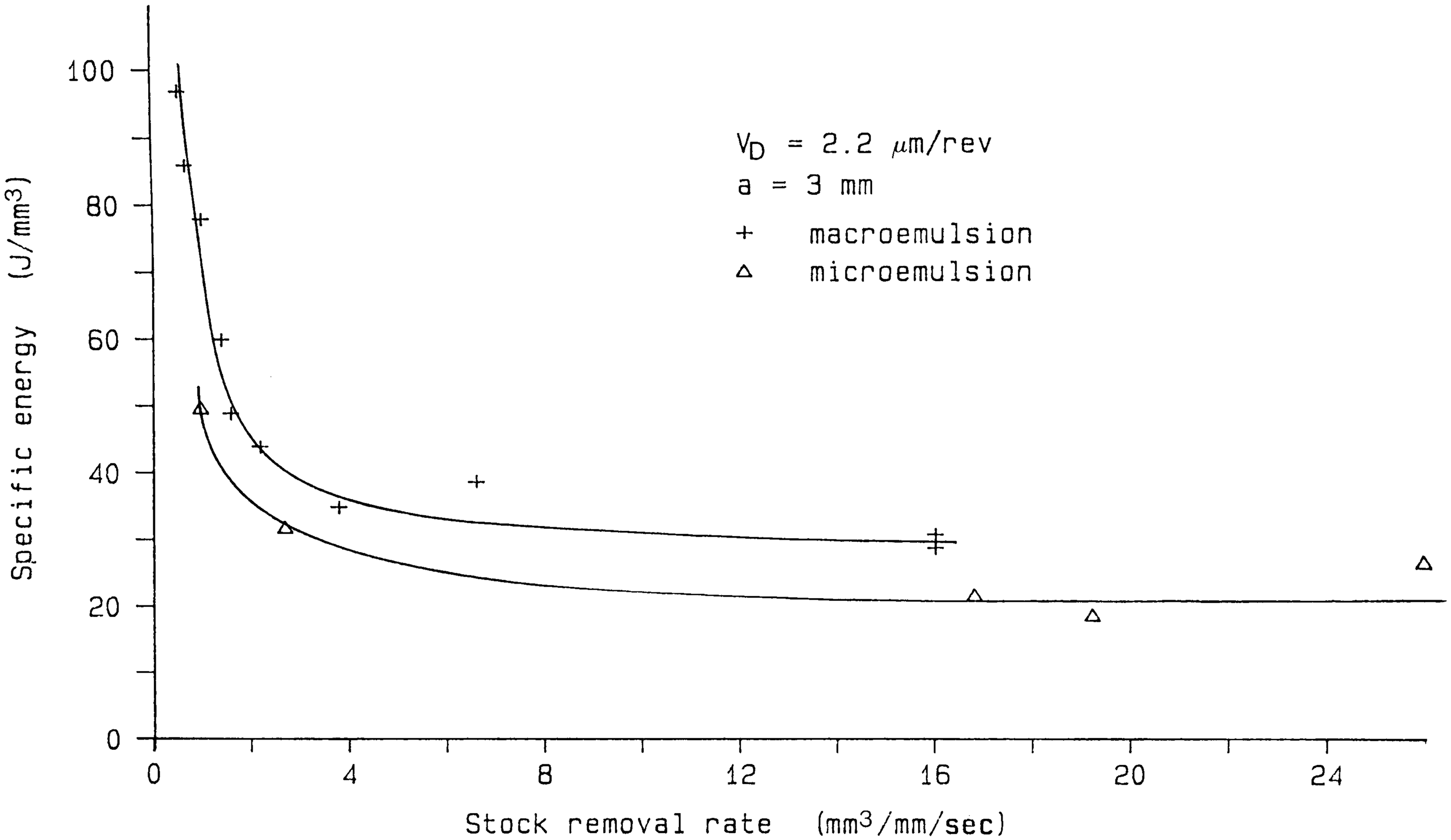

Figure 41. Graph of specific energy versus stock removal rate of Nimonic with water based fluids.

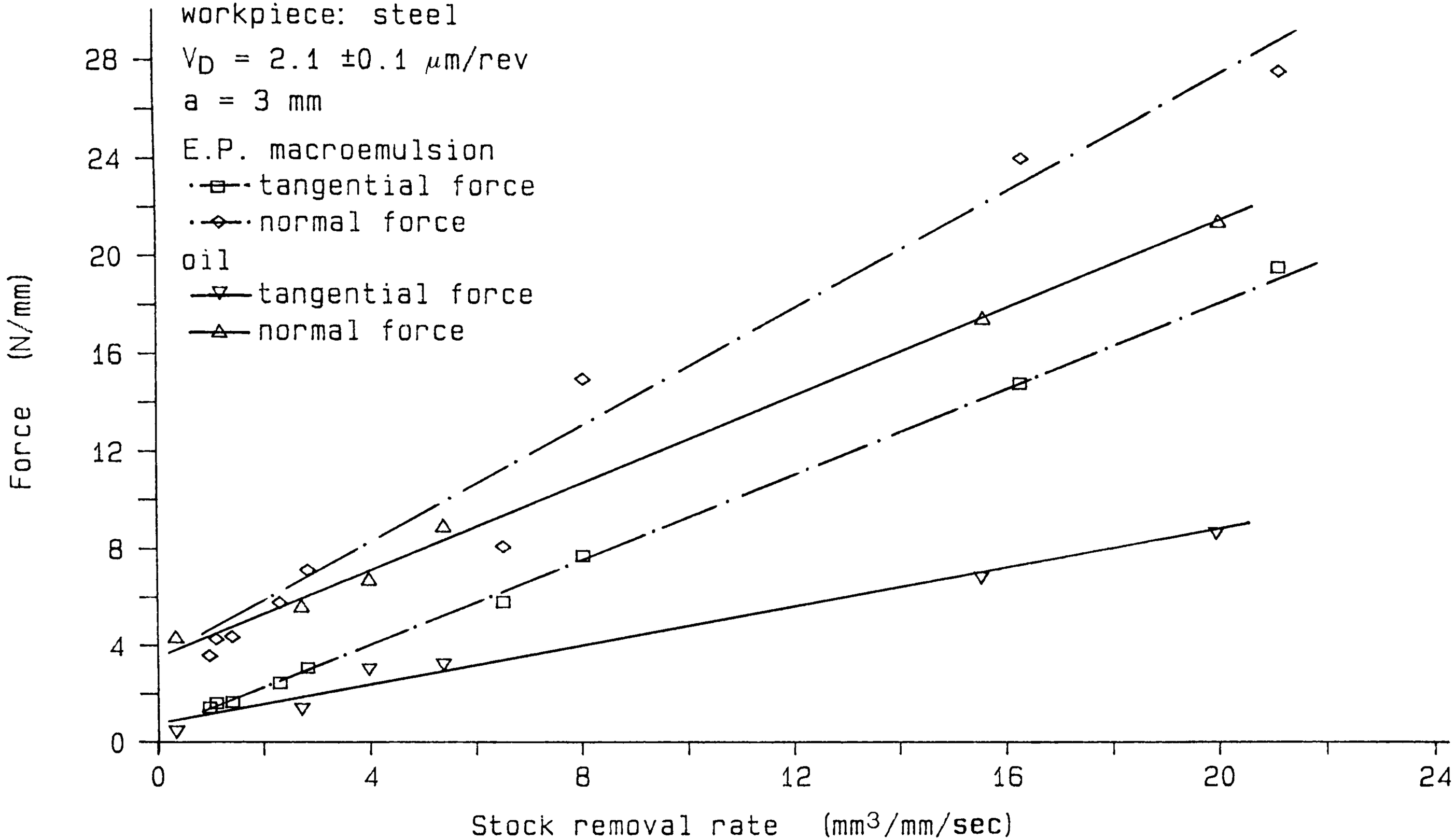

Figure 42. Variation in forces with stock removal rate for steel.

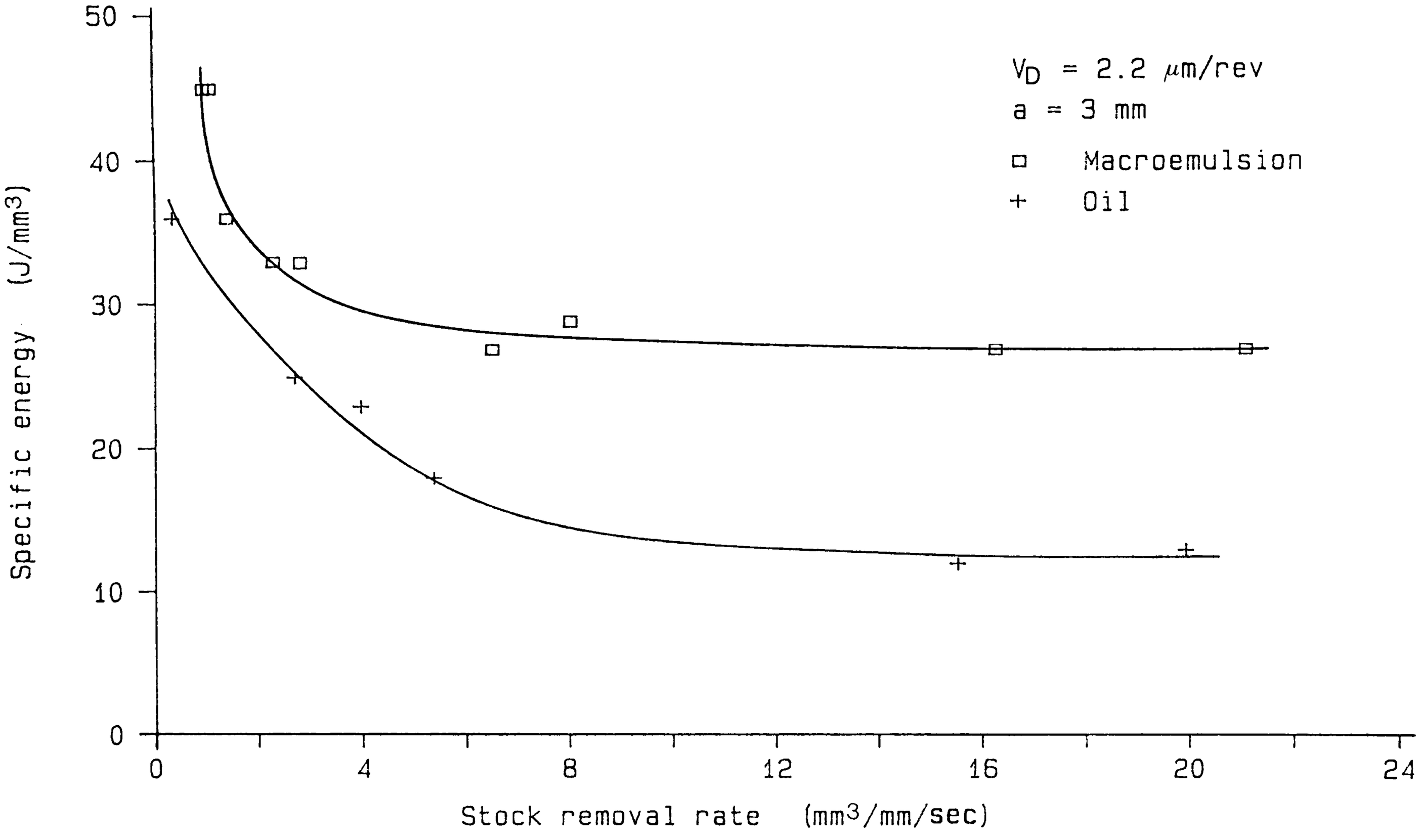

Figure 43. Specific energy variation with stock removal rate for steel.

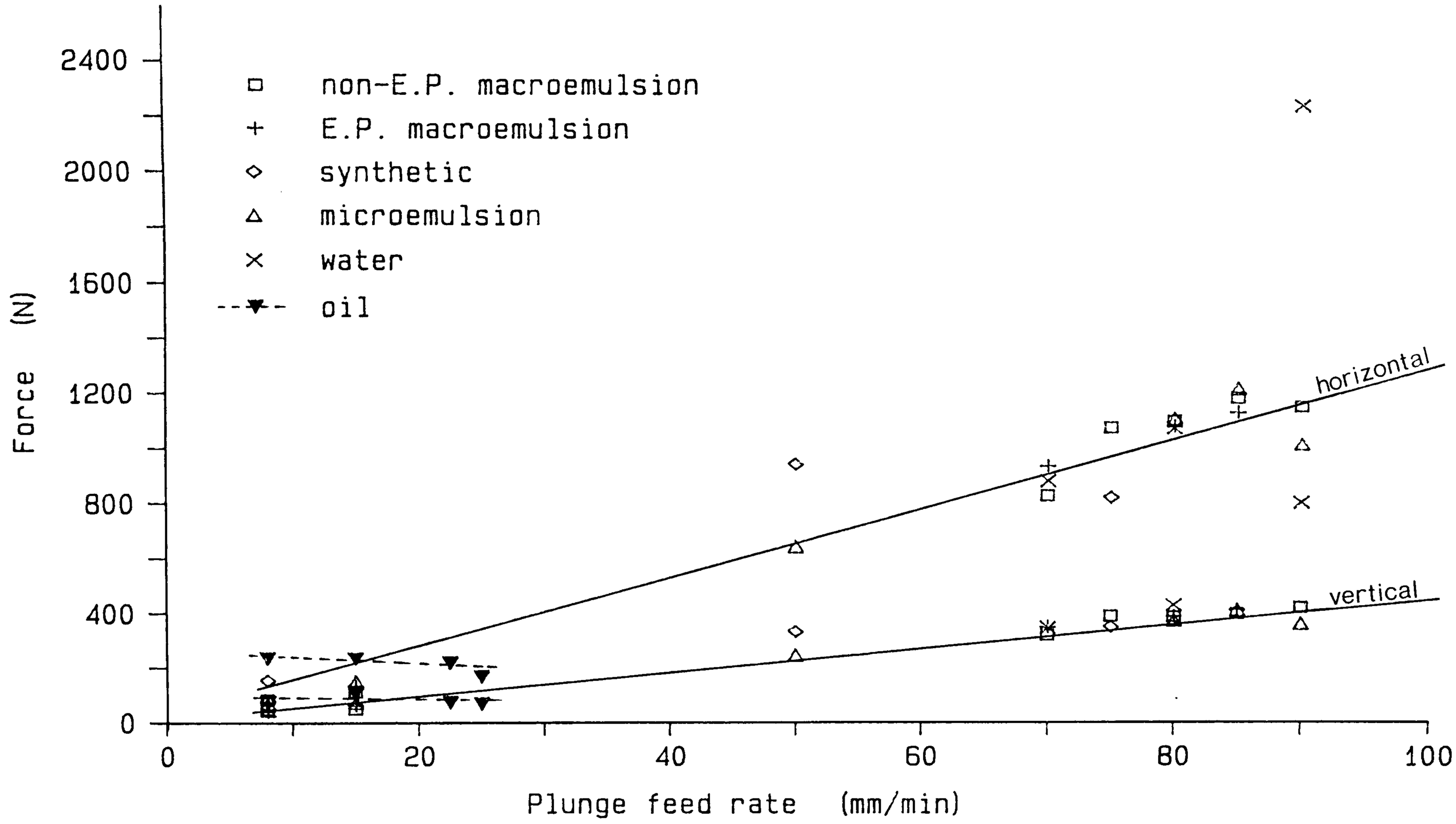

Figure 44. Forces measured versus plunge feed rate for plunge ground steel pins.

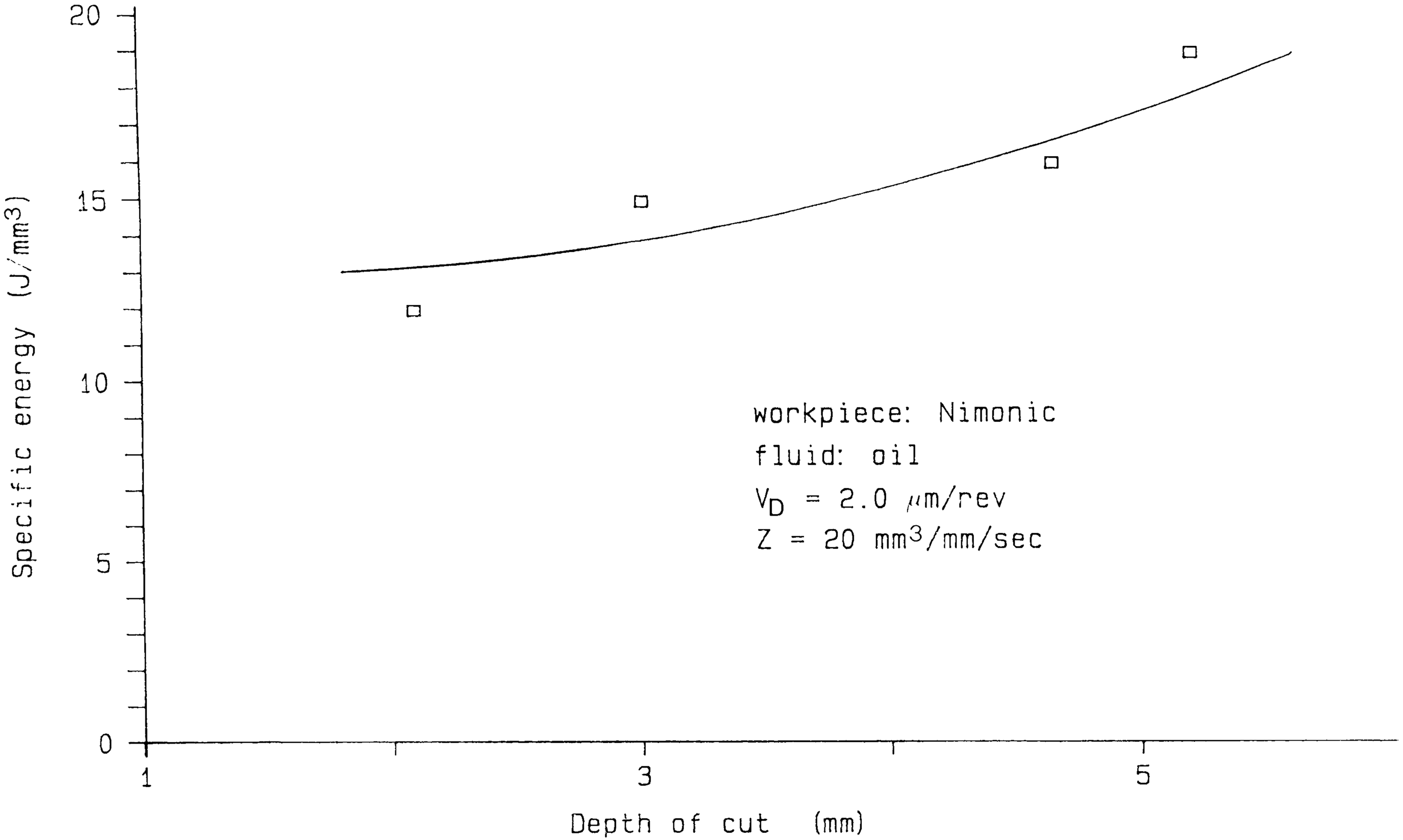

Figure 45. Specific energy variation with depth of cut at high stock removal and dresser infeed rates for the grinding of Nimonic.

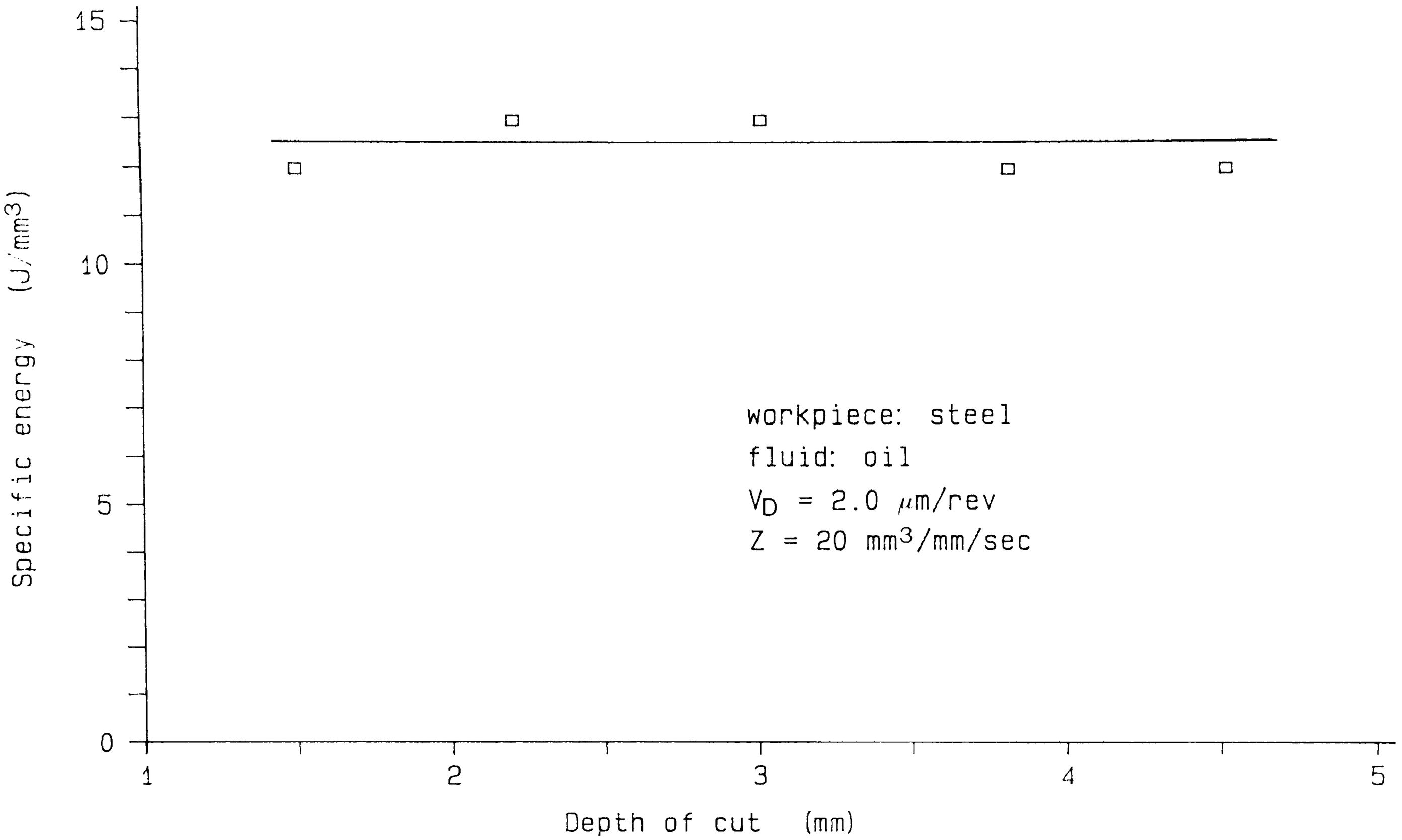

Figure 46. Specific energy variation with depth of cut at high stock removal and dresser infeed rates for the grinding of steel.

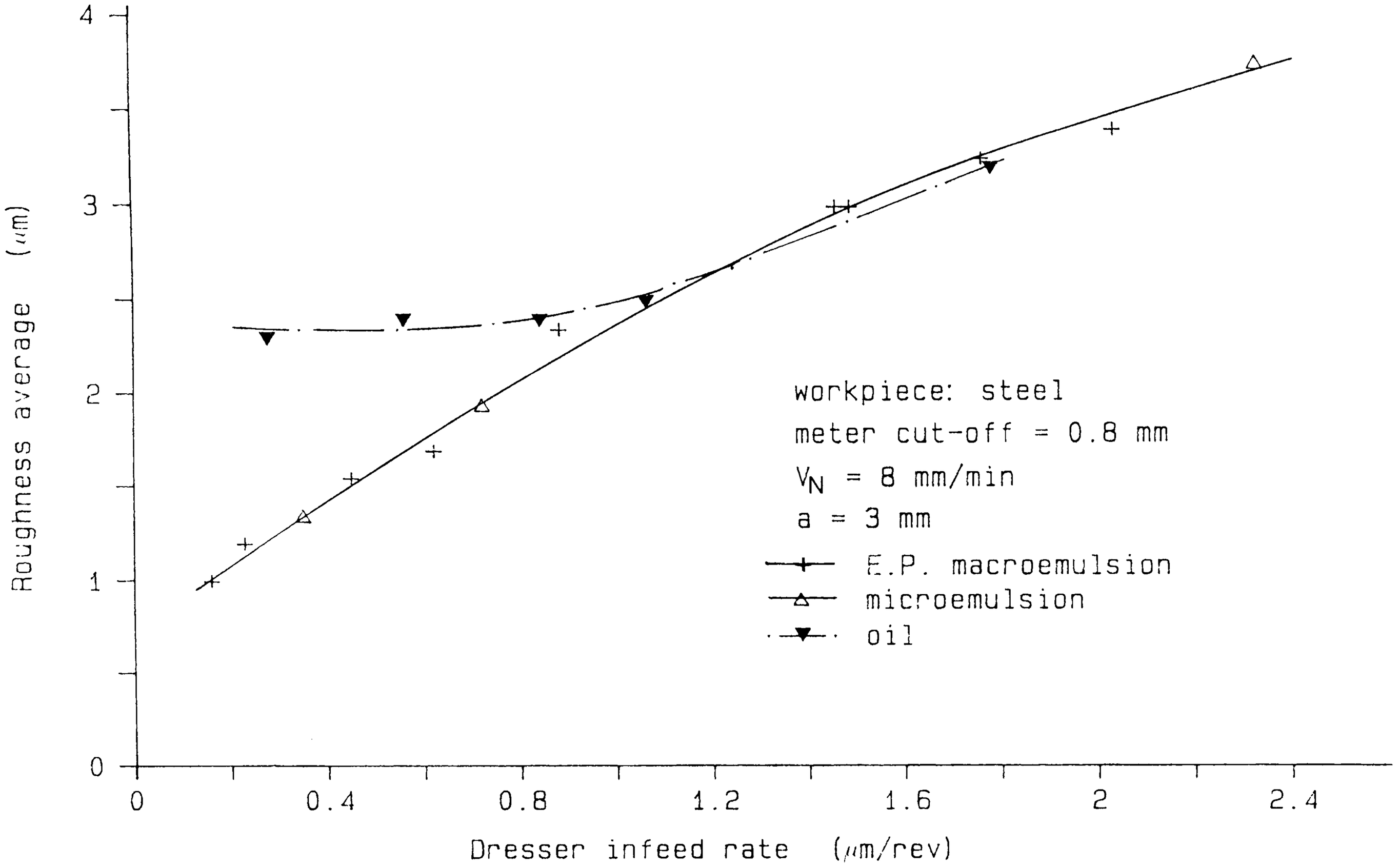

Figure 47. Graph of the variation of roughness averages with dresser infeed rate for steel.

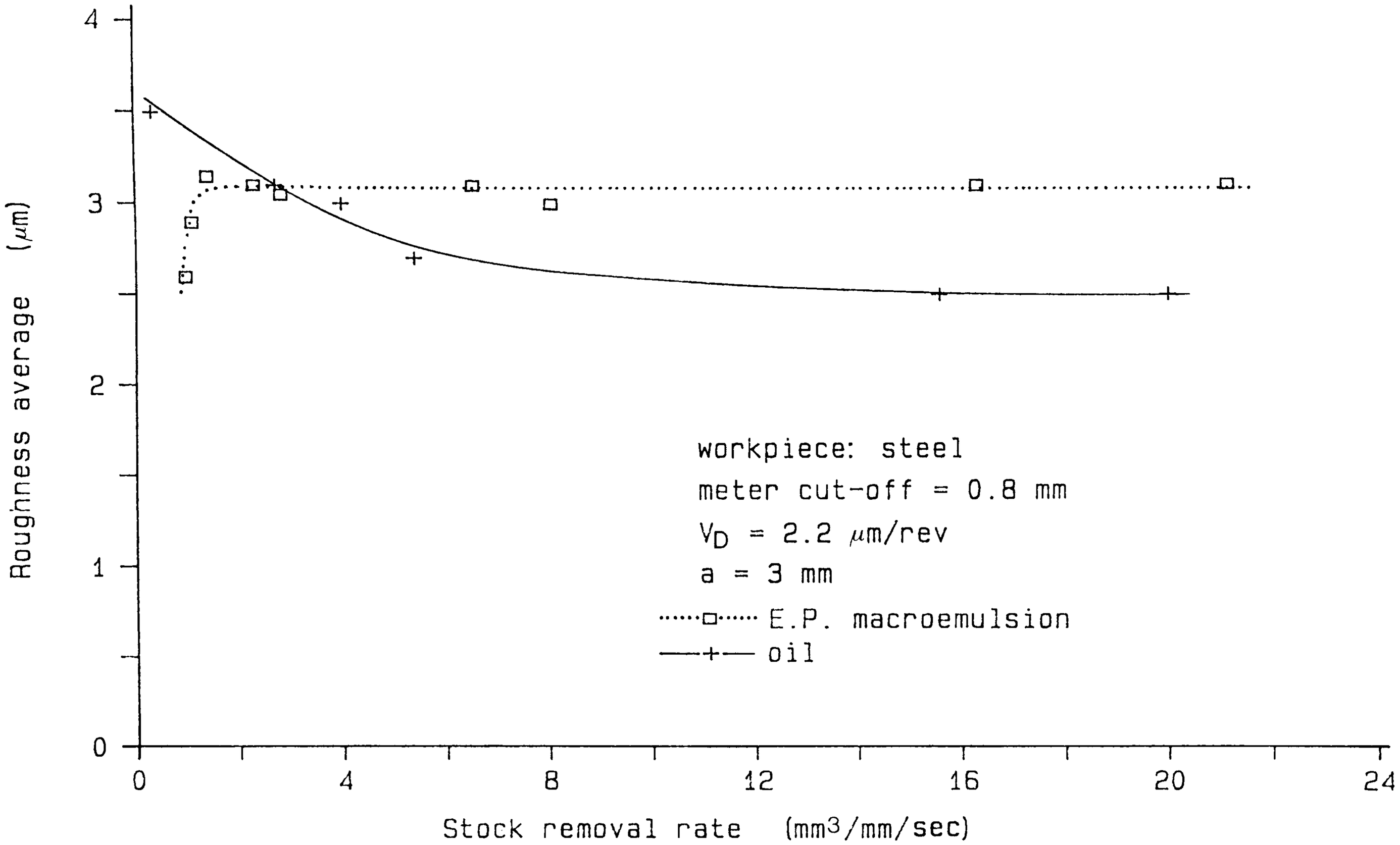

Figure 48. Roughness average versus stock removal rate for steel, corresponding to the specific energy results in Figure 43.

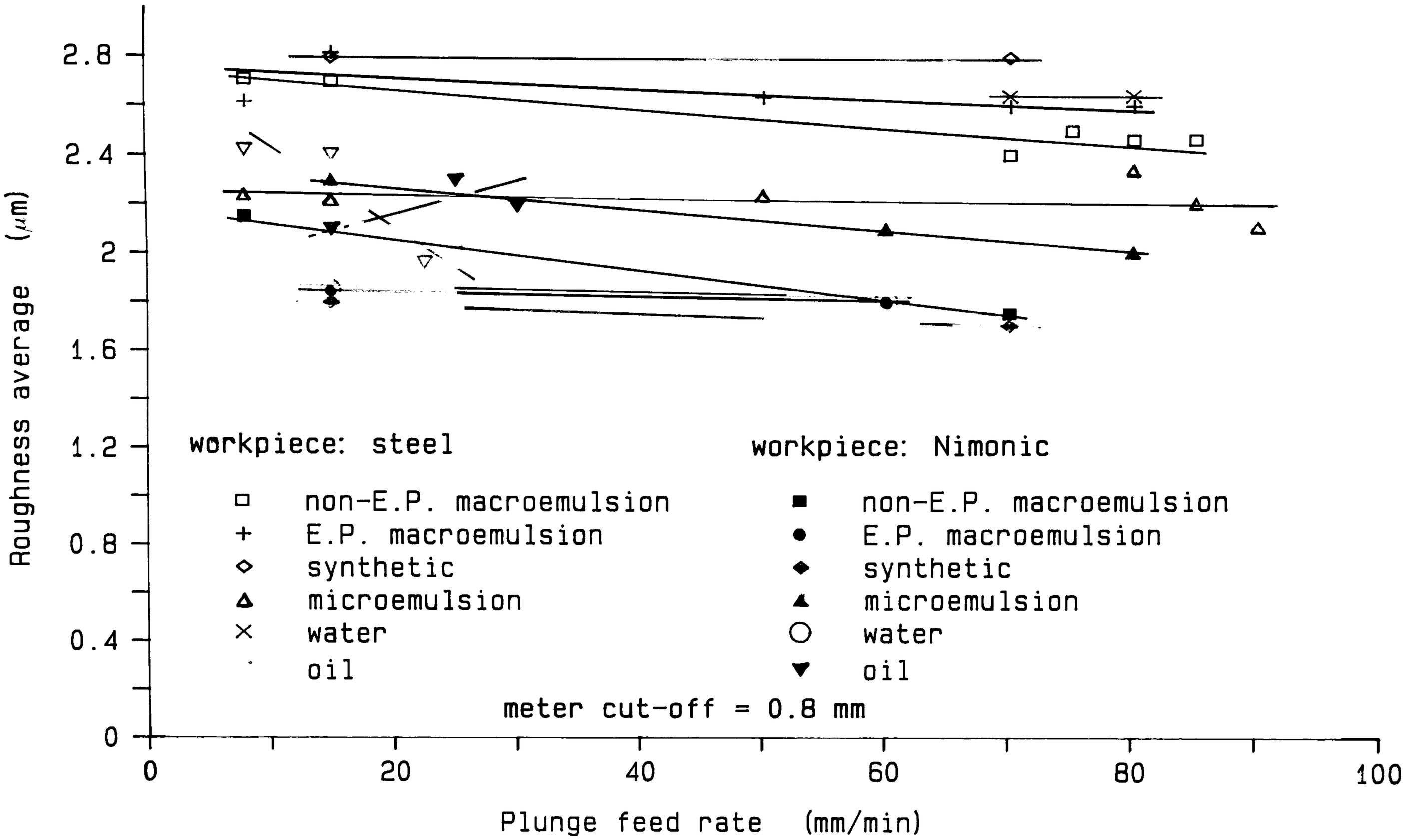

Figure 49. Roughness average measurements for the plunge ground pins, for Nimonic and steel specimens with the full range of fluids

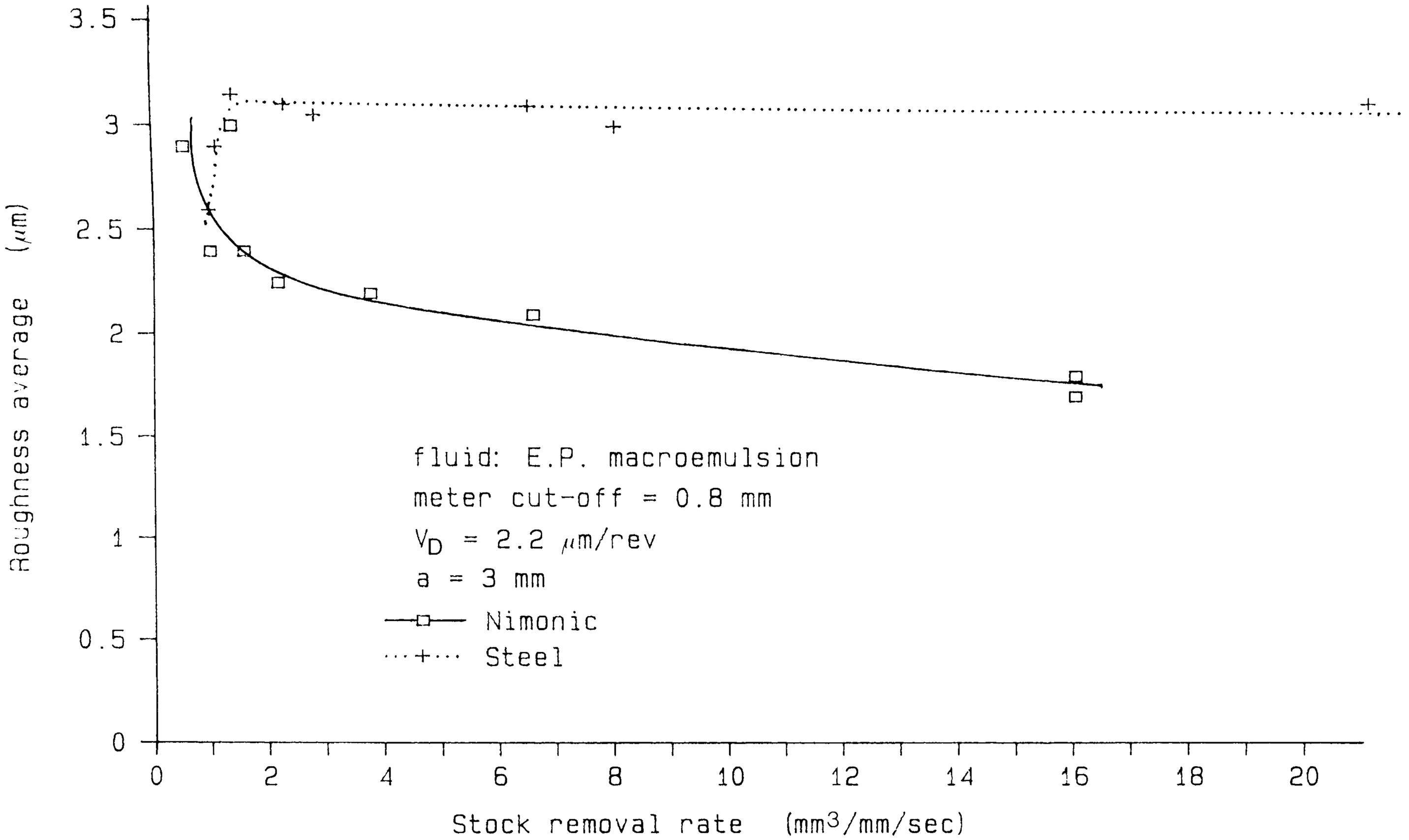

Figure 50. Roughness average versus stock removal rate for steel and Nimonic.

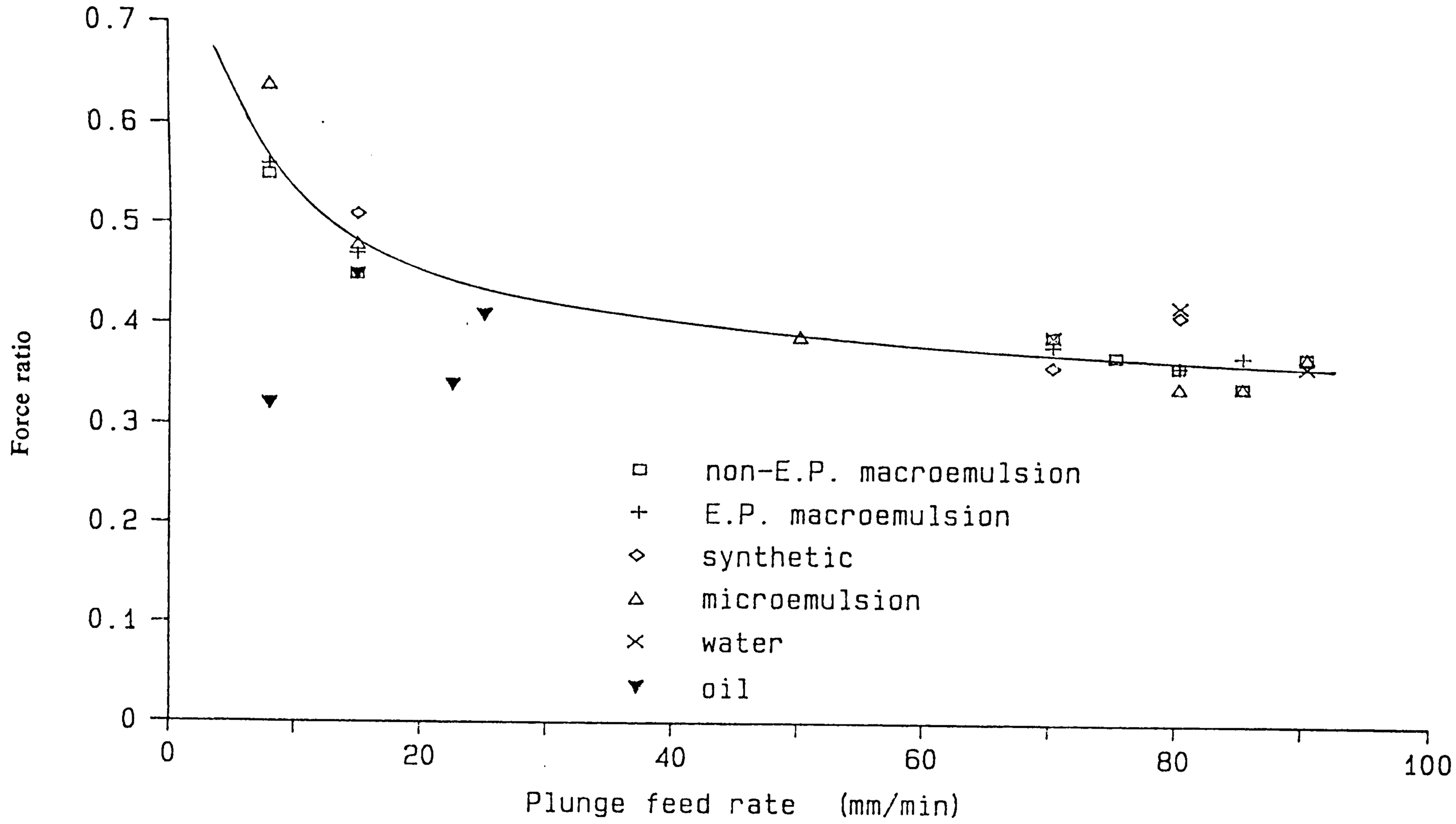

Figure 51. Force ratio versus plunge feed rate for the cylindrical pins.

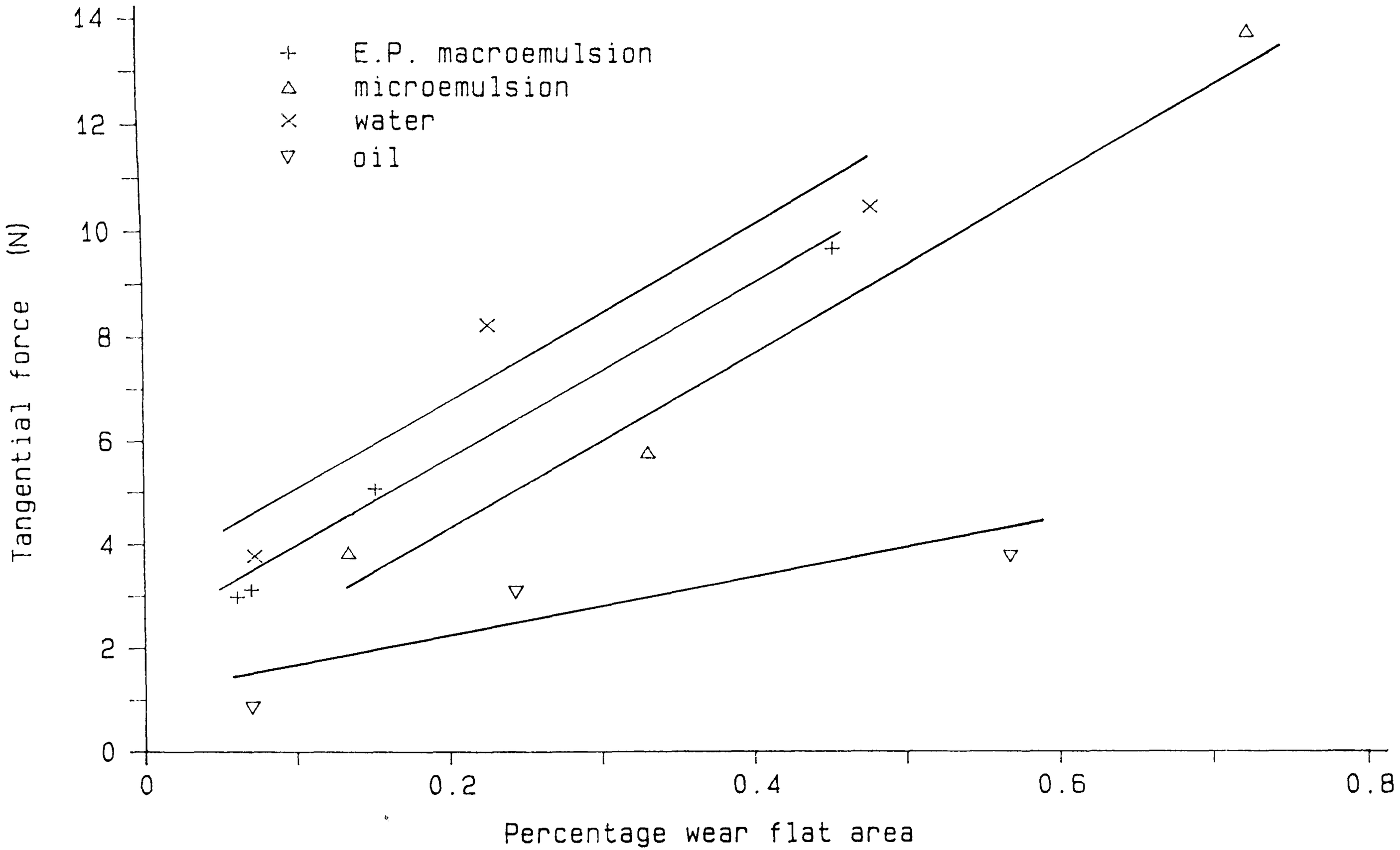

Figure 52. Graph of tangential force versus wear flat area for Nimonic workpieces ground using four different fluids.

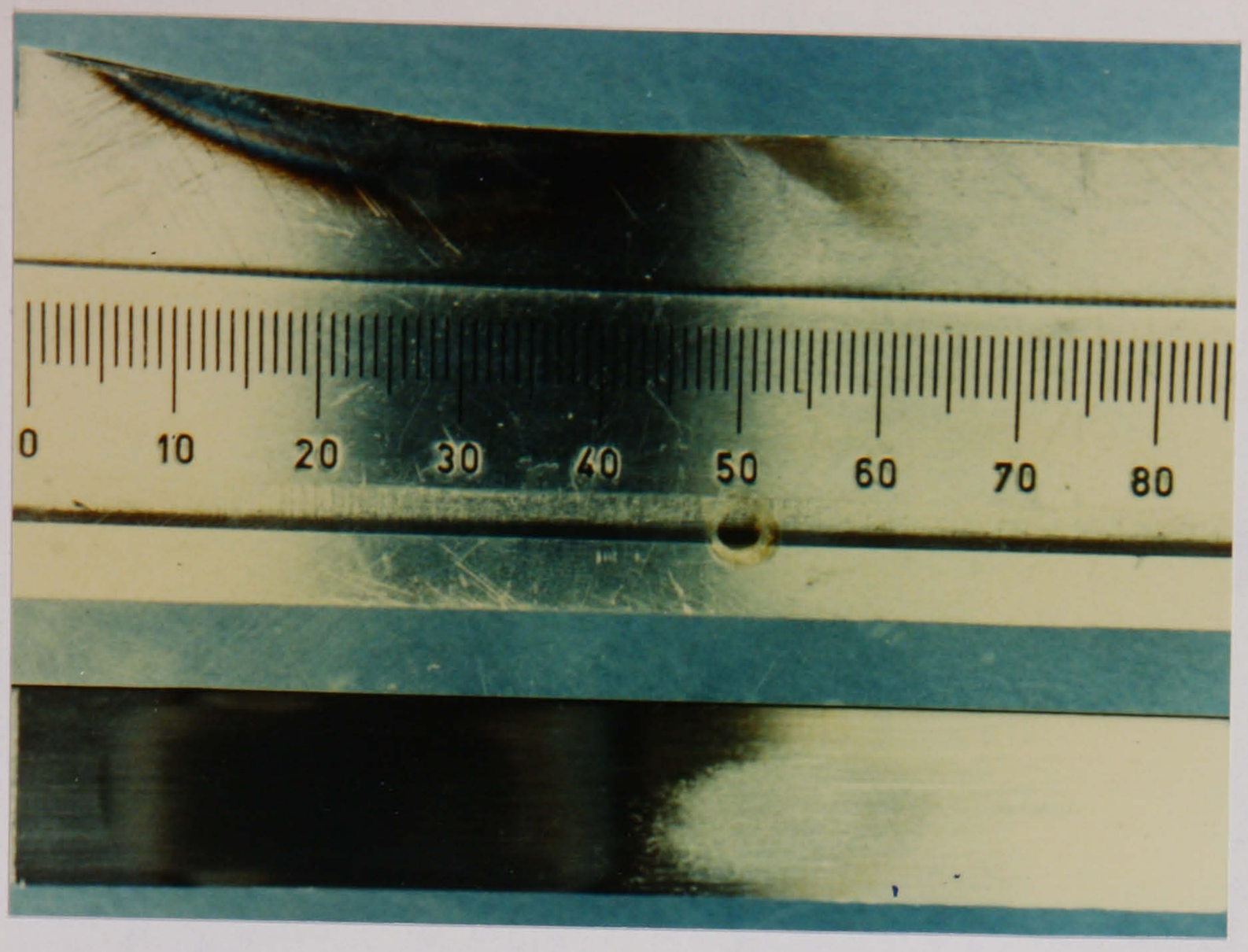

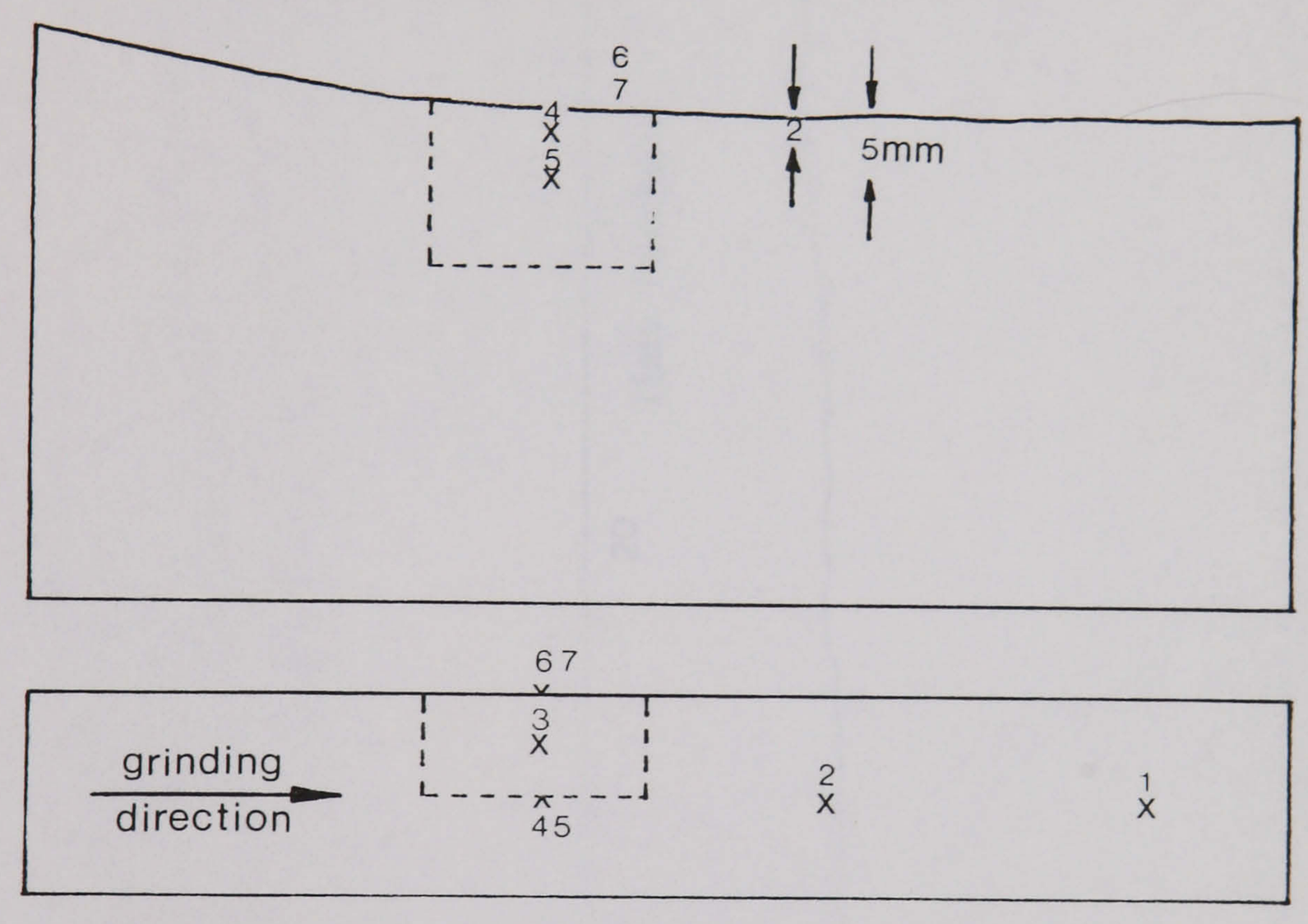

position	direction relative to grinding	
	parallel	transverse
1	-318 ± 33	-340 ± 12
2	-307 ± 36	-264 ± 24
3	-29 ± 22	-299 ± 19
4	-301 ± 44	-464 ± 18
5	-289 ± 31	-455 ± 22
6	116 ± 31	-34 ± 13
7	143 ± 56	137 ± 15

Figure 53. Thermally induced residual stresses (MPa) in a burnt steel workpiece ground using the E.P. macroemulsion.

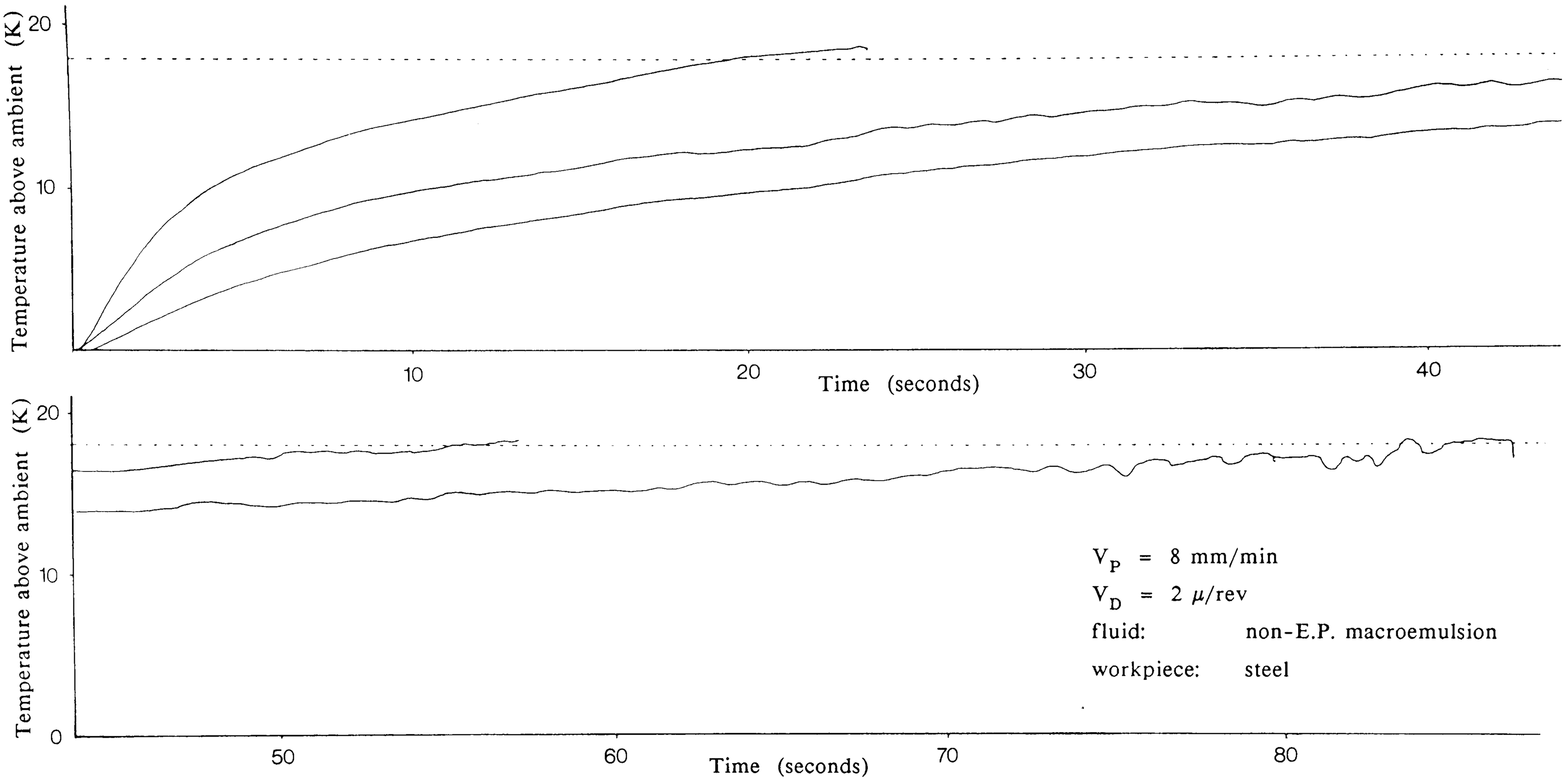

Figure 54. A trace of the output from three thermocouples embedded in a steel workpiece versus elapsed time since the start of grinding with a non-E.P. macroemulsion.

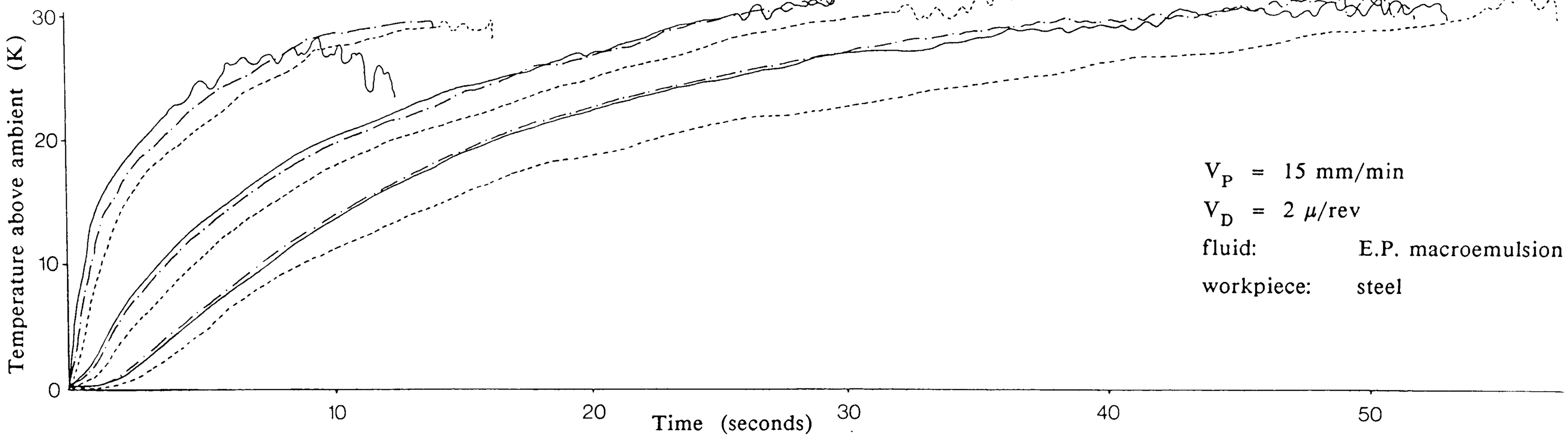

Figure 55. The temperatures recorded during several tests with the same water-based fluid under the same conditions.

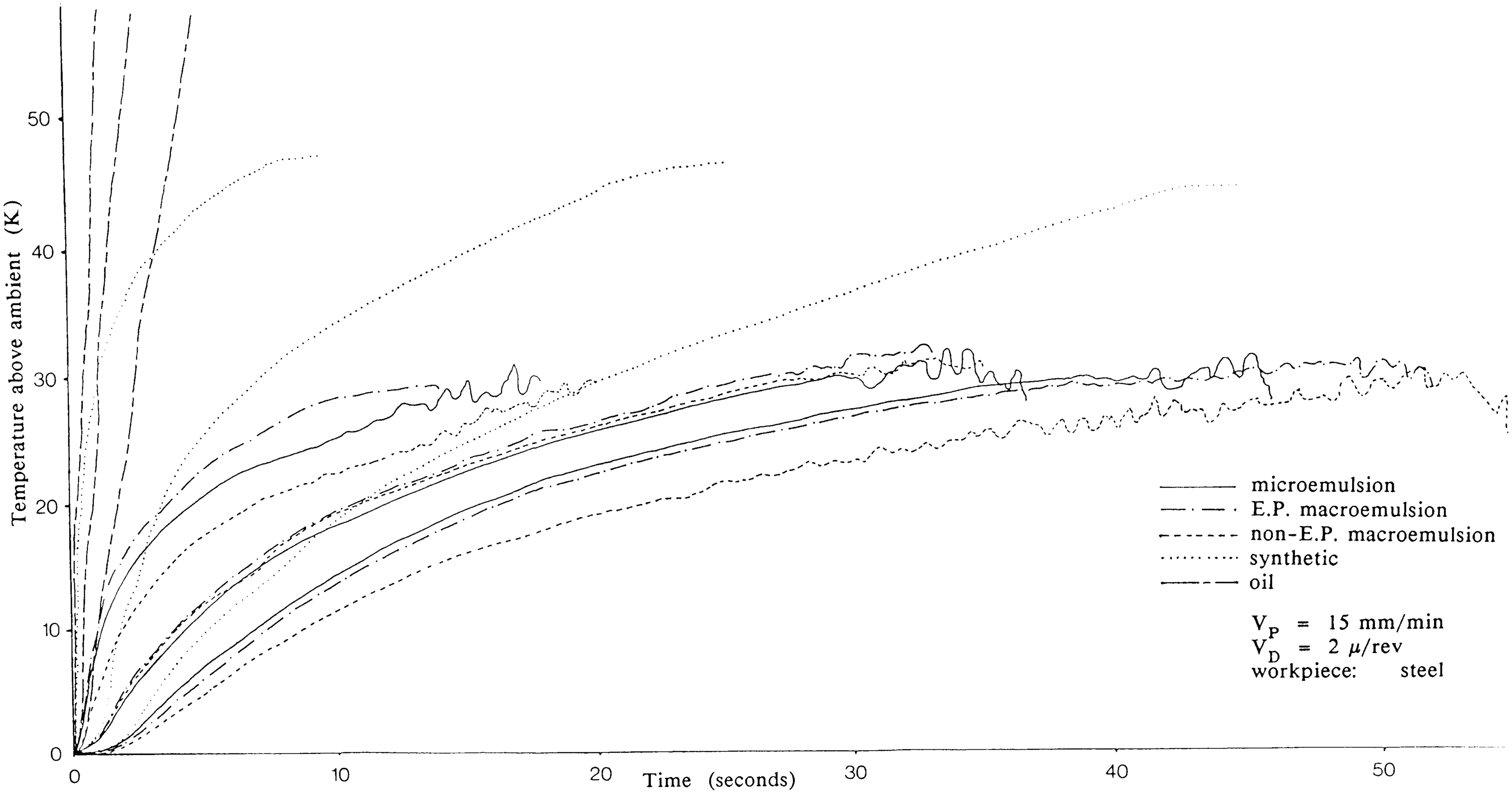

Figure 56. The effect of the grinding fluid on thermocouple temperature traces under the same grinding conditions.

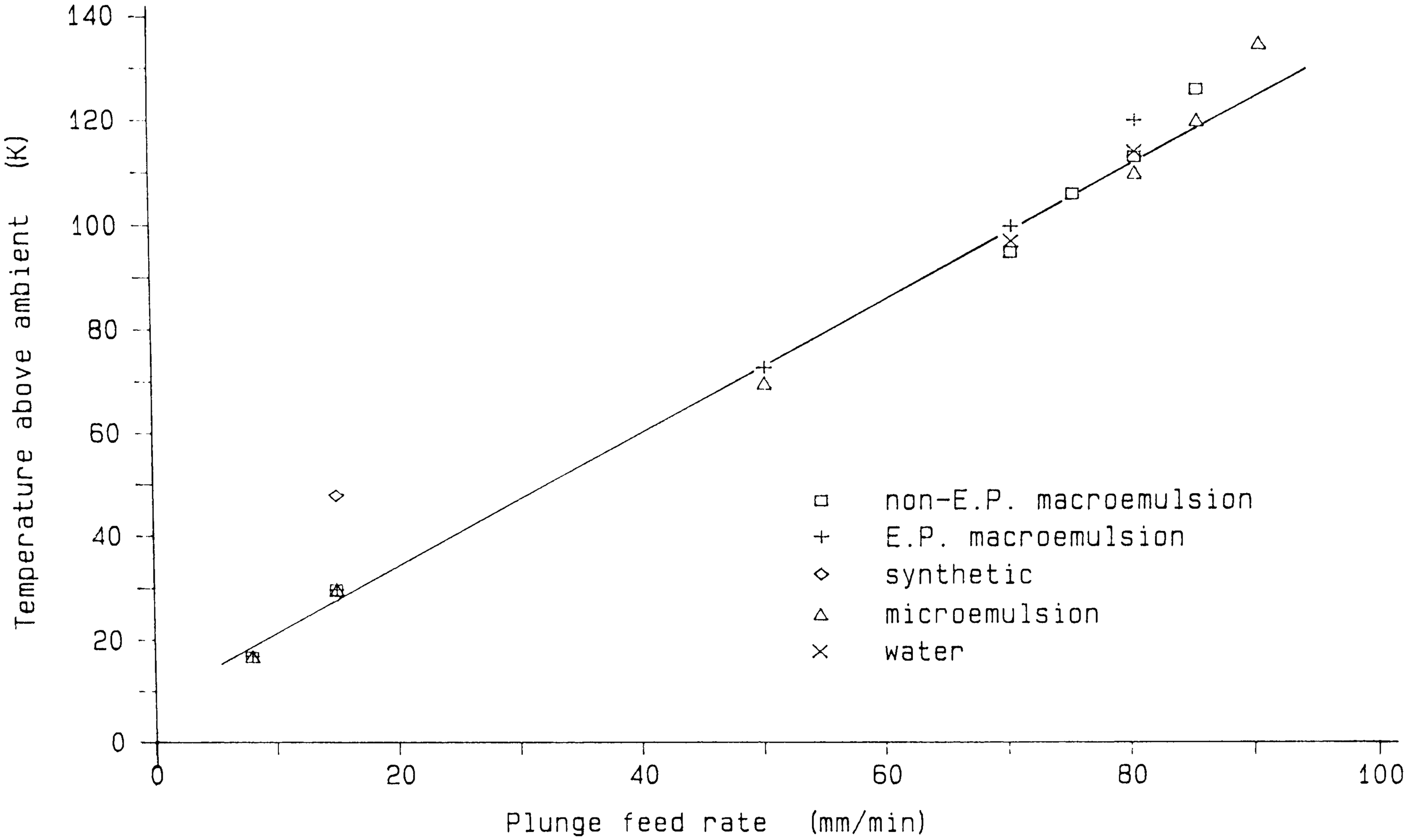

Figure 57. Graph of the apparently stable surface temperatures of the steel workpieces versus plunge feed rate.

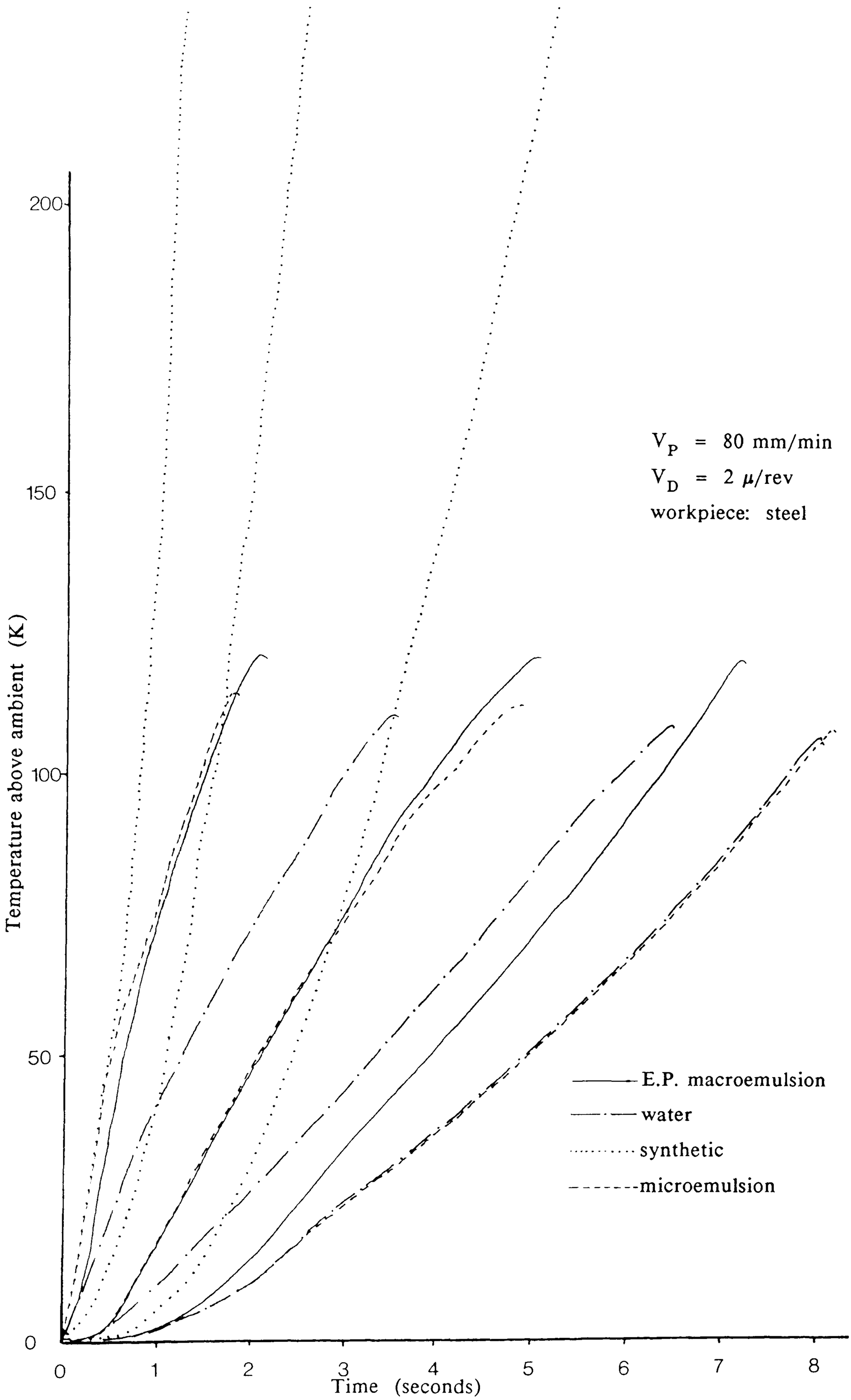

Figure 58. Steel workpiece temperatures using various water based fluids at a plunge feed rate of 80 mm/min.

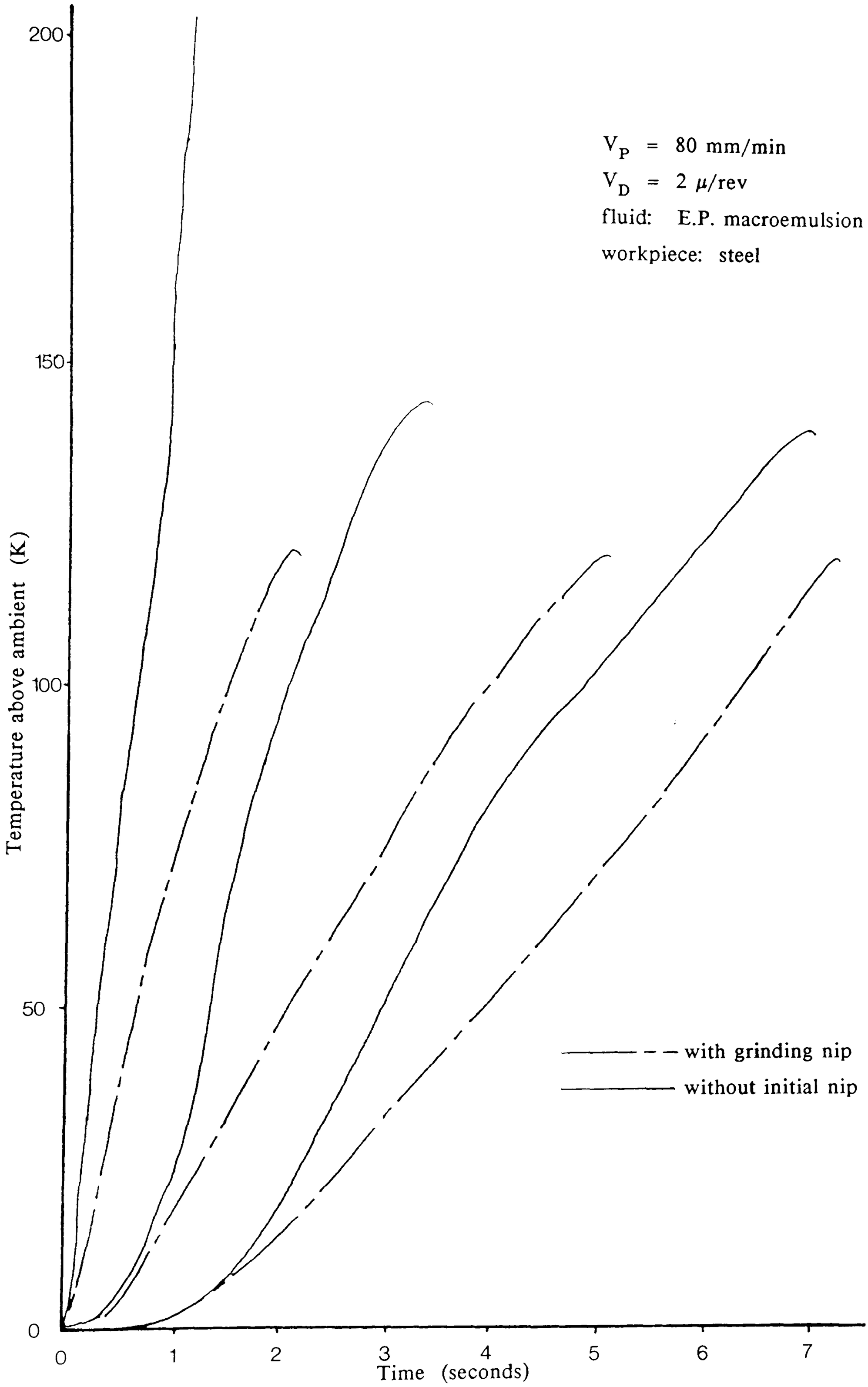

Figure 59. Workpiece temperatures reached with and without a nip (c.f. Figure 58).

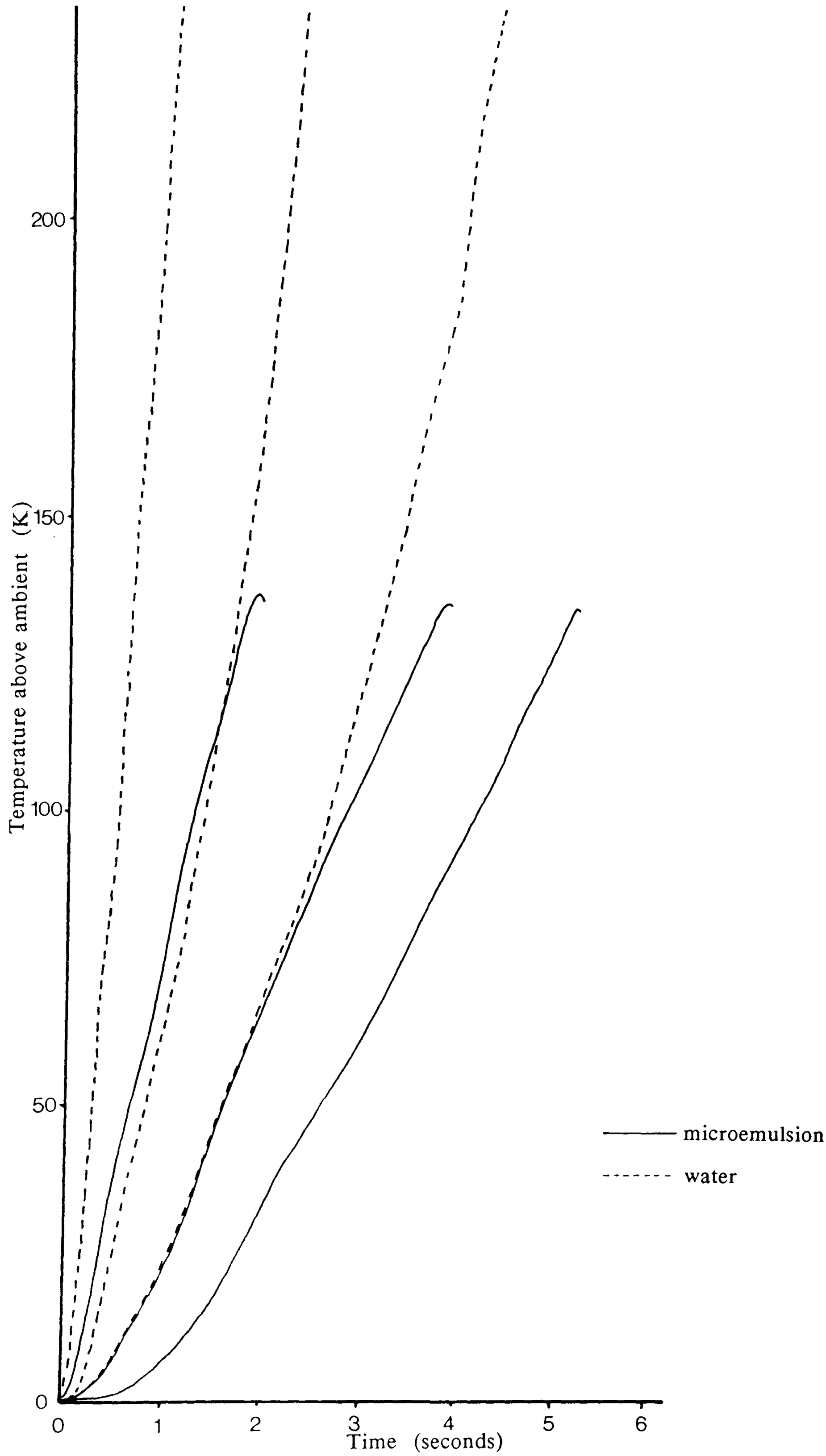

Figure 60. Workpiece temperatures recorded with the microemulsion at a feed rate of 90 mm/min.

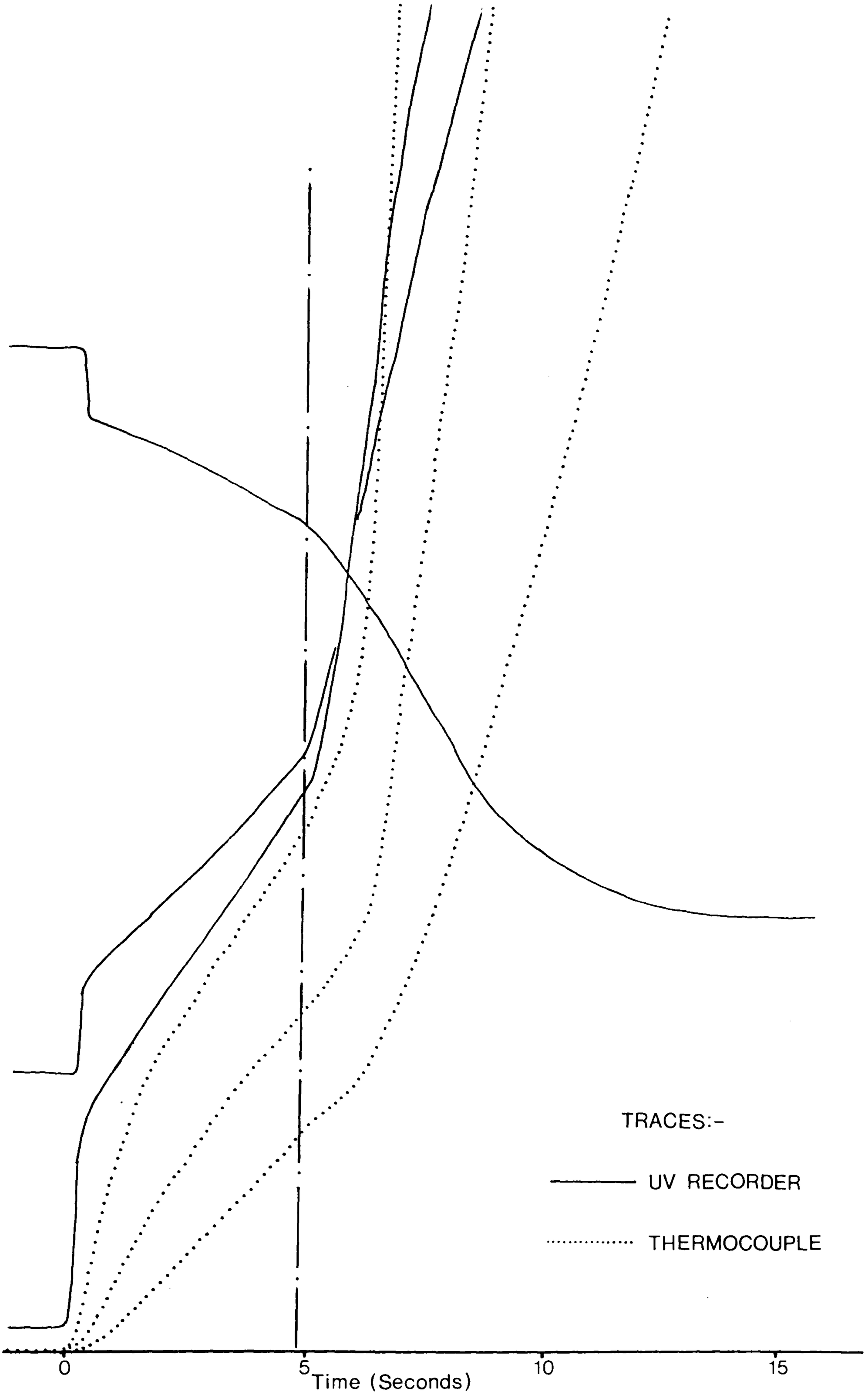

Figure 61. Temperature versus time traces and the corresponding force traces as burn is reached.

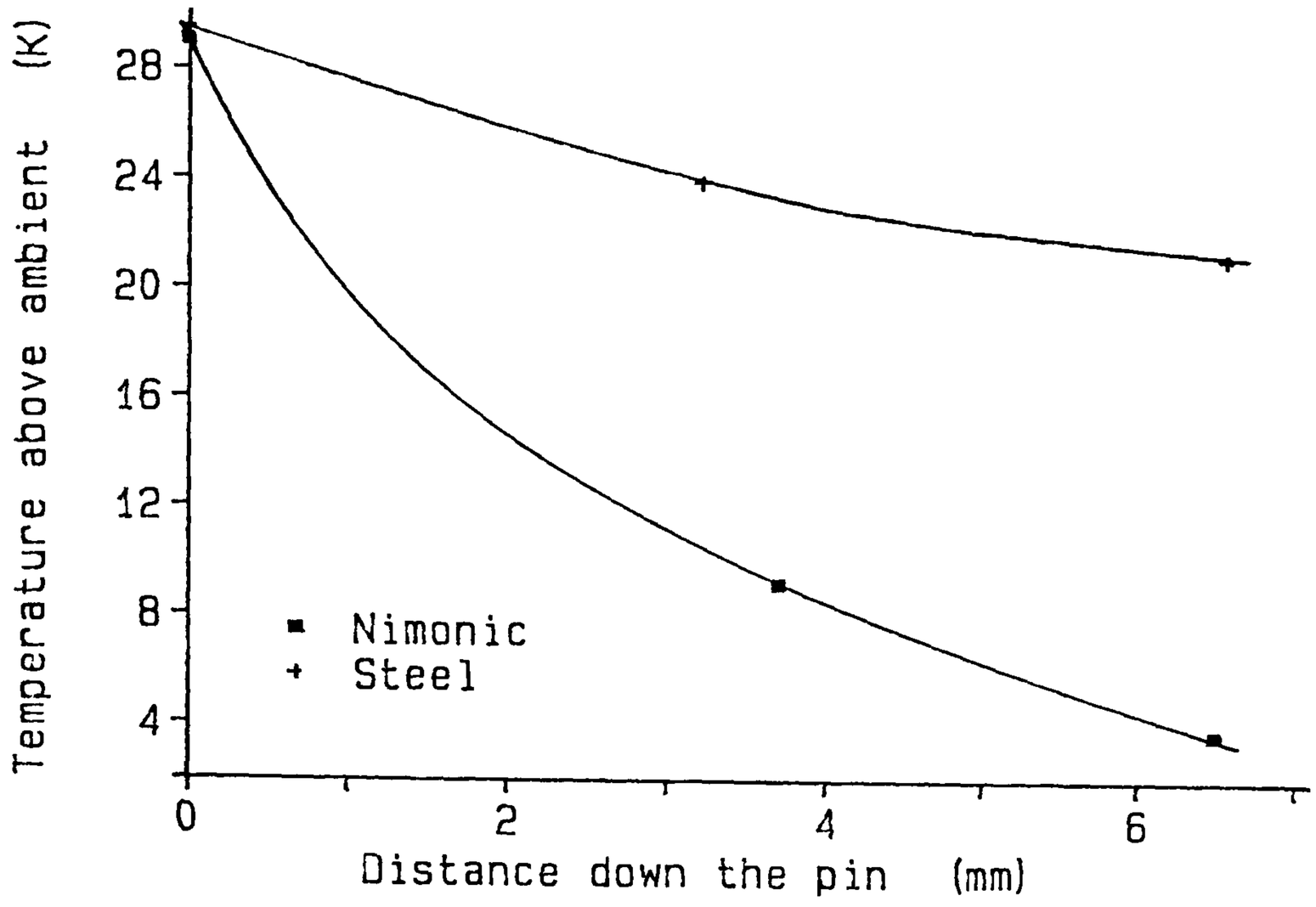

Figure 62. Plot of the temperature profile down the Nimonic and steel pins with a water based fluid.

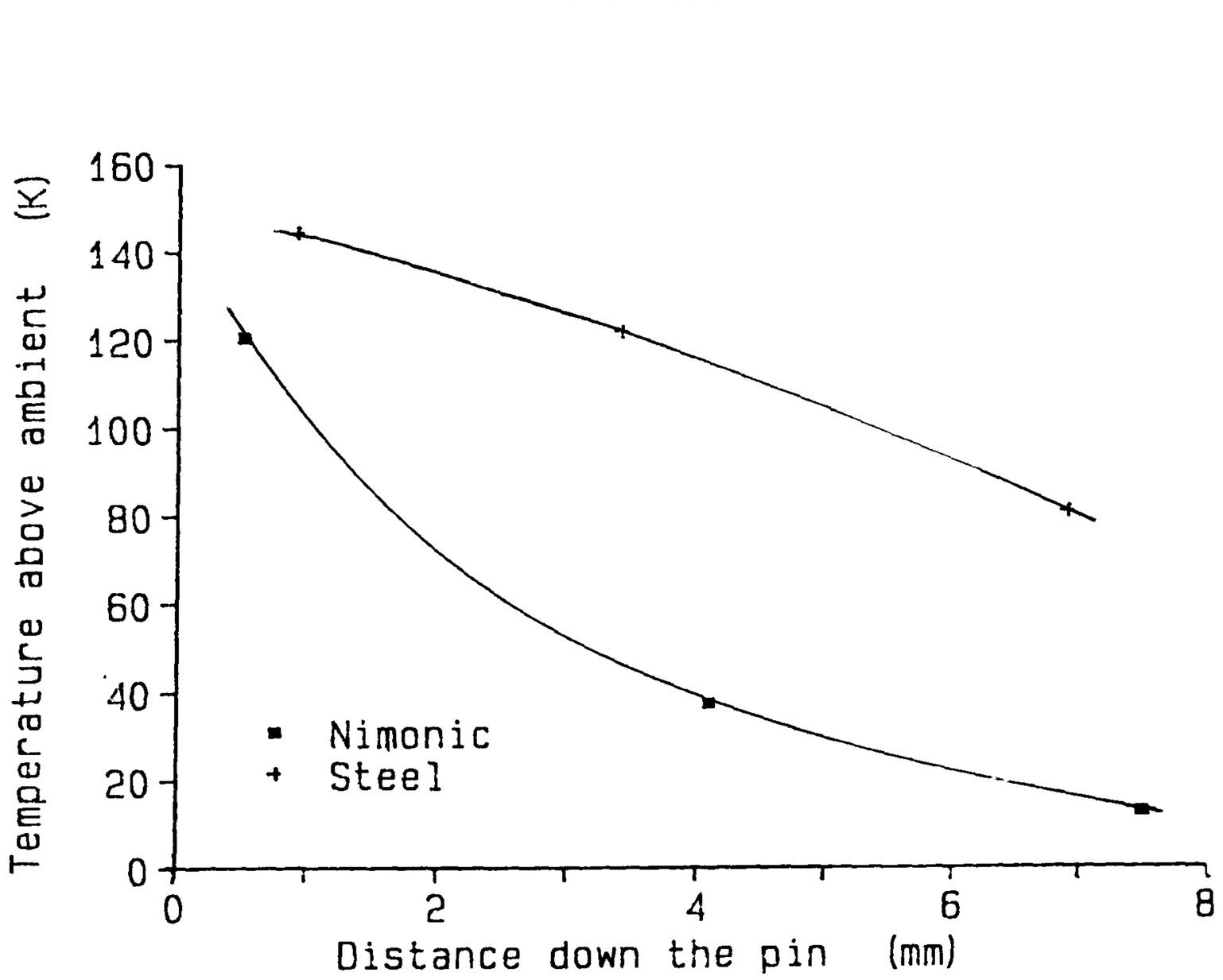

Figure 63. Plot of the temperature profile down the Nimonic and steel pins with oil.

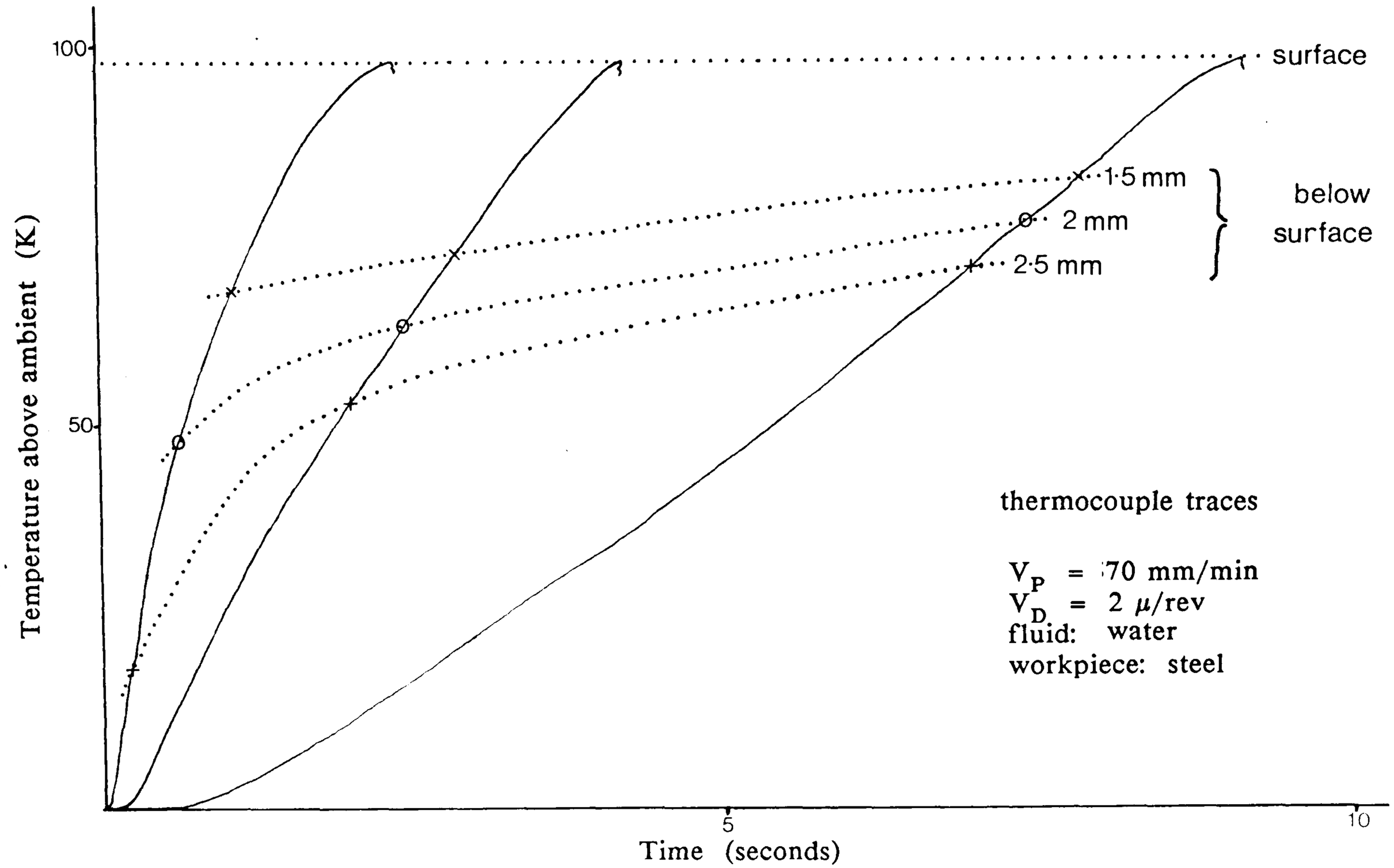

Figure 64. Temperature variation with time below the workpiece surface.

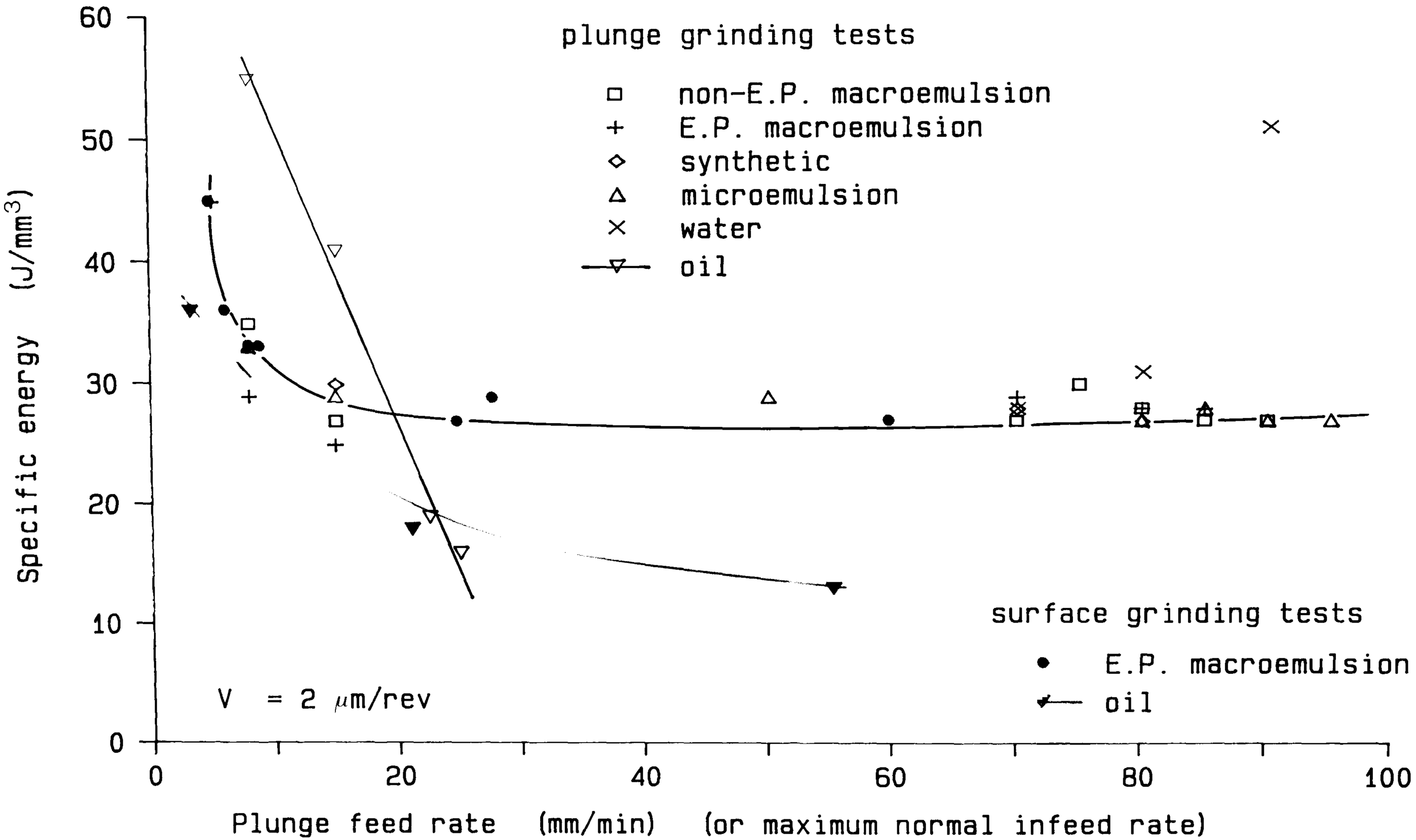

Figure 65: A graph of specific energy versus feed rate on steel pins.

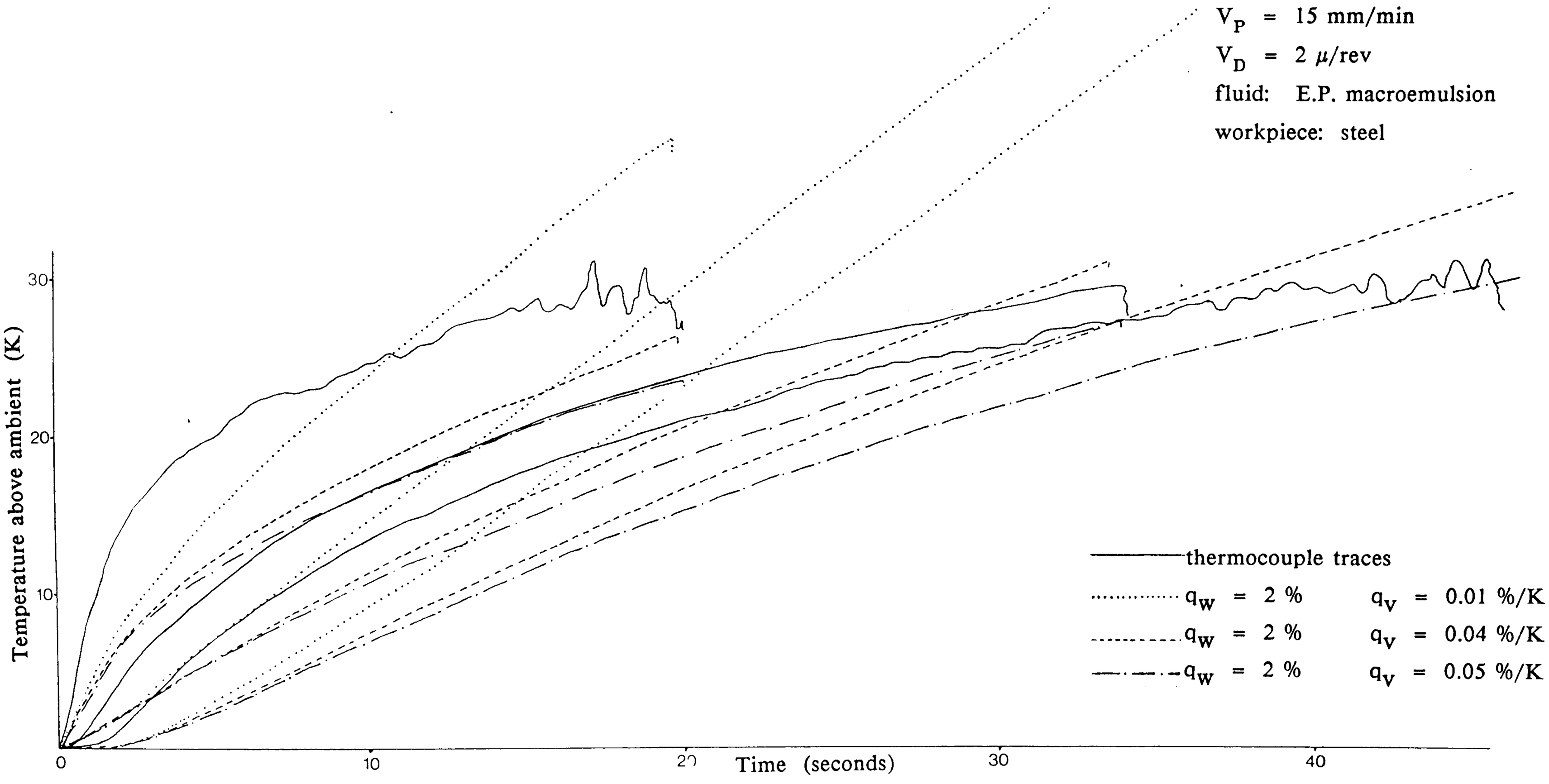

Figure 66. Fitting 2% partitioning values to empirical (thermocouple) traces from an insulated steel pin.

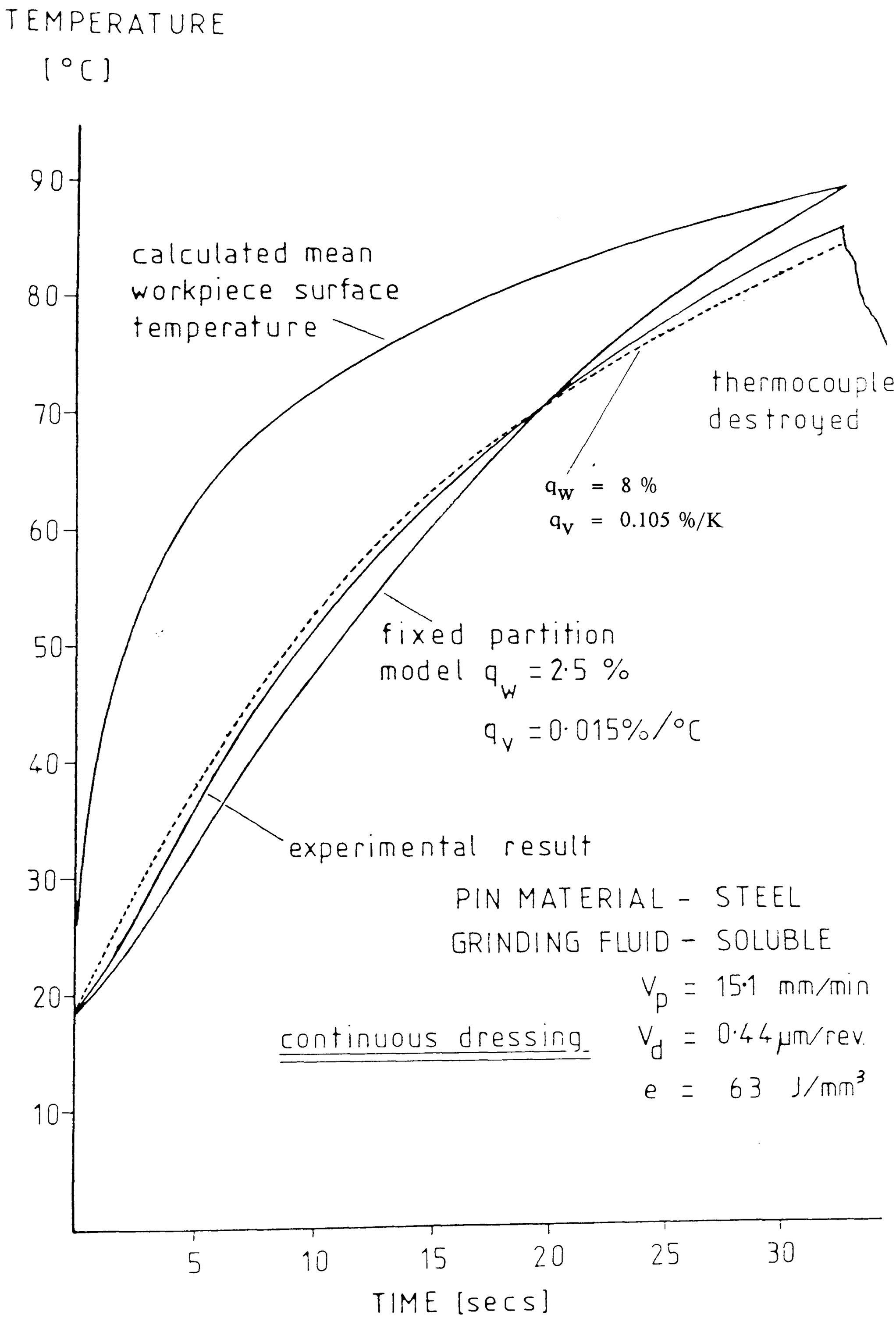

Figure 67. An example of Salter's measured and modelled temperature curves with the E.P macroemulsion [19] and an 8% partitioning fit to the same data.

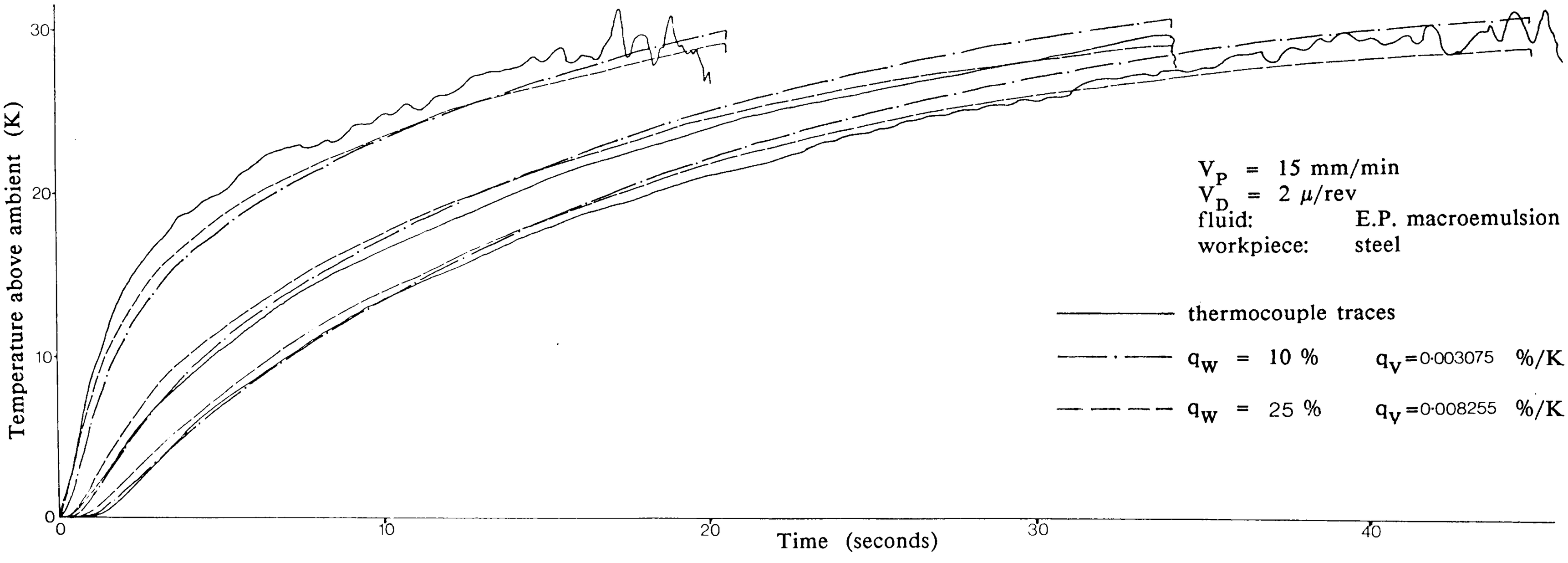

Figure 68. A range of partitioning values from 10 to 25% fitted to temperature curves obtained when grinding steel with a water based fluid.

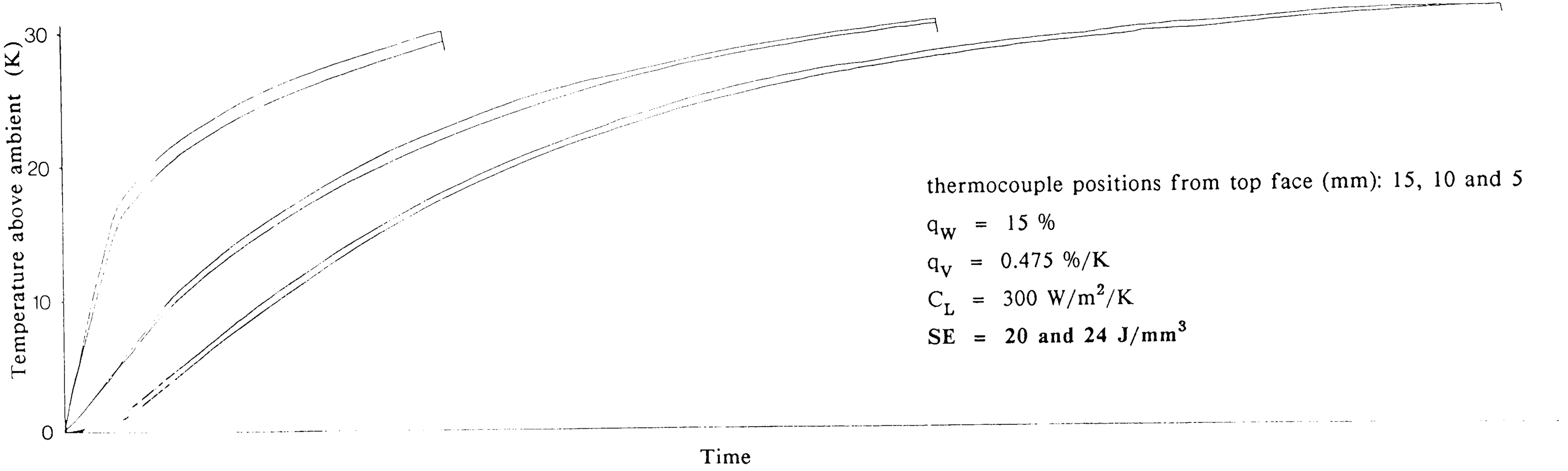

Figure 69. Graph showing the effect on modelled output of uncertainty in the measured value of specific energy.

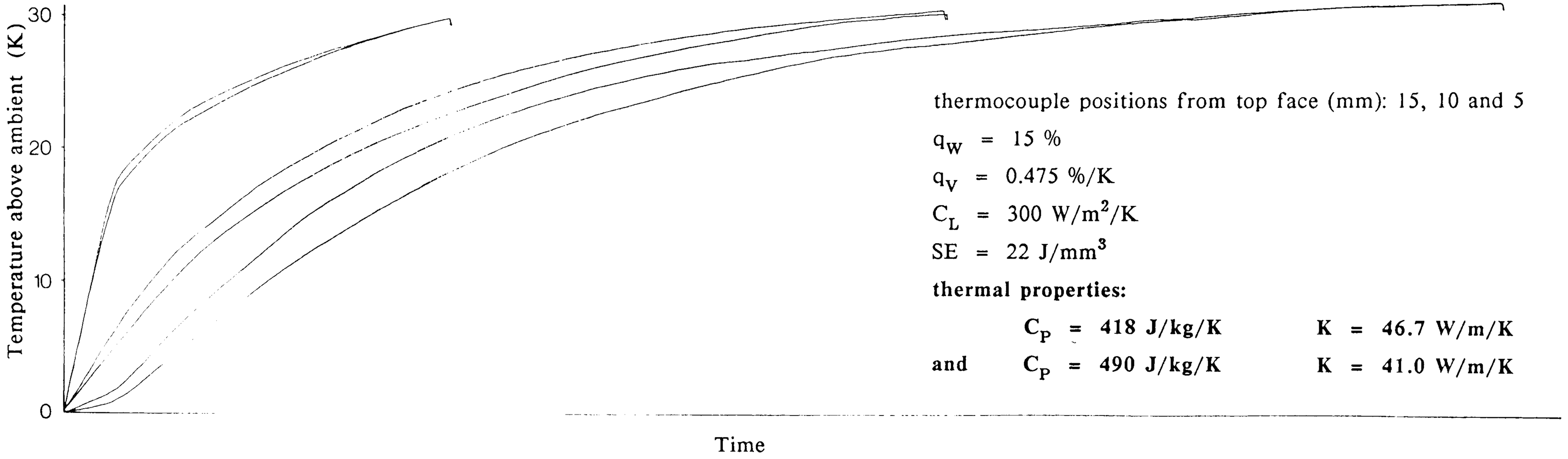

Figure 70. Graph showing the effect on modelled output of uncertainty in the thermal properties of steel.

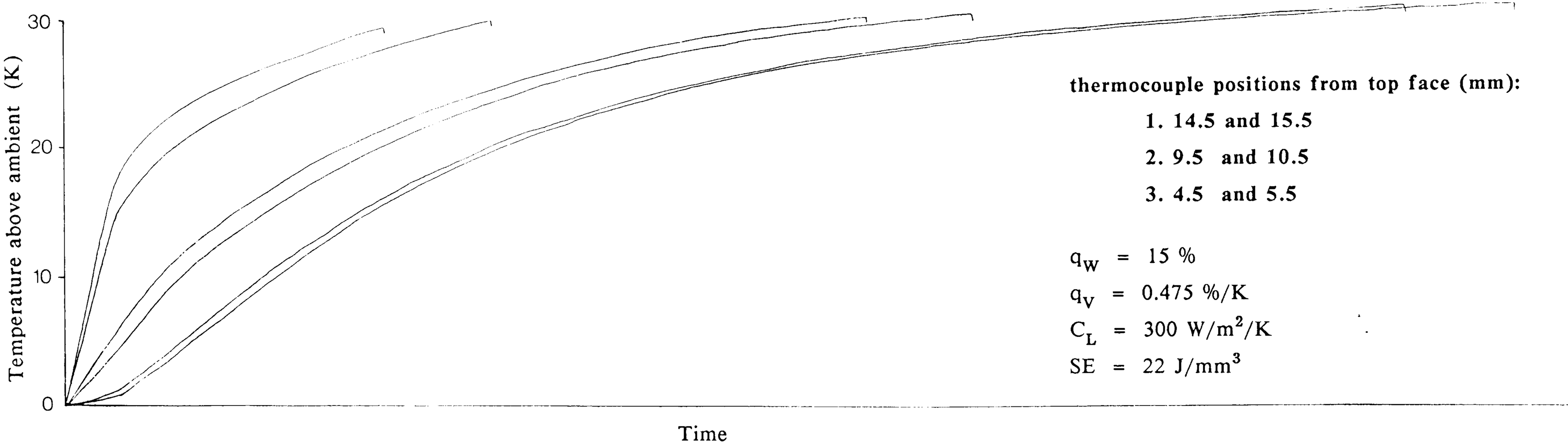

Figure 71. Graph showing the effect on modelled output of uncertainty in thermocouple positions.

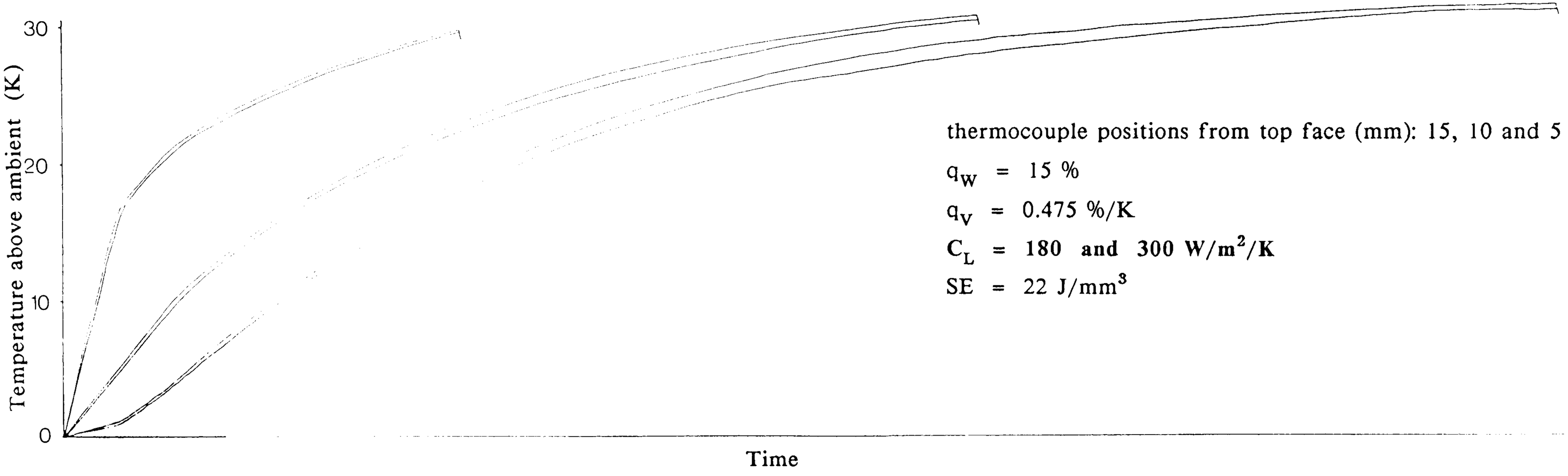

Figure 72. Graph showing the effect on modelled output of uncertainty in the value of the loss term, C_L.

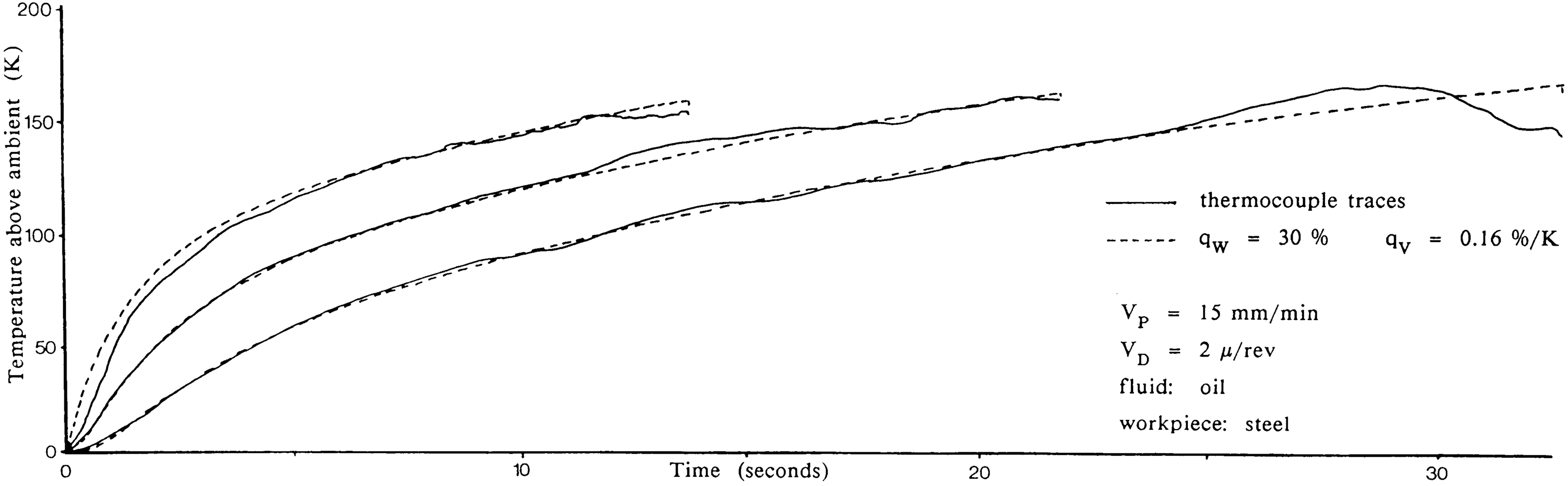

Figure 73. **Partitioning fraction of 30% fitted to experimental results with oil on steel.**

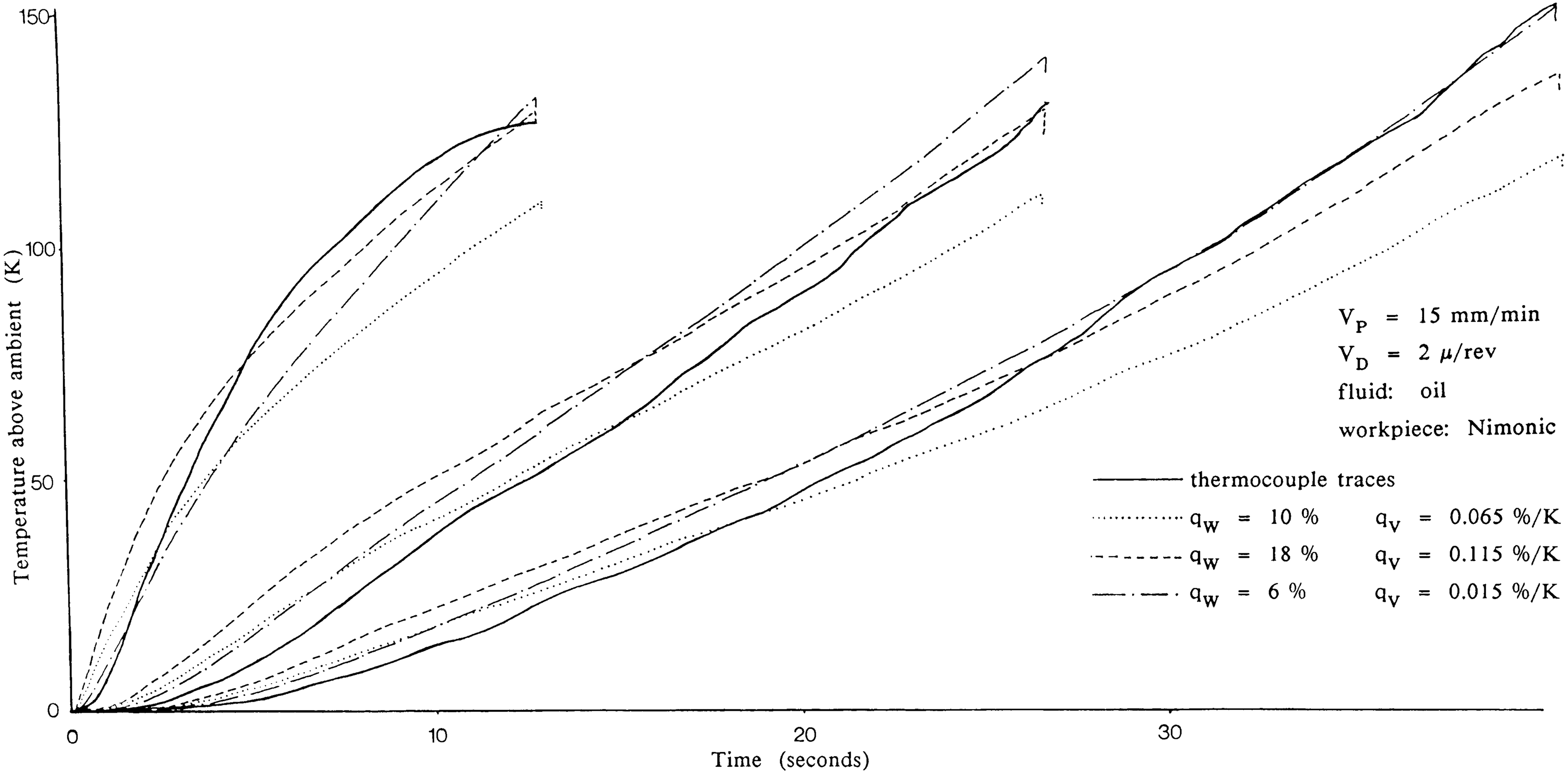

Figure 74. Range of "best fits" for partitioning fractions between 6 and 18% on Nimonic with oil as the grinding fluid.

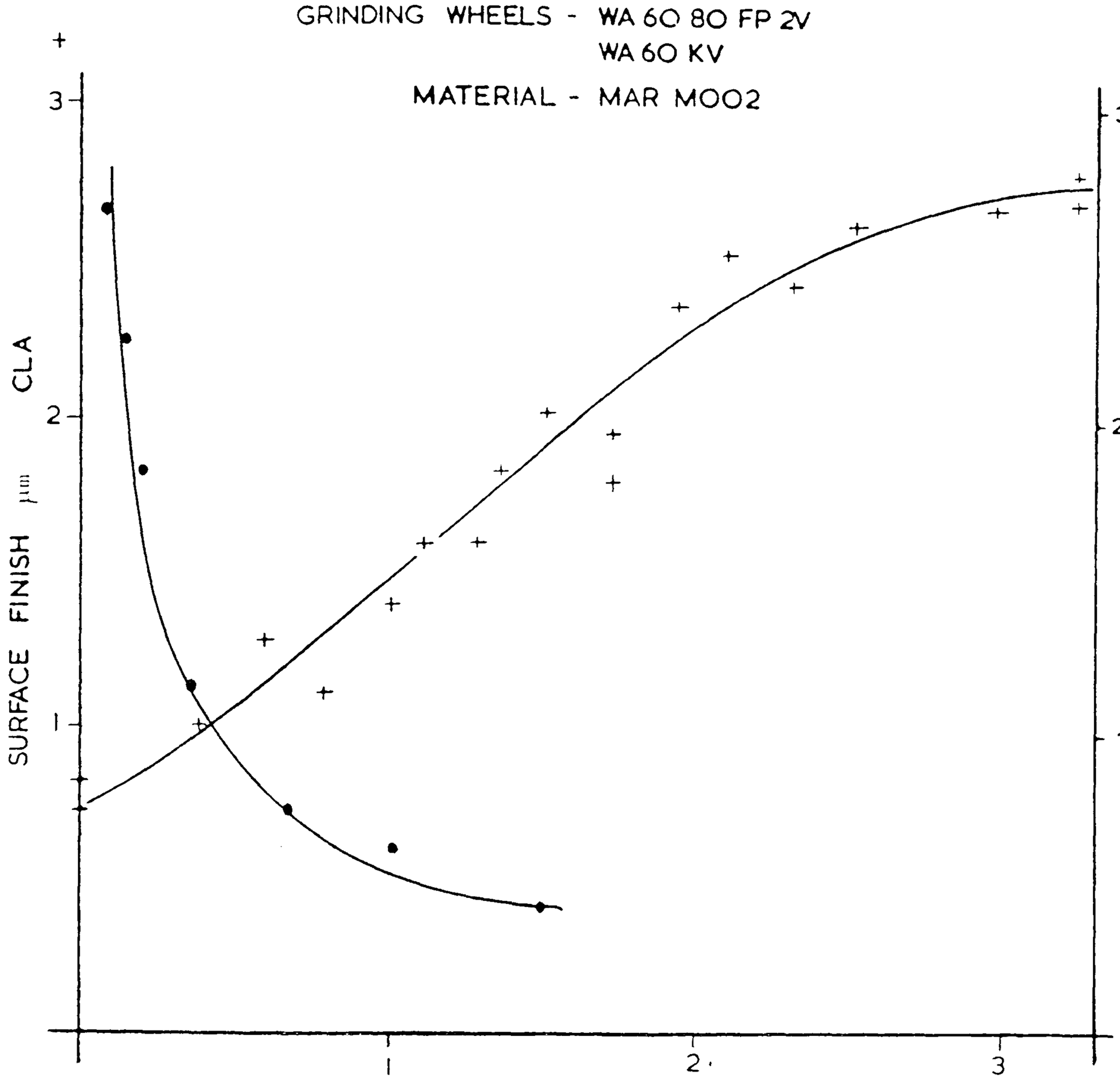

VARIATION OF SURFACE FINISH & SPECIFIC ENERGY

WITH DRESSER INFEED RATE.

FOR MAR M002

Figure 75. Comparison of the dresser infeed rate at which the specific energy and surface finish reach a constant value (after Salmon [65] Figures 17 & 18).

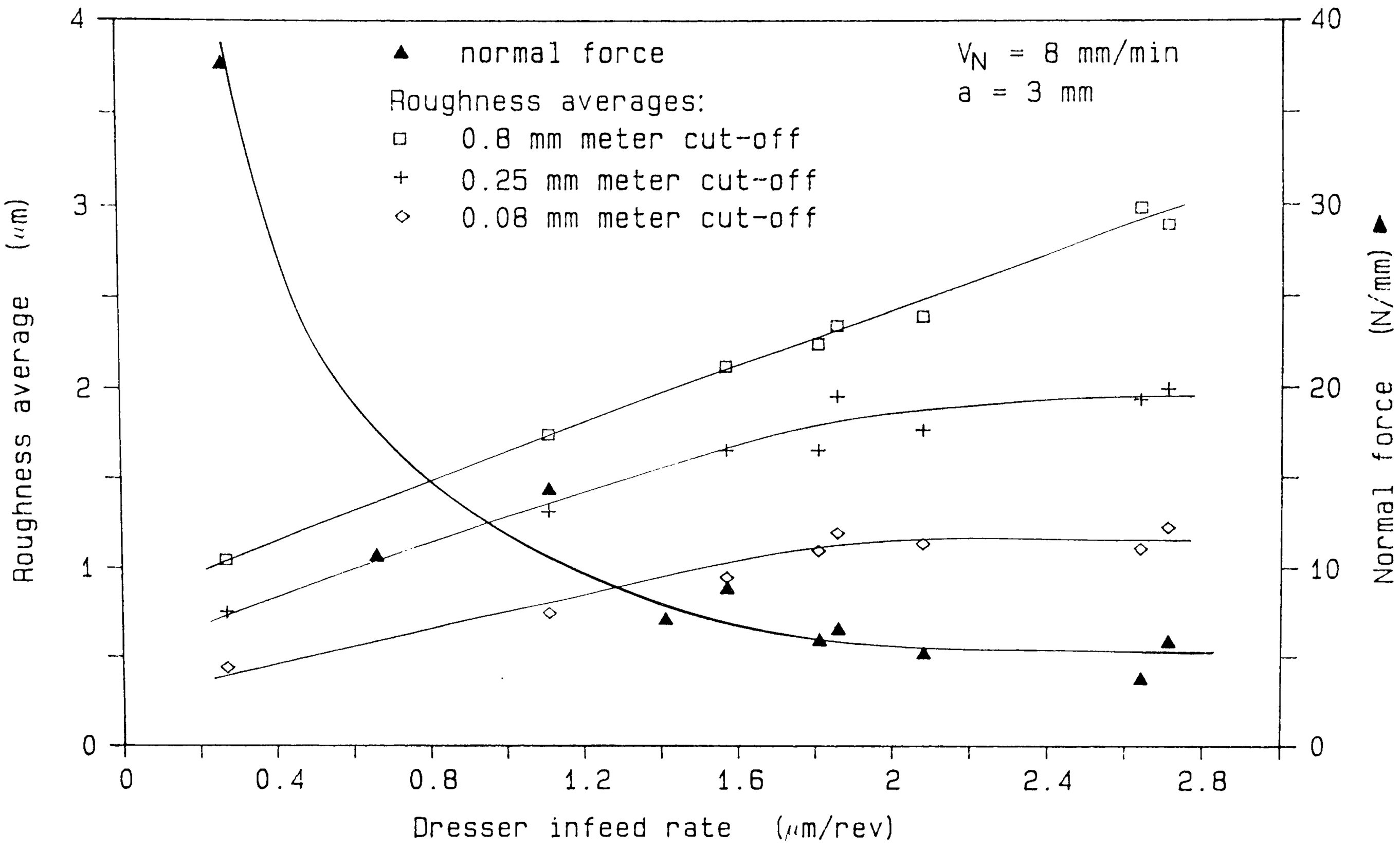

Figure 76. Surface roughness versus dresser infeed rate using three different values for meter-cut-off.

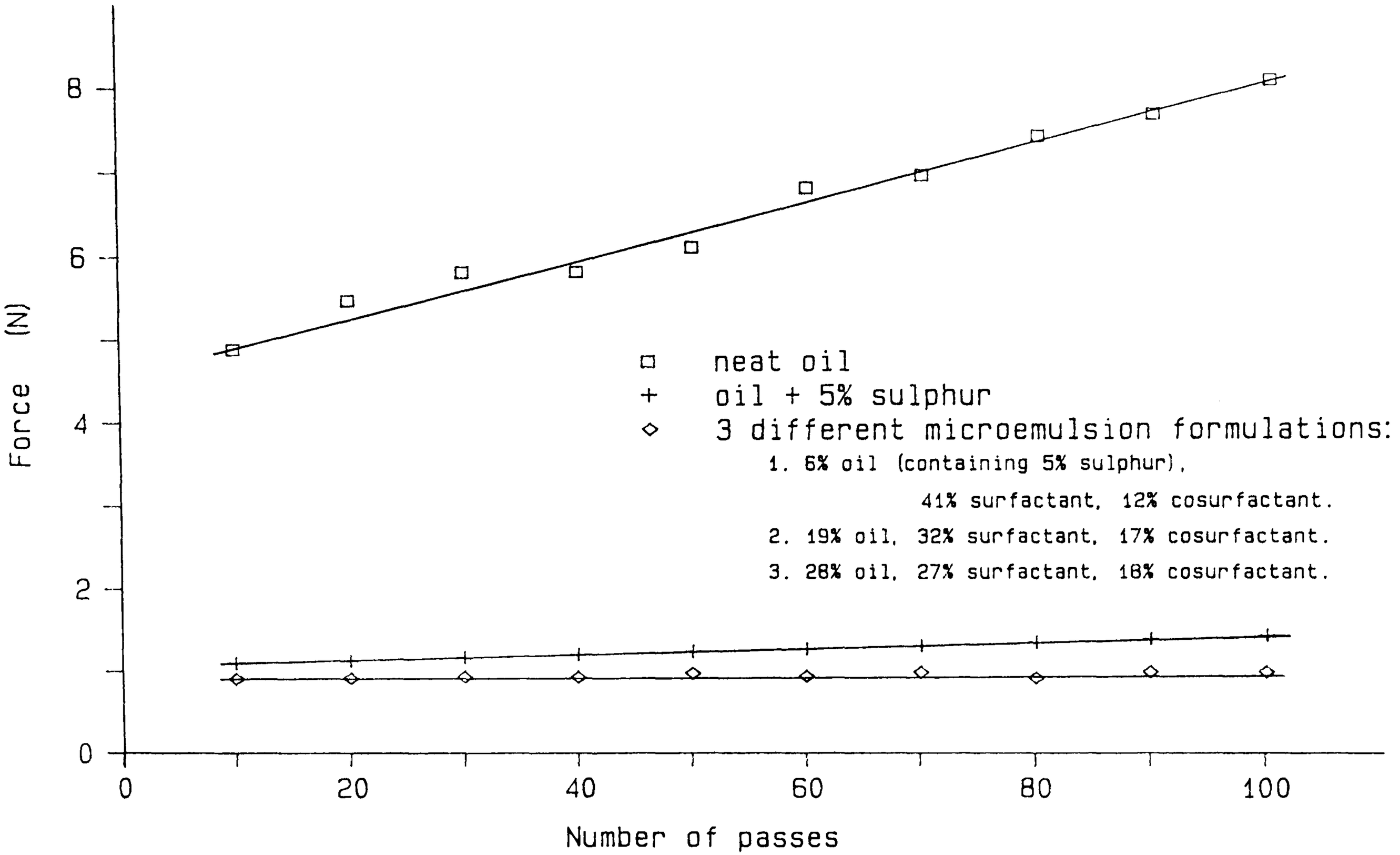

Figure 77. Force versus number of passes for fluids with varying oil contents (after Torrance's Figures 6.3, 6.5 & 6.8 [59]).

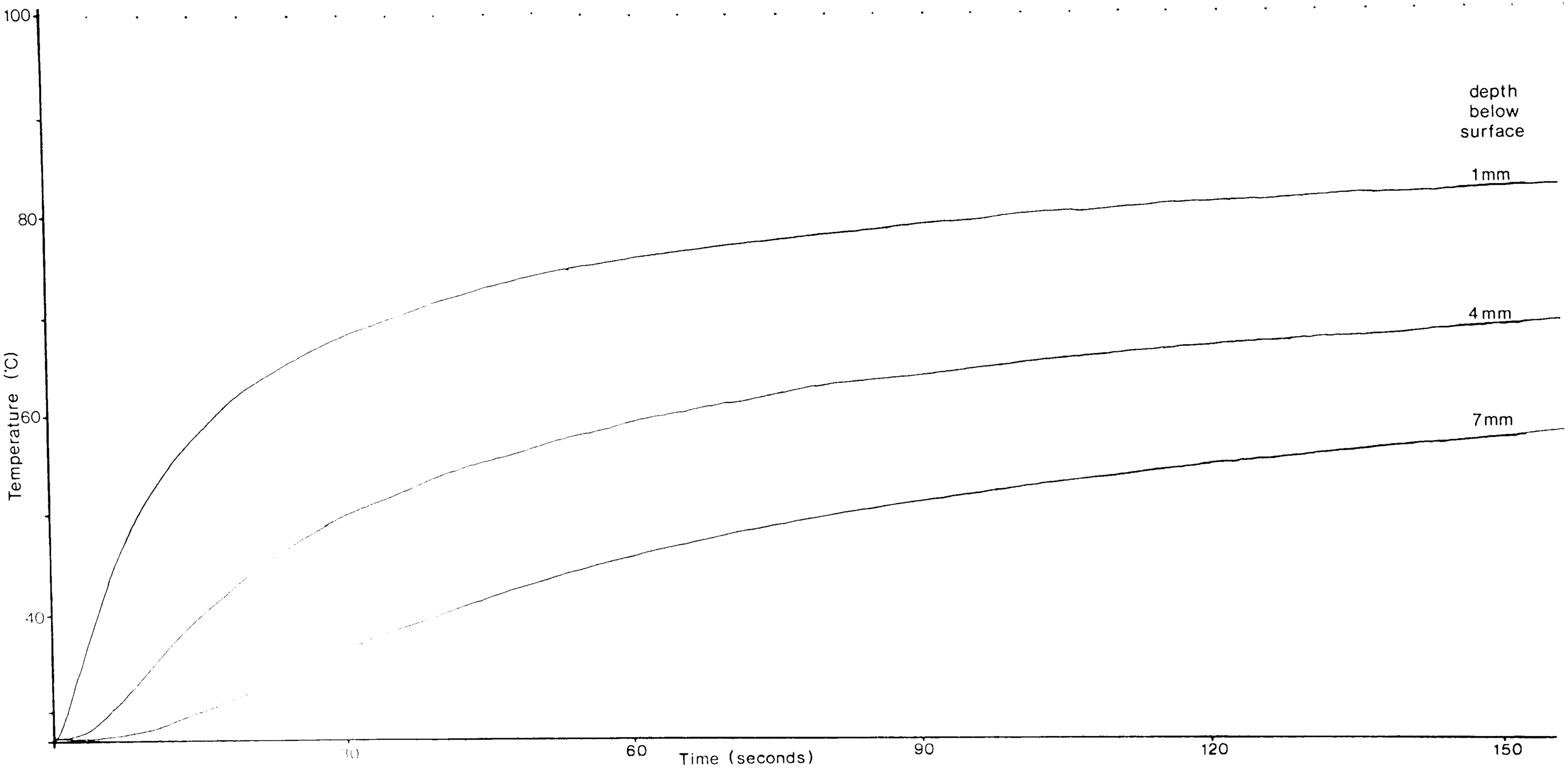

Figure 78. **Temperature versus time at depths in** Sindanyo below a steam **heated surface.**

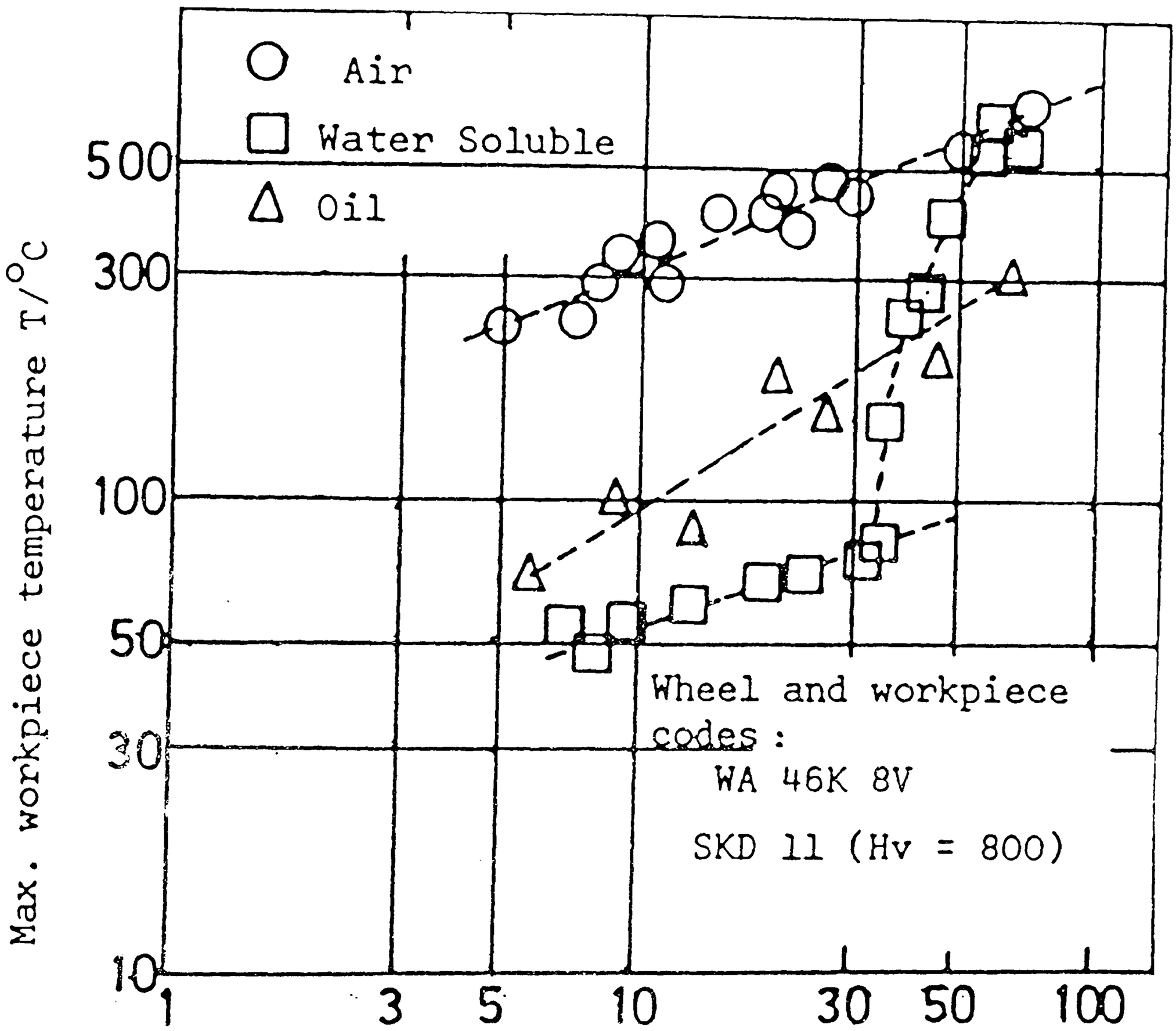

Figure 79. Temperature versus depth of cut (after Yasui & Tsukuda [112]).

INDEX OF AUTHORS

Numbers in square brackets correspond to those used in the list of references.
Numbers in bold text denote the pages where these references are used.